Linking slopes to the wetland: Hillslope hydrology and associated nitrate transport in a tropical valley bottom wetland

Dissertation

zur

Erlangung des Doktorgrades (Dr. rer. nat.)

der

Mathematisch-Naturwissenschaftlichen Fakultät

der

Rheinischen Friedrich-Wilhelms-Universität Bonn

Vorgelegt von

Claudia Schepp

aus

Aachen, Deutschland

Bonn, April 2022

Angefertigt mit Genehmigung der Mathematisch-Naturwissenschaftlichen Fakultät der

Rheinischen Friedrich-Wilhelms-Universität Bonn.

1. Gutachter: Prof. Dr. Bernd Diekkrüger

2. Gutachter: Prof. Dr. Mathias Becker

Tag der Promotion: 7. Juli 2022

Erscheinungsjahr: 2022

To
the love amongst people of different origin,
the beauty of the world and
the curiosity to explore both

&

To my dear friend Juju

Acknowledgments

This phd-journey was a truly special time and it is hard to express how sincerely grateful I am for all the experiences, the adventures, the lessons learnt and, above all, the people, who accompanied and supported me during this journey.

First of all, I would cordially like to thank my supervisory, Prof. Bernd Diekkrüger for always having our back, for his support and guidance not only in scientific matters, for fostering patience when I didn't have it, for always (!) being available for us, even after his retirement, briefly for being a "Doktorvater" in the truest sense of the word. Thank you! I would equally like to thank my second supervisor, Prof. Mathias Becker, for his advice and support and for his ever-positive mind-set and encouragement! I would further like to thank Prof. Weigend and Prof. Mariele Evers, for agreeing to join my doctoral committee and Prof. Evers for kindly "adopting" me to her research group.

This work would not have been possible without the support of all my co-workers in Uganda. My special thanks goes to my field assistant Abdul Kawere, for all his support and constructive inputs during the field work and all the time we spent together. I would like to thank Richard Mukasa, William Anecho, Paul Mayege and Baduru Kyimbugwe for always keeping us save, Steven Nkangi for many miles on the road and Aisha Nakyagaba for taking such good care of our house and being a top roomie! My gratitude goes to Dr. Michael Ugen and the entire GlobE-wetlands team in Namulonge, especially Lozio Makesa. My time in Uganda would truly not have been the same without my very dear friends Jennifer Imou and Hellen Drichiru and their families. Thank you, for introducing me so deeply to Ugandan culture, for opening your homes and your hearts and making Namulonge a second home for me! I would also like to thank my friends Janani Loum for making me part of CEOUganda and Arjen Rottmans for many new perspectives.

Also in Germany, there were many people who helped me realize this project. I would like to thank Camilla Kurth, Gabriele Kraus, Angelika Veits and Hans Böttger for their support in the laboratory and in practical matters, Jonas Limbrock, Florian Wagner and Dr. Pritam Yogeshwar for their advice on Geophysics and the University of Cologne as well as the Geomorphology working group for borrowing me their equipment.

I would like express my gratitude to the Cusanuswerk for their financial support as well as for the many insights into political, social and spiritual matters and the sense of community amongst the scholars.

I am so grateful for all my colleagues from the GlobE-family, the hydrology and the ecohydrology working group, especially and without any special order: Dr. Geoffrey Gabiri, Dr. Julius Kwesiga, Emmanuel Nkundimana, Björn Glasner, Kai Behn, Dr. Katrin Wagner, Susanne Ziegler, Eike Kiene, Dr. Miguel Alvarez, Dr. Andrea Rechenburg, Dr. Konrad Hentze, Layla Hashweh, Vivianne Umulisa, Dr. Matian van Soest, Susanne Hermes, Stefanie Steinbach, Dr. Felix op de Hipt, Dr. Thomas Poméon, Dr. Charléne Gaba, Dr. Yacouba Yira, Gero Steup, Fabian Weidt, Dr. Inken Rabbel, Dr. Britta Höllermann, Dr. Linda Taft, Dr. Adrian Almoradie, Katja Höreth, Rholan Houngue, Dörte Schulz and Joshua Ntajal. Thank you for sharing ideas and worries, the great lunch hours, for being top roomies and travel mates, for the many happy moments we shared in the field, in the office, during conferences and in our free time! I would especially like to thank Dr. Constanze Leemhuis, for helping me to get this work started, Dr. Sonja Burghof for sharing data and thoughts on hydrogeological complexities, Dr. Mouhammed Idrissou, for making the office such a

bright place and setting examples in many ways, Dr. Kristian Näschen, for his great support, mentorship and friendship during so many years, Alex Ahring for our office Saturdays, your open ear and our nitrate talks, and Dr. Tina Grotelüschen, my work work-wife, for having shared all the big and small joys and worries in work and life-related matters during these last years on the road to mission 202x and for having become such a good friend!

Last but not least I would like to thank all these special people around me who have accompanied, encouraged and supported me during this project and beyond. My dear friends for always having an open ear, especially Marion Schley for in addition to that having read so many pages!, my parents and my sister Barbara for all their support since I was little and for having given me such a good start into life and finally Henri Schwaiger, for all his patience and support during the last years and for all the love and joy we share.

Abstract

Valley bottom wetlands are regarded as a white hope for enhancing food security in East Africa. Due to their prolonged water availability, they buffer some of the effects of climate change and further offer fertile soils in otherwise frequently degraded landscapes. For West Africa it has been shown that these attributes are related to water and nutrient fluxes from the surrounding slopes into the valley bottom wetlands, while for East Africa the knowledge on hillslope hydrology and its relevance for water and nutrient transport to the wetland is still limited. The aim of this work is to investigate interflow processes on a saprolitic hillslope and to explore the agricultural relevance of water and nitrate inputs from the slopes to the wetland fringe.

The experiment was set up as a plot study in a representative small inland valley in Central Uganda and a multi-method approach was followed. The hillslope hydrology was investigated via electrical resistivity measurements as well as the monitoring of soil moisture along the toposequence. Furthermore, interflow was collected in trenches at the slope toe, while surface runoff was quantified on runoff plots at the lower slope position. In view of gaining a better process understanding and to formulate management recommendations, the influence of different land use types as well as rainfall characteristics on water and nitrate fluxes from the slopes to the wetland fringe was analysed. To that end, three different land use types were established on plots of 30 x 105 m² on the slopes, including crop production, semi-natural vegetation and bare fallow. The dynamics of nitrate formation and fluxes as well as the seasonal cumulative amount of bio-available nitrate were monitored along the toposequence under the three land use types. In addition, nitrate loads in the interflow as well as in the surface runoff were determined.

The study revealed that due to the fill-and-drain mechanism interflow is not directed along the soil-saprolite interface but passes through the saprolite. A quick as well as a delayed interflow component develops, which contribute to the shallow aquifer in the wetland soils as well as to the aquifer in the valley sediments. The total rainfall amount during the rainy season as well as the distribution of rainfall over the season strongly influence interflow generation, with the delayed interflow component also carrying the signal of the previous rainy season.

Land use type as well as the rainfall characteristics also impact the nitrate translocation along the slope. These factors are the key drivers of soil moisture conditions and the activation of vertical and lateral flow paths in the soil and in the saprolite, but also for the dynamics of nutrient uptake from the soil solution.

Regarding agricultural production, water from the slope is only one amongst several drivers of the soil water status at the wetland fringe. While there was an input of nitrate from the slopes to the wetland, low contents of seasonal bio-available nitrate hint to a quick loss of nitrate at the wetland fringe. Therefore, agronomic measures should focus on water and nutrient conservation along the slopes and at the cultivation of deep rooting crops at the slope toe in order to maintain water and nitrate in the soil-plant system and thus minimize losses.

The study highlights the complexity of subsurface flow processes in saprolitic environments and stresses the importance of a sound knowledge of the local hillslope hydrology to detect catchment-wetland interactions. This knowledge is the basis for pinpointing agronomic interventions, enabling a sustainable

use of the natural resources in inland valley landscapes of East Africa and, hence, contributing to food-security in the region.

Zusammenfassung

Talbodenfeuchtgebiete gelten als Hoffnungsträger für die Verbesserung der Ernährungssicherheit in Ostafrika. Auf Grund der längeren Wasserverfügbarkeit im Oberboden, sind sie resilienter gegenüber klimawandelbedingt vermehrt auftretenden Dürreperioden und verfügen über nährstoffreiche Böden, im Gegensatz zu den oftmals degradierten Produktionsflächen im Umland. Studien aus Westafrika konnten nachweisen, dass diese vorteilhaften Eigenschaften auf Wasser- und Nährstoffflüssen von den umliegenden Hängen beruhen oder durch diese verstärkt werden. Für Ostafrika hingegen sind diese Zusammenhänge bislang noch kaum erforscht. Ziel dieser Arbeit ist es, die Zwischenabflussprozesse an einem, von einer mächtigen Verwitterungsdecke (Saprolith) bedeckten, Hang zu beschreiben und die Relevanz von Hangzugswasser für die Wasser- und Nährstoffverfügbarkeit in der landwirtschaftlichen Produktion am Rand des Talboden-feuchtgebietes zu ermitteln.

Hierzu wurde auf einer Versuchsfläche in einem repräsentativen Feuchtgebiet in Zentraluganda ein Multi-Methodenansatz verfolgt. Um die Abflussprozesse am Hang zu erfassen, wurden geoelektrische Widerstandmessungen und ein Monitoring der Bodenfeuchte entlang der Toposequenz vorgenommen. Darüber hinaus wurde der Zwischenabfluss in Gruben am Hangfuß aufgefangen und quantifiziert, während der Oberflächenabfluss auf abgegrenzten Parzellen am Unterhang erfasst wurde. Mit dem Ziel, ein besseres Prozessverständnis zu erlangen und Bewirtschaftungsempfehlungen zu formulieren, wurde der Einfluss verschiedener Landnutzungsformen, sowie mehrerer Niederschlagsparameter auf Wasser- und Nährstoffflüsse von den Hängen zum Rand des Feuchtgebiets analysiert. Vor diesem Hintergrund wurde auf Streifen von 30 x 105 m² eine Fläche unter Ackerbau, unter Schwarzbrache sowie unter naturnaher Vegetation angelegt. Auf diesen drei Flächen wurden entlang der Toposequenz die Dynamik von Nitratbildung und -verlagerung sowie das saisonal kumulativ pflanzenverfügbare Nitrat analysiert. Zudem wurde die Nitratfracht im Zwischenabfluss sowie im Oberflächenabfluss bestimmt.

Die Ergebnisse der Feldversuche zeigen, dass Zwischenabflussprozesse auf Grund des Fill-and-drain Mechanismus nicht an der Grenzfläche von Oberboden und Saprolith, sondern innerhalb des Saproliths stattfinden. Dabei lässt sich sowohl eine schnelle wie auch eine verzögerte Abflusskomponente nachweisen, welche beide sowohl in das oberflächennahe Aquifer wie auch in das Aquifer in den Talbodensedimenten des Feuchtgebiets entwässern. Die Ausbildung und Effektivität von Zwischenabflussprozessen wird sowohl von der absoluten Niederschlagsmenge, wie auch von der Niederschlagsverteilung während einer Regenzeit bestimmt, wobei die verzögerte Abflusskomponente auch durch die Niederschlagsverhältnisse während der vorangegangenen Regenzeit beeinflusst wird.

Auch die Nitratverlagerung entlang des Hanges wird von den Niederschlagsverhältnissen sowie der Landnutzung beeinflusst. Diese beiden Faktoren sind entscheidend für den Bodenwassergehalt und somit für die Aktivierung von vertikalen und lateralen Fließwegen im Boden sowie im Saprolith. Gleichzeitig beeinflussen sie die Dynamik der Nitratmineralisierung sowie der Nitrataufnahme aus der Bodenlösung.

Hangzugswasser stellt nur einen unter vielen Einflussfaktoren für die Wasserverfügbarkeit am Rand des Feuchtgebietes dar. Nitrat gelangt durch Oberflächen- und Zwischenabfluss ins Feuchtgebiet, jedoch

deuten die geringen Mengen an saisonal pflanzenverfügbarem Nitrat auf einen schnellen Verlust des Nitrats am Rand des Feuchtgebietes hin. Somit sollte eine auf Wasser- und Nährstoffspeicherung im Oberboden ausgelegte gute landwirtschaftliche Praxis an den Hängen, sowie der Anbau tiefwurzelnder Nutzpflanzen am Hangfuß im Zentrum agronomischer Interventionen stehen, um Wasser und Nährstoffe im Produktionssystem zu halten und Verluste zu minimieren.

Die vorliegende Arbeit zeigt die Komplexität von Zwischenabflussprozessen in durch mächtige Verwitterungsdecken geprägten Gebieten und unterstreicht die Bedeutung einer tiefgehenden Kenntnis der lokalen Abflussprozesse am Hang für das Verständnis der Verbindung von Feuchtgebiet und Einzugsgebiet. Dieses Wissen stellt die Grundlage für zielgerichtete agronomische Maßnahmen und damit für eine nachhaltige Nutzung der natürlichen Ressourcen in Talbodenfeuchtgebieten in Ostafrika dar, welche zur Ernährungssicherheit in der Region beiträgt.

Table of contents

List of figures

List of tables

List of abbreviations

API	antecedent precipitation index
BD	bulk density
BERT	boundless electrical resistivity tomography (software)
BMBF	Bundesministerium für Bildung und Forschung
CV	coefficient of variation
ENSO	El Niño-Southern Oscillation
ERT	electrical resistivity tomography
FDR	frequency domain reflectometry
HH2	hand-held moisture meter
HT	hilltop
IF	interflow
ITCZ	inner tropical convergence zone
K_{fs}	field-saturated hydraulic conductivity
K_{sat}	saturated hydraulic conductivity
LS	lower slope
LULC	land use and land cover
MS	mid-slope
NaCRRI	National Crops Resources Research Institute
NALIRRI	National Livestock Resources Research Institute
P	precipitation
PR2	(polycarbonate rod) profile probe
R	resistance
R^2	Spearman's correlation coefficient
RAQ	resin adsorption quantity
rc	runoff coefficient
RESD2INV	resistivity 2D inversion (software)
roh	Spearman's correlation coefficient
ρa	apparent resistivity
SDG	sustainable development goals
SOM	soil organic matter
sr	surface runoff
ST	slope toe
SWAT	Soil Water Assessment Tool
Θ	soil water content
Θs	soil water content at saturation
U	current density
V	electrical field
W	wetland

1 Introduction

1.1 Problem statement

Achieving food security and healthy nutrition for a rapidly growing population in the face of climate change remains one of the central challenges of this century (FAO, 2017). The number of malnourished people in countries of the global South still exceeds by far the target the international community set in the sustainable development goals. In Eastern Africa, 28 % of the population are malnourished (FAO, IFAD, UNICEF, WFP and WHO, 2021) and in order to meet the demand for food products of Sub Saharan Africa in 2050, an increase of the current production by 112 % is needed (FAO, 2017).

In Eastern Africa, food production is still dominated by small-scale farming. In Uganda, for example, 68 % of all agricultural households cultivate an area of less than 1 ha (UBOS, 2018). In this setting, agricultural production in the uplands is frequently impeded by degraded and nutrient-poor soils as well as water scarcity during highly variable rainy seasons and extended periods of drought (Tully et al., 2015). Extending agricultural production into wetland areas could hence be a vital option for increasing food production as wetlands are generally characterised by a prolonged water availability and relatively fertile soils (von der Heyden and New, 2003). For the purpose of this study, wetlands are defined following the definition of the U.S. Army Corps of Engineers which is well suited for ecological studies (W. J. Mitsch and Gosselink, 2015) as "[…] *areas that are inundated or saturated by surface water or groundwater at a frequency and duration sufficient to support, and that under normal circumstances do support, a prevalence of vegetation typically adapted for life in saturated soil conditions".* Specifically, this study focusses on an alluvial valley bottom wetland, as further defined in chapter 2.1.

Wetlands cover about 4.7 % of the land surface in Sub-Saharan Africa (Rebelo et al., 2010) and in Uganda this number even amounts to 11 % of the land area (Government of Uganda, 2016). While an extensive body of literature exists on the bigger wetlands located in the lake Victoria and the Nile basin, little research has been undertaken in small valley bottom wetlands (Sakané et al., 2011). Besides their potential for agricultural production, wetlands offer a wide range of ecosystem services to local communities. These include, amongst others, the supply of fresh water and building materials as well as the regulation of climate processes. Further, they constitute hotspots of biodiversity and places of cultural practice (Millennium Ecosystem Assessment, 2005). At the same time, wetlands are fragile ecosystems (Rodenburg, 2013) and therefore, their wise use has to be the central guiding principle for all management decisions. In the Ramsar Convention, wise use aims at "[…] *the maintenance of [a wetlands'] ecological character, achieved through the implementation of ecosystem approaches, within the context of sustainable development*" (Ramsar Convention Secreteriat, 2016). In Uganda, especially in peri-urban or drought-prone areas, the conversion of pristine wetlands to sites of agricultural production is already progressing quickly and 42.2 % of the country's wetland area have been lost during the last twenty years (NEMA, 2019). Therefore, a sound scientific knowledge is needed to guide the wise use of wetland systems which considers both human needs and environmental sustainability.

Hydrology essentially determines the state, or health of a wetland (Beuel et al., 2016; Kotze et al., 2012). Especially valley bottom wetlands are very sensitive to changes in quality and quantity of their water supply (Erwin, 2009) which depends on surface and subsurface runoff from the surrounding slopes

(Rodenburg, 2013). Therefore, a detailed understanding of water pathways and runoff related processes is crucial to ensure the wise use of a wetland and to account for wetland-catchment interactions. In this regard, surface runoff and interflow are of special importance, as depending on the geology, they can be major contributors to plant available water in the wetland (McFarlane, 1992). Nevertheless, up to now, no detailed study on interflow processes in slopes covered by a deep saprolite and their contribution to the hydrology of valley bottom wetlands in East Africa exists.

Besides their relevance for the wetland hydrology, water fluxes from the slopes further act as carrier for nutrients. These nutrient fluxes can contribute significantly to the nutrient supply of crops at the wetland fringe, as has been shown in inland valleys in Ghana (Asante et al., 2017) and Burkina Faso (Yameogo et al., 2021). In low-input production systems, the nutrition of crops directly depends on the careful management of native soil nutrients and especially of nitrogen (Becker et al., 2007). Also in Uganda, only 35 % of agricultural households apply any kind of fertilizer (UBOS, 2021). Therefore, an adapted management of the wetland fringe position, which aims at bringing nutrient inputs from the slopes into production (e.g., by the cultivation of catch crops (George et al., 1994)) could stimulate agricultural production and hence contribute to food security in the region. Yet, so far little knowledge exists on nutrient inputs from the surrounding slopes into valley bottom wetlands in Uganda and the related hillslope hydrology. This study aims at enhancing the knowledge on spatio-temporal dynamics of water and nitrate fluxes into valley bottom wetlands. For that purpose, the Namulonge valley bottom wetland was chosen as a case study, as it represents a typical wetland system in the undulating topography of Central Uganda and the East African Highlands in general.

1.2 Research questions

Several research questions unfold from the problem statement above that are addressed in this study:

1. **What are the characteristic interflow processes at the hillslopes adjacent to the valley bottom wetland?**

A thorough understanding of the hillslope hydrology is crucial for predicting the hydrological response of the wetland to agronomic interventions and land use change in the catchment (Bullock, 1992). Nevertheless, so far the knowledge on interflow processes in saprolites, i.e., the thick weathering mantle which is commonly found over crystalline rocks in East Africa (Taylor and Howard, 1996), is very limited. A first conceptual model of regional and local hydrogeology in the Namulonge catchment was introduced by Burghof (2017) and hydrological processes under different land use change scenarios were modelled at a catchment scale by Gabiri et al. (2019). Both authors found that interflow processes were active in the catchment, but so far no detailed analysis of interflow and surface runoff processes at the hillslope scale has been conducted. Therefore, the first question focusses on the analysis of interflow processes in the soil body and in the saprolite and on how they contribute to the water supply of the wetland system. The multi-method approach followed in this study, including the installation of runoff trenches, soil moisture probes and geo-electrical measurements, gave valuable insights into the hillslope hydrology of a catchment enclosing a valley bottom wetland.

2. **How do rainfall characteristics and the land use type at the slopes influence water and nitrate translocation from the slopes to the wetland fringe in interflow and surface runoff?**

Nitrate translocation is determined by source factors, i.e., the amount of nitrate present in the soil solution, as well as transport factors, including the water availability and the activation of surface and subsurface flow paths. These factors are directly influenced by, i. a., climatic conditions and the land use type. Hence, the second research question aims at identifying the influence of rainfall characteristics and three different land use types, including bare fallow, crop production and semi-natural vegetation, on the translocation of nitrate along the slopes and the subsequent input of nitrate into the wetland. Considering the strong linkages of the slopes and the valley bottom wetland, such process understanding is the foundation of a sustainable landscape management.

3. **To what extent are soil moisture status and nutrient availability at the wetland fringe driven by water and nitrate inputs by interflow and surface runoff from the slopes?**

The efficient use of soil native nutrients plays a vital role for the increase in production of agricultural commodities and hence contributes significantly to food security in areas which are characterised by nutrient-poor soils and low-input small scale farming. It has been shown for wetlands in West Africa that following the mineralisation peak during the dry to wet transition period, significant inputs of nitrate from the slopes to the wetland occurred, which requires adapted management strategies like the cultivation of so-called catchcrops in order to keep the nitrate within the soil-plant system. For East Africa, this effect has not been investigated upon before this study. Besides the nutrient availability, crop development also strongly depends on the soil water status. Both, too dry and too wet conditions, negatively impact crop development. At the fringe position, water inputs from the slopes might markedly determine the soil water status, if the water enters the wetland system at the transition from upland to wetland geology. Therefore, the third research question of this thesis addresses the nitrate translocation along the slopes as well as water and nitrate inputs into the wetland in order to contribute to a science-based agronomic decision making.

1.3 Objectives of the study

The overall objective of this study is to analyse water and nutrient inputs from the slopes to the wetland fringe in a valley bottom wetland. Thereby, this study contributes to an enhanced understanding of the hillslope hydrology of valley bottom wetlands in East Africa, which is a crucial factor controlling the hydrological conditions in the wetland and thus has to be considered in sustainable management decisions. In addition, this study explores the relevance and seasonality of nitrate dynamics in the soil solution and particularly of nitrate inputs from the slopes for the nitrate availability at the wetland fringe. Such knowledge is seen to guide agronomic management decisions in the wetland as well as on the slopes and thus to contribute to achieving food security in a region characterised by low-input agro-ecosystems. The specific objectives of this study are:

i Explore the sub-surface characteristics of and water pathways in the saprolite along the slope and investigate their connection to the aquifers in the valley sediments.

ii Characterise and localise interflow processes in the soil body and in the saprolite.

iii Analyse the impact of rainfall characteristics, soil moisture and the land use type on interflow processes and surface runoff.

iv Assess the nitrate dynamics in the soil solution on the slopes regarding seasonality as well as vertical and lateral translocation.

v Analyse the effect of different land use types and rainfall characteristics on nitrate mineralisation and translocation along the slopes.

vi Estimate water and nitrate inputs from the slopes into the wetland.

1.4 Research framework

This work was associated to the "GlobE-Wetlands in East Africa"- project (FKZ: 031A250A-H). The project was one of six interdisciplinary German-African research consortia within the "GlobE- securing the global food supply"- initiative which was initiated and funded by the German Federal Ministry for Education and Research (BMBF). The aim of the initiative was to support the development of sustainable and productive agriculture in Africa which is based on sound scientific and traditional knowledge and is driven by the cooperation of the science community with local farmers and political stakeholders. Within this framework, the GlobE-Wetlands project investigated the physical and socio-political environment and the characteristic processes of four wetland ecosystems in Kenya, Ruanda, Tanzania and Uganda and developed sustainable agricultural management options for different wetland types. The project was built around the cognition that, despite their large production potential, wetlands are very fragile ecosystems whose advantageous properties are quickly lost under poor management (Diekkrüger et al., 2018). Therefore, the overarching goal of the project was to reconcile future food production with environmental protection. The project was set up in four clusters. While cluster A focussed on the process understanding of the wetland system, cluster B explored agricultural management options. In cluster C the results of the different disciplines were integrated and future scenarios analysed. Based on these findings, the results were extrapolated to the regional scale and recommendations for farmers and political decision makers formulated in cluster D. Besides the scientific interest, capacity-building and the promotion of North-South as well as South-South co-operations were a major concern of the project. This thesis contributes mainly to cluster A, as it focusses on process understanding of the hillslope hydrology and wetland catchment interactions regarding water and nutrient fluxes. Nevertheless, it also contributes to cluster B, as it explores the effect of different land use types at the slopes and lays the foundation to formulate recommendations for agronomic interventions at the wetland fringe.

1.5 Structure of the thesis

This doctoral thesis comprises eight chapters. In this first chapter, an introduction to the research questions and the context of this work is given. Chapter 2 provides an overview of the current state of

research regarding wetland hydrology and hydrogeology, hillslope hydrology as well as nitrate dynamics and translocation. Chapter 3 describes the study area, focussing on the physical attributes, before the experimental setup and the methodology are explained in chapter 4. In chapter 5, the results of the geo-electrical measurements and the soil survey are presented and interpreted regarding the geological structure of the slopes and the transition from upland to wetland geology at the study site as well as regarding the detection of lateral and vertical flow paths (objective i.). In chapter 6, the results on soil moisture and runoff dynamics at the slopes and at the wetland fringe are presented and discussed regarding interflow processes and the impact of the land use type and rainfall characteristics (objectives ii. and iii.). In chapter 7, the results on nitrate dynamics in the soil solution and in the different runoff components are presented and interpreted regarding seasonality and translocation of nitrate along the slopes as well as regarding the influence of different land use types (objectives iv., v. and vi.). Based on the insights of the previous chapters, conclusions regarding the hillslope hydrology and associated nitrate translocation along the slopes are drawn in chapter 8 and the relevance of water and nutrient inputs from the slopes for agricultural production at the wetland fringe is evaluated. Finally, the study closes with an outlook on future research activities. The conceptual outline of this thesis is visualized in Figure 1.

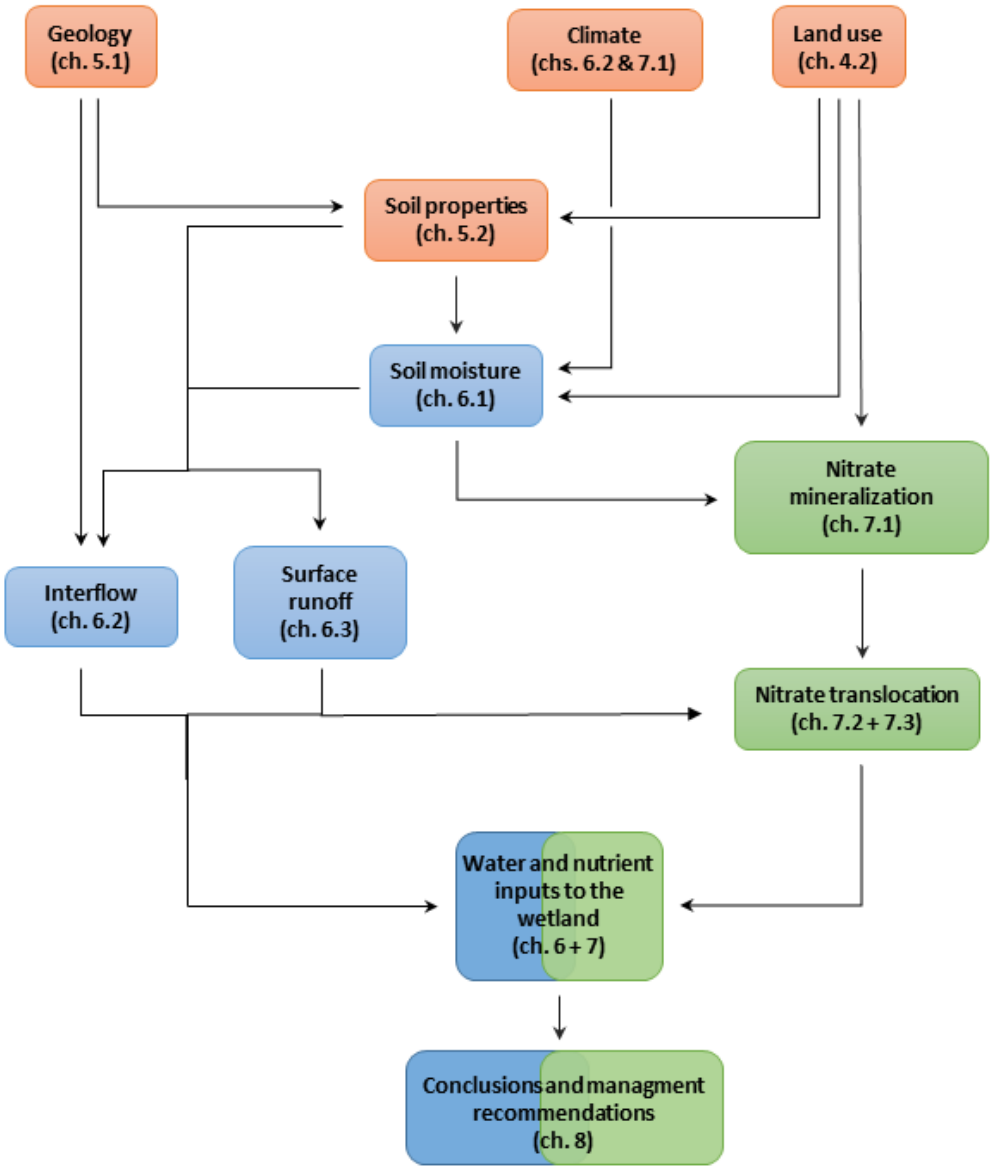

Figure 1 Conceptual outline of the thesis. Elements in the orange boxes refer to the environmental conditions which influence water and nutrient fluxes along the slopes. The blue colour is linked to water dynamics and hydrological processes while the green colour refers to nitrate dynamics and translocation.

2 Current state of research

This chapter reviews the current state of research regarding structures and processes related to water and nitrate fluxes from the adjacent slopes into valley bottom wetlands. In the first section, hydrological and hydrogeological characteristics of valley bottom wetlands are introduced (chapter 2.1). The second sub-chapter reviews the current knowledge on hillslope hydrology, i.e., surface and subsurface runoff processes at the valley slopes (chapter 2.2), while the following section presents the current state of knowledge on nitrogen dynamics and translocation in (tropical) soils (chapter 2.3). The final section of this chapter (chapter 2.4) constitutes a short excursus into the (hydro)geological characteristics of tropical weathering profiles, as these are strongly linked to the interflow processes along the slopes.

2.1 Hydrology and hydrogeology of valley bottom wetlands

Following the Ramsar convention a vast variety of definitions for "wetlands" as a landscape unit exists, depending on the area of interest (Ramsar Convention Secreteriat 2006, p.91). In their review of 245 studies on wetlands, Amler et al. (2015) found that the majority of authors described wetlands as areas of common conditions regarding bedrock formation and hydrology that "together cause and reflect the abundance of water over a time span sufficient to support internally diverse natural riparian vegetation that differs from the surrounding uplands" (p. 5259). Regarding palustrine wetlands, several classification schemes have been developed during the last decades, a non-exhaustive overview of which can be found in Ollis et al. (2015) and in Grenfell et al. (2019). According to Sieben et al. (2018), palustrine wetland classification is either based on conceptual models (top-down approach) or on statistical analysis of field data regarding soils and biota (bottom-up approach). The most common top-down classification is based on hydro-geomorphic features (Ollis et al., 2015), as the flow of water through a wetland and the shape of the basin where it accumulates are accepted key drivers of wetland form and function (Finlayson and van der Falk, 1995). According to the classification scheme of Ollis et al. (2013) which is based on the pioneering work of Kotze et al. (1994), the Namulonge wetland can be classified as a channelled valley bottom wetland. These are defined as "mostly flat wetland areas located along a valley floor often connected to an […] adjoining river […] with a small river channel running through it" (p. 23). In their classification scheme, Grenfell et al. (2019) also include genetic factors, which focus on the mode of wetland formation, as they drive wetland hydro(geo)logy. Following this classification the Namulonge wetland could be further characterised as an alluvial valley bottom wetland, as Burghof (2017) found the valley sediments to be primarily of alluvial origin. Several local names for this type of wetland exist in Sub-Saharan Africa, such as *bas-fonds* (West Africa), *vleis* (South Africa), *mbugas* or *dambos* (South and East Africa), with *dambos* being most frequently referred to in literature (Rodenburg, 2013). These swampy depression are the primary drainage system of the Precambrian basement complex (Giertz et al., 2006) and are characterised by permanent or seasonal flooding regimes (Sakané et al., 2011). According to Acres et al. (1985) dambos are usually associated with granite or metamorphic rocks of the basement complex and can be found in Uganda. They are defined as seasonally waterlogged tropical and subtropical wetlands (von der Heyden, 2004) and might contain a river channel which can be considered the first stage of *dambo* destruction (McFarlane, 1992). Hence, the Namulonge wetland might also be considered a *dambo*-like wetland.

According to Windmeijer and Andriesse (1993), valley bottom wetlands comprise a toposequence in which each element is characterised by a different hydrological regime. These include the pluvial regime at the upper and middle slopes, the phreatic conditions at the wetland fringe and the fluxial regime at the valley bottoms (see Figure 2). Key parameters like the soil type and water availability are closely related to the location within this toposequence.

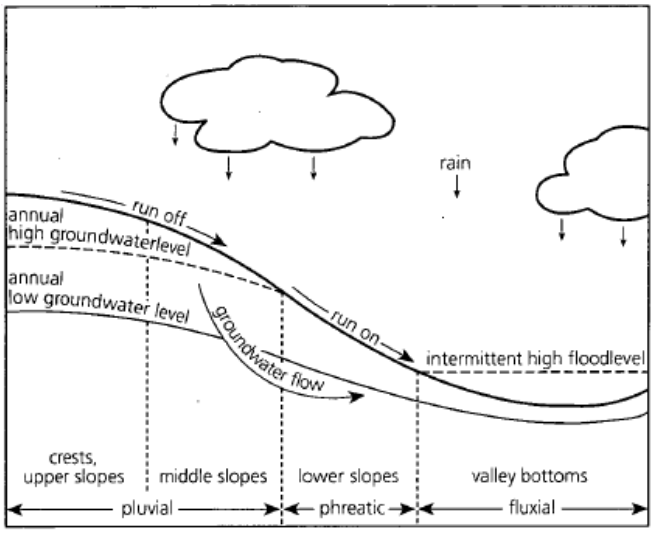

Figure 2 *Landscape elements and hydrological regimes along the toposequence of a valley bottom wetland (Windmeijer and Andriesse, 1993)*

In their review study on *dambo* hydrology, Bullock (1992) identified four major sources of water. These include direct precipitation on the *dambo* surface, subsurface throughflow from the valley slopes, overland flow from the slopes and overbank flow from the valley channel. Yet, other authors argue that upwelling deep groundwater can also contribute to water in the wetland, i.e. (McCartney and Neal, 1999; McFarlane, 1992). Studies trying to identify the major contributors to *dambo* water came up with very different results, identifying either surface runoff (Braun et al., 2002; McCartney, 2000) or subsurface flow (McFarlane, 1992) as the main source of water supply to the wetland. Subsurface movement of water from the slopes depends on the hydraulic gradient, the hydraulic conductivity and the thickness of the water carrying layer. Processes related to the interflow component of lateral flow are further described in chapter 2.2.1. In addition, vegetation and cultivation also strongly influence the water balance of the wetland, as under natural vegetation little surface runoff and instead higher infiltration, and percolation are expected (Windmeijer and Andriesse, 1993). In *dambo*-like wetlands waterlogged conditions in the wetland are related to the presence of a (semi)impermeable clay layer close to the soil surface at the valley bottom. The origin of this clay layer remains a matter of scientific discussion as it is closely related to the debate on the origin of the African weathering surface and the development of the valley bottom wetlands within it. The debate is centred around two models including the fluviatile formation of the wetland and the in-situ development (von der Heyden, 2004). The two models result in different connections and pathways of lateral flow from the slopes to the shallow and deep groundwater in the wetland, see Figure 3. The fluviatile model regards valley bottom wetlands as extensions of the channelled drainage network, where over time rivers have truncated the regolith profiles overlying the saprolite due

to fluvial erosion. Alluvial material was then deposited under reducing energy conditions resulting in a "fining upwards" tendency of the sediments (Boast, 1990). Within these valley sediments, lenses of different texture may be present in the form of fluvial lens deposits whose architecture is determined by the rates of subsidence and the frequency of avulsion (Nichols, 2009). Over time, a colluvial sand layer develops at the wetland fringe which is hydrologically connected to the alluvial sand deposits at the valley bottom underneath the clay layer. Thus, infiltrating surface runoff and interflow from the slopes directly recharges the groundwater in the valley sediments but does not contribute to plant available water above the clay layer (Boast, 1990). The in-situ model as introduced by McFarlane (1989) on the other hand, follows the concept of etchplanation: differential weathering of the basement complex parent material especially at zones of geological faults leads to the local collapse of the material and initiates the formation of lowlands. The groundwater welling up in these lowlands contains dissolved minerals from the weathered slopes which precipitate during evaporation and cause the neo-formation of clay minerals, which continuously formed the characteristic clay layer. Over time, the water table lowers due to the further subsidence of the wetlands resulting from subsurface erosion under the clay lens. The former wetland wedges remain as paleo-dambo clays containing floats of sand. As these clays get exposed to weathering, the clay is washed out and the former sand floats remain, causing the sand accumulation flanking the contemporary wetlands. Thus, water from the slopes reaching the wetland fringe via shallow interflow or as surface runoff which infiltrates in the sandy fringe soils cannot pass the paleo-dambo clay layer and hence discharges at the wetland fringe. At the same time, positive heads in the aquifer under the wetland cause upwelling and spring formation at the fringe of the wetland or generally where the paleo-dambo clays are thin or more permeable. Chemical analysis revealed, that in the Namulonge wetland interflow from the slopes recharges the alluvial wetland aquifer in some positions only. In addition, some springs were found at the wetland fringe and thus Burghof (2017) hypothesize the Namulonge wetland to be a transitional type between the two models elaborated before.

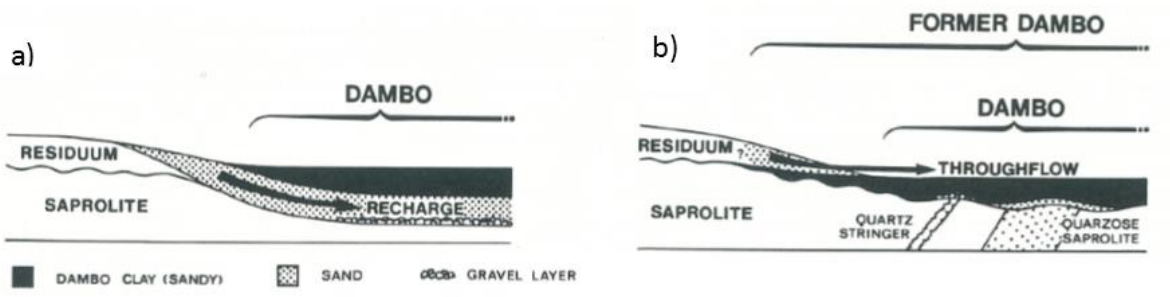

Figure 3 *Schematic cross section of a dambo showing the stratigraphy and possible implications for ground water recharge of the valley sediments following a) the fluviatile model (stripping) and b) the in-situ weathering model (etchplanation) of wetland development (modified after (McFarlane, 1992)).*

Most studies found a seepage zone at the transition from upland to wetland geology at the wetland fringe. This seepage zone is often characterised by pipe flow and small springs and was reported for valley bottom wetlands of fluviatile and in-situ weathering origin. The water at the seepage zone might be derived from upwelling groundwater(Braun et al., 2002; McFarlane, 1992) or from shallow interflow and perched aquifers in the soil or in the saprolite (McCartney and Neal, 1999; Uhlenbrook et al., 2005). These shallow

pathways were also found to be the major route of storm flow and to mainly contribute to the wetland hydrology during the wet season (McCartney, 2000). Lateral flow from the slopes via less permeable pathways commonly continues into the dry season (Bullock, 1992). Nevertheless, the hydrological connection of the slopes and the wetland is still a matter of scientific debate (von der Heyden, 2004) and most studies do not analyse water pathways at the slopes in more detail. Overall, the hydrogeology of valley bottom wetlands is characterised by a complex routing system with considerable differences in residence time and water origin (McCartney and Neal, 1999) and is highly variable between different sites (von der Heyden, 2004). So far, comparatively few studies have been conducted in Uganda (e.g., Burghof, 2017; Mahan and Brown, 2007; Taylor and Howard, 2000).

2.2 Hillslope hydrology

2.2.1 Interflow processes and characteristics

Being at the core of hillslope hydrology, research on lateral subsurface flow and hydrological connectivity has constituted an important area of hydrological research during the last decades (Beven and Germann, 1982; Flügel, 1993; Jarvis et al., 2016; Klaus and Jackson 2018; Meerveld and McDonnell, 2006a). Lately, the emergence of critical zone sciences has revealed "increasing complexities and evermore insights" (Fan et al., 2019, p. 1740) into subsurface preferential flow paths with multiple perched lateral flows. Lateral subsurface flow is known to contribute significantly to catchment runoff and to play a prominent role in the delivery of nutrients and pesticides to rivers in catchments of the tropics as well as the temperate zone (Angermann et al., 2017; Gaskin et al., 1989; Giertz et al., 2006). Nevertheless, up to today, the functioning of tropical catchments is still not well understood (Jacobs et al., 2018a).

Lateral subsurface flow, or interflow as it is referred to from here on, is commonly defined as "the portion of rainfall which infiltrates on the hillslope and percolates through the soil till it reaches a less permeable layer on which it flows under saturated and unsaturated conditions downslope, seeping either directly or via the groundwater aquifer into the river" (Flügel, 1993, p. 215). It can be divided into a quick component which follows preferential flow paths and thus causes a prompt signal in river runoff or groundwater levels in the valley bottom and a delayed component, which is mostly driven by matrix flow and can persist for longer periods of time, depending on the matrix characteristics (Kirkby, 1988). Hence, for the quick component of interflow the existence of a less permeable layer is no prerequisite, as it is bound to the existence of any kind of soil structures which enable preferential flow (see below).

The delayed component of interflow is mostly caused by equilibrium flow in the soil matrix, which means that the flow rate is driven by differences in soil water potential in the matrix (Darcy-flow). Thus, under saturated conditions flow rate and direction are mainly determined by the pore size of the matrix and the gravimetric and hydraulic potential. Under unsaturated conditions, infiltrating water is further driven by differences in the osmotic as well as the matric potential and thus antecedent moisture conditions and mineral concentrations of nearby parts of the soil profile also influence the water flow (Weil and Brady, 2017). A sudden change in the hydraulic conductivity in a sloping stratified soil causes percolating water to impede on the barrier and thereby enables the development of lateral flow towards the valley bottom. This barrier can be the result of an increased bulk density which is frequently found between organic rich and mineral soil horizons (Noguchi et al., 1999) or above a plough pan (Stange et al., 1998). Furthermore,

it can be found at the soil-bedrock interface (Jackisch et al., 2017) or it can be caused by a change in soil texture. At high soil water potentials, the presence of layers with a fine texture following a coarser layer reduces percolation as K_{sat} is significantly lower in a fine textured medium (Weil and Brady, 2017). At lower water potentials, coarse soil underlying a fine soil acts as a capillary boundary, as the matric potential in the fine soil is lower and thereby prevents water from further downward movement (Heilig et al., 2003). In the case of a sloping stratified soil, the result is a lateral diversion of percolating water and hence the initiation of interflow, a process called "capillary diversion". This process persists until saturated conditions are reached in the fine soil and hence the matric potential at the wetting front drops to near zero or becomes positive so that a "complete breakthrough" occurs and water drains freely into the coarse soil (Walter et al., 2000). Nevertheless, in their review study of 17 hillslopes Klaus and Jackson (2018) found that also on slopes which are characterised by interflow generation on top of an impeding soil layer of fine texture, a large share of water infiltrates into the impeding layer, leading to down slope travel distances of less than 30 % of the slope length.

The quick component of interflow, on the other hand, is mostly caused by non-equilibrium or preferential flow. Jarvis et al. (2016) define preferential flow as "the convergence of water flow towards preferential pathways" which is characterized by a "non-equilibrium in terms of differences in water pressure and solute concentration transvers to the flow direction". Hence, preferential flow can occur in an otherwise unsaturated matrix but also under completely saturated conditions. To date various preferential flow processes are known including fingering (Sililo and Tellam, 2000), distribution flow, (Ritsema and Dekker, 1995), funnel flow (Kung, 1990) and, most prominently, macropore flow (Noguchi et al., 1999).
According to Jarvis (2007) large pores with an equivalent diameter of > 0.3 mm allow rapid non-equilibrium flow and can hence be classified as macropores. Nevertheless, following Beven and Germann (1982) a definition of macropores by size alone is not feasible. They stress that pore structure and continuity of a pore is of equal importance for sustaining non-equilibrium channelling flow and that there is a complex relation between void geometry and flow characteristics, so that not every large void can act as a macropore in that sense. Macropores can be continuous for distances of at least several meters in both vertical and lateral direction (Nieber and Sidle, 2010) and vertical macropores can be linked to lateral macropores resulting in an extended network within the soil which is possibly linked to the soil surface (Kienzler and Naef, 2008). Beven and Germann (1982) as well as Jarvis et al. (2016) provide a broad overview of the different types of macropores and their characteristics. They differentiate between biopores which are the result of plant root activity or burrowing activities by the soil fauna, cracks and fissures which result from swelling and shrinking of clay soils or chemical weathering of the parent material, natural soils pipes which are the result of subsurface erosion and macropores caused by soil aggregation. The orientation of macropores in a steep hillslope is strongly related to the formative elements (Noguchi et al., 1999) and influences the effectiveness of lateral flow, as does the tortuosity of the macropores (Sidle et al., 2001). Water flow in macropores may be transitional or even turbulent and can be several orders of magnitude higher than in the soil matrix (Beven and Germann, 2013). Kienzler and Naef (2008) for example, found that rapid flow in large, continuous macropores reached velocities of up to 3 cm/s. Generally, the effect of preferential flow in macropores is greatest, when the hydraulic conductivity of the soil matrix is lower than the average rainfall intensity (Sidle et al., 2001).

Macropores can be activated by surface ponding of water during high intensity rainfall events (input rate > infiltration rate) or in surface depressions as otherwise entrapped air might block the water entry (Lin and Zhou, 2008). In addition, water pressures close to saturation allow water from the soil matrix to enter the macropores, even if these conditions occur in very localized spots only, e.g., due to increased infiltration resulting from stem runoff or due to impermeable structures or layers in the soil or at the soil-bedrock interface (Jarvis, 2007). In this regard, also distribution flow in the uppermost centimetres of the soil can play an important role, as it channels infiltrating rainfall and might thus cause localized saturation at the macropore interfaces even during smaller rainfall events (Ritsema and Dekker, 1995). Nevertheless, the contribution of macropores to subsurface runoff increases with saturation of the soil matrix, as under unsaturated conditions infiltrating water bypasses macropores in large part (Sidle et al., 2001). Therefore, several authors found antecedent moisture conditions and rainfall amount and intensity to be the main factors influencing the share of preferential flow in runoff processes (Beven and Germann, 1982; Gaskin et al., 1989; Meerveld and McDonnell, 2006a). Nevertheless, Lin and Zhou (2008) stress that preferential flow might also play a more prominent role under initially dry soil conditions due to water repellency of the soil. Macroporosity consists of various macropores networks which are separated by smaller pores and include bottleneck constrictions and “dead ends” (Luo et al., 2010; Pierret et al., 2002). Macropore networks can extend during a rain storm or over the rainy season as macropores get connected via “nodes”. These nodes can be either direct physical linkages between macropores or pockets of highly conductive material, e.g., buried organic matter or more permeable soil. The prevailing moisture conditions determine which type of node can be activated during a rainfall event, while generally the expansion of macropore networks is more effective under moist conditions. Nevertheless, activation of nodes can also occur in deep soil layers due to local saturation behind impermeable structures (Nieber and Sidle, 2010; Noguchi et al., 1999; Sidle et al., 2001). Nieber and Sidle (2010) further argue, that macropore networks should be regarded self-organizing flow systems which extend over time due to subsurface erosion. In their line of reasoning, dead ends of macropores lead to the development of very local high hydraulic pressure heads which cause the erosion and thus result in the connection of macropores in the long term. Nevertheless, the importance of self-organization of macropores remains an ongoing debate as, e.g., Beven and Germann (2013) argue that macropore networks are to a large extend constructed rather than constructal.

As mentioned above, preferential flow is not bound to macropores only. Especially in heterogeneous soils with several inclined layers of different texture preferential flow could also be caused by the combination of funnel and column flow (Kung, 1990). As most soils have some interbedded structural and textural discontinuities, e.g., due to preferential weathering of the parent material, and sloping boundaries are common this phenomenon occurs widely. Funnel flow refers to the perching and subsequent lateral runoff of infiltrating water on an inclined layer characterized by abrupt pore size discontinuities, i.e., a fine textured layer in a coarse matrix or a coarser layer in an otherwise fine textured matrix which causes capillary diversion. If the matrix at the end of the impeding layer has a coarse texture the concentrated flow can maintain its areal dimensions, water penetrates downwards as column flow. If various inclined layers of variable texture are found in a soil profile, repeated column flow phenomena occur at the edge of each layer creating a macro-tortuosity of preferential flow paths, similar to a marble run. Depending

on the extent of the macro-tortuosity and the soil texture at the edge of the impermeable layers, funnel and column flow can accelerate subsurface flow by a ratio of between 10 and 100.

Many authors report a threshold behaviour, i.e., a non-linear relationship, of interflow volumes and rainfall, as interflow volumes drastically increase once a location specific rainfall amount is reached (Meerveld and McDonnell, 2006a; Nieber and Sidle, 2010; Sidle et al., 2000; Zehe and Flühler, 2001). There are many different internal hillslope conditions that create this behaviour which are attributed to the activation of preferential flow paths under specific moisture conditions. One frequently cited mechanism is the "fill and spill hypothesis" introduced by Meerveld and McDonnell (2006b) who found a close relation between the micro-topographic relief in the bedrock surface, soil moisture and the sudden increase in interflow measured at the slope toe of the Panola Hillslope in the southern Piedmont, USA. They describe that during a rainstorm, infiltrating water impedes at the soil-bedrock interface and converges in depressions in the bedrock topography where positive pore water pressure develops. Only after this subsurface storage is satisfied water spills over the edge of the depressions and flows laterally towards the slope toe under saturated conditions in bedrock lows. A process, they describe as the analogue to depression storage in overland flow processes.

It is a pertaining field of research to what extent interflow during rainfall events, i.e., subsurface storm flow, consists of (old) pre-event and (new) event water and what the mechanisms behind subsurface mixing of water from different events are (e.g., van Stempvoort et al. 2021, Jackson et al. 2016). Kirchner (2003) summarized the problem as the "old water paradox" and the "variable chemistry of old water paradox", wondering how pre-event water can be released spontaneously during a rain storm and why its chemical signature is different from base flow water. Two conceptual models focussing on the old water component are translatory or piston flow (Hewlett and Hibbert, 1967), i.e., new water entering the saturated zone at a hill slope causes the displacement of old water at the slope toe, and secondly, the transmissivity feedback. The latter refers to the rise of a perched water table in to a surficial horizon with a higher hydraulic conductivity causing fast runoff in the upper horizon (Bishop, 1991). Translatory flow on the other hand might be caused by effects of kinematic wave propagation as suggested by Williams et al. (2002). An early explanation behind high shares of event water in the interflow is the existence of long connected macropores with a direct link to the soil surface (Beven and Germann, 1982). Currently, for most catchments in literature a mixing of event and pre-event water is assumed, while there are different conceptual approaches describing the mixing process. The general idea behind these approaches is the interaction of macropores and the soil matrix. While large continuous macropores deliver event water to deeper soil layers, the development of a perched water table, or even only local saturation, forces event water to enter the soil matrix and thereby mix with pre-event water in the matrix. Downward flow of this mixed water can then occur via the matrix as well as via macro pores in the saturated parts of the soil, a process called "indirect feeding". The share of pre-event water in the interflow thus depends on the spatial extend of these saturated zones (Aulenbach et al., 2021; Kienzler and Naef, 2008; Klaus et al. 2013; McDonnell, 1990). This also determines the chemistry of the interflow, as different parts of the hillslope at a larger scale and of the soil body at a smaller scale contribute to subsurface storm flow under different rainfall conditions and depending on the soil moisture status (Ali et al. 2010; Kirchner, 2003; Klaus and McDonnell, 2013).

Many hydrological studies from sub-Saharan Africa reveal that interflow was the prevailing process along the slopes and can be an important contributor to stream flow in tropical catchments (Bonell, 2005; Giertz et al., 2006; Idrissou, 2020). The processes involved in the formation of the quick as well as the delayed component of interflow described above were also reported for tropical regions. Kahl et al. (2007) for example describe that with higher antecedent moisture contents more preferential flow paths were activated upon further wetting and describe the presence of long preferential flow paths. Wenninger et al. (2008) found interflow in temporarily perched water tables in the soil as well as at the soil-bedrock interface, where a fill-and-spill mechanisms was active. In regions with petroplinthite formation, interflow was frequently found on top of the petroplinthic horizon (Op de Hipt, 2017). Chilton and Foster (1995a) described a quick interflow component within the soil body above the saprolite and a slower component of interflow within the saprolite. Yet, only few studies exist on interflow processes within the saprolite as well as at the soil-saprolite interface.

2.2.2 Surface runoff

Surface runoff is a fraction of the total rainfall which is determined by the runoff coefficient. The runoff coefficient depends on the rainfall characteristics, i.e., rainfall amount, intensity and duration, the vegetation, the infiltration capacity of the soil and thus the soil texture and structure as well as the degree of saturation. Because of the variability of these factors, the runoff coefficients may range from almost 0 % to 100 % for different parts of the slope and during different stages of the rainfall event as well as during different seasons (Windmeijer and Andriesse, 1993). Generally, two generic types of runoff can be differentiated. While saturation excess runoff describes surface runoff which is generated on saturated soils (Dunne and Black, 1970a, 1970b), infiltration excess runoff develops when the water supply rate exceeds the infiltration capacity of a given soil (Horton, 1933). The two processes are non-exclusive and can occur simultaneously during a single rain storm, but are more likely to occur under certain climatic and geomorphic conditions (Nash et al., 2002). Saturation excess runoff is mostly related to subsurface discontinuities, i.e., impermeable layers in the soil body, which prevent or slow down percolation to the groundwater (Needelman, 2002). The infiltration capacity of the soil on the other hand, depends on the soil texture and the presence of macropores, the degree of siltation at the soil surface as well as the pre-event soil moisture conditions. Following the classic infiltration theory, the infiltration capacity changes during water application; it declines sharply at first due to high potential differences in the soil and then tends to level off and remains fairly constant thereafter as it approaches the field saturated conductivity (K_{fs}) (Weil and Brady, 2017). While infiltration excess runoff contains moistly rainwater, saturation runoff is composed of rain as well as soil water due to exfiltration processes (Nash et al., 2002).

2.3 Nitrogen dynamics in (tropical) soils

2.3.1 The nitrogen cycle and nitrogen transformation processes in soils

In the global nitrogen cycle, nitrogen occurs in many valence states and in all three phases of matter (gaseous, liquid and solid) as it undergoes various transformation processes. Here, only the main processes of nitrate transformation and relocation in the soil are depicted. As organic matter decays, microorganisms break down large insoluble N-containing organic molecules into CO_2 and lower-molecular carbon compounds as well as in amino compounds or amino-groups. During the enzymatic process of N mineralization, these units are first hydrolysed and nitrogen is released as ammonium ions (NH_4^+) in the

process of ammonification. Being a hydrolysis, this process requires the presence of water, but not necessarily of oxygen. The ammonium ions are either taken up directly by plants, are adsorbed to colloidal surfaces, or remain in the soil solution. In a second step, ammonium can be oxidized to nitrate (NO_3) in the two-step process of nitrification. Both, ammonium and nitrate might then be immobilized again as they can be absorbed and incorporated into the cellular components of microorganisms or growing plants, contributing to the synthesis of amino acids, proteins, enzymes, chlorophyll and secondary metabolites. Both processes (N mineralization and N absorption) occur simultaneously in the soil and are driven by the activity of aerobic microorganisms. Whether the net effect is an increase or decrease in mineral N content in the soil solution depends on the C/N ratio in the organic components undergoing decomposition (N supply) and the absorption of N by growing vegetation (N demand). Nitrate in the soil solution can further be translocated and finally be lost from the soil by leaching as it cannot be adsorbed to the negatively charged soil colloids. Under anaerobic conditions, nitrate might further be converted to gaseous forms of dinitrogen-oxide (N_2O) and eventually dinitrogen gas (N_2) in a series of widely occurring reduction reactions by facultative anaerobic bacteria (anaerobic respiration), a process termed denitrification (Weil and Brady, 2017).

The fate of nitrogen in soils depends on the environmental conditions. As soil microorganisms are eventually responsible for the mineralisation of detritus, soil conditions which are favourable for the activity of microorganisms generally enhance mineralisation rates. The most important factors in this regard are oxygen supply, soil temperature and soil moisture content (Zech et al., 1997). Microorganisms thrive under warm conditions with an optimum at about 30-35 °C in tropical soils (Sahrawat, 2008). Nevertheless, Sierra (2002) found that nitrate mineralisation in the tropics is increased when the soil is exposed to temperature fluctuations. Oxygen supply is crucial, as most microorganisms involved in carbon mineralisation and those associated with ammonium oxidation or nitrification depend on the presence of O_2 for respiration. Therefore, mineralisation of organic matter is inhibited or reduced under anaerobic conditions due to high levels of soil moisture or in strongly aggregated soils (Robertson and Groffman, 2015). As microbes are aquatic organisms, they depend on a certain level of soil moisture to conduct mineralisation. Both ammonification and nitrification proceed at their maximal rates near 50-60 % water-filled pore space (Weil and Brady, 2017). In addition, the availability as well as the quality of the organic material to be decomposed is responsible for the amount of plant available nitrogen in the soil solution. The C/N ratio of the plant material limits the availability of plant available nitrogen in the soil. In case the input material shows a wide C/N ratio, microorganisms will scavenge mineral nitrogen from the soil solution and accumulate it in their body cells. It is then only after the death of the microorganisms that during the mineralisation of their body cells nitrogen is released to the soil solution (Robertson, 1989; Robertson and Groffman, 2015).

While ammonification and nitrification are generally enhanced by similar environmental conditions, nitrifying bacteria are more sensitive than the broad group of heterotrophic organisms responsible for ammonification. The strongest factor limiting nitrification is the availability of oxygen, as all nitrifiers are aerobic organisms. Excess ammonium can be toxic to nitrifiers and cold temperatures as well as the protection of organic compounds in intercolloid pores of smectites and allophane clays slow down nitrification rates (Weil and Brady, 2017). Some authors state that low pH values are thought to slow down

nitrification rates (Sahrawat, 2008; Zech et al., 1997), as culturable nitrifiers exhibit an optimum at pH 7-8 (Prosser, 2011). At present, results from various field studies suggest that the soil pH value does not impact nitrification rates directly (Bertrand et al., 2007; Prosser, 2011; Robertson, 1989; Robertson and Groffman, 2015).

2.3.2 Nitrogen mineralisation after dry periods

Nitrogen mineralization is increased by alternate cycles of drying and wetting of the soil, an effect first described by (Birch, 1960, 1958) and hence referred to as the "Birch effect". This effect is especially important in tropical and subtropical regions with pronounced wet and dry seasons (Borken and Matzner, 2009). On the basis of experiments on agricultural plots in East Africa in the 1950s and 1960s, Birch showed that cycles of drying and wetting of soils, like the re-wetting of the soil with the onset of the rains after a prolonged dry period, stimulate the mineralization of organic matter, leading to the release of mineral nitrogen and the loss of soil organic carbon (Jarvis, 2007). More recently, Dick et al. (2001) confirmed the significance of the Birch effect in agro-forestry systems in Uganda and Yameogo et al. (2021) in upland agriculture in Burkina Faso, while other authors (Asante et al., 2017; Becker et al., 2007; Bognonkpe and Becker, 2009) stressed the importance of drying and wetting cycles for nitrogen mineralisation and mineral N contribution to wetland rice production in Western Africa.

In his experiments, Birch found that the rate of nitrogen mineralization is significantly increased upon rewetting of dry soil. Hereby, the mineralisation rate is highest during the hours following a rainfall event and then gradually declines again. In the years to follow, several explanations for this effect were found through laboratory and field experiments. During dry periods, microbes die or fall into a dormant stage so that the decomposition of organic matter comes to hold (Voroney, 2007). Upon rewetting, several non-exclusive processes take place. On the one hand, the dead tissue of the microbes is quickly decomposed and nutrients are released (Schimel et al., 2007). Surviving microbes and fungi show a hypo-osmotic stress response, releasing some of the cytoplasmic solutes accumulated during the dry period to equilibrate the sudden water uptake (Halverson et al., 2000). In addition, there is a rapid increase in microbial bio mass and fungal hyphae (Scheu and Parkinson, 1994). On the other hand, shrinking of the soil has exposed new sources of organic matter which were protected inside soil aggregates (Denef et al., 2001). Furthermore, due to the higher soil moisture content diffusion of organic material to the microorganisms resumes (Stark and Firestone, 1995). During remittent wetting and drying, the effect is attenuated from cycle to cycle, as less organic material is available for mineralisation (Birch, 1958) and a shift in the bacterial community composition occurs (Fierer et al., 2003). There is an ongoing discussion on the effect of the intensity and duration of the drying period on the increase of the mineralisation rate. While Birch (1960) states that more severe drying intensifies the mineralisation upon rewetting, e.g., Hentschel et al. (2007) and Schimel et al. (1999) found the opposite to be true. Another question arises around the net effect of drying and wetting cycles on the mineralisation of nitrogen. In their review study, Borken and Matzner (2009) found no consensus on whether the Birch effect causes a net increase in mineralisation, no change or even a decrease as compared to permanently moist conditions. Yet, they found that in most studies which reported a net increase in mineralisation the length of the wetting season exceeded that of the dry spell. In case of an increase in net-mineralisation, the Birch effect can imply a fertilizing effect for crops, especially in small scale farming, where no or little industrial fertilizer is applied (Becker et al., 2007).

Nevertheless, with increasing soil moisture, nitrate can then get lost via denitrification and leaching, especially if the plant cover is not yet well established. Hence, in regions which are characterised by pronounced dry and wet seasons, a typical development of the nitrogen content in the soil can be observed: During the dry to wet transition period (DWT), the nitrogen content in the soil solution increases rapidly during several cycles of drying and rewetting and nitrogen accumulates in the soil. Subsequent water saturation at the end of the DWT then leads to severe leaching and denitrification and thus a decline of mineral nitrogen in the soil (George et al., 1993). Therefore, an adapted crop management, which aims at using the available nitrogen resources at the end of the DWT and thus limits nutrient losses can improve the productivity and thus contribute to food security in the global South. In undulating landscapes characterised by crop production in the upland as well as in the wetland, this might include a land scape approach. Here, nitrate lost from the upland areas by leaching is frequently transported via interflow to the fringe of the wetland, where it might significantly increase the nitrogen content of the soil at the end of the DWT, but is lost during the anaerobic conditions of the following wet season. In this setting the conservation of native soil N by, e.g., the cultivation of a "nitrate catch crop" (George et al., 1994) in the wetland, can significantly increase, e.g., rice yields (Yameogo et al., 2021).

2.3.3 Nitrate losses

Denitrification

Nitrate can be reduced to gaseous forms (mainly N_2O and N_2, but also NO) in a series of biochemical reactions termed denitrification (Weil and Brady, 2017). When the oxygen level of a soil is low, denitrifying bacteria as well as certain fungi and archaea use the nitrate-nitrogen as terminal electron acceptor during anaerobic respiration. As most denitrifying organisms are heterotrophs, the presence of energy-rich carbon sources is necessary for denitrification to take place. In addition, at least 60 % of the soil's pore space should be water saturated, inducing a redox potential of less than 400 mV. Increasing levels of saturation and further lowering of the redox potential lead to higher denitrification rates and concomitant N losses as most denitrifying organisms are facultative anaerobs and will prefer oxygen over nitrogen as terminal electron receptor. Thereby anaerobic conditions within soil aggregates can cause denitrification even when the soil body is not water saturated. The end product of denitrification is di-nitrogen gas (N_2). Nevertheless, nitric oxide gas (NO) as well as nitrous oxide gas (N_2O) are released during intermittent steps in the reduction reaction, with N_2O being one of the main agriculture-related climate-relevant trace gases. Hereby, soil temperature, the level of saturation and the pH of the soil determine the velocity of the reactions and thus the proportion of the three main gaseous products to be released. Generally, N_2 is more likely to be released when oxygen levels are very low, while fluctuations in the aeration status of the soil as well as high acidity favour the release of N_2O (Robertson and Groffman, 2015).

Leaching

Nitrate leaching occurs when the accumulation of NO_3 in the soil coincides or is followed by a period of high drainage of the soil profile (Di and Cameron, 2002). Due to its negative charge nitrate is not adsorbed to the negatively charged soil colloids that dominate most soils. Thus it is easily translocated by water fluxes and finally leached from the soil profile (Weil and Brady, 2017). It is only in some tropical soils which are characterised by positively charged mostly gibbsite or protonated kaolinite clay minerals that nitrate can be adsorbed and held against leaching (Wild, 1972; Wong et al., 1990). Otherwise, the amount, the

timing and the controlling conditions for nitrate loss via leaching are directly related to the amount of water available for nutrient transport (Sharma and Chaubey, 2017) as well as the characteristics of water movement in the soil (vertical movement) and at the hillslope scale (lateral movement). Unless nitrate is leached to the groundwater, its lateral transport occurs via interflow (Nash et al., 2002). The major processes involved in interflow formation and transmission at a hillslope were described in chapter 2.2.1. Generally, nitrate leaching of in-situ mineralised nitrate is increased when the contact time of the infiltrating rainfall and the soil is extended (Rusjan et al., 2008). High moisture levels during longer time spans allow the diffusion of nitrate following the concentrations gradient towards bigger pores where it can then easily be transported towards the slope toe (Mathers et al., 2007; Wild, 1972). A detailed description of the mechanics of the transport of chemicals through the soil can be found in Jury and Flühler (1992). Nevertheless, a very low saturated conductivity of fine textured soil can slow down nitrate transport and increase denitrification losses (Di and Cameron, 2002). Interflow processes which involve the entire soil matrix are more efficient regarding leaching of in-situ mineralised nitrate than rapid preferential flow through macropores (Creed and Band, 1998; Weiler and McDonnell, 2006). Hence, rainfall events of high intensity which are often related to preferential flow via macropores are less effective regarding leaching of in-situ mineralised nitrate than rainfall events causing the saturation of the soil body and hence the washout of nitrate from the extended network of smaller pores (Wild, 1972). In this context, several authors explain the flushing of nitrate after periods of nitrate accumulation (e.g., during drought) as the result of the rise of a perched water table into the topsoil from where it drains via near-surface preferential flow paths, a process called “transmissivity feedback” (Burns, 2005; Creed and Band, 1998; Jiang et al., 2010). Weiler and McDonnell (2006) found that the topography of a hillslope plays a pivotal role in the mobilisation of nitrate, as the slope toe of concave hillslopes experiences saturated conditions more frequently and is thus more likely to be subject to transmissivity feedback flushing processes. In the absence of surface-near perched water tables or at straight or convex hillslopes, nitrate might leach to deeper flow pathways (McHale et al., 2002) which can be considered “transient”, i.e., nitrate appears in the stream months later or “permanent”, i.e., nitrate reappears in the stream years later (Cirmo and McDonnell, 1997). Nevertheless, interflow pathways along the slope might have different characteristics at various positions and can be activated at different times in the course of a rainfall event or under specific rainfall conditions, as mirrored in the variable source area concept (McGlynn and McDonnell, 2003).

The situation is different in case of superficial fertilizer application (Smaling and Bouma, 1992; Sugita and Nakane, 2007) or when nitrogen input via rainfall is high (Hill et al., 1999). In this case rapid preferential flow via macropores leads to quick and efficient leaching of nitrate and thus high nitrate losses from the upslope areas.

As nitrate leaching is strongly linked to interflow processes, a thorough understanding of the prevailing interflow mechanisms at a hillslope and at catchment scale and of how environmental conditions influence these processes is crucial to predict nitrate losses from upland areas and implement adequate management strategies (Mathers et al., 2007). Nevertheless, leaching is a function of all the complex factors affecting the sources, transport and transformations of nitrogen (Jiang et al., 2012). Especially when focussing on the input of leached nitrate into downslope (agro)ecosystems, it has to be considered

that N input is often supply limited (Sharma and Chaubey, 2017), particularly during periods of high nutrient demand by plants but also after long periods of high soil moisture and thus high leaching losses or when nitrate is lost from the soil due to denitrification (Jiang et al., 2012).

Surface runoff

When the infiltration of rainfall into the soil is limited and thus surface runoff is generated, nitrate remaining on or close to the surface may be translocated by surface runoff. Hereby, the depth of the interaction zone of surface runoff and the soil is mostly limited to 2 - 6 cm (Elrashidi et al., 2005), but depths of up to 10 cm can also be assumed (Elrashidi et al., 2005; Lal, 1976). Some authors state that nitrate transport via surface runoff is nominal compared to nitrate transport via subsurface flow (Drury et al., 1993; Sharma and Chaubey, 2017). Yet, others found that when the amount of surface runoff is increased on the expense of subsurface flow in less permeable soils or due to agricultural practices more nitrate was transported via surface runoff (Woodley et al., 2018). According to Kleinman et al. (2006) the combination of transport and source factors determines how much nitrate is transported. While transport factors control runoff generation, source factors control the nutrient availability in the soil. Nevertheless, transport factors are more important regarding the nitrate load (Kleinman et al., 2006; Woodley et al., 2018). Higher nitrate loads were detected in saturation excess runoff than in infiltration excess runoff, as water rich in nitrate dwelled up to the soil surface instead of infiltrating into the soil (Kleinman et al., 2006; Zheng et al., 2004). This is in line with Kleinman's description of a negative correlation on rainfall intensity and nitrate concentration in the surface runoff, as during infiltration excess conditions nitrate is diluted by the rain water.

2.3.4 Fate of nitrogen in wetland environments

In wetland environments, nitrogen can be found in many oxidation states. An overview of which and the related processes is shown in Figure 4. Nitrogen transformations in wetland soils are strongly related to the soil aeration status in the different soil layers and nitrogen availability is directly linked to water fluxes in and out of the wetland system. Nitrogen input is caused by the biological fixation of atmospheric N_2 by bacteria, cyanobacteria or actinobacteria, free-living or in symbiosis with plants, by the (microbial) mineralisation of organic matter or by nitrate input by flowing water either from the slopes or during inundation originating from stream runoff, as well as following the application of N-containing fertilizers. While ammonification potentially takes place in the entire soil body, nitrification is limited to the oxidized layer of the wetland soils and the oxidized rhizosphere. In the reduced layer nitrate is subject to dissimilatory nitrogenous oxide reductions, including denitrification and reduction to ammonia (DNRA), while ammonium is lost from the soil during the process of ANNAMOX (anaerobic ammonium oxidation). Besides these transformation processes, nitrate can also be translocated in or even lost from the wetland due to leaching with surface water flows. Hence the hydroperiod of a wetland has a strong influence on nitrogen transformations, nutrient availability to plants and nitrogen losses (Mitsch and Gosselink, 2015).

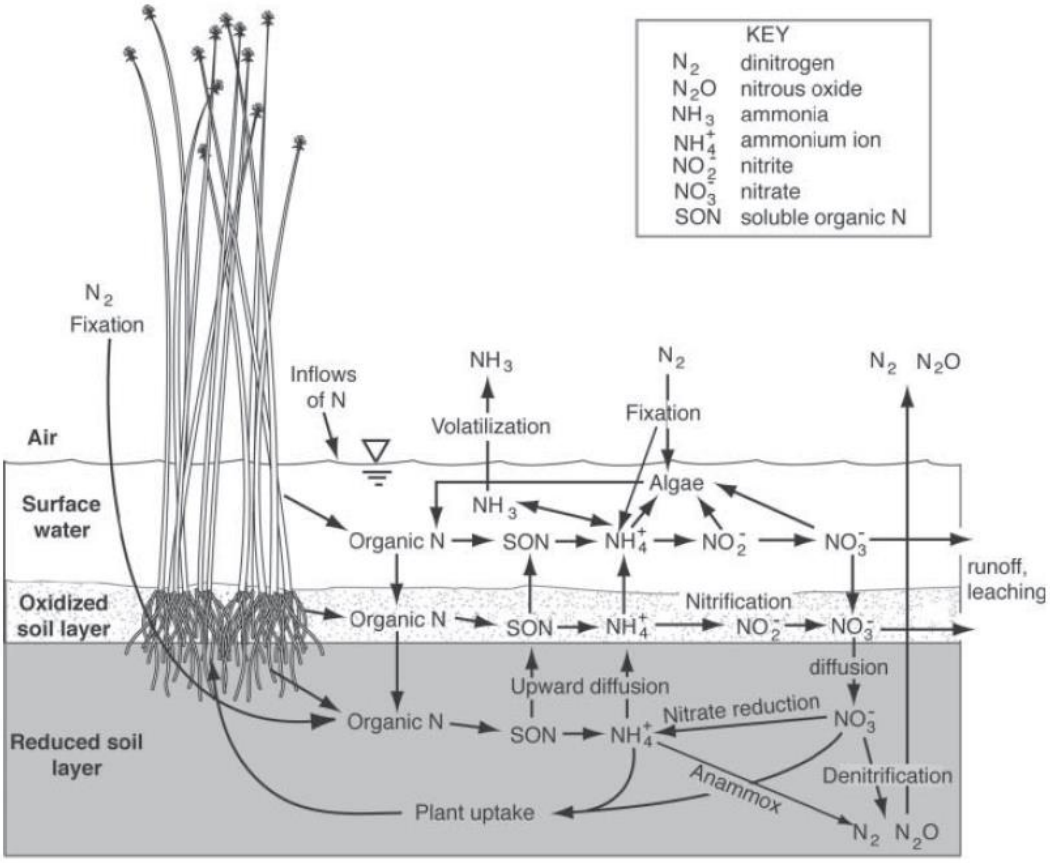

Figure 4 *Transformations and fade of nitrogen in various oxidation states in a flooded wetland environment. Graph by William J. Mitsch and Gosselink (2015).*

To conclude. nitrogen transformations and spatial fluxes are highly dynamic, with nitrate formation (nitrification), its vertical and horizontal translocation along slopes and within wetlands (nitrate leaching) and its microbial reduction by anaerobic respiration (denitrification) being the dominating processes, all of which are closely related to soil hydrology. Thus, large nitrate accumulation rates and subsequent translocations and losses could potentially be expected at the onset of the rainy season in the inland valley landscape and under the seasonally wet climate of Uganda.

2.4 Weathering profiles over crystalline rocks

Most crystalline rocks in Uganda as well as in large parts of Sub-Saharan Africa are covered by a thick weathering profile (Taylor and Howard, 1996, see Figure 5). These profiles generally develop under stable geodynamic condition, where erosion is not the dominant process and in a hydrolysing climate (Dewandel et al., 2006). In East Africa, Precambrian rock formations of the basement complex have been exposed to intense weathering under conditions of high temperatures and high rainfall amounts over a very long time span (Westerhof et al., 2014). The infiltrating acidic rainfall reacted with the alkaline minerals and leached the more soluble and mobile components. At the same time kaolinites and Fe-Al oxides were formed unless under extreme weathering conditions kaolinite dissolution occurred and only quartz sand was left (Chilton and Foster, 1995a). This process of deep weathering or etching ultimately resulted in profiles of alteration products of several tens of metres of depth (Wyns et al., 1999), which follow the paleo-

topography (Taylor and Howard, 2000). Geological features like faults and dykes or contrasts in rock mineralogy or structure locally modified the characteristics of the weathering profile and led to differential weathering and variable weathering products (Taylor and Howard, 1998). While aluminous schists create a clayey lithology, weathering products of granites are sandier. Within the unconsolidated weathering profile hence variable porosity and permeability persist depending on the mineralogy and texture of the parent rock and the advance of the weathering process (Wyns et al., 2004, 1999). Generally, the lithological sequence above crystalline basement rocks can be distinguished by the physical, chemical, mineralogical, geodynamical and paleo-morphological features (Dewandel et al., 2006). Several zonal groupings for the weathering zone above crystalline rocks in tropical conditions have been suggested (Chilton and Foster, 1995a; Koita et al., 2013; Taylor and Howard, 2000; Wright, 1992). For the Namulonge wetland Burghof (2017) found the zonal grouping introduced by Chilton and Foster (1995a) to be the most representative of the local conditions. Within the weathering body they distinguish the residual soil, the saprolite, a zone of basal breccia and the saprock which overly the crystalline bedrock. The residual soil developed from the saprolite through soil-forming chemical, physical and biological processes. In this work, it will be just referred to as 'soil'. The saprolite, which is the result of the deep weathering processes described before, can be further divided into an upper and a lower part. The upper part is characterised by a higher share of kaolinites, while the lower part has a greater abundance of primary minerals and intermediate weathering products, as the weathering front advances downwards. Therefore, a higher hydraulic permeability is usually found in the lower saprolite while preferential flow is likely to be active in the upper part (see Figure 5). Many authors (e.g., Chilton and Foster, 1995a; Koita et al., 2013; Wright, 1992) found the top of the fractured saprock and the base of the saprolite to hold the most important aquifers for water supply in large parts of Sub-Saharan Africa. In addition, also smaller, perched aquifers may develop within the saprolite (Wenninger et al., 2008).

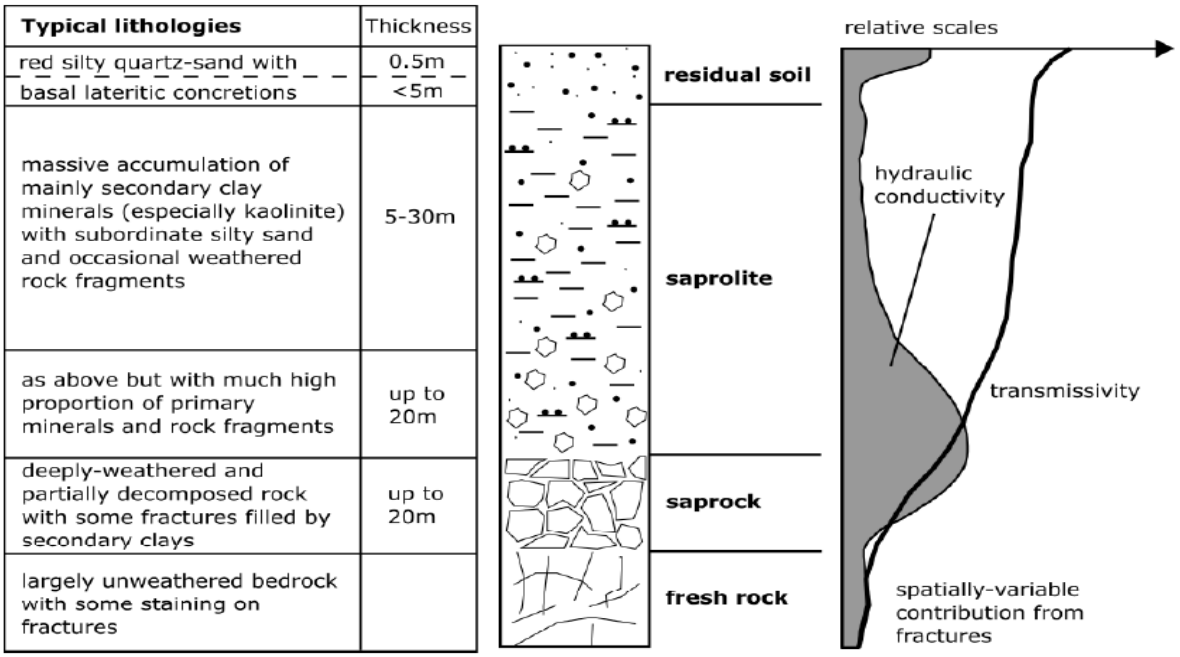

Figure 5 *Typical weathering profile of crystalline rocks in tropical Africa and related hydrogeological properties (modified after Burghof, 2017; Chilton and Foster, 1995a).*

3 Study area

The Namulonge study site is located in the Wakiso district north of Kampala in Central Uganda at around 0.5°N and 33°E and at an altitude of 1100 to 1300 masl. The central field trials of the GlobE-wetlands project as well as the research area of this study are located in the Namulonge inland valley, which is the main valley of the Nasirye catchment and hence situated in the headwater catchment of the Lake Kyoga basin. The Nasirye catchment comprises an area of 33.2 km² (earthexplorer.usgs.gov) of which 4.5 km² are occupied by a valley bottom wetland extending in north-eastern direction (Gabiri, 2018). The physical attributes of the study area are described in the following chapter.

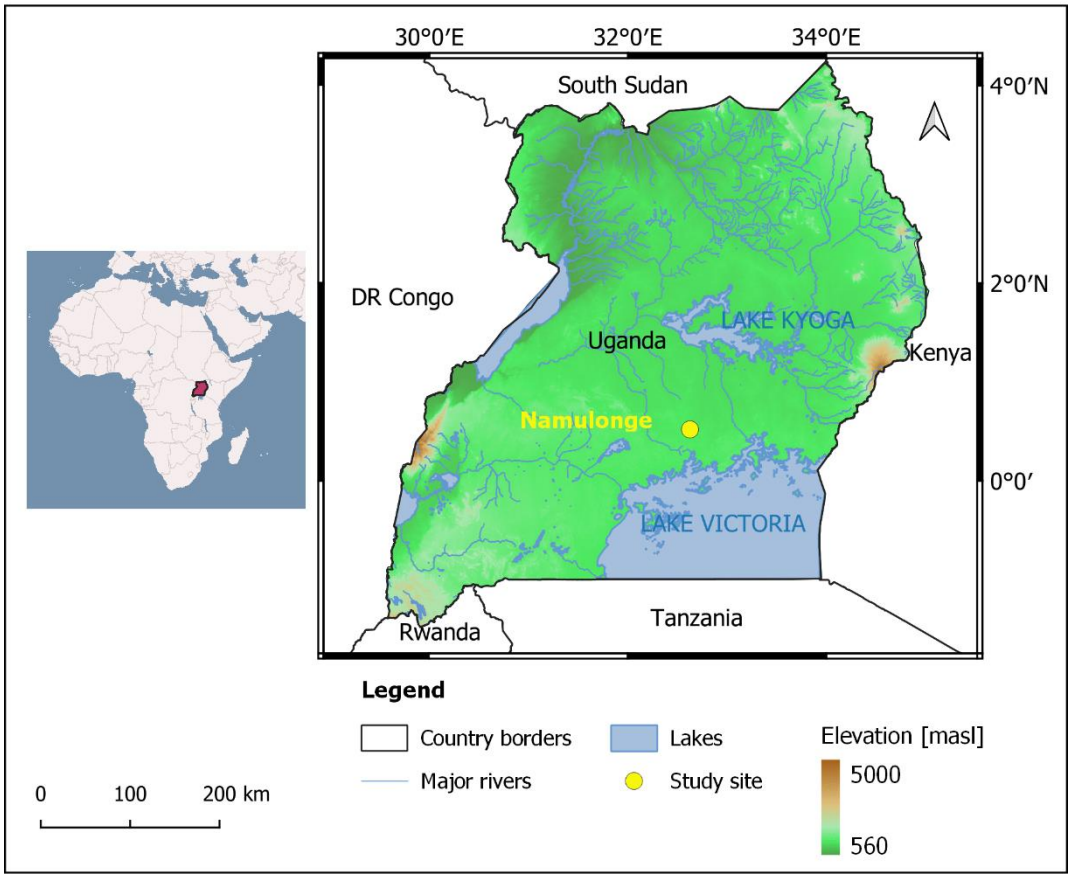

Figure 6 *Topographic map of Uganda and the position of the Namulonge study site. Data sources: elevation (Jarvis et al., 2008), country borders (gadm.org), base map Africa (http://vmap0.tiles.osgeo.org/wms/vmap0), lakes and rivers (NAVTEQ 2011).*

3.1 Climate

According to the updated Köppen-Geiger classification (Peel et al, 2007), the climate at the study site can be classified as tropical savannah climate (Aw). Due to its location near the equator, the climatic conditions are strongly influenced by the annual migration of the Inter-Tropical Convergence Zone (ITCZ) and are thus characterized by a bi-modal distribution of rainfall and moderately high temperatures throughout the year (Nsubuga et al. 2011). As Nicholson (2017) points out, the climate in East Africa is highly complex and driven by several teleconnections as well as the influence of prominent topographical features and large inland lakes. In Central Uganda, the moisture for precipitation is mainly generated over

the Indian ocean and moisture transport to the region is driven by the monsoonal wind system. Nevertheless, lake Victoria, also has a significant influence on the space-time patterns of rainfall and temperature (Ogallo, 1993). In the bi-modal annual cycle of rainfall, the *long rains* last from March to May and are characterised by high rainfall amounts and intensities, while the *short rains* from October to December tend to be more variable. Generally, rainfall variability in East Africa is driven by three low-level circulation systems over the Indian ocean, including the Findlater Jet, the Mascarene High and the Arabian High (Vizy and Cook, 2020). Nevertheless, on shorter timescales also ENSO can significantly influence rainfall amounts in East Africa. In Central Uganda, as in other East African locations which are characterised by a bi-modal rainfall distribution, this mostly affects the short rains. While the El Niño phenomenon causes enhanced rainfall during this period, rainfall is depressed in La Niña years (Phillips and McIntyre, 2000). At the Namulonge study site, the total mean annual rainfall amounts to 1170 mm (Nsubuga et al., 2011), and the transition from dry to rainy season is generally not clearly pronounced. Due to the proximity to lake Victoria, intermittent rainfall events also occur during the dry periods. The average temperature is about 22°C with highest values in February and lowest values in July (Nsubuga et al., 2011), (see Figure 3).

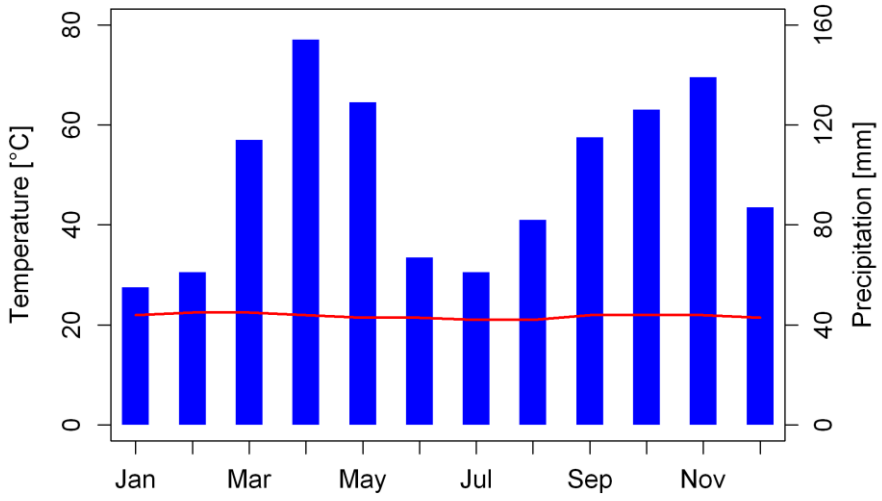

Figure 7 *Climate diagram of the Namulonge research station (NaCRRI) showing long-term average monthly temperature (red line) and precipitation (blue bars) based on the data reported by Nsubuga et al. (2011).*

3.2 Geology

The geology of the Namulonge study site is characterised by Archean rocks from the so-called basement complex as well as by crystalline rocks of Proterozoic age from the Buganda-Toro system (Westerhof et al., 2014), as it is situated at the boundary between the two systems (see Figure 8). Rocks from the basement complex are distributed in small patches over the study site and can be assigned to the Kampala Suite, which comprises Kampala granitoids and orthogneisses (A3KAgr) (GTK consortium, 2012). The Buganda Toro-System is represented by orthoquarzites and conglomerates (P1BVqc) of the Victoria Formation as well as slates, shales and phyllites (P1BNsh) of the Nile Formation (GTK consortium, 2012, Schlüter 1997). Regionally increased metamorphism led to the formation of porphyroblastic phyllites which comprise about 50 % muscovite that locally appears as coarse flakes (Westerhof et al., 2014).

Nevertheless, following geochemical analysis of single drilling logs at the Namulonge study site, Burghof (2017) points to a high uncertainty of the lithologies in the geological map.

As most crystalline rocks in Uganda (Taylor and Howard, 1996), the rocks in the study site are overlain by a thick weathering mantle. As described in chapter 2.4, the weathering mantle is the product of deep weathering, which has been the dominant process in South-Central Uganda since the Miocene (Taylor and Howard, 1998). The regional thickness of the saprolite varies between 17 m and 49 m, while the saprock was found to be up to 36 m thick (unpublished data, Uganda Ministry of Water and Environment). The upper part of the saprolite is characterised by the presence of kaolinitic clay minerals as well as sand and gravel as minor components (Burghof, 2017; Heiß, 2016, unpublished), with the angular shape of the gravel indicating the absence of transport processes of the material (Gilkes et al., 1973). The degree of weathering decreases with depth and thus the lower saprolite contains more primary minerals and its texture is dominated by the middle-sand fraction (Burghof, 2017; Heiß, 2016, unpublished). Hence, the weathering profile acts as a semi-confined aquifer, due to the lower hydraulic conductivity in the clay-rich upper saprolite and the higher conductivity in the sandy lower saprolite (Burghof 2017; Taylor and Howard 1998). Nevertheless, preferential flow paths might be present in the upper saprolite, due to root penetration and cracks or because of the presence of interconnected sand veins (Burghof 2017).

The valley bottoms are characterised by quaternary sediments (GTK consortium, 2012), which were found to be of alluvial nature (Burghof, 2017; Heiß, 2016, unpublished). According to this study, the valley sediments are comprised of interconnected sand and gravel lenses, which are interbedded with clayey deposits, while the texture shows a tendency of fining upwards. The sediments at the valley bottom are underlain by the weathering profile of crystalline rocks.

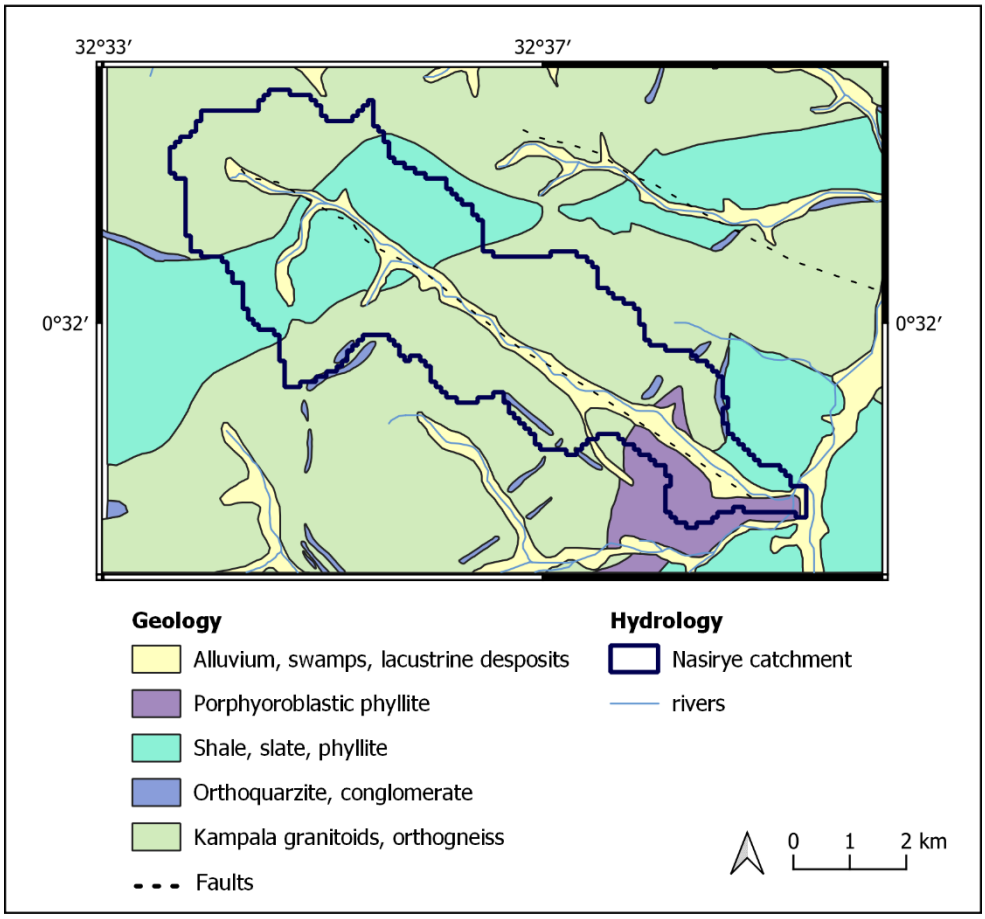

Figure 8 *Geological map of the Namulonge area. Data sources: geology and streams (GTK consortium, 2012), alluvium (Heiß, 2016, unpublished), Nasirye stream (Gabiri, 2018).*

3.3 Hydrology and hydrogeology

The Nasirye stream is situated in the Lake Kyoga basin, which is the second largest sub-catchment in Uganda, extending over an area of 57,233 km² (Government of Uganda, 2016). It drains through the Ssezibwa River into Lake Kyoga, before the water reaches Lake Albert via the Kyoga Nile. The Kyoga basin hosts the highest density and the largest total area of wetlands in Uganda. Most of these wetlands are part of a network of small, vegetated valley bottoms in an undulating landscape. This also applies to the Namulonge wetland (Nsubuga et al., 2014). Nevertheless, 42 % of the wetland area in the Lake Kyoga basin is degraded due to the increasing conversion of wetlands for subsistence cultivation of rice, sugarcane and maize (NEMA, 2019).

The main river channel in the Namulonge wetland only partly follows the local-scale topography, as it was modified for irrigation and drainage of farmer's fields in the wetland (Gabiri et al., 2018). The Nasirye stream is perennial with varying water levels. In the lower catchment, the Nasirye stream has a maximum width of 3 m and a maximum depth of 2 m (Burghof, 2017). The total annual water yield of the Nasirye catchment amounts to ~245 mm/a (Gabiri et al., 2019).

According to Burghof (2017), three ground water bodies can be identified in the valley bottom of the Namulonge wetland. The deep groundwater in the saprolite and the fractured bedrock is part of a regional

aquifer. It is semi-confined and locally connected to the groundwater body in the valley sediments via fractures. The groundwater in the valley sediments is also characterised by confined conditions with an artesian character during the rainy season, as it is separated from the shallow aquifer in the wetland soils and the subsequent vadose zone by a clay layer. This clay layer can be more permeable at some positions so that water from the aquifer in the valley sediments might get connected to the shallow groundwater in the wetland soils locally. Yet, for agricultural production in the wetland, the shallow aquifer in the wetland soil above the clay lens (0.1 - 0.7 m depth) is the most relevant component, as wetland crops usually do not penetrate that layer (McFarlane, 1992). From her geochemical analysis Burghof (2017) concluded that both, the aquifer in the valley sediments as well as the shallow aquifer and the vadose zone of the wetland soils, get recharged by lateral fluxes from the slopes.

3.4 Geomorphology and soils

As most parts of South-Central Uganda, the study site is characterised by an undulating topography with gentle, wavy slopes (Miyamoto et al., 2012) and wetlands in a network of small, vegetated valley bottoms (Nsubuga et al., 2014).

The study site is part of the Buganda surface, which is characterised by moderately deep loamy soils at the hilltops and along the side slopes, which developed in the residuum of quartzite, gneiss, schist and laterite. In some places, hardened laterite and high skeletal fractions can be found. The soils offer a moderate fertility and water holding capacity but might be affected by erosion and phosphorus fixation. Therefore, they are generally well suited for the cultivation of crops, but fertilizer application and a careful nutrient management as well as the establishment of soil erosion protection measures are recommended to increase and sustain the production potential (Yost and Eswaran, 1990). Soils in the wetland developed in alluvial material and have gleyic properties, which are the result of reoccurring water saturation. They are usually characterised by a high organic matter content in the top soil and hence a high CEC. Their fertility is governed by the prevailing hydrological conditions. While waterlogging increases the availability of phosphorus due to a rise in the soil pH, nitrogen availability can be limited due to low mineralization rates and denitrification (Windmeijer and Andriesse, 1993).

According to the Soil Atlas of Africa (Jones et al., 2013), the dominant soil type in South Central Uganda are undifferentiated Nitisols. During his detailed soil mapping campaign of the Namulonge valley, Gabiri et al. (2019) also classified the soils along the valley slopes as Eutric rhodic Nitisols, which are of colluvial character at the lower parts of the slope. At the fringe of the wetland, Eutric Gleyic Arenosols were found, while the soils in the valley bottom were classified as Eutric umbric Gleysols or Eutric Gleyic Fluvisols along the tributaries of the main stream (see Figure 9).

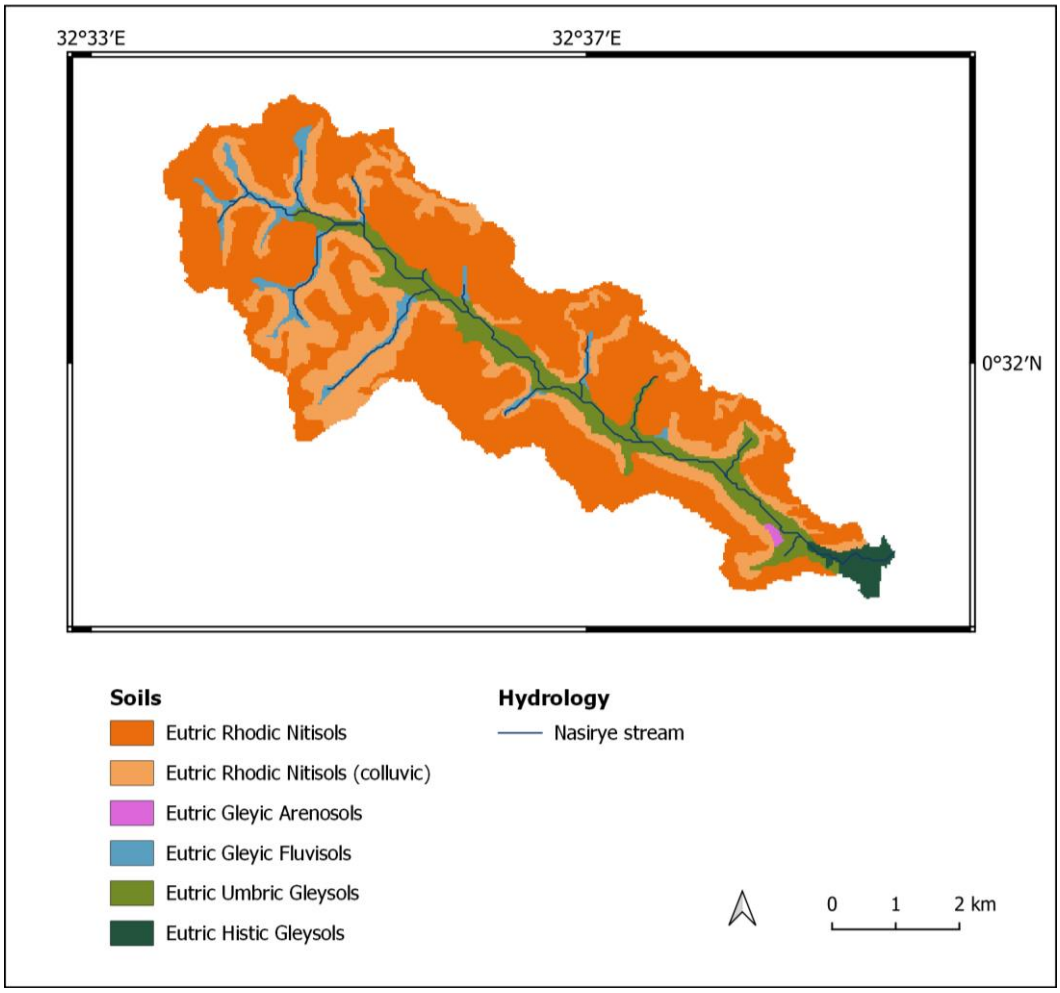

Figure 9 *Soil map of the Nasirye catchment (modified after Gabiri, 2018).*

3.5 Land use, land cover and vegetation

The Nasirye catchment belongs to the sub-humid agro-ecological zone of the Lake Victoria Crescent (Miyamoto et al., 2012). While the natural vegetation in the valley bottom wetlands is papyrus (*Cyperus papyrus*) (Denny, 1993), the potential natural vegetation in the upland areas of the Nasirye catchment is Lake Victoria drier peripheral semi-evergreen Guineo-Congolian rain forest (van Breugel et al., 2015). According to White (1983) in (van Breugel et al., 2015), semi-evergreen forests are characterised by briefly deciduous species in the canopy cover and mostly evergreen species in the understorey. In current days, only small patches of the natural vegetation can be found in the Nasirye catchment. Most of the area is cultivated by smallholder farmers or either used for the establishment of research fields by the National Crops Resources Research Institute (NaCRRI) or for grazing grounds of the National Livestock Resources Research Institute (NALIRRI). Gabiri et al. (2019) developed a land use / land cover map of the catchment (see Figure 10), which differentiates six LULC classes including agriculture, mixed forest (tropical rain forest), evergreen forest (plantations of, e.g., eucalyptus), pasture, sparsely populated urban areas and water bodies. He found that the predominant LULC classes are agriculture, covering 64.8 % of the area, mixed forests with 11.8 % and evergreen forests with 11.7 %. Due to the high share of smallholder farmers cultivating the land, LULC in the Nasirye catchment is highly fragmented and thus small patches of all LULC classes are found in close proximity throughout the entire catchment. In the agriculturally used areas,

typical upland crops like maize (*Zea mays*), beans (*Phaseolus vulgaris*) and sweet potatoes (*Ipomoea batatas*) are cultivated at the valley slopes. Main crops in the valley bottom wetland include rice (*Oryza sativa*) and taro (*Colocasia esculenta*), which are cultivated under saturated or near-saturated conditions, while vegetables are grown on raised ridges or in drained areas.

In recent days, subsistence and commercial agricultural activities still provide 30 - 50 % to household incomes in the Wakiso district (Mugisa et al., 2017). A major part of the agricultural goods produced in the area serves the market demands of the metropolitan area (Sabiiti & Katongole, 2016). Nevertheless, as urbanization in Kampala is proceeding rapidly, the metropolitan area is constantly expanding into rural trading centres and towns (Shuaib et al., 2005). As a consequence, the competition for land in the peri-urban areas is increasing and agricultural production is being slowly pushed-back as land is increasingly valued for housing development and recreation (Sabiiti and Katongole, 2016).

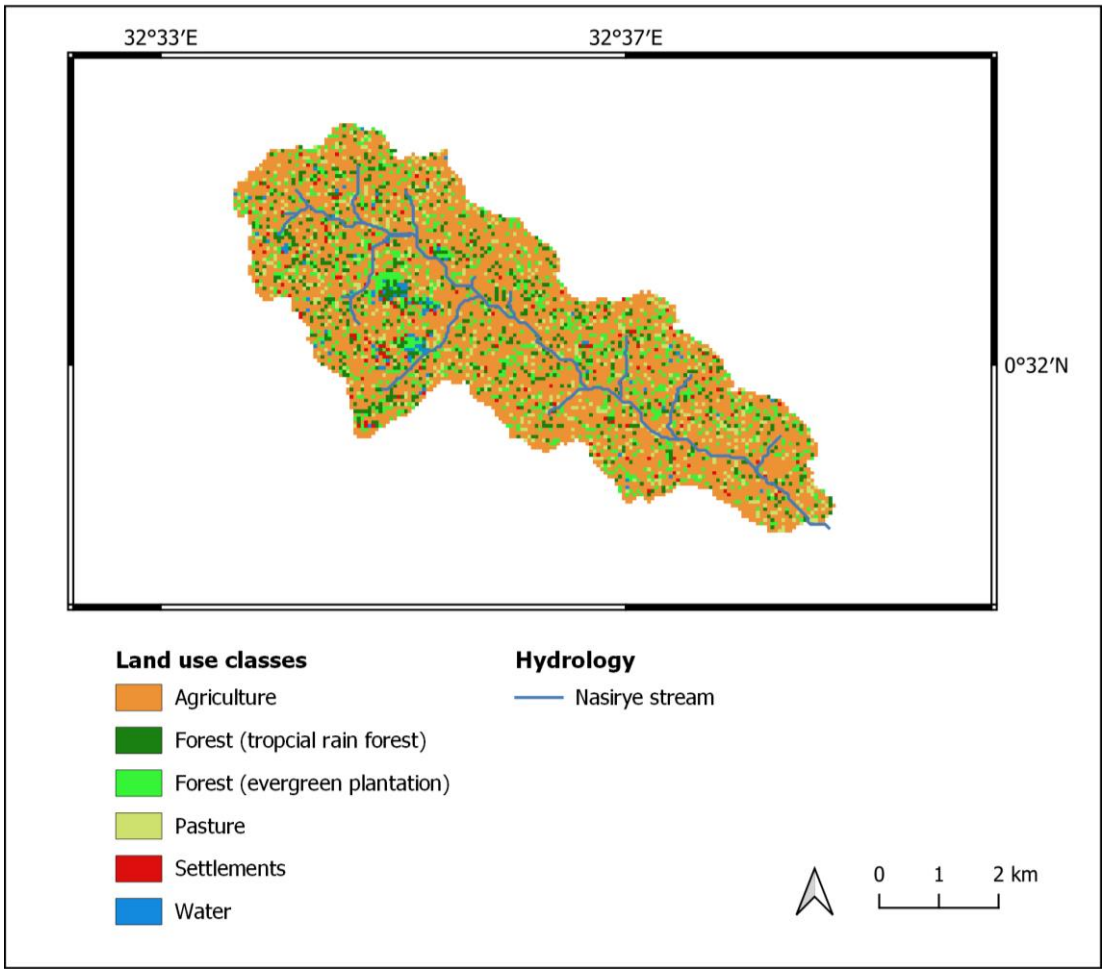

Figure 10 *Spatial distribution of land use and land cover types in the Namulonge inland valley (modified after Gabiri, 2018).*

4 Materials and methods

4.1 Experimental design

Hydrological as well as geological data availability in central Uganda is still very limited. For the Namulonge wetland though a basic data set exists, as it has been subject of a multi-year interdisciplinary research in the frame of the GlobE-wetlands in East Africa project. Yet, most of the data were generated at the agricultural field trials (further described in Grotelüschen et al. (2021)), which were located in the valley bottom some 200 m upstream of the study site. Some studies conducted in the scope of the GlobE-wetlands project further focussed on catchment hydrology (Gabiri, 2018) and catchment hydrogeology (Burghof, 2017). In these studies data were collected along four transects perpendicular to the stream which were spread out between the inlet and the outlet of the wetland. These transects covered the different hydrological zones of the wetland (centre, middle and fringe position) but did not extend further upslope than the slope toe. The present work aims to characterise the hydrological connectivity of the slopes and the wetland and the linkage of these two systems. Therefore, the spatial focus of this study's experimental setup was at the slopes and at the transition zone from upland to wetland hydrology.

Blume and Meerveld (2015) stated that hillslope-stream (or in this case: wetland) connectivity can be investigated by studying "how, when and where water moves through a hillslope" (p. 179). They point out that most studies have used a multi-method approach as it strengthens the interpretation of the single measurements. The present study follows this approach by combining geo-electrical measurements with the monitoring of soil moisture dynamics and direct surface and subsurface runoff measurements paired with the analysis of nitrate dynamics which also served as a tracer.

The study was designed as a plot study to allow for a detailed characterisation of subsurface structures and hydrological processes, and to be able to identify the impact of different land use types on water and nutrient transport to the wetland fringe. The study area was located at a slope in the lower part of the Namulonge wetland (see Figure 11). It comprised an area of 14000 m² and extended from the fringe of the wetland to the middle of the slope. Only the geo-electrical measurements reached up to the hilltop. Three plots of 30 x 105 m² per plot were demarcated, on which the different land use types (bare fallow, crop production and semi-natural vegetation) were established. On each plot, measurements were taken at different slope positions along transects covering the fringe of the wetland, the slope toe, the lower slope and the mid-slope position. At each position, soil moisture (chapter 4.4.1) and nitrate concentration in the soil solution (chapter 4.5.1) were measured and physical and chemical soil properties determined (see chapter 4.3). An overview of the experimental setup is provided in Figure 12.

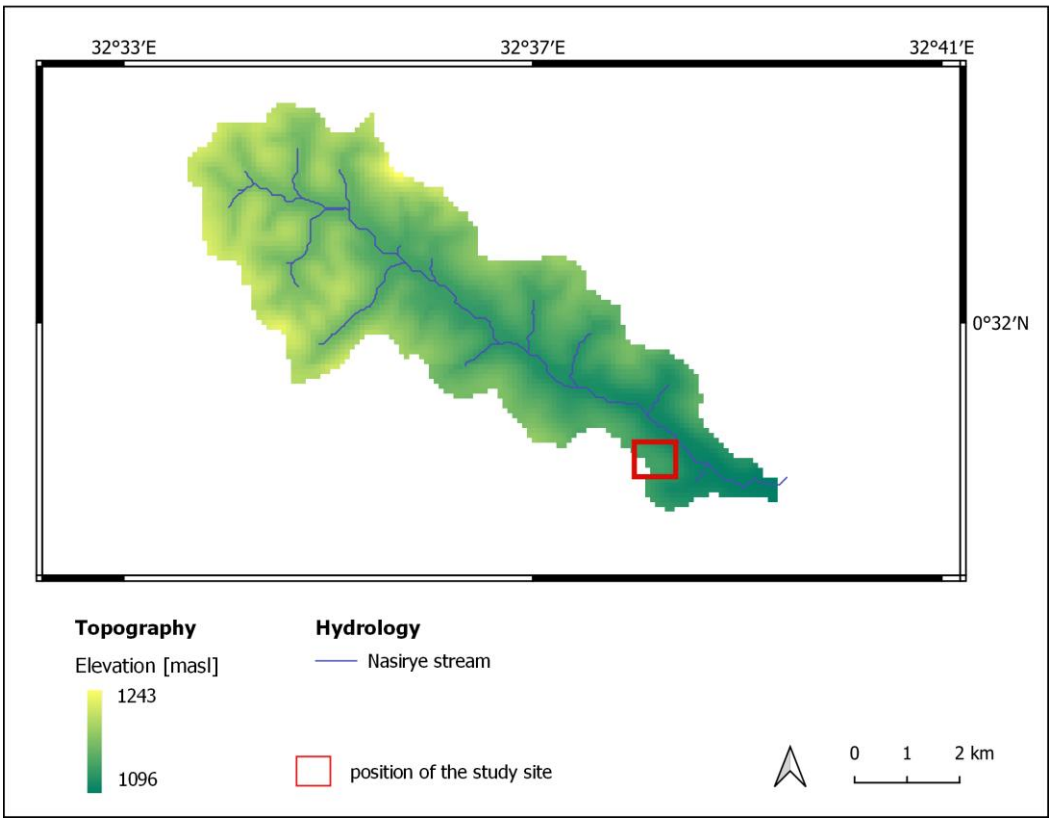

Figure 11 *Position of the study site in the Nasirye catchment near Namulonge. Data sources: Elevation (Jarvis et al., 2008), Nasirye stream (Gabiri, 2018).*

To analyse the water and nutrient translocation in the upper soil layers, three pits of 3 x 2 m² each were excavated at the lower slope at each land use type and soil moisture and nitrate in the soil solution were measured upslope and downslope of each pit. The pits were excavated down to a depth of 40 cm below the surface of the saprolite. As the saprolite was found at varying depths along the slope, depth of the pits also varied between 1.05 m and 2.30 m. Next to each pit, a reference plot was installed on which measurements were taken at the same slope positions but without preventing potential upslope contributions through the installation of the pit. At the mid-slope position, three parallel measuring points were installed.

On each plot, a trench for interflow collection was installed at the slope toe (chapter 4.4.2). At the lower slope, surface runoff was collected from runoff plots, including three repetitions per land use type (chapter 4.4.3).

No measuring point could be installed at the fringe of the wetland on the plot under semi-natural vegetation, as the field was cultivated by local farmers. On the plot under crop production two measuring points were installed at the fringe of the wetland. This is due to the fact, that local farmers started cultivating Banana plants at the slope toe in March 2017, which could potentially influence nitrate delivery to the wetland. Therefore, a second measuring point was installed some meters aside the first point. Appendix 1 shows the different measuring points at the experimental plots and the corresponding labels.

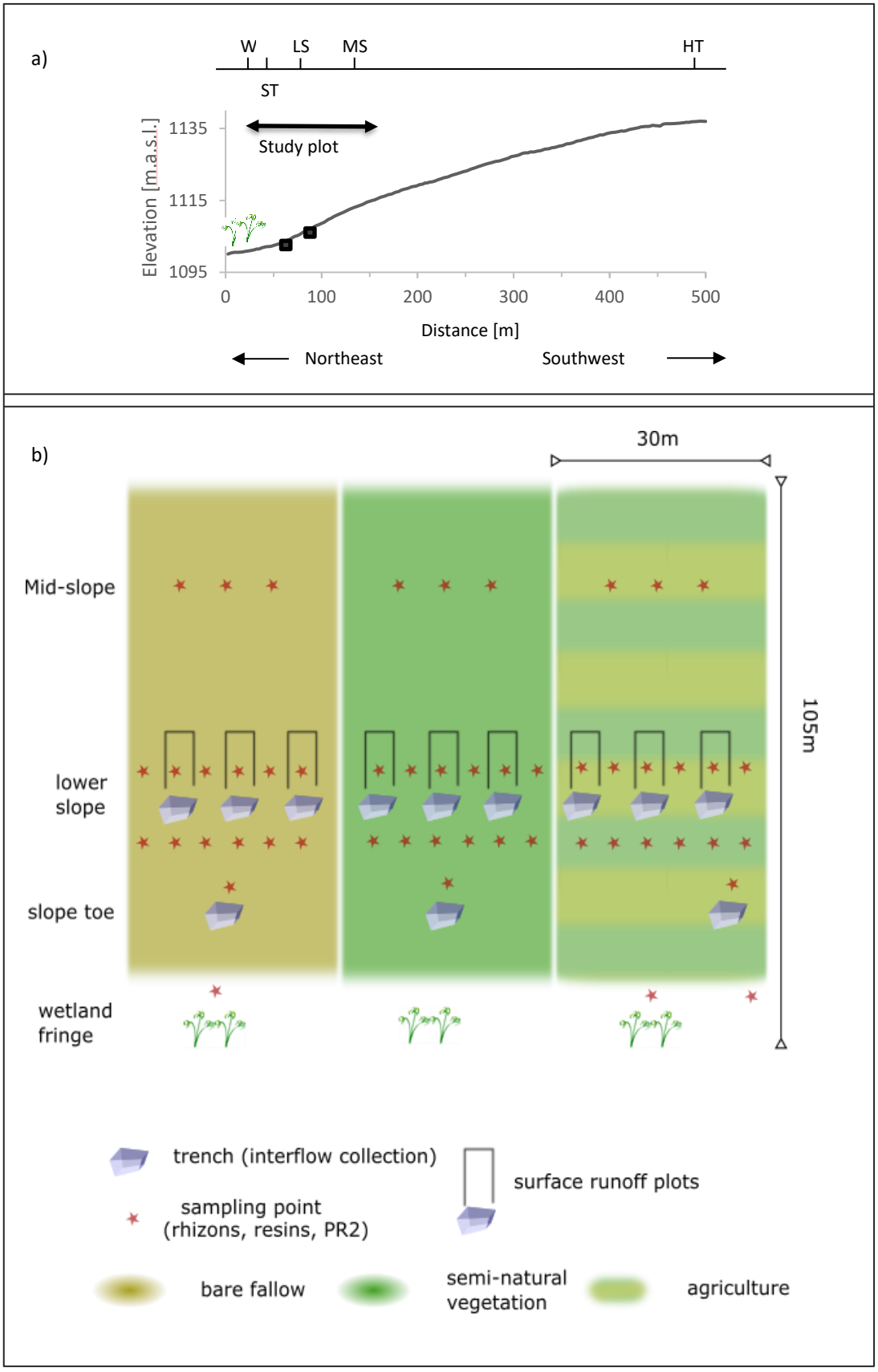

Figure 12 *a) position of the study area along the hill slope transect (W= wetland, ST= slope toe, LS= lower slope, MS= mid-slope, HT= hilltop) and b) overview of the experimental setup.*

4.2 Treatment application

Three land use types were established and then investigated in the study area. The first plot represented bare fallow conditions. At the beginning of the measurement period, the land was ploughed by tractor to eradicate the vegetation which previously grew on the plot. Afterwards it was kept weed free by uprooting the weeds manually using a hoe or by applying a herbicide when weed growth was not pronounced. Table 1 presents the dates of ploughing and herbicide spraying.

Table 1 *Weeding dates and practices on the bare plot.*

Year	Month	Treatment
2015	Beginning of December	Ploughing by tractor
2016	End of February	Ploughing (hoe)
	Mid-April	Ploughing (hoe)
	End May	Ploughing (hoe)
	Mid-August	Ploughing (hoe)
	Beginning of October	Ploughing (hoe)
	End November	Ploughing (hoe)
2017	End January	Ploughing (hoe)
	End March	Spraying
	End April	Spraying
	End June	Ploughing (hoe)
	Mid November	Spraying

The plot under crop production was managed by a local farmer, who applied common management practices used by small scale farmers in the region. Therefore, different crops were grown in rather small patches along the slope. This included a belt of cassava plants (*Manihot esculenta*) at the slope toe, followed by maize (*Zea mays)* intercropped with beans (*Phaseolus vulgaris*), followed by sweet potatoes (*Impomea batatus*) at the lower slope and beans at the mid-slope position. During the study period, no fertilizer or herbicide was used on this plot. Cassava plants were perennial and maize, sweet potato and beans were harvested at the end of each rainy season and replanted at the beginning of the next rainy season, while some of the sweet potato plants remained in the field even during the dry season. As 2016 was an unusually dry year due to the impact of the La Niña phenomenon, sweet potato plants dried up in December 2016 and had to be replanted at the beginning of the first rainy season 2017. Sweet potatoes were planted on small soil hills banked up manually before planting. Soil at the lower and mid-slope

position was ploughed before planting at the beginning of each rainy season. The plots in the wetland were located at local farmer's fields. In the wetland beneath the plot under crop production sweet potato was grown at point W1 whereas point W0 was covered by short grasses. The wetland point beneath the bare plots (W2) could not be kept bare as it was used by a local farmer to cultivate Taro (*Colocasia esculenta*). The plot under semi-natural vegetation was not treated during the study period and was densely covered by high grasses (up to 2m height) and shrubs.

4.3 Exploration of vadose zone structures and properties

4.3.1 Electrical resistivity tomography (ERT)

Geophysical methods can complement traditional hydrometric investigations in order to gain further insights into the subsurface structure and its composition (Wenninger et al., 2008). In this study, 2-D electrical resistivity imaging surveys were conducted and used in a reconnaissance fashion to assist in the interpretation of hydrological processes. ERT has been praised to be a valuable, cost-effective and non-intrusive tool in geomorphological investigations (Smith and Sjogren, 2006), and during the last years its relevance for hydrogeological investigations has been increasingly recognised (Blume and Meerveld, 2015). Here, the most basic benefit from the application of geophysical methods in hydrology is their subsurface spatial context information (Koch et al., 2009). There are many studies who successfully applied ERT measurements in hydrological research in tropical regions. Uhlenbrook et al. (2005), for example, used ERT to support their interpretation of hillslope flow pathways in research catchments in South Africa, while Riddell et al. (2010) combined classical hydrological methods and ERT sounding to characterise hydro-geomorphic controls within a headwater wetland.

ERT sounding is based on Ohm's law which relates the current density (U) and the electrical field (V) to the resistance (R) of an electrical conductor. In the field, an electric current is induced to the ground via current electrodes and while the potential difference is measured at the potential electrodes. The implementation of a geometric factor which is related to the distance between the electrodes then allows to infer the apparent resistivity (ρ_a) of the conductor. Potential and current electrodes can be arranged in different configurations, so called arrays, which allow for a different degree of vertical or lateral resolution. The distance between the current electrodes influences the penetration depth of the induced current. Therefore, in 2D profiling, measurements are taken with several electrode spacings at different positions along a transect so that a pseudosection showing the apparent resistivity at each assigned survey level and lateral position can be constructed. To calculate the true resistivities, an iterative process of inverse and forward modelling is applied, where the inverse problem is usually formulated as a regularized optimization problem, which involves minimization of an objective function comprising both data misfit (measured vs. modelled) and a penalty term which accounts for deviations from desired model attributes. Hereby, commonly a finite elements approach is followed for reasonable calculation efforts (Binley and Kemna, 2005). The resistivity of subsurface strata is mostly determined by the conductivity of the pore-filling fluid and therefore strongly influenced by the porosity and degree of saturation of a medium, which is described by Archie's law (Archie, 1942). Nevertheless, also clay mineralogy (due to surface conduction effects) and the presence of ore minerals and graphite impact the resistivity of the subsurface (Everett, 2013).

In this study, ERT surveys were conducted along three transects using the ABEM SAS 300C terra-meter in combination with the ABEM electrode switcher ES464 and multi-core cables to establish a multi-electrode resistivity system. Two transects extended from the fringe of the wetland to the upper slope or the hilltop, while the third transect was oriented in a slope parallel direction and located at the lower slope in order to capture lateral subsurface heterogeneities along the slope (see Figure 13). Transect 1 and transect 3 were measured with different electrode spacings (0.7 m, 2.5 m and 5 m at transect 1, and 1 m and 3.5 m at transect 3) to allow for the resolution of shallow as well as deep structures and to allow for a cross-check between the measurements. Measurements were conducted using carpenter's steel nails of 10 cm length as electrodes, as these were locally available, knowing that this does not promote an optimal transmission of the electrical current into the ground. However, due the reconnaissance character of the ERT measurements in this study, this limitation was acceptable. The electrodes were arranged following the Wenner array, as one of its attributes is a high signal strength and its high resolution of horizontally layered subsurface structures (Berktold, 2005). As it was known before the measurement campaign that a layer wit high quartzite content was present close to the soil surface, this seemed desirable in order to obtain as much information about the underlying layers as possible. Measurements of all profiles were taken as roll-along readings, as the desired length of the transects exceeded the maximum cable length. Yet, as a rather old model of the ABEM was used, measurements of one profile section could take several hours and therefore one traverse was measured on different days, while the positions of the electrodes were not changed between the measurements. An overview of the measurement days is given in Table 2. For the inversion process, the software RES2DInv (Locke, 2018) was used and the inversion parameters optimized for the best possible resolution which was compatible with prior knowledge of the subsurface in this region. All profiles were displayed with the same colour scheme. This made it possible to compare the different profiles more easily even if in a few cases structures with a less pronounced resistivity difference were not visualised. RES2DInv allows for the inclusion of topographical information in the inversion process as well as in the display of the model sections. The topography of each profile (i.e., each electrode spacing) was determined in the field using a handheld clinometer ("Necli").

According to Koch et al. (2009), there are two major difficulties involved in the application of geo-electrical measurements in hydrological investigations. On the one hand, uncertainty evolves from the inversion process described above, as the best mathematical solution does not always reflect the true natural conditions in the field and thus computational artefacts may be part of the computed images. Furthermore, there are physically based uncertainties which concern the understanding of the interactions of the induced current with the subsurface materials as well as the translation of modelled resistivities into soil properties or hydrological conditions. Furthermore, geo-electrical methods are prone to the problem of equivalence (Sanuade et al., 2019), as several subsurface configurations could produce the same model output. These uncertainties can be reduced by combing the geo-electrical measurements with data from drilling logs and hydro-chemical and hydrometric datasets (Koch et al., 2009). Unfortunately, deep drilling logs and hydrometric datasets related to the saprolite were not available for the transects where the ERT measurements were conducted. Nevertheless, several shallow drilling logs were sunk along each transect and soil properties of the samples were analysed, as described in chapter 4.3. The study of Burghof (2017) provided drilling log information of the upper saprolite, which was

collected about 500 m from the study site. Information on the structure of the saprolite and the position of groundwater bodies within it was derived from deep drilling logs taken by the Ugandan Ministry of Water and Environment within a radius of about 2 km around the study site. In addition, soil moisture of the upper soil horizons was monitored at several positions along the transects.

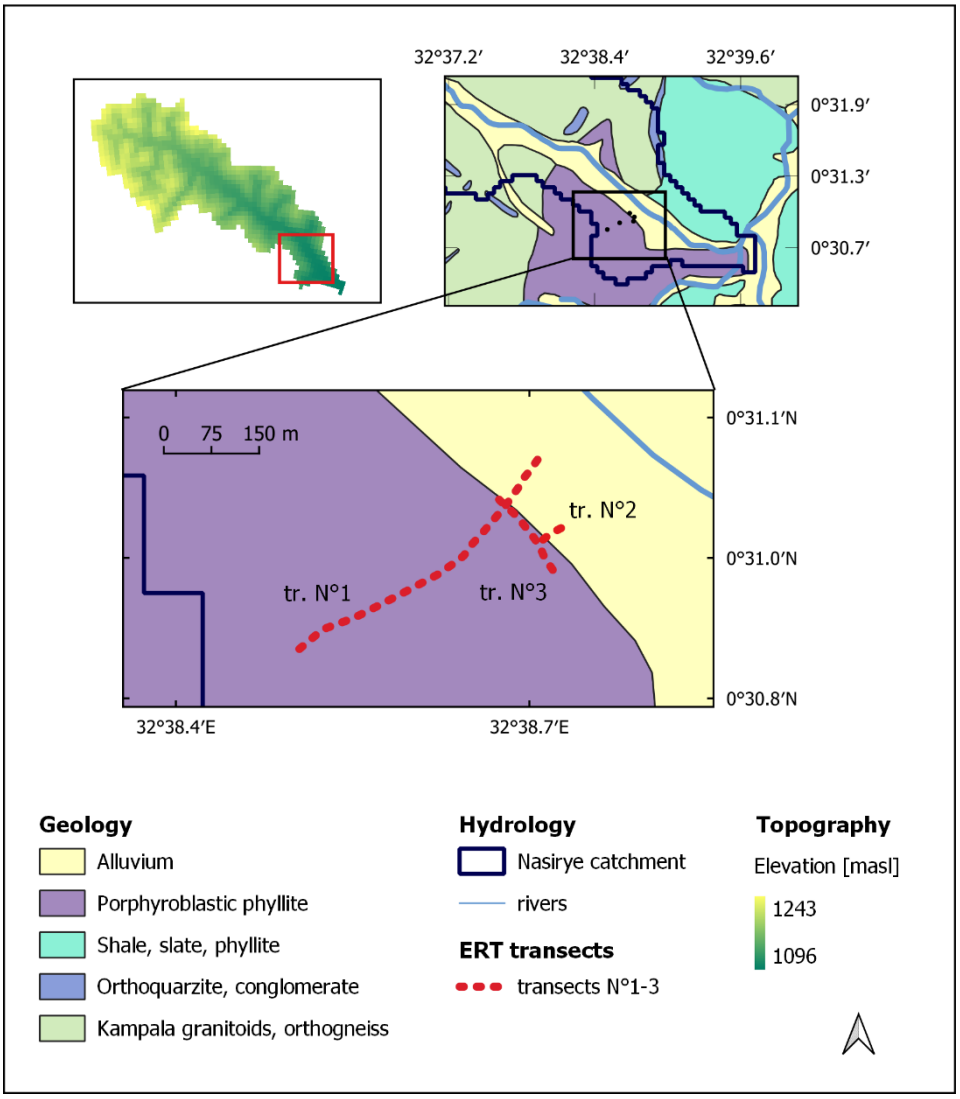

Figure 13 *Position of the ERT transects in the Nasirye catchment. Data sources: elevation (Jarvis et al., 2008), geological map (GTK consortium, 2012), alluvium (Heiß, 2016, unpublished), Nasirye stream (Gabiri, 2018).*

Table 2 *ERT measurement dates and corresponding 7-day antecedent precipitation index for each profile.*

Transect N°	Profile N°	Profile sections	Measurement dates	Antecedent precipitation Index (7 days)
1	1	0-300 m	13.05.2017	5.3 mm
		300-500 m	03.05.2017	2.4 mm
1	2	0-150 m	15.04.2017	0.6 mm
		150-250 m	25.04.2017	19.0 mm
		250-350 m	26.04.2017	11.4 mm
		350-500 m	28.04.2017	8.9 mm
1	3	0-56 m	07.04.2017	4.0 mm
		56-98 m	10.04.2017	8.5 mm
		98-126 m	11.04.2017	6.4 mm
		126-168 m	12.04.2017	5.1 mm
		168-210 m	13.04.2017	3.9 mm
2	4	0-42 m	19.04.2016	13.9 mm
3	5	0-140 m	02.05.2017	1.5 mm
3	6	0-40 m	27.04.2017	12.9 mm
		40-80 m	24.04.2017	23.1 mm
		80-140 m	22.04.2017	14.8 mm

4.3.2 Soil texture and bulk density

Soil samples of each horizon were collected at every measuring point to determine the soil texture. When the subsoil horizon was deeper than 70 cm, two samples were taken and analysed separately. Samples of the upper saprolite were only taken from the bottom of the pits at the lower slope as well as from the trenches at the slope toe and from three sampling points at the mid-slope position due to accessibility constraints. Samples were oven-dried at 105 °C and grinded. The skeletal fraction was determined via sieving. Soil particle size distribution was analysed using the laser diffraction particle size analyser Horiba L950. In a second step soil texture classes were determined following the USDA soil texture classification.

In addition, undisturbed soil samples were collected from the A and upper B-horizon at each measuring point (2 replicates) using a double cylinder core sampler with a volume of 100 cm^3. Samples were oven-dried at 105 °C for 48 h and weighed. The bulk density was then calculated as:

$$BD = \frac{dryweight\ [g]}{cylinder\ volume\ [cm^3]}$$

4.3.3 Field saturated conductivity (K_{fs})

A single ring infiltrometer was used to determine the field saturated hydraulic conductivity (K_{fs}), applying a single constant head approach (Reynolds and Elrick, 1990). In this method, an infiltration process of ponded water is initiated which after a transient phase characterised by decreasing infiltration rates reaches steady conditions. Field saturated hydraulic conductivity can then be estimated from the steady-state flow rate. The single ring infiltrometer method enables a relatively fast and reliable measurement of vertical infiltration rates as well as an easy spatial replication of the measurements and is widely accepted in the science and engineering community (Di Prima et al., 2019; Reynolds, 2008). In addition, it can easily be conducted using locally available materials, which makes it suitable for research in countries of the global South.

K_{fs} was determined for the soil surface, the topsoil, the subsoil and the uppermost saprolite. It has to be noted, that the results include the effect of macropores on K_{fs} as a positive pressure head was applied. The measurements in the different soil horizons were conducted at the mid-slope position of each land use type, while, due to accessibility issues, K_{fs} of the upper saprolite was determined in the drainage of the pits at the lower slope. Measurements were always taken in the first 10 cm of each horizon. For each depth, three rings with a diameter of 11 cm were carefully inserted 2 cm into the soil using a hammer and a lath in order to ensure tight contact of the rings and the soil (see Figure 14). Except for the measurement at the soil surface, the ring was dug out and removed while breaking the soil inside so that a fresh surface, which was not impacted by digging, was created and, thus, soil pores were not clogged. Afterwards, the ring was inserted as described before at the same circular surface. Water was then carefully poured into the ring to a height of 12.5 cm avoiding a direct impact of the jet of water on the soil surface in order to reduce splash effects and clogging of superficial soil pores. Before each measurement, the soil was pre-wetted by allowing the infiltration of 4 cm water column into the soil. During the measurements, the infiltration time of 1 cm water column was recorded and the water level of 12.5 cm restored until a quasi-steady state was reached. K_{fs} was determined from the field data following the cumulative drop method described in Bagarello et al. (1999). In this method, the steady state infiltration rate is obtained from linear regression of the visually determined first linear curve section of the cumulative infiltration vs. time plot. Linearity was assumed when R = 0.99 was attained. The slope of the regression equation then gives K_{fs}. The data of the measurements where a steady state was not reached after 6 hours were discarded. The aim of the infiltration trials in this study was to detect major differences in K_{fs} between the single soil horizons in order to identify favourable conditions for the formation of interflow rather than to specify exact values of Kfs. Therefore, no further correction of K_{fs} for the effects of sorptivity or horizontal fluxes was undertaken, as suggested by, e.g., Di Prima et al. (2019) and Lassabatère et al. (2006). Weiss and Gulliver (2015) described, that K_{fs} is usually overestimated, when the arithmetic mean was calculated over the replicates at a certain position, while the geometric mean tends to underestimate K_{fs}. In this study, except for one position, no significant difference between the geometric and the arithmetic mean was detected and thus the arithmetic mean was chosen.

Figure 14 *Infiltration trials via single-ring infiltrometers in the upper B-horizon.*

4.3.4 C/N ratio

Total C and total N contents of the soil samples which were collected at every measuring point (see Figure 12b) were determined via dry combustion using an elemental analyser (EURO EA Elemental Analyser series 3000, EURO-EA Vector Pavia, Italy).

4.3.5 Soil pH

Soil pH of the soil samples which were collected at every measuring point (see Figure 12b) was determined from air-dried and grinded soil samples in a 1:1 H_2O and a 1:1 1 M KCL solution. Afterwards ΔpH was calculated as

$$\Delta pH = pH\ (KCl) - pH\ (H_2O).$$

4.4 Analysis of slope water processes

4.4.1 Monitoring of soil moisture dynamics

Soil moisture was monitored to detect water fluxes along the slope and the impact of different land use types on these fluxes as well as to compare and connect moisture dynamics in the wetland to the dynamics in the upland. Furthermore, moisture data were correlated to nitrate mineralisation at the different slope positions. Soil moisture was monitored at each measuring point at the different slope positions described in chapter 4.1 (see Figure 12). Thereby, a higher spatial coverage was achieved to account for spatial variability in soil water responses, as single-transects upslope are often not representative (Blume and Meerveld, 2015). Measurements were taken every two to three days during the rainy season and once a week during the dry season. Soil moisture was measured using a profile probe type PR2 (Delta-T Devices Ltd, 2016), which is a FDR (Frequency-Domain-Reflectometry) device. The profile probe measures soil moisture at 10 cm, 20 cm, 30 cm and 40 cm depth when inserted into an access tube, a thin-walled tube which maximises the penetration of the electromagnetic field into the surrounding soil. The probe consists of a sealed polycarbonate rod, ~25 mm, with an electronic sensor

every 10 cm along the rod. When power is applied to the profile probe, it creates a 100 MHz signal, which is then transmitted to the soil as an electromagnetic field extending 100 mm into the soil. The permittivity of the soil (a measure of a material's response to polarisation in a magnetic field) is dominated by its water content and changes the applied electromagnetic field, which finally results in a stable voltage output. This output can then be converted to % soil moisture according to the soil specific calibration functions. Delta-T devices supply two calibrations, one for mineral and one for organic soils, which allow measurements of an accuracy of ~±0.06 %vol. A soil specific calibration would normally decrease this error to ~±0.05 %vol. (Delta-T Devices Ltd, 2016). In addition, Böhme et al. (2013) proved that the standard calibration produces an error of ~±0.07 %vol. for wetland soils in tropical conditions. For this study, the accuracy attained by the general calibration was sufficient and therefore no manual calibration was conducted. As the investigated soils were classified as mineral soils, the calibration function was chosen accordingly. Data were collected manually using a handheld HH2 moisture meter (Delta-T Devices Ltd, 2017), which is connected to the profile probe. Access tubes were installed following the guide-lines established by (Delta-T Devices Ltd, 2005).

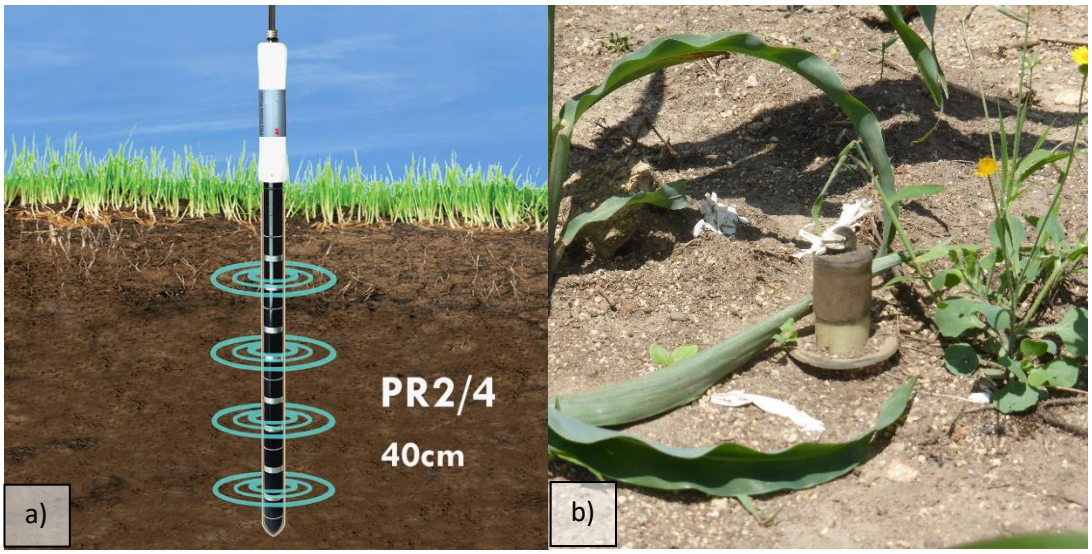

Figure 15 *Schematic representation of the PR2 Profile probe when inserted into the soil (a) (https://www.delta-t.co.uk/product/pr2/) and picture of the access tube installed in the field (b).*

To compare soil moisture in the wetland and at the slope as well as moisture at different slope positions, the arithmetic means of the different slope positions or of the upland and wetland positions were calculated. Measuring point PX.1, which was located behind the pits at the lower slope, was not included in the calculation of mean values as it was hydrologically separated from the rest of the slope by the installation of the pits.

The soil water content at saturation Θs for each measurement depth was calculated using the pedotransfer functions introduced by Rawls and Brakensiek (1985) and the correction factors for the effect of the skeletal fraction as described in (Flint and Childs, 1984). Data on bulk density and sand / clay content, which are the basic input parameters for the pedotransfer functions, were only available per soil horizon and not for each 10 cm step covered by the PR2 probe. In addition, soil samples were taken in close proximity to the PR2 access tubes but not at the exact same position, which might have led to

imprecisions. As a result, the maximum measured volumetric soil water content sometimes exceeded the Θs derived from the pedotransfer functions. In these cases, after the removal of outliers, measured maximum volumetric soil water contents were assumed to represent Θs. The soil water content Θ in % saturation was then derived by

$$\Theta\,[\%\ \text{sat.}] = \frac{\Theta\text{v}[\ \%\ \text{vol.}]}{\Theta\text{s}\ [\%\ \text{vol.}]} * 100$$

with Θ_v being the volumetric water content of the soil as determined by the PR2 measurements.

4.4.2 Monitoring of interflow dynamics

An overview of approaches and methods to characterize hillslope-stream connectivity can be found in Blume and Meerveld (2015). In the present study, a hillslope-centred approach in which water fluxes are studied directly at the slope was chosen over a stream-centred approach where the fingerprints of hillslope water in the stream are observed. A stream centred approach would not be feasible for the purpose of this study, as the analysis of stream responses would rather allow conclusions on the catchment behaviour than to analyse the impact of different land use types at a single slope. Also, not all the water coming from the slopes reaches the stream, as a major part gets stored in the valley bottom wetland or at least has to pass through it (Rodenburg, 2013), which complicates an elaborate EMMA (end member mixing analysis). A wide range of methods and approaches exists which follow a hillslope-centred approach. Those included, e.g., tracer experiments (Kahl et al., 2007), dye staining and excavation (e.g., Noguchi et al., 1999), groundwater level and soil moisture measurements (Lin and Zhou, 2008), geophysical measurements (e.g., Angermann et al., 2017) and trench measurements (Meerveld and McDonnell, 2006b). Besides geo-electrical measurements to collect information on subsurface structures and possible water pathways and monitoring of soil moisture dynamics along the slope to detect water movements, trench measurements were chosen as a central approach in this study. Trench studies offer a direct method to quantify subsurface runoff and to observe flow from macropores as well as matrix flow. Even if the installation and maintenance of the trenches is time-consuming, trench trials can be set up using local materials only. Most importantly though, trenches can be used for sampling subsurface flow and thus study hillslope nutrient fluxes (Burns et al., 1998; van Verseveld et al., 2009).

As no interflow could be detected in the pits at the lower slope, three micro-trenches of 2 x 3 m² were excavated at the slope toe at each plot (bare fallow, semi-natural vegetation and crop production) (see Figure 16 and Figure 17). Each trench was excavated down to 60 cm below the surface of the saprolite and covered by corrugated metal sheets. Water from the matrix as well as from macropores was jointly collected in gutters of 1,5 m length at a depth of about 30 cm below the surface of the saprolite. The upper saprolite has a high skeletal fraction of about 50 % at this position. Therefore, no pipes could be installed to collect the interflow, as no smooth transition to the saprolite could be achieved resulting in water seeping under the pipes. Therefore, the gutters were directly carved in the upper saprolite and sealed using clay, as due to the constant input of water concrete could not be used. Interflow from both sides of the gutters converged in the middle and was directed to an outlet from where it was collected using measuring cylinders. The trenches were drained to the wetland so that water did not impound in the trenches. In front of the trench, a metal gutter was placed in the soil to divert the surface runoff

directly to the drainage and prevent it from entering the trench. As interflow entered the trenches via a sandy loam layer in the upper part of the profile, the walls of the trench had to be fixated using a fine mash, which would allow water to pass but prevent the soil from collapsing. Due to static issues, the trenches could not be extended further downwards so that not all the lateral flow could be captured. The measured interflow volumes thus only represent a part of the interflow and, hence, the possibilities for quantification remained limited. Nevertheless, also qualitative observations of interflow processes at a site are of "considerable pedagogic value" (Jarvis et al., 2016), as the dynamics related to land use type, seasonality and rainfall patterns could be captured and nutrient contents could be measured.

Interflow volumes were measured on the same days as soil moisture, which was every two to three days during the rainy season and once a week during the dry season. Interflow volumes were determined by placing a measuring cylinder under the outlet of the runoffs for one minute. During each measurement, three repetitions were taken. On November 14th 2017, samples were taken before and one hour after a heavy rainstorm, to analyse the quick component of interflow.

Figure 16 *Front view of a micro-trench for interflow collection at the slope toe.*

Figure 17 *View of the channels draining the micro-trenches at the slope toe at a) the plot under semi-natural vegetation and b) the plot under bare fallow.*

4.4.3 Monitoring of surface runoff dynamics

Besides the subsurface runoff component, water and nutrient delivery from the slopes to the wetland also occurs via surface runoff. In order to understand the conditions favouring each runoff component and the contributions they made to the soil moisture and nutrient status in the wetland, surface runoff dynamics were monitored on runoff plots at the lower slope (see Figure 18). As described in chapter 4.1, three runoff plots per land use were installed to account for spatial variability following the recommendations made by Hudson (1993).

At the lower end of each runoff plot, surface runoff entered a metal gutter and was then directed via pipes to steel drums (runoff collectors) placed in the pits. Each drum accommodated 245 l. The pits were fully drained so that drums did not float when water entered the pit. All pits were covered by a metal roof. After each rainfall event, the gutters and connecting pipes were cleared so that entering water was not blocked. The gutters were covered to avoid direct collection of rainfall. As the collectors at the plot under bare fallow frequently overflew during the first measurement period, a second collector was placed in the pit and connected to the first one so that the maximum collector volume was increased to 490 l in seasons 2017.1 and 2017.2. At first, each runoff plot covered an area of 42 m² until the area was decreased to 30 m² on the 31st of March 2017 in order to reduce runoff volumes and avoid overflow of the collectors. The runoff plots were confined by corrugated sheet iron, which was dug about 5 cm into the ground and had an above-ground height of 20 cm. Surface runoff volumes were determined by measuring the height of the water table in the drums after each rainfall event. When the water table was below 5 cm, runoff volumes were quantified using a measuring glass. When rainfall occurred during night hours, the runoff volumes were quantified in the morning of the following day.

Figure 18 *View of the surface runoff plots and runoff collectors at the lower slope position and impression of a measurement of the water table in the collectors.*

4.4.4 Precipitation

In order to conduct a field-based analysis of the hydrological reaction of the different runoff components and the soil moisture to different rainfall conditions, precipitation was measured at the experimental site using a tipping bucket rain gauge with a resolution of 0.2 mm (Theodor Friedrichs & Co. Type 7041). The rain gauge was installed at the slope toe position at the plot under bare fallow in September 2016. Before that and during single days of equipment failure, precipitation data were derived from the tipping bucket in the Central Field trials 700 m further upstream or from the automated weather station at the NaCRRI research station 2 km northwest of the experimental site. Precipitation data were recorded at a 1 min interval. For further analysis the data were summarized to daily values for a 24 h time interval starting at 17 h and ending at 17 h on the following day, while the data are always assigned to the date of the end of the interval. This time frame was chosen in order to facilitate correlations with the other measurements, i.e., to relate the precipitation received during night hours to the measurements of soil moisture, surface runoff volumes, etc. on the following day. Rainfall intensity was calculated as the maximum amount of rainfall received during 15 min on each day. The antecedent 7-day precipitation index API_7 was calculated as

$$\mathrm{API} = \sum_{i=1}^{7} \frac{Pi}{i}$$

where P_i is the precipitation on the i^{th} day beforehand (McDonnell et al., 1991).

4.5 Analysis of nitrate dynamics

4.5.1 Measurement of nitrate in the soil solution

4.5.1.1 Short term dynamics

Nitrate concentrations in the soil solution were measured at 10 cm and 20 cm depth at each measuring point along the slope (see Figure 12) in order to analyse short term dynamics and deduct possible leaching of nitrate from the topsoil. During the rainy season, a measurement interval of 2 - 3 days was chosen. During the dry season, measurements were conducted once a week until the soil dried up. Soil solution was extracted using rhizon soil moisture samplers as shown in Figure 19 (Eijkelkamp, 2019). The rhizon moisture samplers were installed in small trenches which were covered between the measurements. Samplers were frequently replaced as they got damaged by termite activity. To abstract the water, syringes were connected to the Luer-Lock and vacuum applied. The samplers generally function until a water suction in the soil of > 500 hPa, which limited data availability during dry periods.

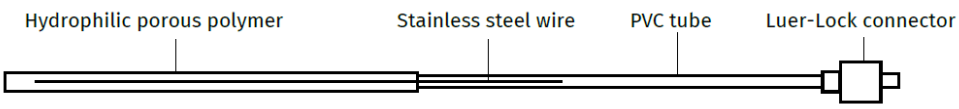

Figure 19 *Schematic representation of a rhizon soil moisture sampler (Eijkelkamp, 2019).*

Figure 20 *Rhizon soil moisture samplers installed in micro-trenches in the field and syringe connected to the rhizon during the sampling of soil solution.*

Dissolved nitrate in the soil solution was quantified in-situ using a hand-held Nitracheck reflectometer (Eijkelkamp, 2004) in combination with Merckoquant® test stripes. The Nitracheck has a measurement range of 5 - 500 ppm nitrate. When the nitrate concentration fell below 5 ppm, the value was set to 2.5 ppm for further analysis, while it was set to 500 ppm when the concentrations exceeded the

measurement range. Every measurement was repeated at least once and the arithmetic mean was used for further analysis to reduce measurement inaccuracies. The nitrate content in the soil solution was determined by multiplying the nitrate concentration with the volumetric soil moisture (see chapter 4.4.1) at the respective measurement depth.

4.5.1.2 Seasonal cumulative bio-available nitrate

In-situ installation of ion exchange resins without subsequent mixing action provides a reliable index of nutrient bioavailability (Skogley and Dobermann, 1996). It has been successfully used in submerged wetland soils (Dobermann et al., 1997) as well as in upland soils which are not permanently saturated (Turrion et al., 1997) and has proven to yield valuable results in solute transport studies (Li et al., 1993; Pampolino et al., 2000). In this study, ion exchange resins caps (UNIBEST International) were used in order to analyse seasonal effects of the different land use types and of potential leaching processes on the bio-available nitrate in the soil solution. Ion exchange resin capsules contain resin beads charged with either H^+ or OH^- ions which act as a strong sink for ions from the soil solution. Once inserted into the soil, an exchange process occurs and nutrients from the soil solution are adsorbed to the resin beads while the H^+ or OH^- ions are released (see Figure 21a). The amounts of exchanged ions depend on the concentration in the soil solution surrounding the resin capsule. Hence, the exchange process resembles the activities of plant roots as it is equally dependent on the initial nutrient concentration in the soil solution as well as the diffusion rate of nutrients towards the resin capsule and is thus effected by soil physical and chemical properties (Skogley, 1992).

Three resin caps were installed at 10 cm and 20 cm depth at each measuring point at the beginning of the rainy seasons. Resins were attached to metal wires and installed with a spacing of 5 cm in small holes with a diameter of 1.5 cm (see Figure 21b). After the installation, the holes were closed with loose soil material from the respective soil horizon. At the end of the rainy season the resins were dug out and loose soil material was removed using a small brush. Afterwards, the resins were kept refrigerated until the extraction in the laboratory. In the following season, resins were installed in new holes which were created in close proximity to the previous sampling points but not at the same position in order to avoid the effects of soil disturbance on water fluxes in the soil. The arrangement of the resins described before was adopted starting from season 2016.2. During the first season all three resins were installed successively in the same hole while maintaining a distance of 5 cm. Analysis of the data later on gave significantly higher nutrient loads for the resins positioned at the end of the line, as they probably had better soil contact. Therefore, for season 2016.1 only the highest value of the three replicates was considered and the installation was adjusted as described before.

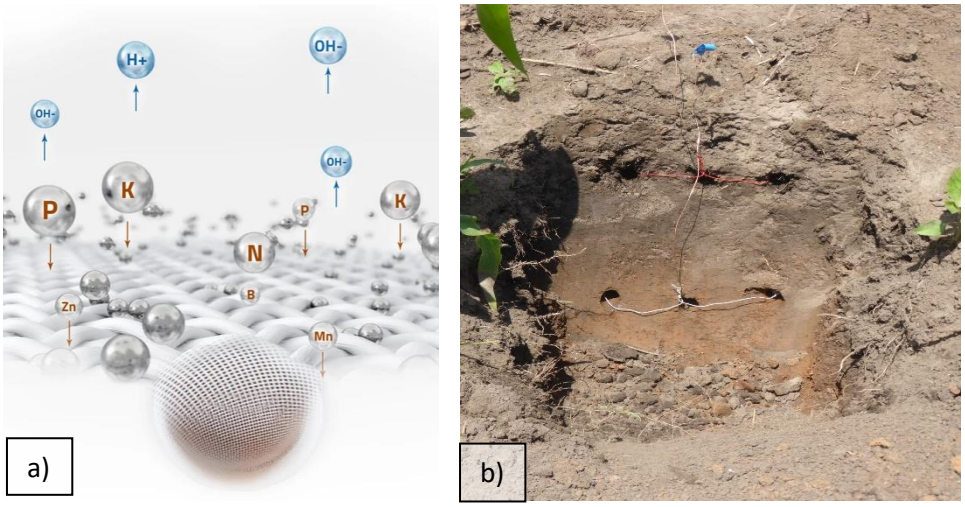

Figure 21 *Illustration of the ion exchange process at the surface of an ion exchange resin capsule (a) (https://www.mysoiltesting.com/technology), and in-situ installation of resin capsules in the field (b).*

For seasons 2016.1, 2017.1 and 2017.2 the nutrients adsorbed by the resin capsules were recovered by sequential shaking of each capsule in three batches of 20 ml 2M HCL for 20 min as described in Dobermann et al. (1997). In 2016.2 three capsules were eluted at once following the same approach. Nitrate content in the HCL eluates was then analysed photometrically using a continuous flow analyser. The quantity of nitrate adsorbed by the resins was expressed as ion loading (RAQ, resin adsorption quantities [µmol/cm²]):

$$RAQ = \frac{C \cdot V}{M \cdot A}$$

C = NO_3-N concentration in the eluate [mg/l] V= Volume of the extraction solution (60ml)
M= Molar weight of nitrogen (14.01 g/mol) A= surface area of the capsule (11.4 cm²)

4.5.2 Measurement of nitrate in the interflow and in the surface runoff

Nitrate concentrations in the interflow and in the surface runoff were also determined in-situ using the Nitracheck reflectometer in combination with the Merckoquant® test stripes (see chapter 4.5.1). Measurements were repeated twice and the arithmetic mean was calculated for further analysis. Concerning the interflow, nitrate concentrations were measured by placing the test stripe under the small jet of water leaving the runoffs in the trenches at the slope toe for 1 second. To determine the nitrate concentration in the surface runoff, a small water sample was taken from the collectors and the test stripe was dipped into the sample for 1 second. As for the soil solution, when the concentration was below the measurement range of the Nitracheck, i.e., < 5ppm, values were set to 2.5 ppm for further analysis. Nitrate content in the surface runoff was then calculated by multiplying the mean nitrate concentration with the respective runoff volume. As, due to logistical reasons, event-based measurements of the nitrate concentration in the interflow and in the soil solution were not possible, analyses of correlation were conducted by correlating the data collected on the last measurement day before the rainfall event with the surface runoff volumes and corresponding nitrate concentrations measured after the event.

4.6 Statistical analyses

The data were analysed using the statistical software *R*. The aim of the analysis was to gain a better understanding of the processes driving the different runoff components and to analyse the effect of rainfall characteristics and the three land use types on hydrological processes and nitrate relocation. In order to analyse the strength of association between two variables correlation coefficients were calculated. To analyse the data for linear relationships between two variables, Pearson's correlation coefficient r was selected. As a standardized measure of an observed effect, it is commonly used to measure the size of an effect, whereby generally absolute values of $0.3 < r < 0.5$ represent a weak correlation, absolute values of $0.5 < r < 0.7$ a moderate correlation and absolute values of $r > 0.7$ a strong correlation (Mindrila and Balentyne, 2016). Nevertheless, it has to be considered that the interpretation of the coefficient regarding the effect size varies according to the object of research and that the values given before can only serve as a rough guide line (Field et al., 2012). In order to then describe how much of the variability in one variable is shared by the other variable, the coefficient of determination R^2 was calculated which further describes the substantive importance of an effect. In addition, Spearman's correlation coefficient rho was calculated to analyse the data for non-linear monotonic correlations. As none of the data sets was normally distributed, non-parametric tests were used to analyse for differences between two or several groups. The two-sided Wilcoxon rank sum test was used to test whether the central tendency of two groups was significantly different at $p=0.05$. To test for significant differences between several independent groups, the Kruskal Wallis test was applied. This test determines whether all groups have identical distributions, but it does not show which group is different, in case the null-hypothesis was rejected (Helsel and Hirsch, 2002). Therefore, a multiple comparison post-hoc test was conducted subsequently .

5 Vadose zone structure and properties

This chapter gives a more detailed description of selected geological and hydrogeological characteristics as well as soil properties of the vadose zone at the slope and at the fringe of the wetland. The results of the geo-electrical measurements are presented and discussed in chapter 5.1, while chapter 5.2 focusses on physical and chemical soil properties.

5.1 Geological structure of the slope

An ERT (Electrical Resistivity Tomography) survey was conducted, to further investigate the structure of the weathering body and to identify groundwater bodies and major water pathways within it. Furthermore, the ERT measurements improved the understanding of the transition from the upland to the wetland. As described in chapter 4.3.1, ERT measurements were conducted at three transects (see Figure 13): transect 1 stretching from the wetland fringe to the hilltop, transect 2 stretching from the wetland fringe to the mid-slope position of the experimental plots and transect 3 which was oriented in a slope parallel direction. Transects 1 and 2 both passed next to the trenches at the slope toe where subsurface runoff was monitored. All transects were measured with at least two different electrode spacings (three in the case of transect 1) in order to reach both, a greater depth of investigation as well as a good resolution of smaller near-surface structures. The results and the interpretation of the different measurements are presented hereafter.

Transect 1

For the first profile, an electrode spacing of 5 m was chosen, which is the maximum spacing the available cables allowed. The inversion model including topography is displayed in Figure 22. With resistivities of down to 46 Ωm, the lowest resistivity values of the transect were found between 0 m and 30 m profile length. Starting from 95 m and reaching up to the hilltop, a layer of very high resistivity emerged. Between 95 m and 200 m profile length, this layer was modelled to reach down to a depth of about 10 m while it reached down to 15 m depth further upslope. Between 95 m and 280 m, the resistivity of this layer varied between 600 Ωm and 900 Ωm, while it increased in upslope direction where the resistivity was about 1400 Ωm. Within this layer single blocks of higher resistivity were found reaching up to 1100 Ωm in the lower part and up to 1800 Ωm in the upper part of the profile. Below this layer and down to the bottom of the model section, lower resistivities of about 100 - 400 Ωm were found, with the lowest values appearing between 95 m and 190 m profile length. A small layer with a resistivity of about 300 Ωm emerged here and there on top of the layer of high resistivity described above between 205 m and 460 m profile length. The high values in the left bottom corner of the profile were classified as inversion artefacts and are therefore not considered further. Modelled resistivity and resulting spatial patterns were very similar when inverting the apparent resistivity values measured in the field with another inversion software (“Bert”), see Appendix 2. Yet, here the range of modelled resistivities was smaller, as the low values at the beginning of the profile reached down to 71 Ωm only and the maximum modelled resistivity in the resistant upper layer did not exceed 1440 Ωm.

For the second profile taken over the same transect, the electrode spacing was reduced to 2.5 m. The inversion model including topography is displayed in Figure 23. The profile reveals the same greater

structures like the first profile. At the beginning of the profile, between 0 m and 30 m profile length, again very low resistivity values of down to 42 Ωm occurred. Yet, at this resolution it becomes clear that below this area, starting at about 6 m depth, the resistivity was about 250 Ωm. The area of lower resistivities extended to 50 m upslope, even if resistivities increased with increasing profile length and was overlain by a more resistant area starting from 25 m profile length. The highly resistant layer which was also found in the first profile is a dominant feature starting from 92 m profile length. Yet, here the resistivity reached up to 2280 Ωm. The trend of increasing thickness and increasing modelled resistivity of this layer in upslope direction became even more obvious at this resolution. Nevertheless, the modelled layer thickness was less than in the first profile as the bottom of the layer could be found between 6 m and 11 m depth in this profile. Between 230 m and 250 m profile length, a more resistant area of about 600 Ωm was present even beneath this layer. But, as this could neither be found in the first profile nor in the minimum resistivity model, it is not considered further. The highly resistant layer was overlain by a layer of very variable resistivity (50 - 500 Ωm) starting from 95 m profile length, while the less resistant areas could mostly be found towards the hilltop, interrupted by a short segment of very high resistivity (6000 Ωm) at 445 m profile length. At 92 m, a sudden lateral change in resistivity appeared. Yet, this will not be considered further as the structure does not appear when applying a different colour scheme.

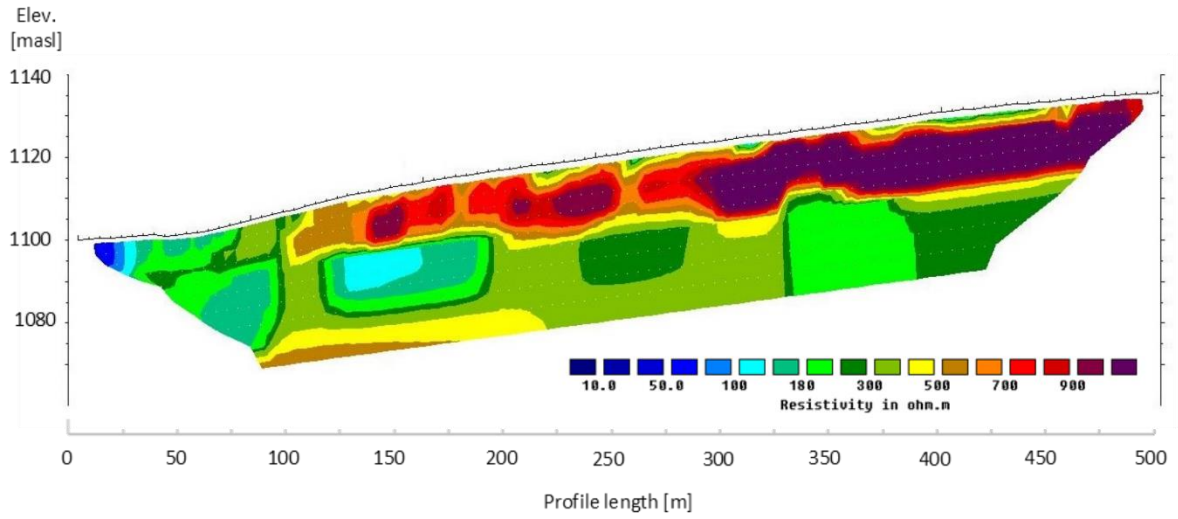

Figure 22 *Model resistivity with topography of profile N°1 at transect 1. Iteration 6 and abs. error = 2.5, unit electrode spacing 5 m. Elevation and distance along the profile are displayed in meters.*

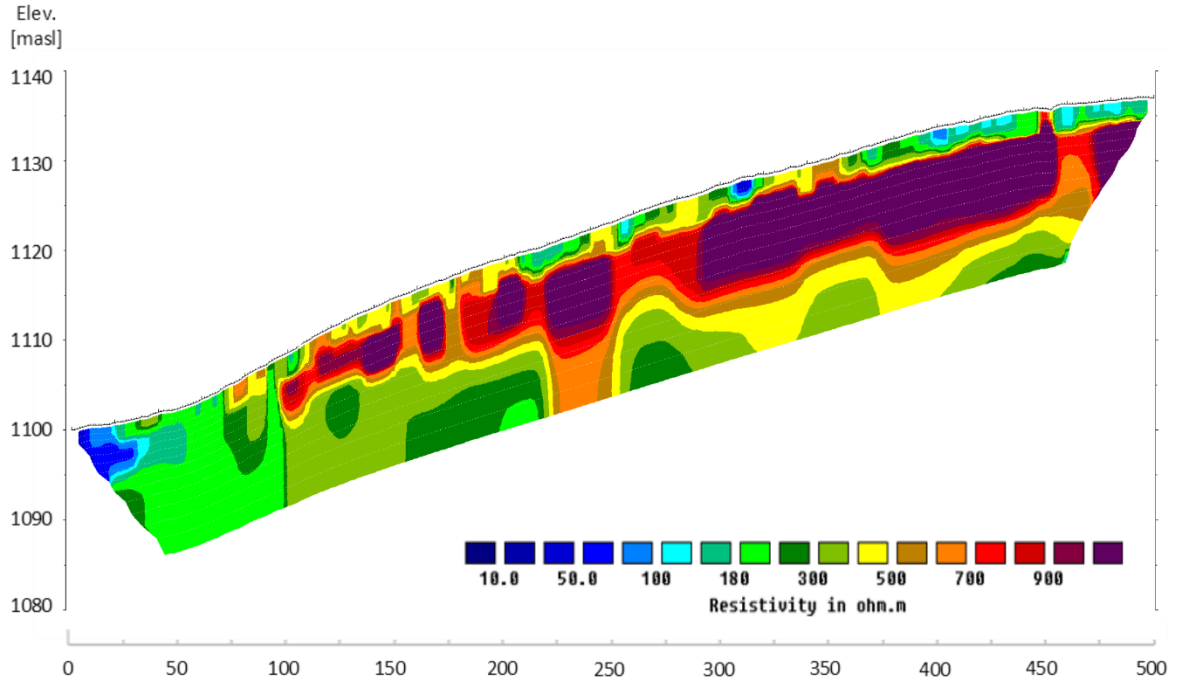

Figure 23 *Model resistivity with topography of profile N°2 at transect 1. Iteration 6 and abs. error = 2.9, unit electrode spacing 2.5 m. Elevation and distance along the profile are displayed in meters.*

The third profile was measured with an electrode spacing of 0.7 m. Due to time constraints, not the entire transect was captured but measurements stopped at 200 m profile length. The smaller spacing allowed for a better resolution of the regions closer to the soil surface. In this profile, the less resistant layer on top of the highly resistant layer reached down to a depth of about 1 m and showed a wavy surface structure (see Figure 24). This fits to the results of the drilling campaign as discussed below. Resistivity values in this layer varied between 50 Ωm and 350 Ωm, while the lowest resistivity was found at about

100 m profile length. The highly resistive layer appeared more heterogeneous in this profile and resistivity values varied between 500 Ωm and 2600 Ωm. The penetration depth of this spacing was not high enough to reach the layer of lower conductivity which was found at the bottom of the previous profiles. At the beginning of the profile, between 0 m and 60 m profile length, again a very conductive layer was found with a resistivity between 16 Ωm and 180 Ωm, while the underlying structures of higher resistivity were considered artefacts of the inversion. At this resolution it becomes apparent that this area was covered by a less conductive layer of about 1 m depth. Between 58 m and 70 m profile length, this superficial layer again showed a comparably low resistivity of 70 - 180 Ωm and in this model section there appeared to be a connection to the deeper conductive layer described before. At this slope position, this underlying layer was already more resistant than at the same depth further downslope (180 - 250 Ωm). At this resolution no sudden lateral change was modelled at 92 m profile length, but here as well the highly resistive layer was interrupted. Furthermore, the highly resistive layer reached down to about 2 - 2.50 m only and was thus more shallow than further upslope and also more shallow than it was modelled in the other two profiles.

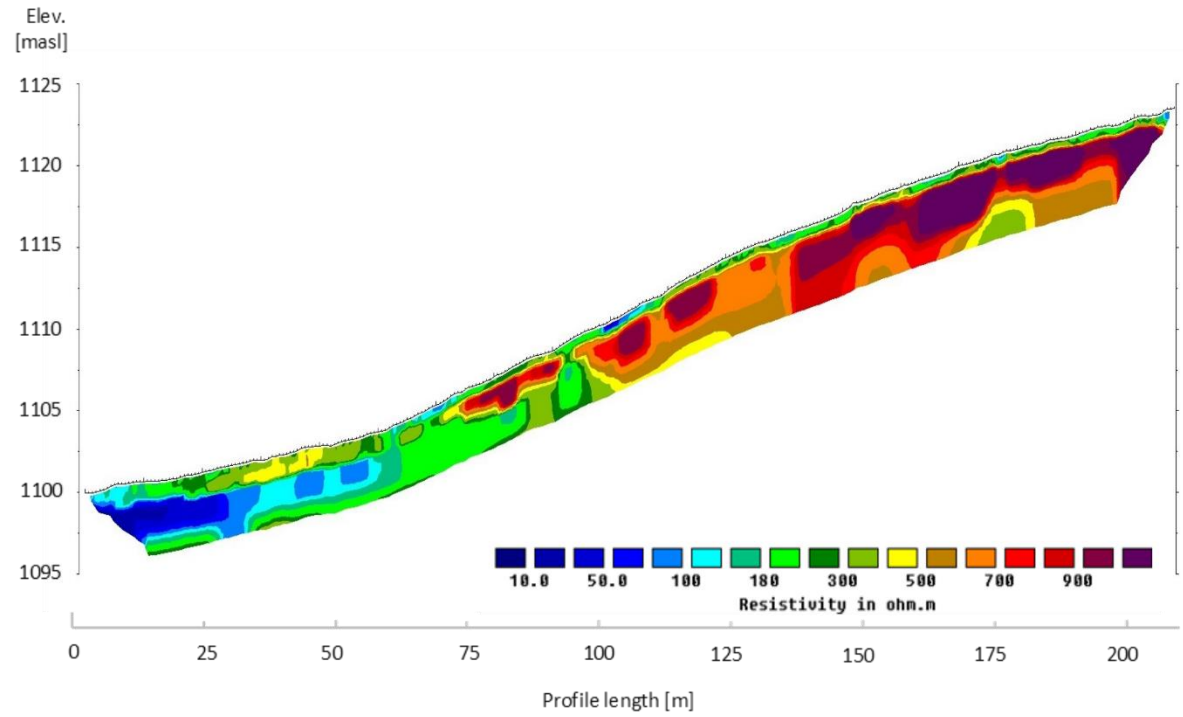

Figure 24 *Model resistivity with topography of profile N°3 at transect 1. Iteration 6 and abs. error = 2.2, unit electrode spacing 0.7 m.*

Transect 2

Many features described above could also be detected in profile N°4, where the electrode spacing was set to 0.7 m again (Figure 25). Here as well, a layer with low resistivities (about 100 Ωm) was found at the bottom of the slope. Furthermore, a near-surface layer of high resistivities (400 - 1200 Ωm) was present between 7 m and 37 m profile length while resistivities below this layer were about 200 - 400 Ωm. Nevertheless, the thickness of the resistive layer was about 1 m only and it was not continuous in upslope direction, as between 35 m and 46 m profile length a low resistivity of about 100 - 300 Ωm was modelled.

For most of the profile, the superficial layer of lower resistivities compared to the underlying areas was also present, but in this profile it was not as explicit as at transect 1. The high values below 1 m depth at the beginning of the profile were regarded as inversion artefacts.

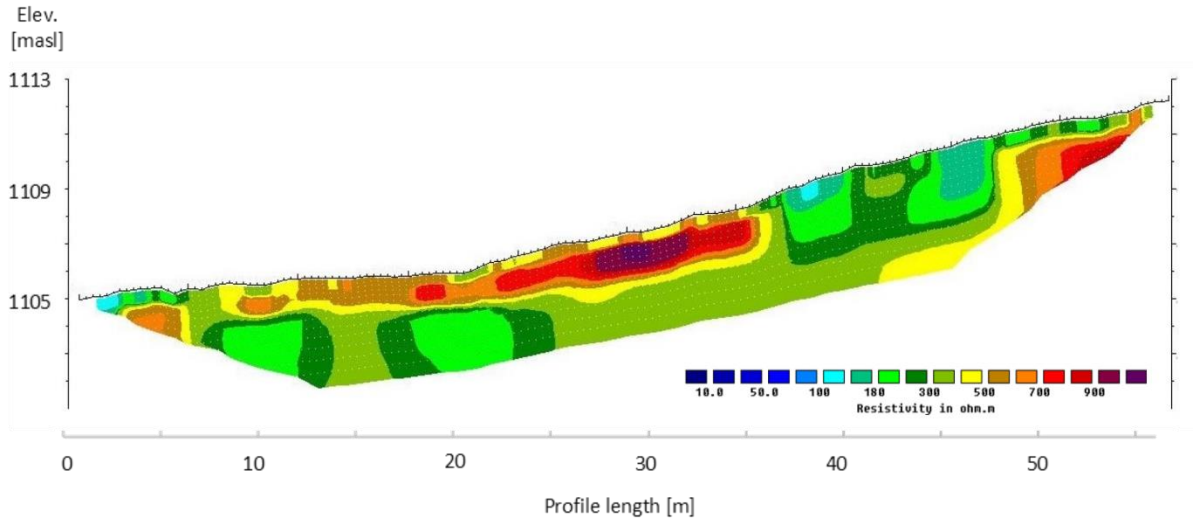

Figure 25 *Model resistivity with topography of profile N°4 at transect 2. Iteration 6 and abs. error = 1.9, unit electrode spacing 0.7 m.*

Transect 3

Transect 3 was oriented in a slope-parallel direction and intersected with transect 1 at 123.7 m profile length (95 m along transect 1) and with transect 2 at 49 m profile length (45 m along transect 2). Profile N°5 had an electrode spacing of 3.5 m. It can be seen that the near-surface layer of high resistivity also extended in a slope-parallel direction, but in this profile the resistivities were generally lower (400 - 1000 Ωm) than the resistivities measured for the profiles in upslope direction (see Figure 26). When using a different colour scheme with a higher differentiation between 200 Ωm and 400 Ωm, it became clear that the layer could be found along the entire profile, but the resistivities varied widely. As before, a layer of lower resistivities (150 - 400 Ωm) was detected below that at about 10 m depth. Starting at 70 m profile length, a resistivity of about 150 Ωm was modelled for that layer. As described for the other transects, the layer of high resistivities was covered by a layer of lower resistivities, in this model section 200 - 400 Ωm, which reached down to 5 m depth. The layer was not continuous though, as between 49 m and 72 m the high resistivity layer reached up to the surface.

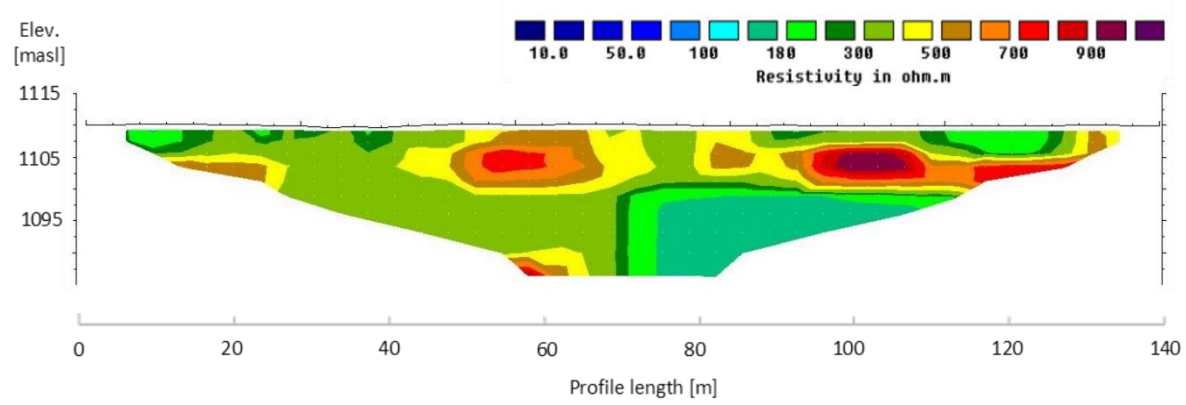

Figure 26 *Model resistivity with topography of profile N°5 at transect 3. Iteration 6 and abs. error = 3.3, unit electrode spacing 3.5 m.*

As for transect 1, measurements at transect 3 were repeated with a smaller electrode spacing of 1 m to achieve a better resolution of shallow structures (see Figure 27). At this resolution, the superficial layer of lower resistivities extended to a depth of about 1.5 m but commonly did not exceed a depth of 1 m. It can be seen that the resistivities within this layer were very variable but generally lower than for the other profiles (70 - 180 Ωm from 0 - 32 m profile length and 56 - 180 Ωm from 88 - 130 m profile length). The stretch between 32 m and 88 m profile length displayed higher values, especially between 64 m and 74 m where the resistivity reached up to over 500 Ωm. The following layer showed higher resistivities, but as could already be seen in profile N°5 the resistivity was very variable. Lower values of about 300 - 500 Ωm were detected between 0 m and 50 m, while after that resistivities between 600 Ωm and 1100 Ωm were modelled. The layer was interrupted by an area of lower resistivity (about 200 Ωm) between 115 m and 123 m, a structure which could not be found in profile N°5. The thickness of the more resistant part was also variable and reached from 2.5 m to over 5 m. Concerning the intersection of transect 2 and transect 3, the low resistivity encountered at the point of intersection in profile N°4 (150 Ωm) was not found in profile N°6 where a resistivity of about 250 Ωm was modelled. Nevertheless, the modelled thickness of the superficial layer was about 2 m for both profiles, which is deep compared to most other parts of the profile. At the intersect of transect 1 and transect 3, the thickness of the superficial layer was also identical. Yet, the modelled resistivity in profile N°6 was about 120 Ωm while it was about 200 Ωm in profile N°3, which can probably be explained by higher soil moisture values as discussed below. In profile N°6, the highly resistive layer was interrupted by an area of lower resistivity (described above) at the position of the intersect with transect 1. This interruption could not be found at the same position in transect 1, but 3 meters downslope of the intersection point.

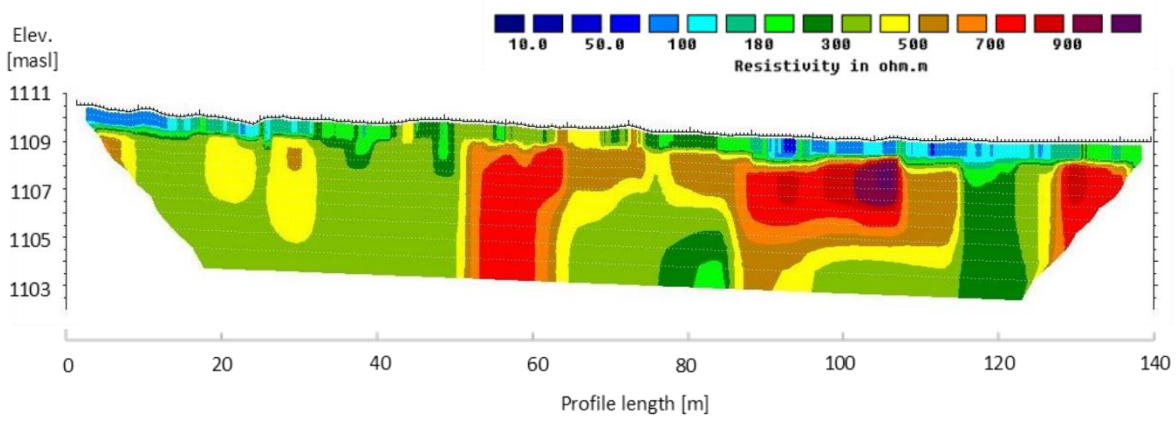

Figure 27 *Model resistivity with topography of profile N°6 at transect 3. Iteration 6 and abs. error = 2.3, unit electrode spacing 1 m.*

The transects which followed the slope gradient stretched from the fringe of the wetland to the hilltop (transect 1) or to the mid-slope position (transect 2). Therefore, they covered alluvial sediments as well as the weathering profile at the slope. At transect 1, the weathering profile was found from 52 m profile length onwards, while at transect 2, it started at about 7 m profile length. According to Chilton and Foster (1995a), the weathering body in tropical Africa can be divided into the residual soil overlying the saprolite which gradually turns into the saprock due to decreasing impact of weathering with depth before the crystalline rocks are met (see chapter 2.4). The occurrence of this typical weathering profile in Uganda was confirmed by Taylor and Howard (2000). The residual soil was apparent in all profiles as the superficial layer of low to intermediate resistivities. Nevertheless, at bigger electrode spacings either the thickness was overestimated or it was not captured at all in some parts of the profile. Considering the electrode spacings of 0.7 m and 1 m, the residual soil was modelled to be about 1 m deep, while in some positions it could reach down to a depth of 1.5 m, and in other locations the model resolution was to coarse to capture it, as it was very shallow. Thus, throughout the study area the saprolite was shown to have a wavy surface structure, which was confirmed by drilling logs, as was the average thickness of the residual soil (see chapter 5.2.1). As described above, resistivities of the residual soil displayed in profile N°6 were significantly lower between 0 m and 32 m as well as between 88 m and 130 m profile length than in profiles N°3 and N°4. As the drilling logs did not show any specific differences in soil texture (i.e., more clayey soil in these profile sections), the low resistivities were the result of higher soil moisture levels after some days of rainfall before the measurement on the 22nd of April 2017 (20 mm on 18th, 13 mm on 20th and 26 mm during the night of the 22nd). Nevertheless, soil moisture values were high along the entire profile. Between 32 m and 88 m though, there were many areas where the saprolite was found rather close to the surface, which caused the higher resistivities despite high moisture values. Yet, this does not apply to all positions. At 48 m profile length, for example, drilling logs indicated a soil depth of 90 cm and soil moisture at this position was comparable to the positions mentioned before as was the soil texture. Interestingly, in this profile the section of higher near-surface resistivities corresponded to the extent of the plot under semi-natural vegetation. So far, no explanation for this correlation was found, as soil moisture under semi-natural vegetation was actually higher during the rainy season and soil texture was not significantly different from the other plots. As described above, high conductivities of the residual soil were also found between 99 m and 106 m in profile N°3. As for profile N°6, the high conductivity at this

position was most likely caused by higher soil moisture. At this position, the land use changed from a perennial cassava field to a ploughed field where beans were cultivated. At the border line, a small terrace (a geomorphological feature referred to as "*Ackerrandstufe*" in German) developed, which increased infiltration at this position. The very high resistivities (about 800 Ωm) between 448 m and 453 m profile length of profile N°2 on the other hand, were correspond to the position of the dirt road crossing the slope, where the soil was highly compacted due to the impact of frequently passing vehicles.

It can be deducted from profiles N°1 and N°4 that the weathering body was more than 30 m deep, as no change to higher resistivities was detected at the bottom of the profiles. The area of higher resistivities at the beginning of profile N°1 was regarded to be an artefact from the inversion, as the depth of investigation (DOI) and model resolution were weak at this position (resolution per unit area index < 10). This fits to the results of 2 deep drilling logs which were sunk by the Ugandan Ministry of Water and Environment close to the profile line (drilling log descriptions can be found in Appendix 5). Both drilling logs were located at a similar slope position relative to the wetland, and at a distance of 800 m from the ERT transects. While the first drilling log (DWD12992) was sunk at the same hill, the second drilling log (DWD12993) was located at the opposite site of the wetland. The logs indicated that the crystalline rock was only met at 52 m and 45 depth at the first and second position respectively, which is well below the penetration depth of the ERT profiles measured in this study and within a range typical for tropical weathering profiles (Chilton and Foster, 1995a). According to the log description, "weathered bedrock" was met at about 38 m depth at the first and 23 m depth at the second positions. This suggests that the ERT profiles presented in this study only covered the saprolite and the residual soil. Nevertheless, the transition from saprolite to bedrock is diffuse and thus difficult to capture precisely both by drilling (Burghof, 2017) and by ERT sounding (Muiuane, 1999). All the profiles presented above were conform regarding the presence of a highly resistive layer of 600 Ωm to >1000 Ωm below the residual soil, which was followed by an area of higher conductivity (100 - 500 Ωm). In literature, a wide range of resistivity values for saprolitic material in tropical areas was found, which can be attributed to the very different characteristics of saprolites in different regions but also at the local scale. Muiuane (1999) states that the resistivity of a saprolite depends on the mineral composition and the degree of weathering of the material, which again impacts, e.g., porosity, conductivity of included soil moisture as well as moisture content, clay content and the type of clay minerals. In their frequently cited study, Palacky (1987) found 250 Ωm to be the typical resistivity for weathering profiles over African weathered granite. In saprolite which developed from granitic geology, Riddell et al. (2012) reported resistivities between 10 Ωm and 100 Ωm in South Africa, while Beauvais et al. (1999) found resistivities of 130 - 480 Ωm in West Africa, and Barongo and Palacky (1991) measured resistivities of 50 - 200 Ωm in western Kenya. Thus, the resistivities encountered in the lower layer of the profiles roughly fall in the same range and hence the geological interpretation of this layer is saprolite. The resistivities of the upper layer on the other hand were by far higher than the typical values for saprolitic material. Many authors reported similarly high resistivities for ferrungineous zones: Palacky (1987) found resistivities of over 1000 Ωm in a ferrungineous zone in lateritc soils in Brazil and Peric (1981) reported resistivities of 600 - 1200 Ωm from a Ferralite in Burundi. Kižlo and Kanbergs (2009) describe that in every soil which contains significant amounts of oxidized metals microscopic cracks and oxidation of surfaces within the limits of individual grains lead to a significant

increase in resistivity. Drilling results showed that there was no ferralite or duricrust present in the study area. Nevertheless, the share of oxidized Fe_2O_3 was about 11% in the layer of high resistivities (Burghof, 2017) and thus similar to values reported from ferrugineous zones (Chandran et al., 2004). In the lower layer, <5% Fe_2O_3 was detected. Therefore, the high share of oxidized iron might have increased the resistivity of the layer under the residual soil. Furthermore, due to the higher degree of weathering, the mineralogy of the clay mineral differed between the upper and the lower layer. The upper layer contained mostly kaolinite, which is known to have a reduced electrical conductivity as compared to Montmorrillionite (McNeill, 1980). At the same time, the layer consisted of 22 % to 40 % angular quartzites and in places rocks of up to 1 m in diameter were found when digging into that layer. When drilling down to 7 m depth at a position about 200 m northwest of the study site at the lower slope, Burghof (2017) also reported that the share of gravels decreased significantly at about 6 m depth. This corresponds to the depth where at a similar slope position the less resistive layer started in profile N°2. In addition, the lower resistivity of the upper layer at the lower slope as compared to the hilltop corresponds to a reduction of the skeletal fraction down to 20 %. Therefore, the high resistivities in the upper layer are expected to be related to the accumulation of iron oxides as well as to the high share of quartzites. As both attributes are the result of in-situ-weathering processes, the highly resistive layer is interpreted to be the upper part of the saprolite regardless of the uncommonly high resistivities. According to the results of the mineralogical analysis, Burghof (2017) deducts that the weathering of the parent material decreases with depth, which would not lead to expect the presence of quartzites in the upper and their absence (or reduced occurrence) in the lower saprolite. Therefore, the different characteristics of the upper and lower saprolite concerning the occurrence of high amounts of quartzites in the upper layer, were probably the result of heterogeneities in the parent rock material or could be related to quartz stringers which are a common feature of the local geology (GTK consortium, 2012). At the same time, a wide range of resistivities was found even within the upper saprolite. While very high resistivities were probably related to the presence of big quartzite rocks, the more conductive regions are less well understood. Having a closer look at the intersection of transect 2 and 3, for example, a segment of comparably low resistivities (150-300 Ωm) was found in all three profiles which covered this area. Yet, shallow drilling logs did not reveal higher clay contents or a lower skeletal fraction in the first centimetres of the upper saprolite. Nevertheless, the residual soil was rather deep at this position (about 1 m). This could hint to very local differential weathering which could be caused either by heterogeneities in the parent material or by preferential infiltration of water at this point or most likely the combination of both. Thus, it can be assumed that throughout the study area, there are regions where an enhanced infiltration of rainwater into the upper saprolite can occur.

When compared to the resistivities of saturated saprolitic material reported in literature, the resistivities of the lower saprolite were too high to suggest the presence of groundwater. Anudu et al. (2014), for example, found resistivities of 29 - 116 Ωm in a water saturated highly weathered gneiss in Nigeria. Furthermore, the structures displayed in the sounding profiles did not hint to the presence of intermediate water bodies within the saprolite. Nevertheless, while installing a deep water pump at the experimental site, the drilling company hit an intermediate water body at about 27 m depth. Therefore, it has to be concluded that smaller water bodies within the saprolite were not captured by the ERT

sounding. This is a common issues in groundwater exploration in highly weathered material and can be explained by suppression problems, i.e., a thin highly conductive layer situated between two layers of similar resistivity is not captured in the sounding curve (Muiuane, 1999; Sanuade et al., 2019). According to Blume and Meerveld (2015 and Muiuane (1999), combining direct methods with GPR (ground penetrating radar) or EM (electromagnetic geophysics) measurements can be an option to overcome this problem, but the implementation of further geophysical methods was not possible within the scope of this work. Another factor which hindered the detection of intermediate water bodies were the high resistivities encountered in the upper saprolite. This dampens the penetration of the electric current to deeper areas and thus the model resolution of the lower saprolite was rather limited.

The extent of the highly conductive area at the beginning of transect 1 and transect 2 corresponded well to the extent of the wetland observed in the field. Therefore, this part of the profiles is interpreted as the wetland aquifer in the alluvial sediments at the valley bottom. The ERT profiles allowed several conclusions regarding the hydrogeological characterisation of the wetland. Firstly, the profiles indicated that the aquifer in the valley sediments reached down to a depth of about 7 m at the wetland fringe. Secondly, the higher resistivities at the soil surface hint to the fact, that the shallow aquifer in the wetlands soils was separated from the aquifer in the valley sediments. This was also suggested by Burghof (2017) based on water chemistry and groundwater pressure heads. The increasing conductivity of the material towards the centre of the wetland probably resulted from higher degrees of saturation of the valley sediments further inside the wetland. As described above, the transition from the wetland to the upland geology was characterised by low resistivities (about 200 Ωm) of the lower saprolite which persisted up to 84 m profile length. The gradual decrease of the resistivity from the wetland towards the upland does not suggest the presence of a paleo-dambo clay layer demarking a sharp boundary at the transition between wetland and upland geology as described in McFarlane (1992). Between 57 m and 67 m profile length, also the upper saprolite was significantly more conductive than further upslope. Between 67 m and 91 m, the resistivities of the upper saprolite were similar to those further upslope, but the layer of high resistivities only reached down to a depth of between 2 m and 3 m. At the same time, low resistivities of about 100 Ωm were measured in the residual soil. Shallow drilling logs revealed that up to 75 m profile length, the upper saprolite was covered by a sandy loam layer and that both, the sandy loam layer and (parts of) the saprolite were water saturated (see chapter 5.2.1). Therefore, the low resistivities of the surface layer were most likely caused by the very wet conditions. Interestingly, this was not captured by profile N°4 at transect 2, even if field observations revealed the presence of a water saturated sandy loam layer on top of the saprolite at the slope toe (12 - 18 m profile length). Nevertheless, less interflow was measured at this transect compared to transect 1, as described in chapter 6.2.1. At transect 1, a drilling log was sunk down to a depth of 2 m below surface at 68 m profile length. The results showed that below 1.5 m depth, dry conditions were met again, which was supported by the fact that the colour of the upper saprolite changed from grey to beige-orange (see chapter 5.2.1). This also fits to the results of the ERT measurements, as, at this position, a more resistive layer was still found below the residual soil. Unfortunately, drilling logs further down slope could not be sunk down to that depth. Therefore, it is not known whether the low conductivities of the upper saprolite towards the wetland indicated the absence of dry regions in the upper saprolite and hence a possible discontinuity of the clay-muscovite layer (see

chapters 5.2.1 and 6.2.1) at this slope position. At 58 m profile length, the ERT profile suggested a connection of the residual soil and the aquifer in the valley sediments. Nevertheless, there is a high uncertainty related to the interpretation of structures of such small magnitude from resistivity sounding and the connection might as well be the result of the inversion process. No deep drilling logs or piezometer data were available at the slope toe. Therefore, it cannot be confirmed whether the low resistivities of the lower saprolite were caused by saturated conditions and thus displayed the position of the deep aquifer. Nevertheless, resistivities of water saturated granitic saprolite reported in literature were an order of magnitude lower than the resistivities found here, as was described before. Therefore, the resistivities of the lower saprolite could also indicate higher moisture conditions due to, e.g., capillary effects in the clayey matrix related to the proximity to the wetland or to the deep groundwater. At the same time, a change in the composition of the saprolite could be the reason behind the change of resistivities at this slope position. Deep drillings logs and further hydrometric data sets would be needed for a sound interpretation of the resistivity values found at this slope position and thus no conclusions regarding the connection of the regional and the local aquifer at the slope toe could be drawn from the ERT measurement. This is a common problem. As Blume and Meerveld (2015) describe, near surface geophysical measurements are an important addition to conventional hydrological approaches as they provide information on bedrock topography, soil layering and moisture content. Nevertheless, it is an indirect method and the challenge lies in the translation of the geophysical data into hydrologically relevant information.

5.2 Soil properties

This subchapter describes selected physical and chemical soil properties of the soils along a transect stretching from the wetland to the hilltop and at the single measuring points. The data offer the foundation for the interpretation of the dynamics of soil moisture and nitrate content in the topsoil as well as the deduction of water and nitrate fluxes along the slope in the following chapters (chapter 6 and chapter 7).

5.2.1 Physical soil properties

Depth of the soil body, soil texture and soil colour

The depth of the soil body at the experimental site varied widely between 25 cm and 150 cm. Variations were found at a very small scale, i.e., differences in depth of up to 1 m were found within a few meters lateral distance. Thus, as already suggested by the ERT measurements (see previous chapter), drilling results revealed an undulating surface of the upper saprolite in both, slope parallel and upslope direction.

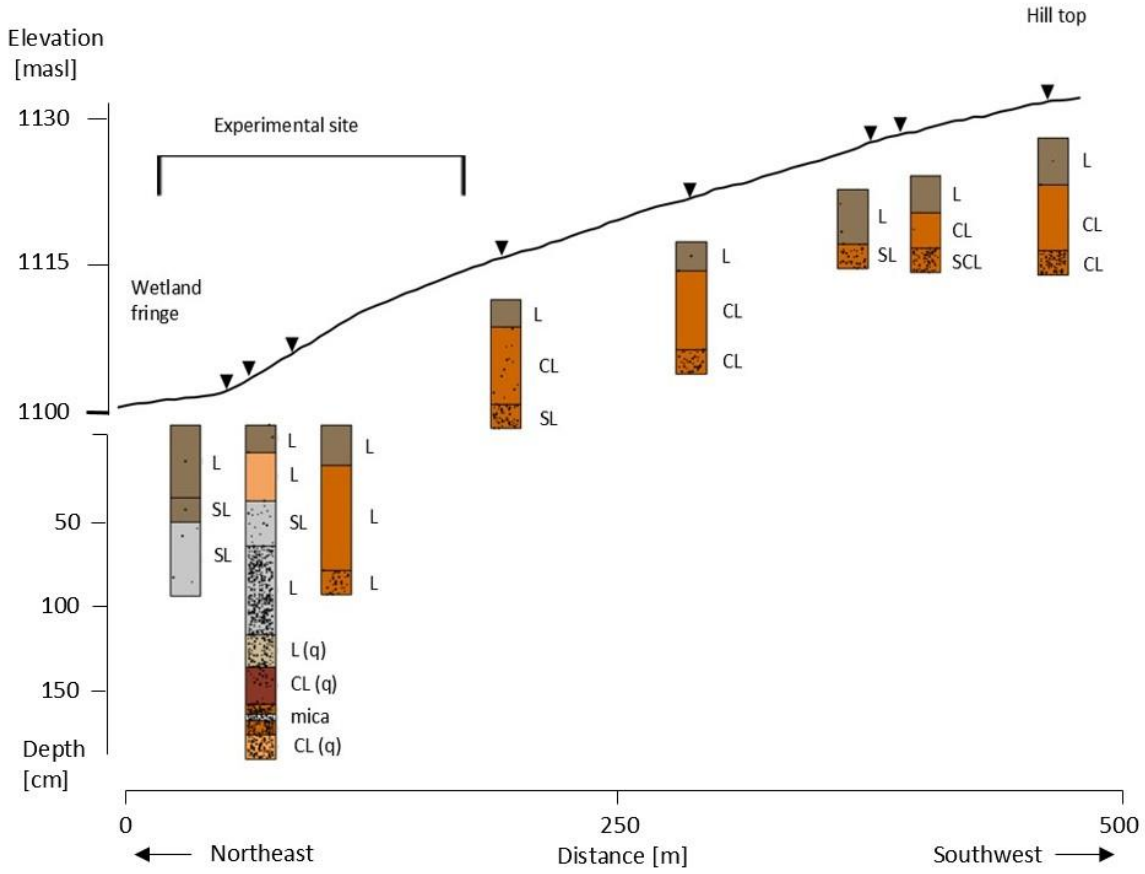

Figure 28 *Soil profiles along a catena stretching from the wetland fringe to the hilltop. The catena follows the ERT transect N° 1. (q) indicates that texture was determined manually in the field and not via laser diffraction in the laboratory. The colours are chosen according to qualitative observations in the field.*

Figure 28 shows the soil profiles along a catena stretching from the wetland fringe to the hilltop. Here, as in the following graphs, soil texture classes are abbreviated by capital letters (L= loam, SL= sandy loam, CL= clay loam, SCL= sandy clay loam). As can be seen, the study area was characterised by loamy soils with varying shares of clay (4 - 36 %) and sand (26 - 80 %). The clay content of the B horizon increased towards the hilltop. At the slope toe, a sandy loam layer was found on top of the saprolite, while at the wetland fringe a sandy loam layer was found on top of a layer of clay loam (see Figure 29). The soil profiles at the slope toe and at the wetland fringe showed hydromorphic features, while the upland soils were characterised by ferralisation processes. Beneath the soil body, the upper saprolite was met, which was characterised by a loamy matrix and a high skeletal fraction of 12 - 64 % (mean 39 %). The matrix of the upper saprolite also consisted of variable amounts of sand and clay but the composition cannot be related to a certain slope position. A detailed description of the mineralogy of the saprolite can be found in Burghof (2017) and an overview of the soil texture at each measuring points is given in Appendix 6. In the following section, the soil profiles at the wetland fringe and at the slope toe are analysed in more detail.

Figure 29 shows the texture and the soil colour of the drilling logs at the wetland fringe. All horizons were characterized by redoximorphic features, which fits well to the position at the wetland fringe where the soil was saturated or near saturation during most days of the year. The profiles show that at all three measuring points the sandy loam layer continued into the wetland. With increasing depth, the clay

content of the sandy loam layer increases as well, which is most likely the result of lessivage. At point W2 and point W0, a beige-grey marbled clay loam layer was found below the sandy loam layer. This layer was also described in Burghof (2017) and is expected to separate the aquifer in the valley sediments from the shallow aquifer in the wetland soils.

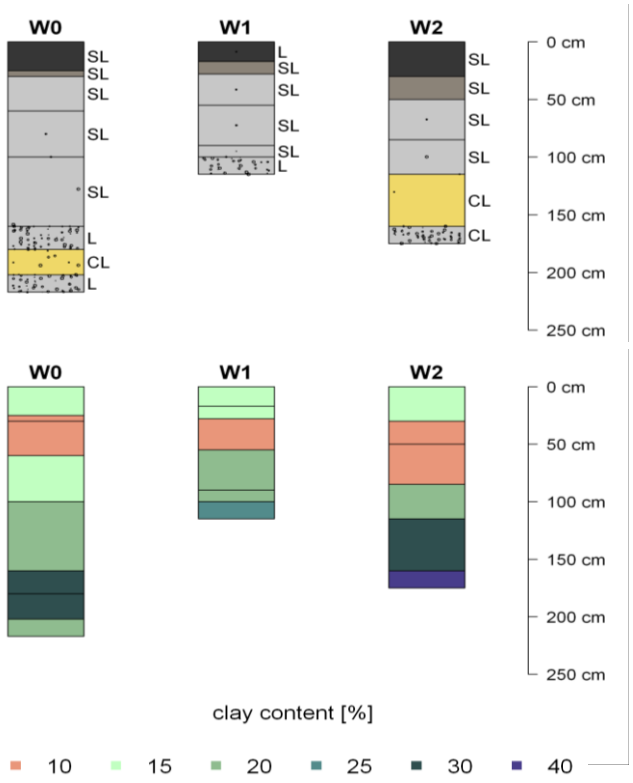

Figure 29 *Soil profiles of the measuring points at the wetland fringe. The upper panel shows the soil colour (as observed qualitatively in the field), the skeletal fraction symbolized by the share of the plot area covered by the black circles and the soil texture. The lower panel displays the clay content in the different soil layers.*

Figure 30 shows the drilling log profiles of the measuring points at the slope toe. At all three measuring points, both, the uppermost part of the saprolite as well as the soil layer on top of it, were characterised by redoximorphic features, as the grey soil colour indicated that these layers experienced water saturated conditions during most of the time (Scheffer et al., 2010). At P10 and P11, the submerged layer had a sandy-loam texture and was covered by a transitional horizon (AB) and a humic A-horizon on top. The reddish colour of the AB horizon at P10 indicates that here oxidization of mineral particles had started. At P12, a yellowish-brown sandy loam layer was found below the AB horizon. According to the colour, this layer was not exposed to continuous saturation but also not characterized by oxidation processes unless the mineral composition was different than at the other slope positions, i.e., the layer contained more goethite, which oxidizes to a more yellowish colour (Scheffer et al., 2010). Unfortunately, the mineralogical composition of the soils is not known. Burghof (2017) hypothesized that the sandy loam layer at the slope toe was of colluvial origin. The fact that soil-forming processes were not as advanced here as further upslope supports this hypothesis as does the continuity of the sandy loam layer into the wetland, as described above. At the same time, colluvial deposition is not the dominant recent process, as a humic A-horizon has already formed. At P12, the saprolite was covered with a loamier layer. The

reddish-orange stains in that layer show that water saturation in this layer took place periodically. At the same time, the clay content of the matrix of the uppermost saprolite was significantly higher (21 % compared to 7 % at P10 and 13 % at P11) and the skeletal fraction significantly lower than at the other measuring points at the slope toe (12 % compared to 52 %). At P10, the drilling was continued until 2 m depth (about 1.20 m into the saprolite). This revealed that a layer with a higher clay content, characterised by an intensely dark reddish colour and a high skeletal fraction, was located below the hydromorphic layer. Yet, besides the subangular quartzites which were also present in the layer above, here also highly weathered quartzite residues were present. Beneath that, a layer of horizontally layered muscovite was found, which also showed signs of oxidation, especially at the upper and lower boundary. Below this layer another pale reddish clay loam with a high skeletal fraction (see Figure 31 d-f) was found. The present stratigraphy shows that the impoundment of water was favoured by the horizontally layered muscovite. This probably led to an intense weathering of that layer, resulting in the dark-reddish clay loam, which at present acts as water-impermeable layer. Nevertheless, the dark reddish colour indicates that this layer is temporarily under the influence of water, as reduced metal minerals from the layer on top of it were probably washed in and then oxidized.

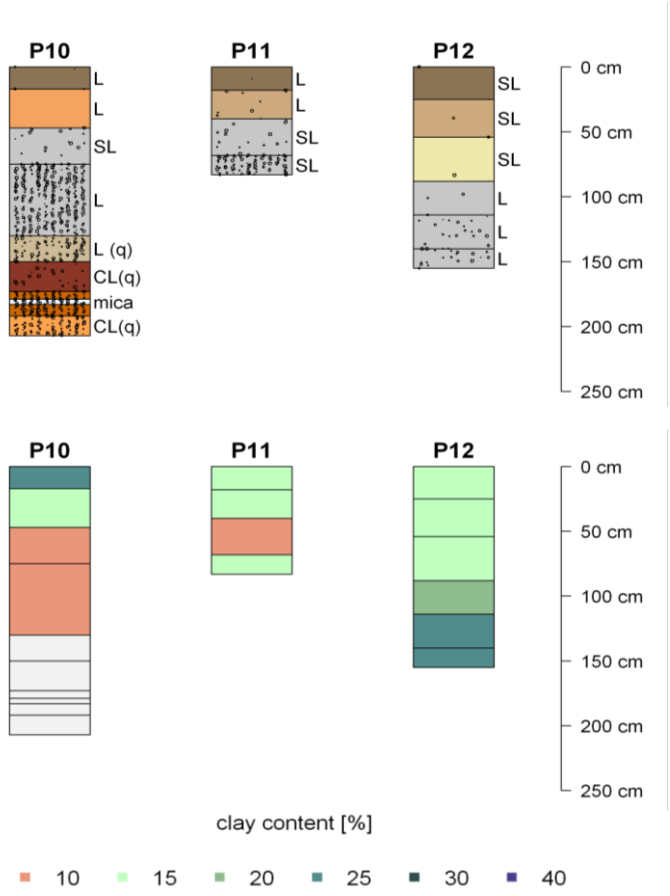

Figure 30 *Soil profiles of the measuring points at the slope toe. The upper panel shows soil colour (as observed qualitatively in the field), texture and skeletal fraction, while the lower panel displays the clay content in the different soil layers. Note that the last four horizons at point P10 were analysed manually in the field, so clay percentages are not included in the figure.*

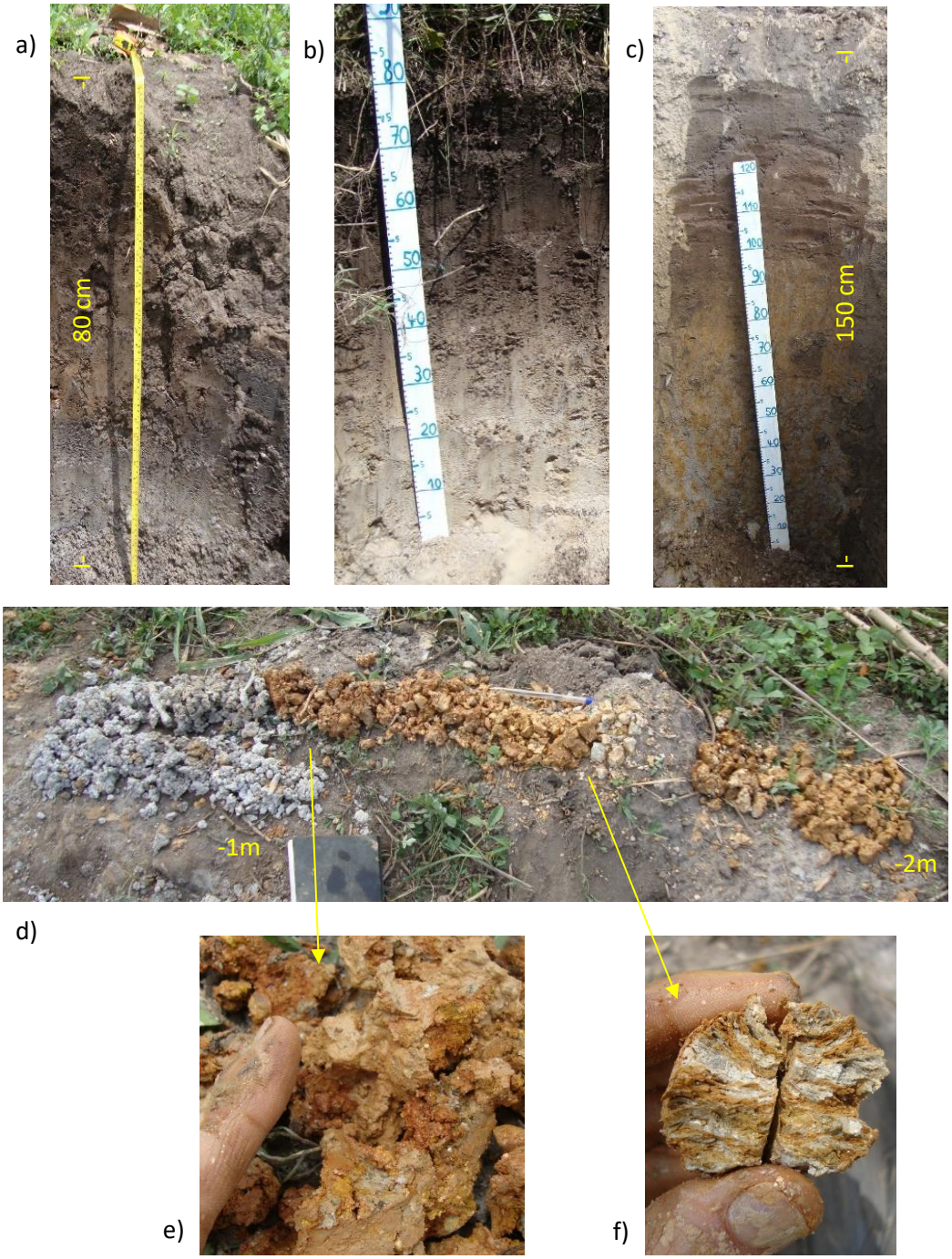

Figure 31 *Soil profiles at P10-12 (a-c) and drilling log of the lower part of the profile at P10 (1 m - 2 m depth) (d), highly weathered quartzites in dark-reddish matrix (e) and horizontally layered muscovite (f).*

A closer look: upslope-extent of the sandy loam layer at the slope toe

As can be seen from the data presented above, the greyish sandy loam layer was found only at the slope toe but not at the lower slope position. Therefore, a qualitative drilling campaign (samples were not taken to the laboratory for analysis) was conducted to gain a better understanding of the extent of the sandy loam layer and the corresponding water table found at the slope toe. The profiles along the transect

upslope of P11 are displayed in Figure 32 and were comparable to the profiles along the transect upslope of P10. The results show that the greyish sandy loam layer could be found up to 17 m upslope from the wetland fringe, and that the water table in the sandy loam layer had the same extent. At this position, the soil colour changed to pale beige - brown while the texture remained a sandy loam until the upland soil conditions described before were met about 10 m further upslope, i.e., reddish loamy soils. The results confirm that interflow passed through deeper areas of the saprolite along the slope and not at the soil - saprolite interface. Nevertheless, the connection of interflow pathways to the sandy loam layer at the slope toe remains unknown. The pale colours of the dry part of the sandy loam layer could either be the results of increased leaching of metallic minerals due to the higher porosity of the soil or suggest that in former times the water table reached further upslope. The course of the sandy loam layer connecting the slopes and the wetland also supports the hypothesis of Burghof (2017) that this layer is of colluvial origin and was deposited after the valley sediments, as described by Wright (1992) for similar wetlands. Therefore, following the two models introduced by McFarlane (1992), see chapter 2.1, interflow from the slopes is likely to contribute water to the shallow aquifer in the wetland soils.

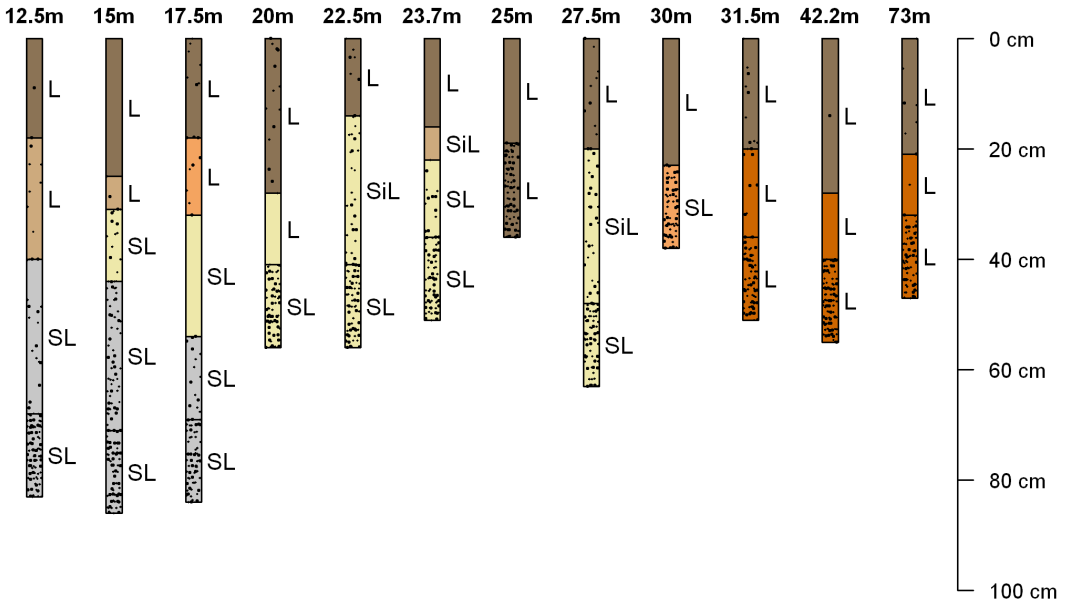

Figure 32 Results of the drilling campaign following the sandy loam layer from the slope toe (P11) to the lower slope position. The positions relate to the length along the ERT profile N°4 (see *Figure 25*). As before, soil colours are chosen as qualitatively observed in the field. Except for the first and the last profile, soil texture was determined in the field and not via laser diffraction.

Bulk density

At the upland positions, bulk density at the study site varied between 1.19 g/cm³ and 1.54 g/cm³. Bulk density of the upper subsoil layer was significantly higher than the bulk density of the A horizon and varied between 1.48 g/cm³ and 1.93 g/cm³. There was no significant difference between the three land use types considering the bulk density of the topsoil as well as the subsoil.

Field-saturated hydraulic conductivity (K_{fs})

As described in chapter 4.3.3, field-saturated hydraulic conductivity of the soil surface, the topsoil and the subsoil as well as of the upper saprolite was determined via infiltration trials at the mid-slope position of each land use type (see Table 3). At the plot under crop production and under bare fallow, K_{fs} at the soil surface was very similar to K_{fs} in the topsoil, while it was lower in the subsoil. At the plot under semi-natural vegetation, K_{fs} was an order of magnitude higher at the soil surface than in the topsoil and increased slightly in the subsoil. At the soil surface and in the topsoil, K_{fs} was slightly higher at the plot under bare fallow than at the plot under crop production, while this trend was reversed in the subsoil. K_{fs} was highest at the soil surface of the plot under semi-natural vegetation. Higher conductivities in the topsoil compared to the subsoil can be explained by the lower bulk density as well as by a higher share of macropores created by soil organisms and plant roots in that layer (Weil and Brady, 2017). The high infiltration capacity of the soil surface at the plot under semi-natural vegetation was probably caused by the lack of siltation at the soil surface due to the protective effect of the dense plant cover. The lower K_{fs} in the topsoil is surprising though, as more macropores would be expected at this land use type (Jarvis, 2007). The fact that no tillage or weeding operations were applied at that land use type could have influenced the field-saturated hydraulic conductivity but as the bulk density was comparable to that of the plot under crop production this effect does not seem to be prominent. The higher K_{fs} values at the soil surface of the plot under bare fallow as compared to the plot under crop production were also unexpected, as more siltation and hence less infiltration would be expected at the plot under bare fallow, and also more surface runoff was measured under this land use type (see chapter 6.3). Here, the difference in soil texture at the position the measurements were conducted was probably the vital factor, as the topsoil at the plot under crop production had a higher share of clay. This soil texture was not characteristic of the whole area though, so no general conclusions regarding the potential infiltration at this land use type can be drawn from the infiltration trials. At the plot under semi-natural vegetation and under bare fallow, K_{fs} of the upper saprolite was significantly higher than in the subsoil, while there was no difference at the plot under crop production. Yet, at the plot under crop production, only one measurement could be conducted while at the plot under semi-natural three measurements were conducted, which revealed some variability between the repetitions. At this depth, the land use type is not expected to influence the saturated conductivity significantly, so differences in K_{fs} between the measuring points resulted from inherent attributes of the saprolite, such as the degree of weathering, the occurrence of macropores and the soil texture. The higher saturated conductivity of the upper saprolite compared to the subsoil affected the nature of interflow processes, as discussed in chapter 6.2.1. During their study at the slopes of the lake Victoria basin, Mulumba (2004) found similar values of K_{fs} of the topsoil ranging from 32 mm/hr to 58 mm/hr, which they classified as moderately low for tropical soils. Bamutaze et al. (2010) found big variations of saturated conductivity during their study in Eastern Uganda, covering values of 12 mm/hr to 3600 mm/hr, which they attributed to a high spatial variability concerning the presence and characteristics of macropores. While Mulumba (2004) did not find a significant difference between various land use types (forest, bush fallow and annual crops), they reported a significant difference between slope positions. In addition, Weil and Brady (2017) describe saturated conductivity to be the most variable physical soil property at very small scales. Therefore, one critical

shortcoming of the infiltration trials in this study is the weak spatial coverage, as only one position per land use type was investigated and neither the different slope positions nor the variable soil textures within the fields were covered. Nevertheless, even with a more comprehensive spatial design, the high spatial variability always limits the validity of field measurements of K_{fs} for the characterisation of the hydrological properties of a hillslope (Jackisch et al., 2017). In the present study, the aim of the infiltration trials was not to find universal characteristics of the soils in the experimental area but to detect major differences in K_{fs} between the different soil layers, which enable a better understanding of pathways and processes related to the generation of subsurface flow. To that end, the results presented before add valuable insights.

Table 3 *Field saturated conductivity K_{fs} [mm/hr] and coefficient of variation, bulk density and texture of the soil surface, topsoil, subsoil and the upper saprolite at the mid-slope position of each land use type.*

		Crop production	**Semi-natural vegetation**	**Bare fallow**
Soil surface	**Mean**	47 mm/hr	131 mm/hr	62 mm/hr
	CV	13 %	22 %	26 %
Topsoil	**Mean**	55 mm/hr	25 mm/hr	63 mm/hr
	CV	10 %	6 %	23 %
	BD	1.25 g/cm³	1.28 g/cm³	1.37 g/cm³
	Texture	Clay loam	Loam	Loam
Subsoil	**Mean**	29 mm/hr	35 mm/hr	18 mm/hr
	CV	69 %	38 %	13 %
	BD	1.56 g/cm³	1.52 g/cm³	1.54 g/cm³
	Texture	Clay loam	Loam	Clay loam
Upper saprolite	**Mean**	31 mm/hr	70 mm/hr	113 mm/hr
	CV	-	87 %	14 %
	BD	-	-	-
	Texture	Loam	Loam	Sandy loam

5.2.2 Chemical soil properties

Carbon content and C/N ratio

Mean carbon contents and C/N ratios in the topsoil and in the subsoil at the different slope positions are shown for each land use type in Table 4 and Table 5 respectively. Carbon was measured as C_{total}, but as the parent-material was non-calcareous and liming practices were not common in the region, the values are expected to roughly represent C_{org}. In the topsoil, the mean organic carbon content was about 2 % at the plot under crop production and under semi-natural vegetation and slightly lower at the plot under bare fallow with 1.6 %. At the plot under semi-natural vegetation and bare fallow, carbon contents at the slope toe were lower than at the other upland position, while the highest content was found at the mid-slope position. Yet, none of the differences was statistically significant. C/N ratios were around 14 at all land use types, while overall slightly narrower ratios were found at the plot under bare fallow. No trend regarding differences between the slope positions could be detected. Nevertheless, a ratio of 12 was measured at the mid-slope position at the plot under crop production, while ratios of 10 and 17 were found at the slope toe position at the plot under semi-natural vegetation and bare fallow respectively. Carbon content in the subsoil was significantly lower for all land use types. Very low carbon contents of about 0.1 - 0.2 % were found in the subsoil of the wetland soils and at the slope toe. At the upslope positions, more carbon was found in the subsoil at the plot under semi-natural vegetation than at the other two land use types. At the plot under crop production, the C/N ratios were slightly narrower than in the topsoil, while at the plot under bare fallow and semi-natural vegetation, they were slightly wider than in the topsoil.

Robertson and Groffman (2015) state that as a rule of thumb C/N ratios below 25 stimulate mineralisation of soil organic matter and Weil and Brady (2017) describe that at C/N ratio below 20, nitrogen is rather released into the soil solution than immobilized by micro-organisms. Thus, the present data show that at all positions (with the exception of the subsoil at the slope toe position at the plot under semi-natural vegetation) mineralization of nitrogen was stimulated and nitrate was possibly released into the soil solution. Nevertheless, Zech et al. (1997) found that even if narrow C/N ratios promote mineralization and increase turnover rates, climatic factors like rainfall and temperature are more important than chemical parameters like the C/N ratio or the soil ph. The C/N ratios and carbon contents in the topsoil of the upland soils found in the scope of this study were comparable to values reported in literature. Aitkenhead and McDowell (2000), for example, found C/N ratios of 14 for tropical savannah soils, while Pincus et al. (2016) reported C/N ratios of 12 and carbon contents of 2 % for agricultural fields in central Uganda. Fatumah et al. (2021), on the other hand, found higher carbon contents of about 5 % and highly variable C/N ratios depending on the cropping system during their study in the Wakiso district (central Uganda). They reported a C/N ratio of 9 under maize intercropped with beans and of 20 under sole crop sweet potato, while they found a C/N ratio of 17 under semi-natural vegetation. These differences were not found in the present study. The carbon content of the A horizon in the wetland was in the same order of magnitude as the values reported by Sakané et al. (2011), who found a mean carbon content of 2.4 % during their inventory of 44 inland valley wetlands in East Africa. The mean C/N ratio of 9.5 reported in their study though, is narrower than in the present study. Nevertheless, Touré et al. (2009) reported a

C/N ratio of 13 and a carbon content of 2.04 % for their study in an inland valley wetland in the Ivory Coast, which fits well to the results presented here.

Table 4 *Mean carbon contents and C/N ratios of the A horizon at the different slope positions and at each land use type. For the lower slope position (LS), the measuring points downslope of the pits (LS-X1), measuring points at the same position at the reference plot (LS-1) and measuring points upslope of the pits including reference plot positions (LS-2) are shown separately.* C_{total} *was determined, but as the parent-material was non-calcareous and liming practices were not common in the region the values are expected to roughly represent* $C_{org.}$

Topsoil	**Crop production**		**Semi-natural vegetation**		**Bare fallow**	
	C [%]	**C/N ratio**	**C [%]**	**C/N ratio**	**C [%]**	**C/N ratio**
Mean (upland)	2.1	14	1.98	14	1.61	14
Wetland	1.79	15	-	-	1.91	14
Slope toe	2.36	14	1.51	10	1.38	17
LS-X1	2.1	14	2.02	14	1.37	13
LS-1	1.89	15	1.99	16	1.66	14
LS-2	2.09	14	1.93	14	1.44	13
Mid-slope	2.2	12	2.2	14	2.23	14

Table 5 *Mean carbon contents and C/N ratios of the B horizon at the different slope positions and at each land use type. For the lower slope position (LS), the measuring points downslope of the pits (LS-X1), measuring points at the same position at the reference plot (LS-1) and measuring points upslope of the pits including reference plot positions (LS-2) are shown separately.*

Subsoil	**Crop production**		**Semi-natural vegetation**		**Bare fallow**	
	C [%]	**C/N ratio**	**C [%]**	**C/N ratio**	**C [%]**	**C/N ratio**
Mean (upland)	0.65	13	0.76	15	0.51	14
Wetland	0.13	18	-	-	0.11	16
Slope toe	0.21	13	0.12	26	0.21	18
LS-X1	0.62	13	0.9	15	0.46	14
LS-1	0.62	14	0.58	14	-	-
LS-2	0.64	12	0.76	14	0.52	14
Mid-slope	0.8	13	1.02	17	0.75	11

Soil pH

Soil pH in the study area was between 5 and 6 (see Table 6 and

Table **7**). In the A horizon, soil pH was slightly lower for the plot under bare fallow. In the B horizon, the pH at the plot under semi-natural vegetation was slightly higher than at the other two land use types. At the plot under crop production, the pH was slightly lower in the B than in the A horizon. Overall, no significant difference between the different slope positions was found, but at the plot under bare fallow, the pH was slightly higher in the wetland and at the slope toe than at the upslope positions.

The Δ pH values serve as an indicator for the net charge of the colloidal system of a soil (United States Department of Agriculture, n.d.). For all measurements points in both, the A and the B horizon, Δ pH values were negative. This means that the colloidal system had a net negative charge and thus leaching of nitrate can be expected. Nevertheless, Black and Waring (1979) found, that up to a strongly negative Δ pH of > -1.5, adsorption of nitrate to positively charged soil colloids, which can occur in variable-charge soils with a high share of kaolinites in tropical areas (Wong et al., 1990), can still be expected. In addition, Sheppard et al. (2001) did not find a correlation between negative Δ pH values and the absence of nitrate accumulation in the subsoil during their study in Western Kenya. Hence, the data presented here show that even if nitrate leaching is likely to occur, the adsorption of nitrate anions to positively charged soil colloids cannot be ruled out.

Table 6 *pH and Δ pH values of the A-horizon at the different slope position for the three land use types.*

A-horizon	Crop production		Semi-natural vegetation		Bare fallow	
	pH (1:1 H_2O)	Δ pH	pH (1:1 H_2O)	Δ pH	pH (1:1 H_2O)	Δ pH
Mean (upland)	5.6	-0.72	5.6	-0.95	5.2	-0.69
Wetland	5.8	-0.95	-	-	5.7	-1
Slope toe	6	-0.7	5.4	-1	5.5	-1.1
LS-X1	5.5	-0.77	5.6	-0.93	5	-0.7
LS-1	5.6	-0.63	5.7	-1.03	5.1	-0.7
LS-2	5.5	-0.64	5.6	-0.88	5.2	-0.63
Mid-slope	5.7	-0.87	5.5	-1	5.2	-0.67

Table 7 *pH and Δ pH values of the B-horizon at the different slope positions for the three land use types.*

B-horizon	Crop production		Semi-natural vegetation		Bare fallow	
	pH (1:1 H_2O)	Δ pH	pH (1:1 H_2O)	Δ pH	pH (1:1 H_2O)	Δ pH
Mean (upland)	5.1	-0.9	5.5	-1.15	5.1	-0.88
Wetland	5.6	-1.62	-	-	5.5	-1.5
Slope toe	5.9	-1.8	5.9	-1.6	5.7	-1.67
LS-X1	4.9	-0.8	5.7	-0.93	4.6	-0.3
LS-1	5	-0.85	5.4	-1.18	-	-
LS-2	5.1	-0.88	5.5	-1.17	5.1	-0.79
Mid-slope	5.2	-0.92	5.3	-1.23	5.2	-0.78

6 Water dynamics

This chapter presents the findings on soil moisture dynamics on the slopes (chapter 6.1) as well as on interflow dynamics (chapter 6.2) and surface runoff (chapter 6.3). The data are interpreted to deduct processes related to (sub)surface runoff generation and routing and to characterise the hydrological connection of the slopes and the valley bottom wetland.

6.1 Soil Moisture

Soil moisture in the topsoil was measured every two to three days at four depths and different slope positions ranging from the wetland to the middle of the slope (see Figure 12). In the following subchapter, the data are analysed regarding the in-situ dynamics as influenced by the establishment of three land use types (bare fallow, semi-natural vegetation and crop production), seasonality and the effect of different soil depths overlying the saprolite. In addition, the soil moisture dynamics at different slope positions and on plots interrupted by shallow dug-out pits are interpreted regarding the presence of shallow subsurface flow in the soil above the saprolite.

6.1.1 In-situ dynamics

Seasonality of moisture dynamics

This section describes the soil moisture in the upland as well as in the wetland during rainy and dry seasons, and reflects on the differences between the two land scape positions as well as on the moisture variability between the measuring points in the wetland.

Figure 33 shows the mean soils moisture in % saturation (see chapter 4.4.1) of all upland positions for each land use type at 10 cm, 20 cm, 30 cm and 40 cm depth. The effect of dry and rainy seasons could be seen for all upland positions, yet, the difference was not genuinely significant. The strongest effect was found at 10 cm depth where soil moisture ranged from 33 - 75 % sat. in the rainy season and from 22 - 60 % sat. in the dry season. At 20 - 40 cm depth, soil moisture showed less fluctuation between as well as within the seasons. Here, values range from 46 - 98 % sat. in the rainy season and from 38 - 86 % sat. in the dry season. Moisture conditions were very similar during all four dry seasons as well as during three of the rainy seasons investigated in this study. The second rainy season 2016, though, was exceptionally dry as there was only little and irregular rainfall due to the impact of the La Niña phenomenon on East Africa. In this particular season soil moisture values did not exceed 62 % sat. at 10 cm depth and 83 % sat. at 20 - 40 cm depth. The effect of the land use type on soil moisture fluctuations is discussed in the section “Impact of land use type”, and is not considered further at this point. The intra-seasonal soil moisture dynamics as impacted by different climatic conditions during the four rainy seasons 2016 - 2017 are described in more detail in chapter 7.1, where they are further analysed regarding their influence on nitrate mineralisation and leaching.

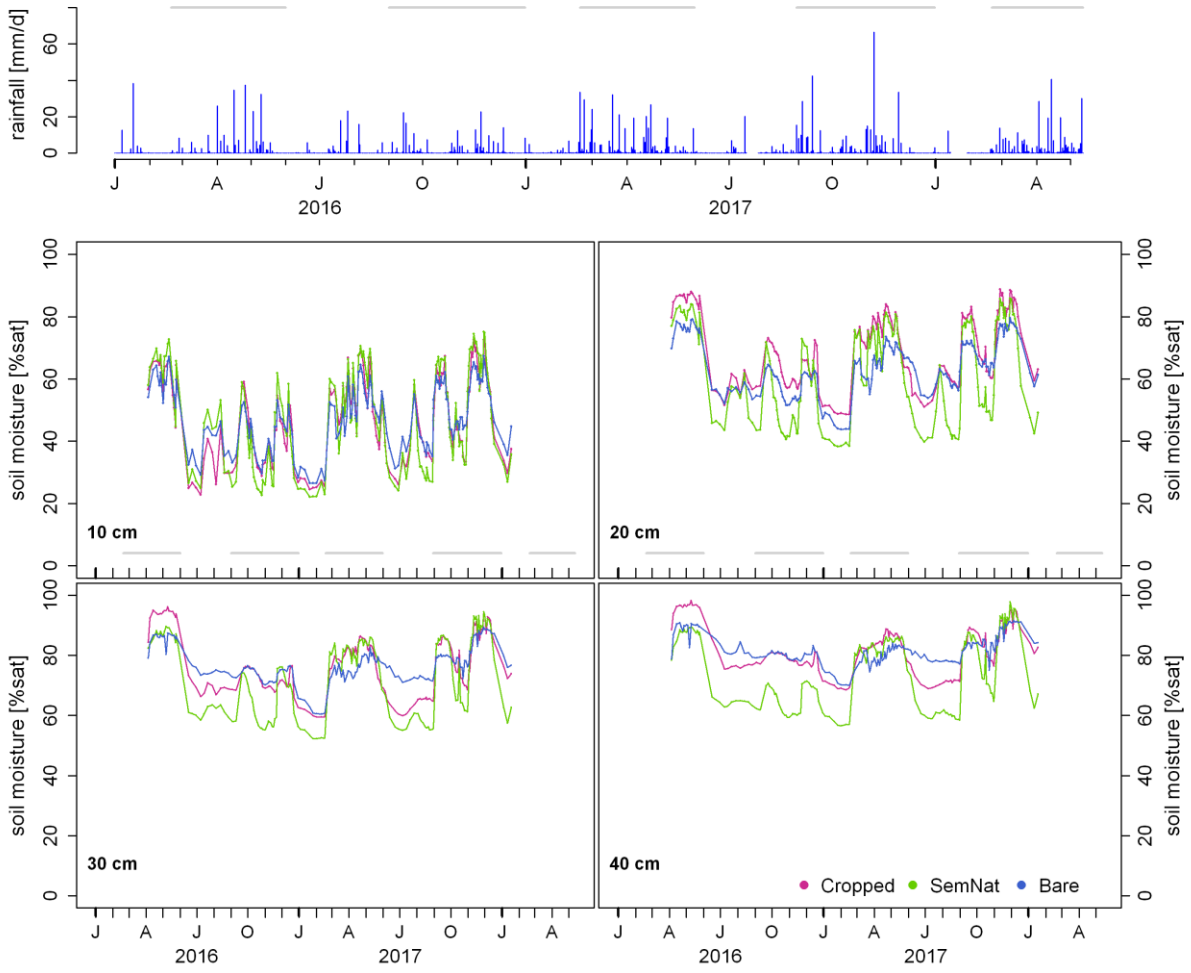

Figure 33 *Mean soil moisture at the upland positions for the three land use types and at the four measurement depths. Grey bars indicate the duration of the rainy seasons.*

In the wetland, soil moisture remained at values close to saturation throughout the year, i.e., seasonality was not pronounced (see Figure 34). Only the upper soil layer (10 cm depth) reflected the impact of dry and rainy seasons at two of the three measuring points (W1 and W2), whereupon dynamics were more pronounced at point W2. Drying and wetting patterns were similar to those at the upland positions. Nevertheless, high moisture levels in the upper 10 cm persisted longer after the start of the dry season in the wetland soils. During the rainy season, maximum moisture levels in the wetland soils were higher than in the upland soils and were only reached at a later point during the season. This hints to the fact that soil water in the wetland was not fed by rainfall alone, but also by (sub-) surface runoff from the surrounding slopes as well as by upwelling water from the shallow groundwater aquifer in the wetland sediments, as described in (Burghof, 2017). Nevertheless, the three measuring points in the wetland also showed different dynamics. At position W1, variations were less pronounced during the second rainy season 2016 than during the following seasons. At 20 cm depth, this was still true for the first dry season 2017. Point W0 was installed in the first rainy season 2017 after banana was planted on the lower slope above point W1 and was also located beneath the plot under crop production, 10 m right of point W1. Here, soil moisture variations were very small, and values remained close to saturation throughout the study period.

The different dynamics at the three measuring points in the wetland indicate that even within the wetland local variations in soil moisture existed. This could be related to various reasons, e.g., small scale variations in soil texture, micro-topography, local upwelling from the groundwater in the valley sediments through more permeable areas in the clay layer separating it from the soil water, varying input of slope water or agricultural management practices. For W2, the most likely explanation are agricultural management practices, as W2 was located in a local farmer's field, where Taro was cultivated. This crop is grown in small pits, which are water filled and separated by ridges. This cultivation practice causes water to drain from the ridge areas into the dug-out pits leading to spatially very heterogeneous moisture conditions and partial drainage of the upper soil layers. This could explain, why rainfall patterns influenced soil moisture more directly at this position, as access water was drained to the small pits. Differences between point W0 and W1 might be caused by the agricultural practices on the slopes, as banana plants use more water than cassava plants (Lu et al., 2002; Oguntunde, 2005), which could reduce interflow from that area. Yet, the two points were very close to each other and, as discussed in chapter 7.2, lateral subsurface mixing of waters is expected over larger areas. Furthermore, soil water in the wetland was not only fed by rainfall and interflow water, as explained in chapter 6.2.2. Thus, this strong effect of crops at the slope would be rather surprising at such a small scale. More likely, lateral variations in the extent of the wetland might explain the differences here. The fringe of the wetland did not follow a straight line, but rather meandered along the valley bottom. Therefore, even if the two measurements points were at the same line, point W0 was located further inside the wetland than point W1. In addition, the texture at W1 was sandier and no underlying clay layer could be detected. This might further be related to the position at the very edge of the wetland sediments and could prevent the impounding of water and thus lead to higher variability of soil moisture. The correlation of soil moisture in the wetland and water input from the surrounding slopes is discussed in more detail in chapters 6.2.2 and 6.3.

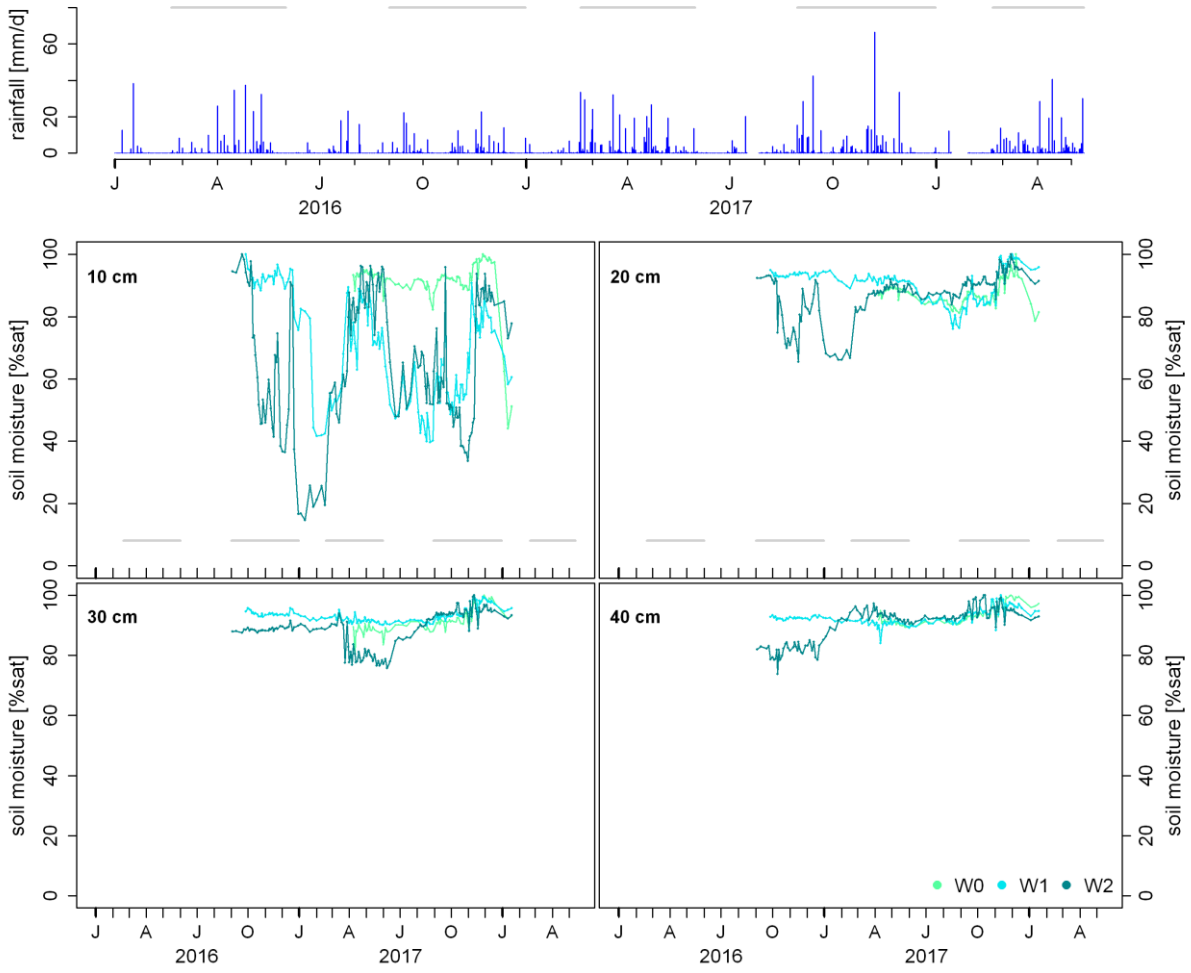

Figure 34 *Soil moisture at the three wetland positions bordering the plot under crop production (W0, W1) and bordering the bare fallow plot (W2). Grey bars indicate the duration of the rainy seasons.*

Effect of land use types

There was no significant difference in the mean soil moisture between the three land use types analysed in this study. Nevertheless, the dynamics of wetting and drying were specific to each land use type (see Figure 33). There were higher fluctuations of soil moisture between dry and rainy seasons for the plots under crop production and semi-natural vegetation. Both reached higher moisture values in the rainy and lower values in the dry season than the bare fallow plot. This trend became more pronounced with increasing depth. Especially the plot under semi-natural vegetation dried out more intensely and more quickly than the others, while the biggest differences were found at 40 cm depth. Grasses and shrubs on the plot under semi-natural vegetation were perennial and had an extended root system. Therefore, water dynamics at the plot under semi-natural vegetation were strongly influenced by the effect of transpiration, leading to higher water losses especially from the lower soil depths. The maize and beans which were grown at the plot under crop production dried up at the beginning of the dry season and their root network was not as dense and did not reach as deep as that of the semi-natural vegetation. Therefore, the effect of transpiration was not as pronounced at this land use type. Nonetheless, the crops persisted long enough into the dry season to cause the soil to dry out more than under bare fallow

conditions. During the rainy season, there was more infiltration and less surface runoff from the plots under crop production and semi-natural vegetation compared to the bare fallow plot (see chapter 6.3), which led to higher soil moisture values. Looking at the topsoil (10 cm depth), dynamics were rather similar for all three land use types. Interestingly, the bare fallow plot showed a distinct reaction to smaller rainfall events during the dry season. This can be explained by missing interception by the plant cover compared to the other land use types.

Effect of shallow soils on moisture dynamics

The surface of the saprolite was undulating along the slope (see chapter 5.1). Therefore, some soils were shallower than others and sometimes the 30 cm and 40 cm measuring points of the PR2 device were already situated in the saprolite. As the soil-saprolite interface is expected to play a crucial role for the activation of macropores and therefore the generation of subsurface runoff (see chapter 6.2.1), these positions are analysed in more detail in the following section.

In shallower soils, saturation or at least very moist conditions are expected to develop faster than in deeper soils. At the same time, the soil at the non-bare plots should dry up more quickly during the dry season as it has less water storage capacity. As discussed in chapter 6.2.1, water is further expected to impound on top of the saprolite until the matrix potential is reduced to the point that water drains freely into the meso- and macropores of the saprolite (the reason why no shallow subsurface flow was generated). Yet, the data collected in shallow soils did not reflect these assumptions. Figure 35 - Figure 38 show soil moisture dynamics at different slope positions at the measuring points where the PR2 excess tubes reached down to the saprolite (coloured lines) in comparison to the dynamics of mean soil moisture of the measuring points located in deeper soils at the corresponding slope position at the same land us type (black lines). The position of each measuring point is presented in Appendix 1 and the properties of the corresponding soil profiles can be found in Appendix 6 and Appendix 7. Soil moisture conditions varied widely between the different measurements points in shallow soils and, when compared to the mean values of measuring points in deeper soils, no clear trend could be inferred. The data suggested that microscale factors were more important than the mere soil depth or position in the saprolite to explain the moisture dynamics. In this regard, one important factor was soil texture. Point P4.3 for example, showed higher soil moisture values (volumetric water content and % saturation) than the deeper soils under the same land use and at the same slope position (see Figure 38), even if the saprolite was already found at 40 cm depth and had a very high skeletal fraction of 60 %. At this position the soil as well as the saprolite matrix were classified as a clay loam with a clay share of 28 %, while soils at the other points were classified as loam. This might explain the higher soil moisture values at point P4.3 even during the dry season. The opposite effect was found at points P4.2, P7.1 and partly R6.1 (30 cm and 40 cm) and R7.1 (10 cm and 20 cm), where a more sandy texture of 45 - 50 % sand content might have led to comparably low moisture values during dry and rainy seasons (see Figure 35, Figure 36 and Figure 37). Yet, this was not true for all measurement depths, as, e.g., R6.1 (10 cm and 20 cm) and R7.1 (30 cm and 40 cm) had moisture values higher than the average even though soil texture was comparably sandy (45 % and 60 % respectively).

For some points in the C horizon, no information on soil texture was available, so that a correlation of moisture and texture was only possible for some few samples. Therefore, it is not known if the high moisture values in the upper saprolite at points P7.1, P4.2 and R6.2 were related to the small scale variability in the soil texture of the matrix, as they do not fit to the otherwise drier conditions in the overlying sandier soils.

Measuring point R9.1 was drier at all depths than the other measuring points in shallow soils at the lower slope of the bare fallow plot. Nevertheless, the texture was very similar to that at point R7.1. At this position, biogenic structures created by termite activity characterised the surrounding soil and probably induced rapid drainage of the soil. Other possible factors influencing soil moisture in shallow soils are the characteristics of the root system (for the plot under semi-natural vegetation), the density of macropores, as well as the micro-relief of the saprolite. These parameters were not analysed in the frame of this study and can therefore not be related to the moisture values presented here.

Impounding of water due to the effect of capillary boundaries as well as the resulting breakthrough of water into the saprolite (Heilig et al., 2003) was not reflected in the soil moisture dynamics in shallow soils. This supports the hypothesis presented in chapter 6.2.1, that infiltrating water was diverted to the depressions in the undulating saprolite topography (thus the positions with deeper soils) due to capillary diversion at the soil-saprolite interface. Thus, a continuous monitoring of soil moisture or preferably soil suction down to the saprolite at the deeper soil profiles would be necessary to demonstrate this effect.

Nevertheless, uncertainty is also related to the moisture values as such. As the skeletal fraction of the saprolite was quite high, installation of the PR2 access tubes might be faulty at some positions, as adequate soil contact of the tube might not have been given. In addition, soil samples for the analysis of soil texture were taken in close proximity to but not at the exact position of the excess tubes. Due to the very high spatial variability of soil properties, this might obscure the findings. Another limitation is the timely resolution of the measurements. To detect the effect of capillary boundaries, continuous measurements would be necessary, which could not be realized due to limited financial resources. The measurement interval of 2 - 3 days as well as the distance between the moisture sensors was most likely too coarse to show impounding of infiltrated rainfall at the soil-saprolite interface, especially as capillary diversion takes places in a small layer of some centimetres only (Heilig et al., 2003).

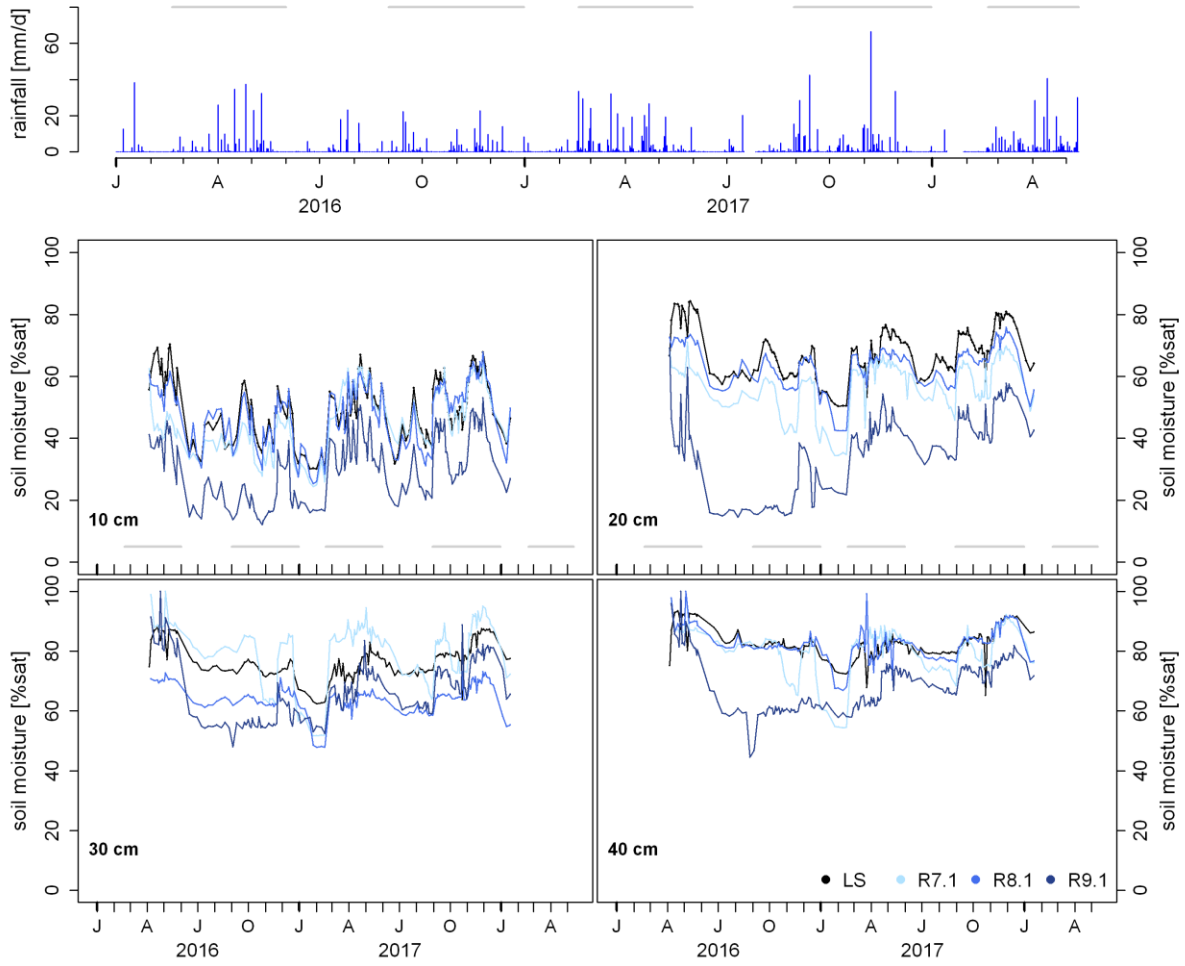

Figure 35 *Mean soil moisture at the lower slope of the bare fallow plot (black line) compared to soil moisture at measurements points with shallow soils at the same slope position. Measurements taken in the saprolite: R7.1: 30 and 40 cm, R8.1: 40 cm, R9.1 40 cm. Grey bars indicate the duration of the rainy seasons.*

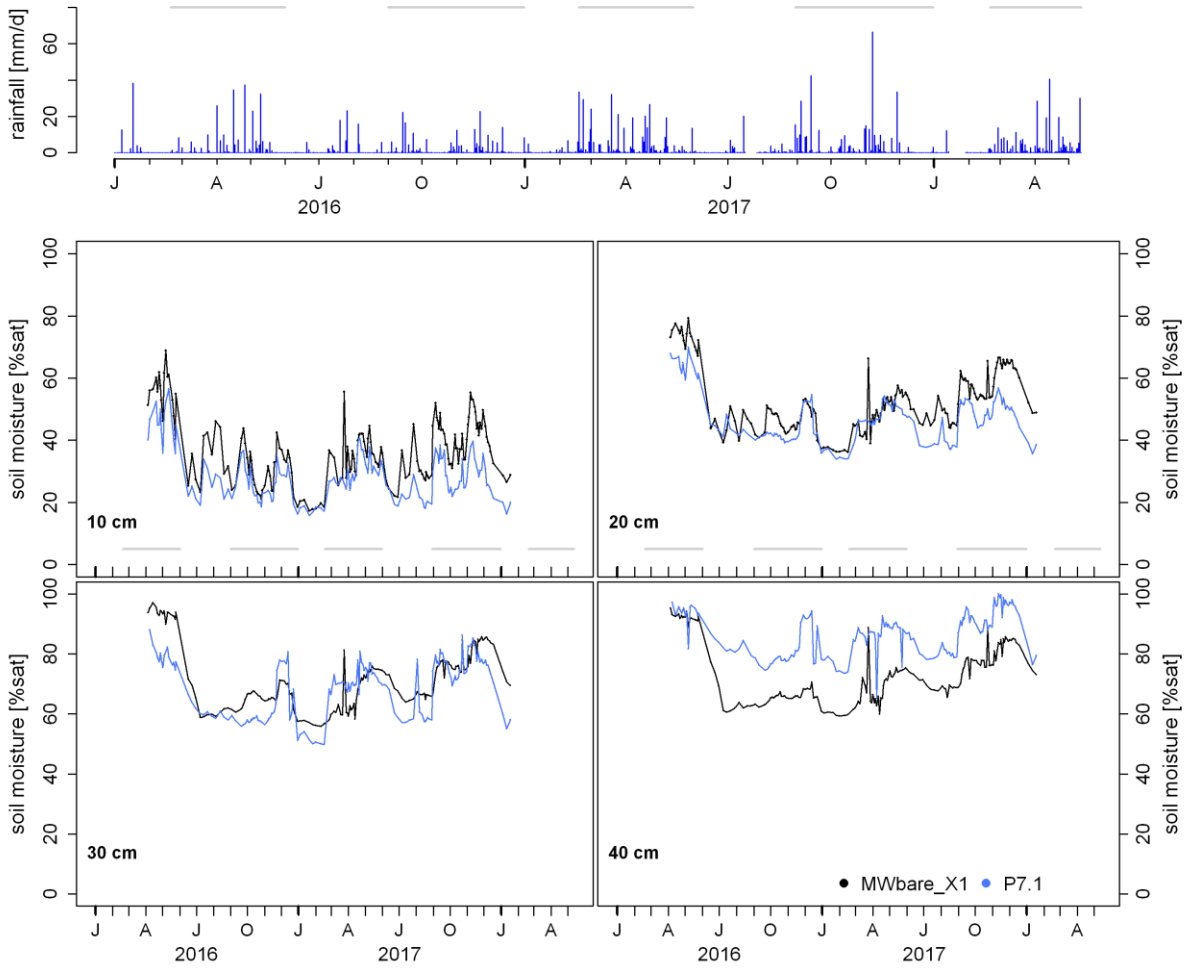

Figure 36 *Mean soil moisture downslope of the pits at the bare fallow plot (black line) compared to soil moisture at the measuring point with shallow soil. Measurements taken in the saprolite: P7.1: 30 and 40 cm. Grey bars indicate the duration of the rainy seasons.*

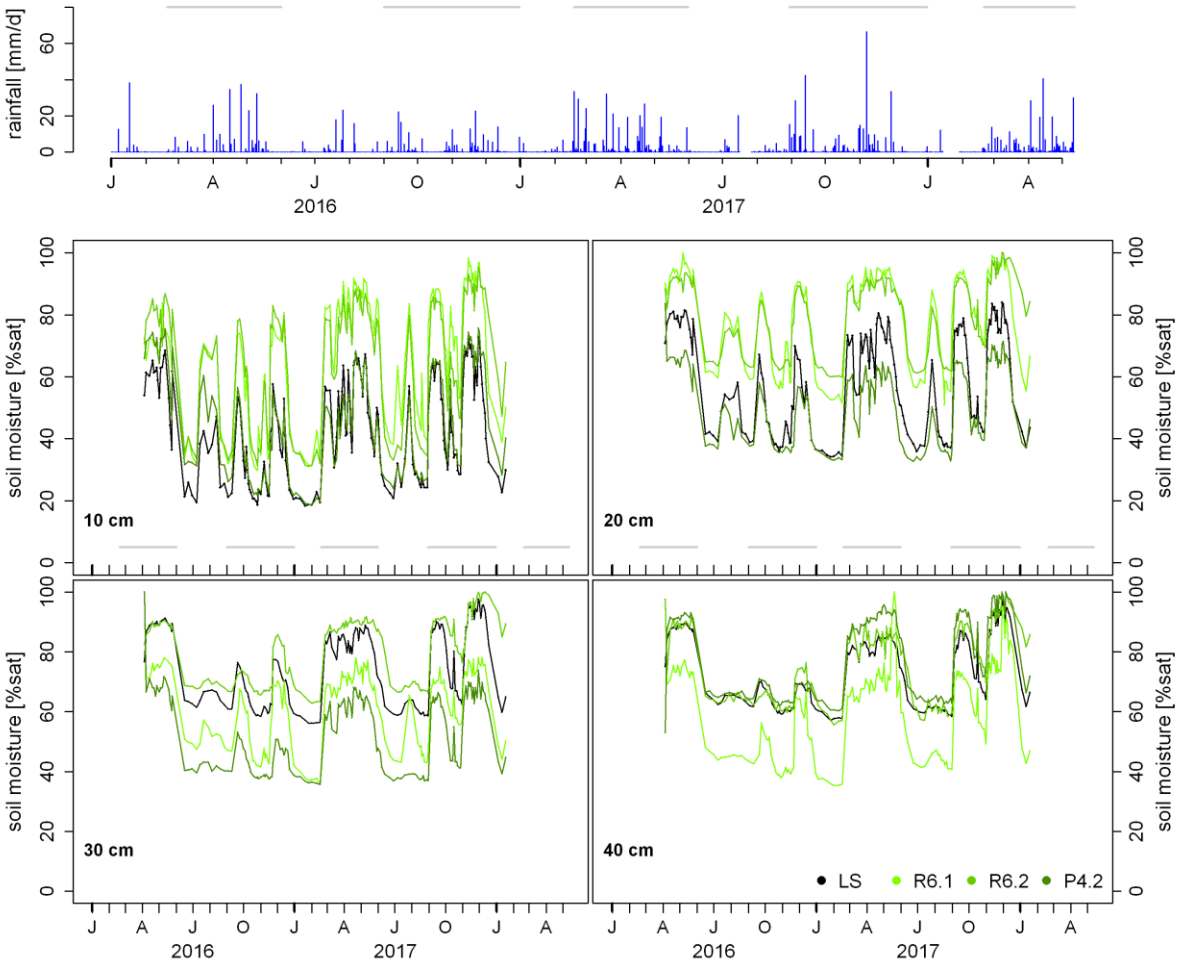

Figure 37 *Mean soil moisture at the lower slope at the plot under semi-natural vegetation (black line) compared to soil moisture at measurements points with shallow soils at the same slope position. Measurements taken in the saprolite: P4.2: 30 and 40 cm, R6.1: 30 and 40 cm, R6.2: 40 cm. Grey bars indicate the duration of the rainy seasons.*

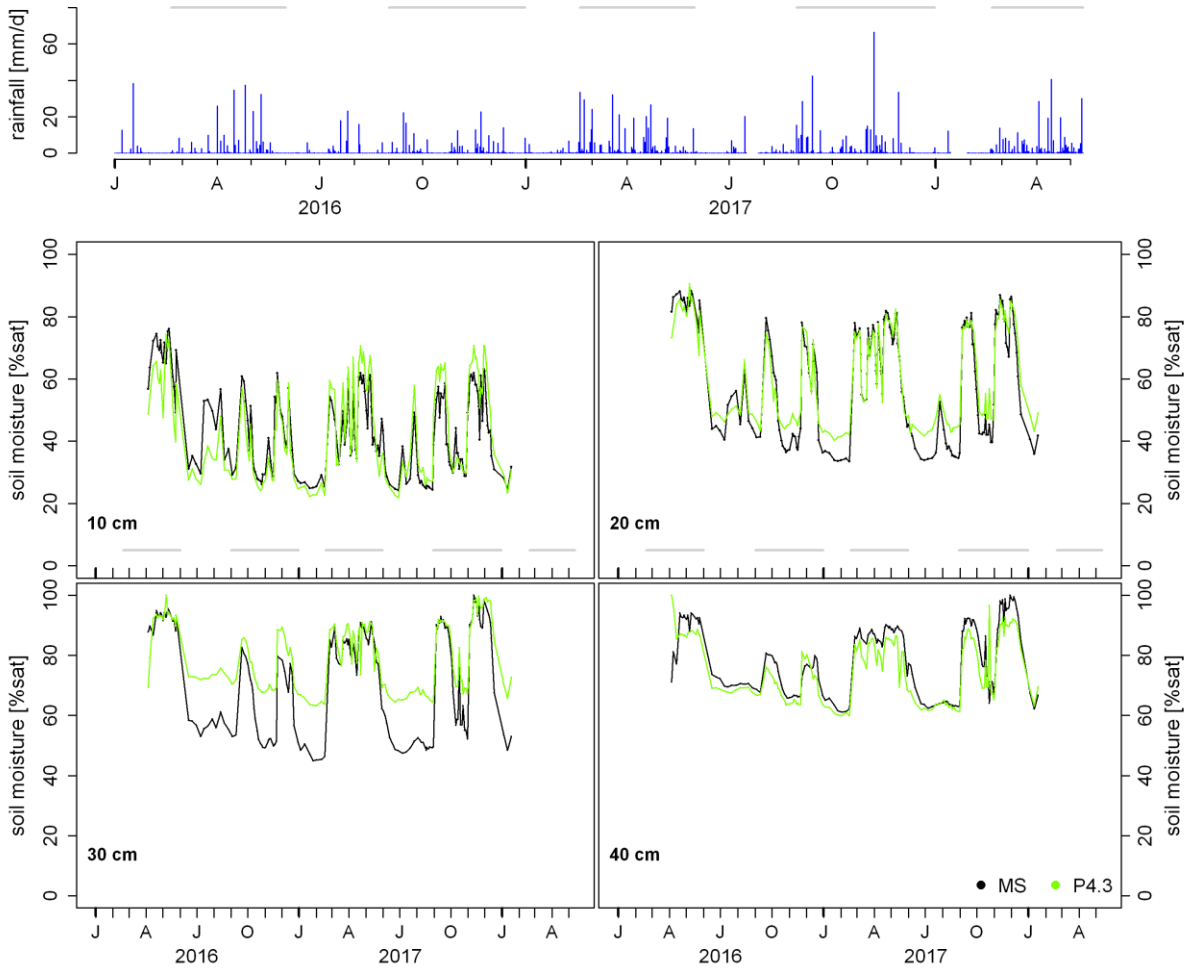

Figure 38 *Mean soil moisture at the mid-slope position of the plot under semi-natural vegetation (black line) compared to soil moisture at a measuring point with shallow soil at the same slope position. Measurements taken in the saprolite: P4.3: 40 cm. Grey bars indicate the duration of the rainy seasons.*

6.1.2 Lateral water fluxes in the soil

Effect of the slope position

In the following section, differences in the soil moisture between the three slope positions in the upland (slope toe, lower slope and mid-slope position) are analysed and interpreted regarding the presence of lateral sub-surface flow in the soil.

Soil moisture was not significantly different at the three upland slope positions. Nevertheless, certain trends could be observed which allow to infer water fluxes along the slope (see Figure 38-Figure 41). Overall, the slope toe positions were drier compared to the lower slope and mid-slope positions. This effect was more pronounced at the first 20 cm and at the plot under bare fallow and crop production. Under semi-natural vegetation, the soil at the slope toe was drier in the dry season but showed very high moisture values during the rainy seasons at 30 cm and 40 cm depth. At first this seems surprising, as generally higher soil moisture would have been expected at the bottom of the slope due to infiltrating surface runoff and more gentle terrain (Zehe and Flühler, 2001) and due to the proximity to the upwelling

interflow. Therefore, moisture conditions found here were probably the result of soil texture rather than slope position and associated water supply from upslope areas, as the soil was sandier at the slope toe than at the upslope positions (see chapter 5.2.1). Thus, it can be assumed that infiltrating surface runoff would quickly percolate and not be stored in the upper soil layers. Yet, a continuous measurement approach would be necessary to confirm this assumption. The sandy texture further explains why the proximity to the interflow did not buffer dry season effects, as capillary rise is very limited in coarsely structured soils (Weil and Brady, 2017). Nevertheless, the high moisture dynamics at 30 cm and 40 cm depth under semi-natural vegetation were not dominantly related to the soil texture. Here, two other factors might be of importance. Firstly, the height and density of the grasses at the slope toe were higher compared to the upslope positions and secondly, interflow could already be found at 60 cm depths. Therefore, during the rainy season interflow might have risen into the soil profile and caused high moisture levels. During the dry season though, interflow at this trench was reduced drastically so that plant roots could not reach it (see chapter 6.2.1). At the same time, the high water demand of the denser vegetation induced higher water losses from the soil due to transpiration, which caused the lower soil moisture values compared to the upland positions in the dry season.

Comparing the lower slope and the mid-slope positions gave no clear results. Overall, there was no difference between these positions except for the bare fallow plot at 20 - 40 cm depth, where on average soil moisture was higher at the mid-slope position. When looking at the time series in Figure 39 to Figure 41, different dynamics were found at the different slope positions for each land use type and within the land use type for the different years and soil depths. On the plot under crop production, soil moisture was higher at the lower than at the mid-slope position during the first two rainy and dry seasons at all depths. This trend changed with the first rainy season of the second year of investigation (2017) when soil moisture at the lower slope position was lower or equal to the mid-slope position. So far, no explanation for that behaviour was found as the cultivation of the plot did not differ between the two years of the study. The values for the first two dry and rainy seasons seem rather surprising, as, due to the more clayey soil texture at the mid-slope position, higher values for this plot would have been expected. For the bare fallow plot, soil moisture at the mid-slope position was higher in the rainy and in the dry season except for the first dry season in 2017. This trend was even more pronounced for 30 cm and 40 cm depth. This can be explained by the higher clay contents and greater soil depths at the mid-slope position at this land use type. At the lower slope, many measuring points at 30 cm and 40 cm were located in the saprolite leading to lower moisture contents. At the plot under semi-natural vegetation, soil moisture at the mid-slope position was generally higher than at the lower slope.

It has to be considered that the soil properties and moisture conditions varied widely within the plots and that the higher number of measuring points at the lower slope makes it difficult to compare the different slope positions in the upland. Yet, the data at hand did not suggest that there was a lateral flow component in the soil above the saprolite, which is in accordance with the results from the pit trials at the lower slope discussed below.

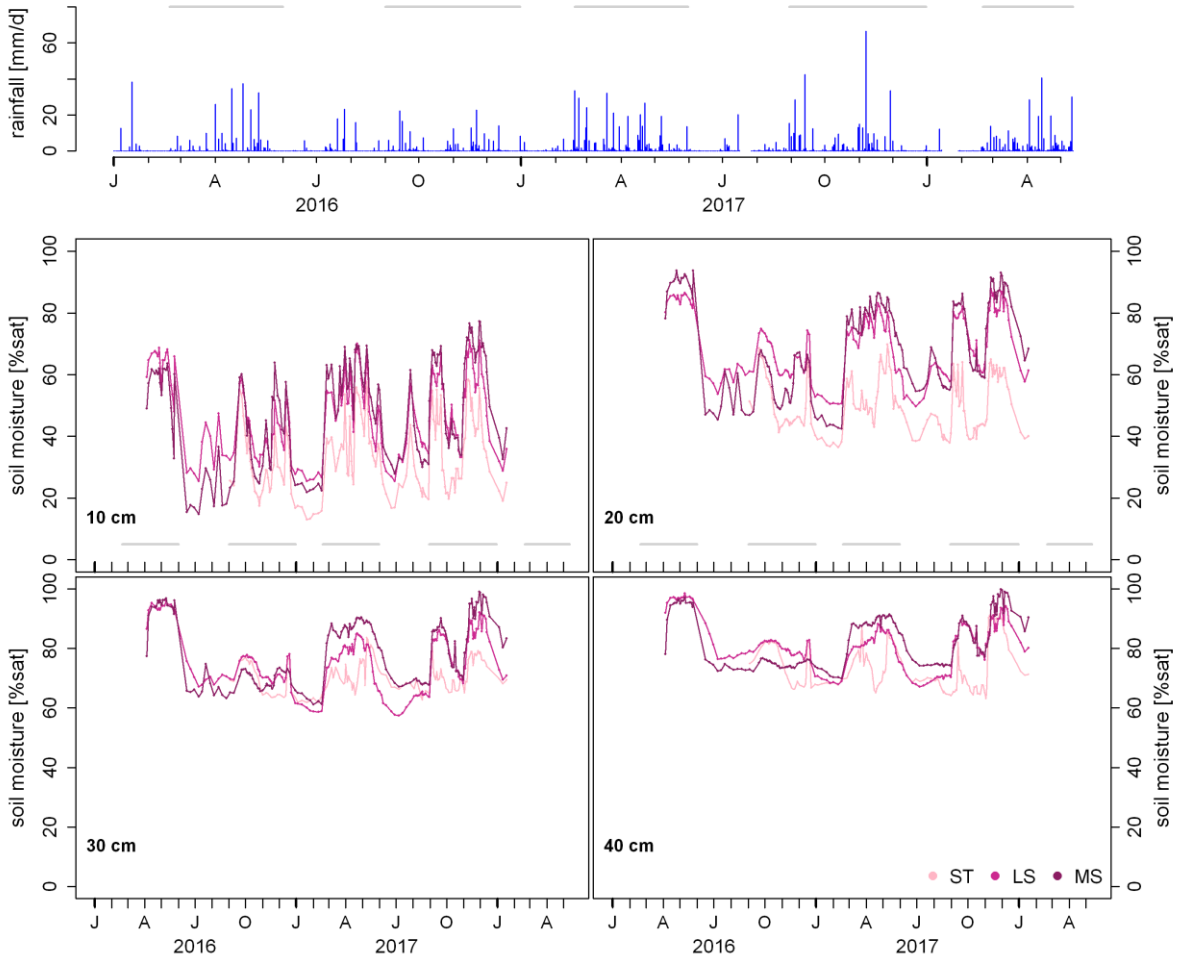

Figure 39 *Comparison of soil moisture at the plot under crop production for the different upland positions: Slope toe (ST), Lower slope (LS) and Mid-slope (MS). Grey bars indicate the duration of the rainy seasons.*

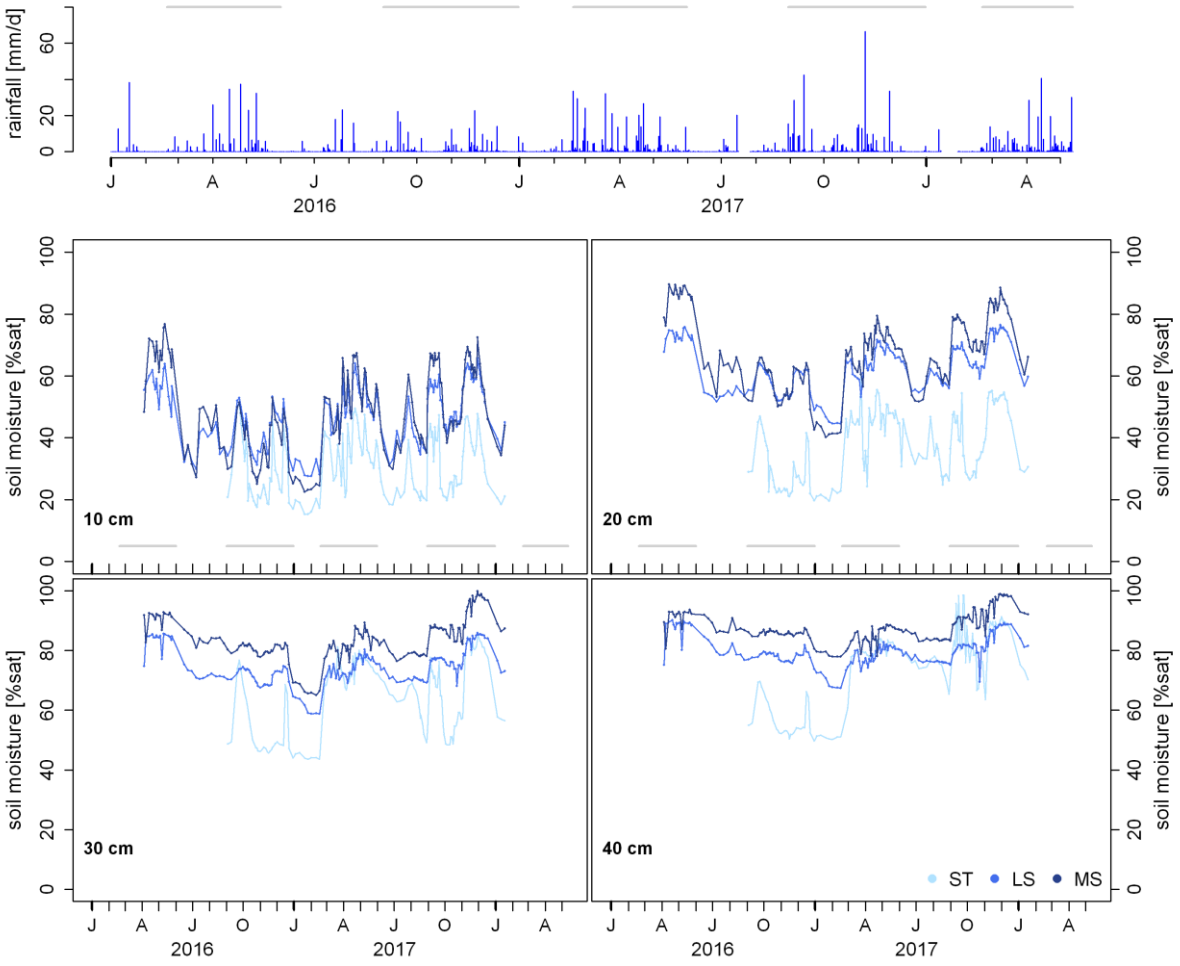

Figure 40 *Comparison of soil moisture at the different upslope positions (Slope toe (ST), Lower slope (LS) and Mid-slope (MS)) at the bare fallow plot. Grey bars indicate the duration of the rainy seasons.*

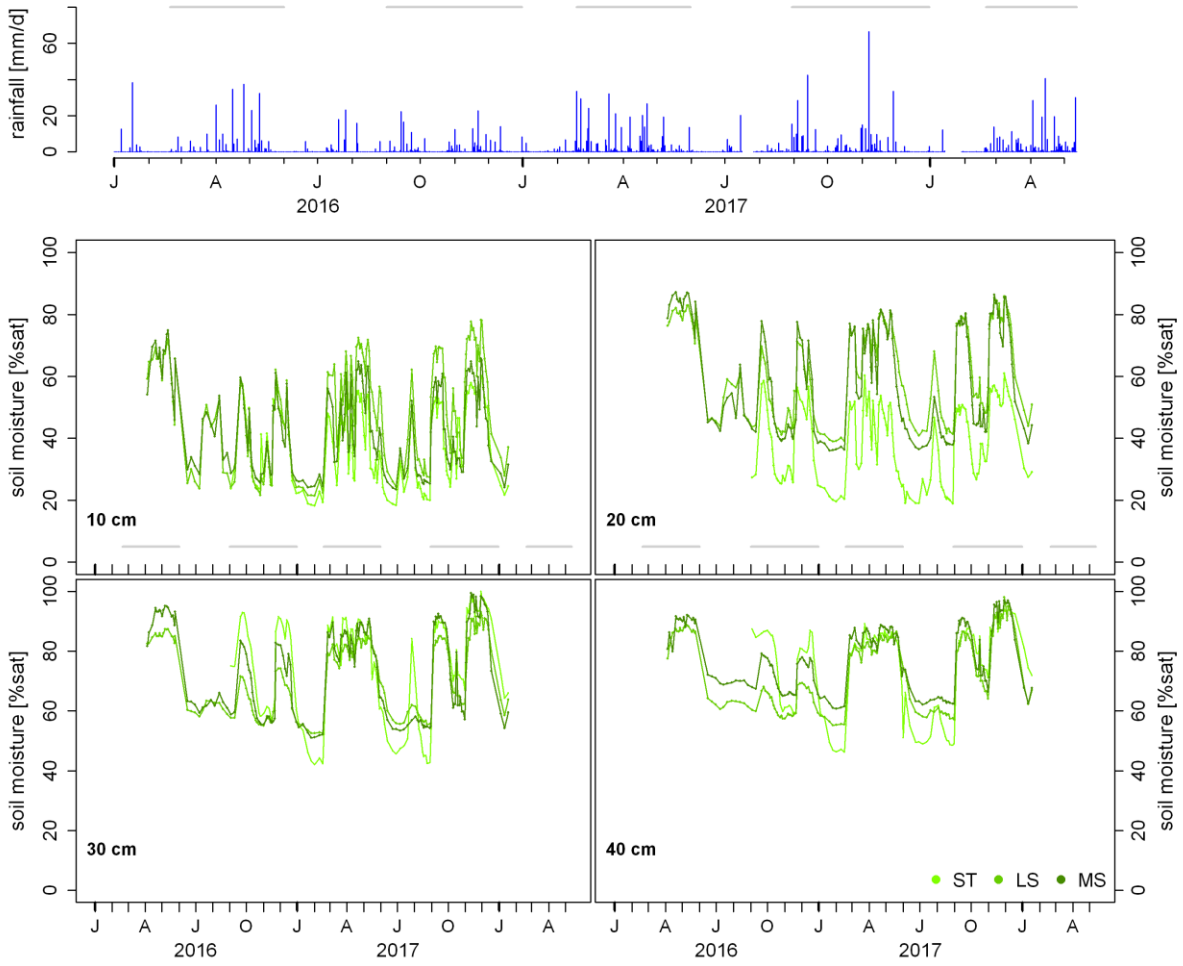

Figure 41 *Comparison of soil moisture at the different upslope positions (Slope toe (ST), Lower slope (LS) and Mid-slope (MS)) at the plot under semi-natural vegetation. Grey bars indicate the duration of the rainy seasons.*

Effect of shallow dug-out pits

As described in chapter 4.4.3, pits were excavated at the lower slope position down to about 30 cm into the saprolite to detect shallow subsurface flow in the soil or at the soil-saprolite interface. Soil moisture measurements were taken upslope and downslope of the pits and at reference plots aside (see Figure 12). In this section, the results of these measurements are discussed regarding the presence of shallow subsurface flow in the soil above the saprolite.

Shallow subsurface flow could have been expected at the interface of the organic rich (A) and mineral (B) soil horizons (e.g., Kahl et al., 2007; Noguchi et al., 1999) and at the soil-saprolite interface (e.g., Braun et al., 2002; Ribolzi et al., 2018). In this study, direct observations of the pits during and after rainfall events did not reveal the presence of shallow subsurface flow at the slope, neither between the A and B horizon nor at the soil-saprolite interface. The higher K_{fs} values of the upper saprolite (see chapter 5.2.1) already suggested that shallow subsurface flow on the saprolite would be unlikely even if the matrix was more clayey than the residual soil at many measuring points. The soil moisture measurements upslope and downslope of the pits and at the reference plots did not suggest the existence of shallow subsurface flow

in soil above the saprolite, either. If shallow subsurface flow had been present, the pits would have interrupted the water supply from upslope and, thus, measuring points downslope of the pits would have shown lower soil moisture contents compared to the points upslope of the pits and at the reference plots. This was only true for the bare fallow plot (see Figure 42). Here, soil moisture at 10 cm and 20 cm depth was lower downslope of the pits during almost the entire measurement period, the difference being statistically significant during the dry seasons at 20 cm depth. At 30 cm and 40 cm depth, soil moisture downslope of the pits could reach higher values than at the other positions at the peak of the rainy season. Nevertheless, the drier conditions downslope of the pits at the bare fallow plot were probably caused by the sandier texture compared to the other measuring points (see profiles in Appendix 6 and Appendix 7).

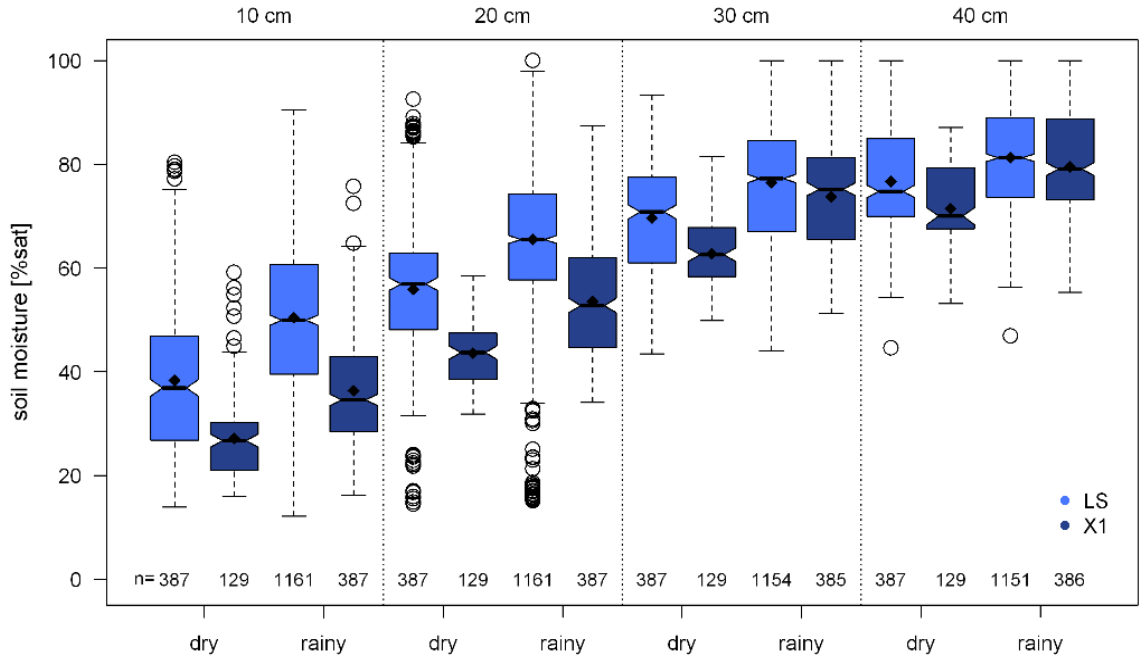

Figure 42 *Soil moisture at the bare fallow plot downslope of the pits (=potential water input by shallow interflow is prevented) (X1) and upslope of the pits and at the reference plots (= open to potential water input by shallow interflow) (LS) during rainy and dry seasons at the four measurement depths.*

At the plot under semi-natural vegetation, soil moisture downslope of the pits was similar or even higher than upslope of the pits and at the reference plots at all depths (see Figure 43). One reason could be that the vegetation downslope of the pits was younger and shorter than at the other positions, as it was cut or removed during the installation process. This would lead to less transpiration and therefore less water loss from the soil.

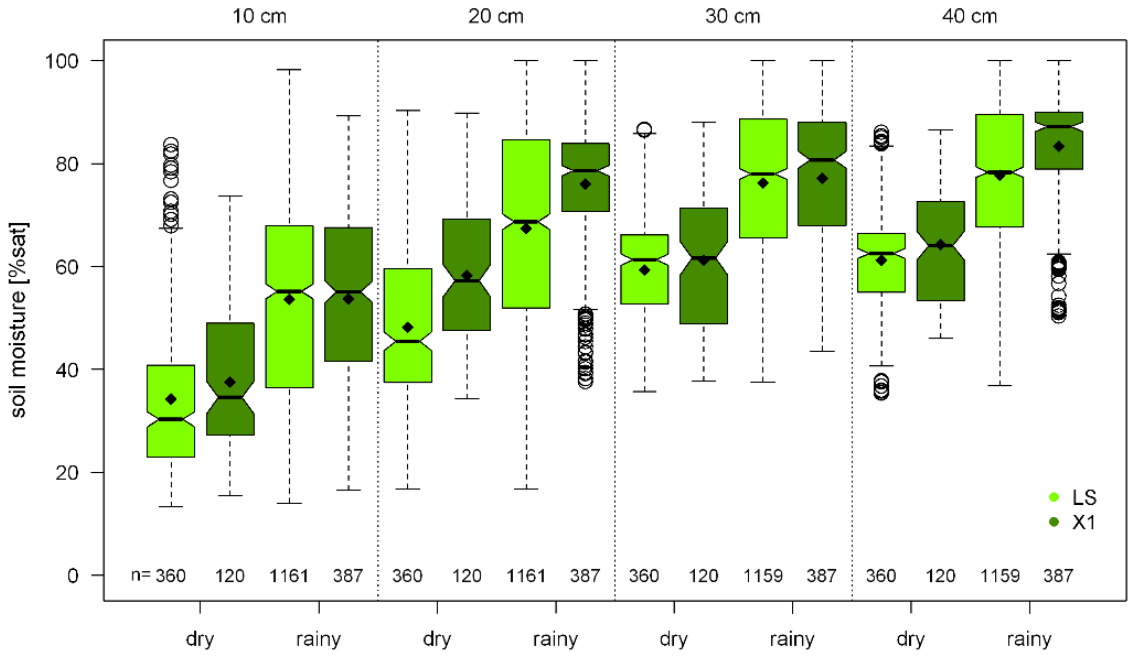

Figure 43 *Soil moisture at the plot under semi-natural vegetation downslope of the pits (=potential water input by shallow interflow is prevented) (X1) and upslope of the pits and at the reference plots (= open to potential water input by shallow interflow) (LS) during rainy and dry seasons at the four measurement depths.*

At the plot under crop production, soil moisture downslope of the pits was only lower compared to the other positions at the lower slope at 10 cm depth. At 20 - 40 cm depth, soil moisture downslope of the pits was actually higher during the dry seasons and slightly higher during the rainy season (see Figure 44). Soil texture and depth to bedrock were not different at this plot. Therefore, the way the pits were constructed most likely entailed the results described above. The pits were covered by metal roofs (see chapter 4.4.3) and the runoff from these roofs was collected and deviated away from the plots in dug-out channels downslope of the pits. These channels were about 15 cm deep and not sealed. Therefore, water could infiltrate into the soil downslope of the pits (position X1). This would explain why, starting from 20 cm depth, soil moisture was higher downslope of the pits, as additional water was added to the soil body. This effect was not present at 10 cm depth, as infiltration occurred from the base of the channels which was below the 10 cm measuring point.

The findings presented above do not suggest the presence of shallow subsurface flow along the slope. This is further supported by the fact that for all land use types the variation between the different measuring points upslope of the pits was higher than the differences between the measuring points upslope and downslope of the pits.

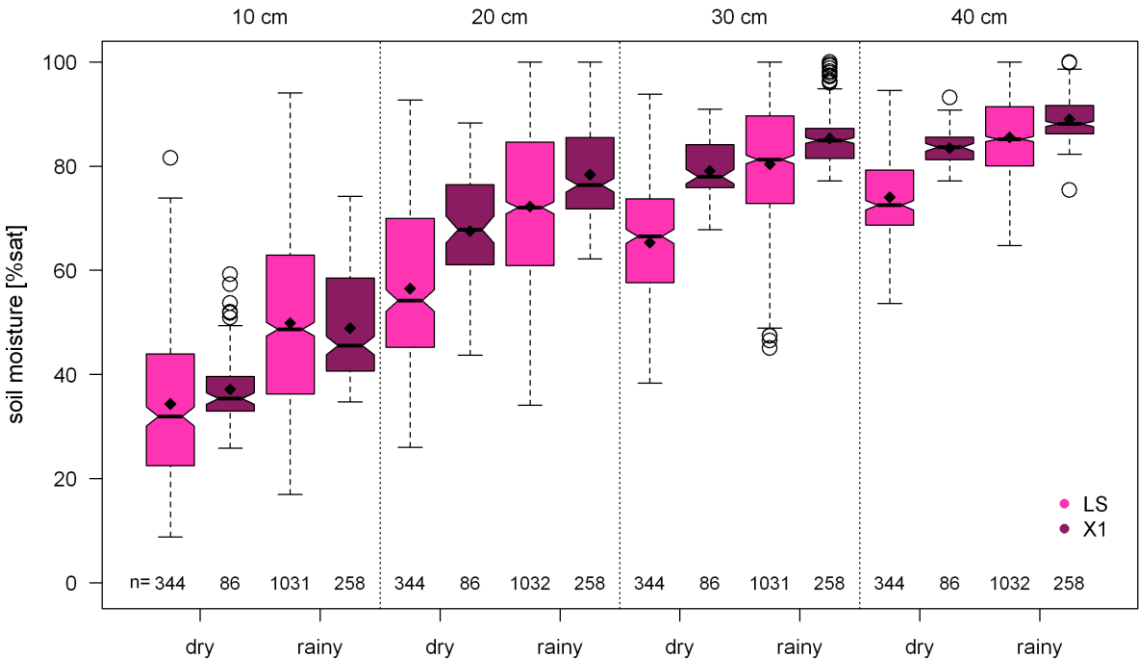

Figure 44 *Soil moisture at the plot under crop production downslope of the pits (=potential water input by shallow interflow is prevented) (X1) and upslope of the pits and at the reference plots (= open to potential water input by shallow interflow) (LS) during rainy and dry seasons at the four measurement depths.*

6.2 Interflow

Various studies describe the importance of lateral subsurface (storm) flow for catchment hydrology and solute transport in tropical regions (e.g., Giertz et al., 2006; Kahl et al., 2007; Ribolzi et al., 2018; Uhlenbrook et al., 2005; Wenninger et al., 2008). At the same time, quantity and timing of water and nutrient delivery to the valley bottom by the interflow depend on the subsurface runoff processes along the slope (Angermann et al., 2017). In the following chapter, the results on interflow volumes measured at the slope toe are introduced and interpreted regarding interflow processes in the saprolite along the slope. In the second part of the chapter, the hydrogeological connectivity of the interflow to the wetland aquifers as well as the influence of interflow on soil moisture dynamics at the wetland fringe is analysed.

6.2.1 Interflow related processes at the slope

The first part of this section describes the results of field observations and the interflow measurements conducted at the slope toe. The second part introduces some hypotheses on interflow routing through the saprolite and reflects on the influence of rainfall characteristics and the different land use types on interflow related processes along the slope.

As described in chapter 4.4.2, interflow was collected in trenches at the slope toe. In contrast to the other slope positions (see previous section), here interflow was found close to the soil surface at between 60 cm and 100 cm depth. At this position, lateral flow in a sandy loam layer overlying the saprolite as well as

in the top layer of the saprolite was observed in the trenches. Interestingly, an upwelling of the interflow water via macropores in the top layer of the saprolite was also detected (see Figure 47 c). As shown in Figure 45, interflow was active during the entire rainy season and partially also during the dry season. Interflow volumes and dynamics varied between the different seasons as well as by land use type. Rainfall amount as well as rainfall distribution and intensity during the rainy seasons determined interflow volumes (see Table 8 and Figure 45), but unlike the results described for the soil moisture of the soil above the saprolite, the characteristics of a single rainy season still influenced interflow volumes in the following seasons. The dynamics of interflow volumes measured at the slope toe during each season are briefly summarized hereafter.

At the plot under crop production, despite little rainfall (214 mm), season 2016.2 was characterised by a constant interflow of about 400 l/d, which pertained into the dry season and then slowly decreased to 150 l/day in February 2017. Despite the significantly higher total rainfall amounts (447 mm), the total interflow volume recorded during season 2017.1 was similar to season 2016.2 (see Table 8). Following rainfall events of high intensity (related to the data recorded in this study), interflow volumes increased slowly at the beginning of the season and showed a delay of several weeks compared to the increase in soil moisture. During the second part of the season, interflow volumes of 600 l/d were recorded, before they decreased steadily over the dry season to about 200 l/d and then briefly dropped to very low values of 30 l/d in August 2017. The second rainy season 2017 was characterised by a bi-modal distribution of rainfall and single big events of high intensity (e.g., 66 mm at a max. intensity of 15 mm/15 min in November 2017). The bi-modal distribution of the rains was also reflected in the interflow volumes. The big rainfall events at the beginning of both wet periods led to a rapid increase in interflow and a peak flow of 950 l/d in November 2017. At the same time, the decrease in interflow after each wet period was fast compared to the other seasons and almost parallel to the decrease in soil moisture. The total interflow recorded for season 2017.2 was significantly lower than for the other two seasons. In January 2018, interflow ceased completed until it increased again to about 400 l/d in season 2018.1. At the plot under semi-natural vegetation, similar dynamics were found in seasons 2017.1 and 2017.2. Nevertheless, interflow volumes were significantly smaller under semi-natural vegetation than under crop production and interflow under semi-natural vegetation reacted faster to dry conditions. For one, interflow decreased and finally even ceased more quickly during the dry seasons. In addition, the dry conditions in 2016.2 led to a steady decrease of the interflow during the rainy season, while the interflow under crop production was not yet affected. Nevertheless, the interflow volumes measured at these two land use types were overall well correlated with R^2= 0.66 and rho= 0.82 and hence interflow related processes seem to have been driven by similar external conditions.

Besides the long term observations of interflow, flow levels before and after one rainfall event were analysed to get a better understanding of the processes involved in subsurface flow along the slopes (see Table 9). The event took place in mid-November 2017 and was rather small compared to typical rain events during the rainy season. Soil moisture levels were already high before the event and water contents in the deeper saprolite can also be expected to have been high, as the end of a wet rainy season was close. Measurements one hour after the rain event showed an increase in interflow of 31 % at the plot under crop production and of 17 % at plot under semi-natural vegetation.

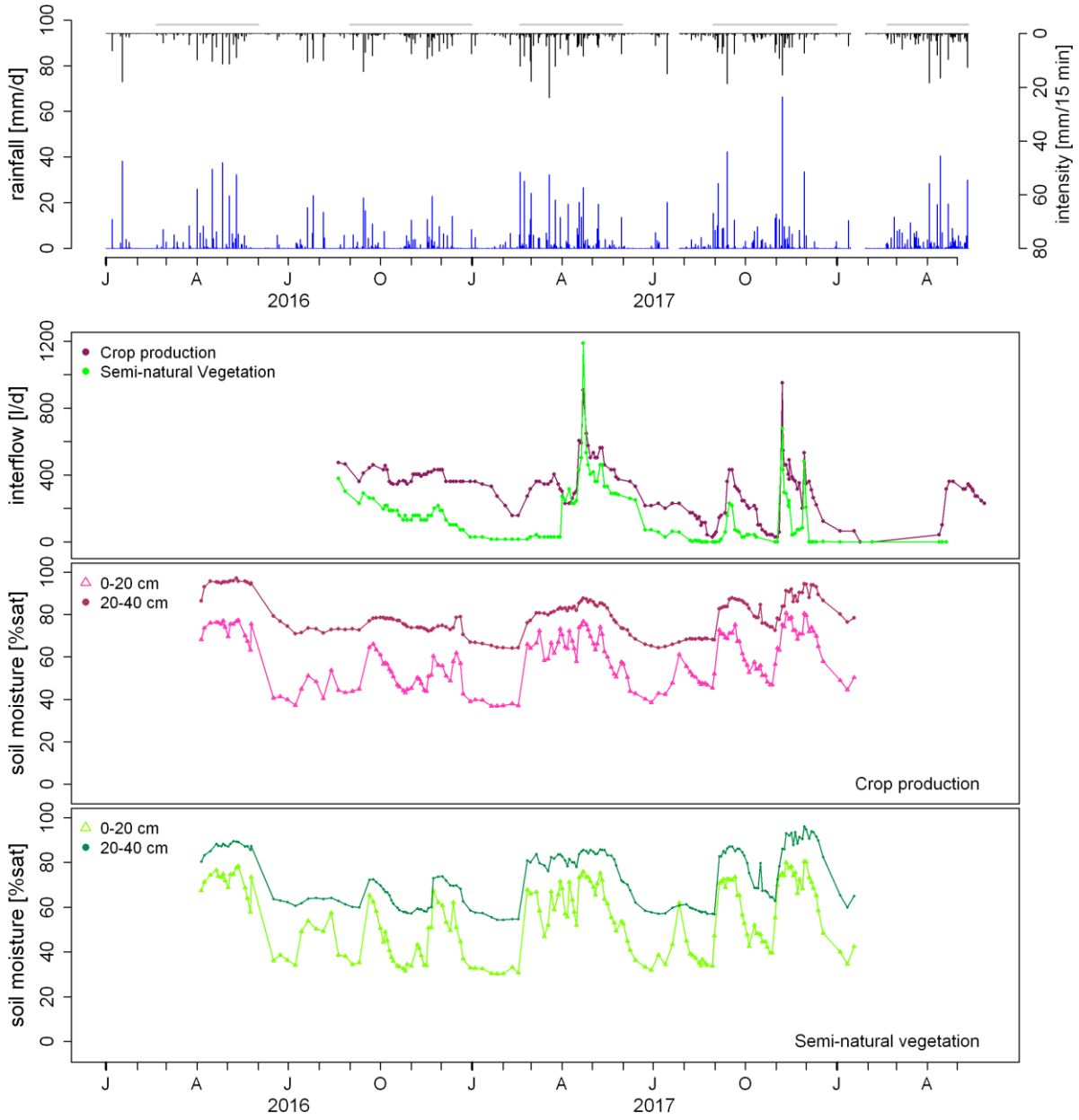

Figure 45 *Interflow at the plot under crop production and the plot under semi-natural vegetation during the investigation period (second panel), related to daily rainfall and max. 15 min. rainfall intensity (blue and black bars in the first panel) and soil moisture dynamics [%sat] at 0 - 20 cm and 20 - 40 cm depth under crop production (third panel) and under semi-natural vegetation (fourth panel). Grey bars indicate the duration of the rainy seasons.*

Table 8 Total rainfall, cumulative interflow volumes as generated per m² on the slope as well as the coefficient indicating how much of the rainfall collected on the slope reached the wetland fringe as interflow during each season. Values embrace the rainy and the following dry season to account for the delayed component of the interflow.

Season	**Rainfall total [mm/m²]**	**Cumulative interflow [l/m²/season]**		**Share [%]**	
		Cropped	***Semi-natural***	***Cropped***	***Semi-natural***
2016.1	353	-	-	-	-
2016.2	214	143	49	67	23
2017.1	447	142	80	32	18
2017.2	395	73	20	18	5

Table 9 *Observations of hydrological parameters related to a single rainstorm on 14th of November 2017.*

	P10 (crop production)		**P11 (semi-natural vegetation)**	
	Before event	**After event**	**Before event**	**After event**
Interflow [l/d]	375	490 (+31 %)	210	245 (+17 %)
NO_3-N concentration interflow [mg/l]	2.8	4.3 (+54 %)	1.4	1.1 (-21 %)
Mean soil moisture slope (0 - 20 cm) [%sat]	77.8	-	77.5	-
Mean soil moisture slope (30 - 40 cm) [%sat]	90.7	-	92	-
Mean NO_3-N in soil solution [mg/l] (10 cm)	2	-	0.44	-
Mean NO_3-N in soil solution [mg/l] (20 cm)	9	-	0.38	-
Surface runoff [l/m²]	1.7		0.07	
Runoff coefficient	23 %		1 %	
NO_3-N concentration surface runoff [mg/l]	16		15	
Rainfall characteristics	7.2 mm, max. 15 min intensity: 5.2 mm, antecedent 7day precipitation index: 16 mm			

Geochemical analysis confirmed that the origin of the water in the trenches was unlikely related to the deep groundwater (Burghof, 2017). Therefore, as no interflow could be detected in the soil above the saprolite at the other slope positions, water must have been conducted towards the slope toe via flow paths within the saprolite. During the drilling campaign, a layer of horizontally layered muscovite covered by some centimetres of clay was found at about 180 cm depth at the slope toe position (see Figure 31). Hence, water coming from the slope probably impounded on that layer and passed into the overlaying part of the saprolite through macropores before it drained laterally into the wetland. It is not known though, whether and if for how far this muscovite layer continued upslope or whether interflow from within the saprolite met this layer only at the bottom of the slope. Different scenarios could cause the upwelling of the interflow water at this slope position. Firstly, if the muscovite layer featured a U-shape over some distance upslope, water input along the slope would cause an upward movement of the water at the slope toe. In the second scenario, the lateral passage of interflow from the saprolite into the aquifer in the valley sediments was impeded by lower hydraulic conductivities of the valley sediments compared to the saprolite. This could be expected when the interflow does not meet a sand or gravel lens in the valley sediments but instead the clayey deposits which enlace them (see chapter 3.3). Therefore, the sources at the slope toe as described by Burghof (2017) and mentioned in chapter 2.1 do not necessarily hint to etchplanation as a crucial factor in the formation of the Namulonge wetland, as the presence of the clay muscovite layer was more likely the major driver for the upwelling of interflow water at this slope position and not the presence of a paleo-clay dambo. Nevertheless, the situation might be different in other parts of the wetland, if a paleo-clay dambo or its remains are present.

The presence of interflow throughout the entire rainy season and more importantly during the dry season showed that interflow had a strong delayed component. This is in accordance with the results of Burghof (2017), who deducted long transit times of slope water from her isotope analysis of interflow water. The highly heterogeneous texture of the saprolite favours the (temporal) development of small perched aquifers in the weathering profile (Burghof, 2017). Observations made by a field assistant, who reported that a small aquifer was found at about 30 m depth at the mid-slope position when a company was drilling to install a pump, correspond to that. These perched aquifers might get connected during the rainy season and thereby contribute to lateral flow within the matrix of the saprolite, causing the pronounced delayed component of the interflow. This could also explain why persisting high volumes of interflow were related to long periods of rainfall which allow for the saturation of larger regions of the saprolite.

The water infiltrating into the soil probably entered the saprolite by a process which (following the fill-and-spill mechanism described in Meerveld and McDonnell (2006b)) we term “the fill-and-drain-mechanism” (see Figure 46). As described in chapter 5.1, the subsurface topography of the saprolite showed an undulating structure in both slope parallel and perpendicular direction. The higher K_{fs} values of the upper saprolite as compared to the A and B horizons of the soil (see chapter 5.2.1) impede infiltration of water from the soil into the saprolite during unsaturated conditions. Under these conditions, a capillary diversion and thus the generation of interflow occurs on inclined soil layers (Heilig et al., 2003). As indicated before, at the microscale this effect was probably active at the high points of the saprolite topography, where impounding water was diverted to the surrounding depressions. The water then pooled in the depressions until the matric potential got high enough and a complete breakthrough as

described by Walter et al. (2000) occurred. Thus, at the slope scale, subsurface topography of the saprolite prevented the initiation of shallow subsurface flow along the capillary boundary at the soil-saprolite interface over larger distances and instead favoured the infiltration of rainwater to the deeper saprolite.

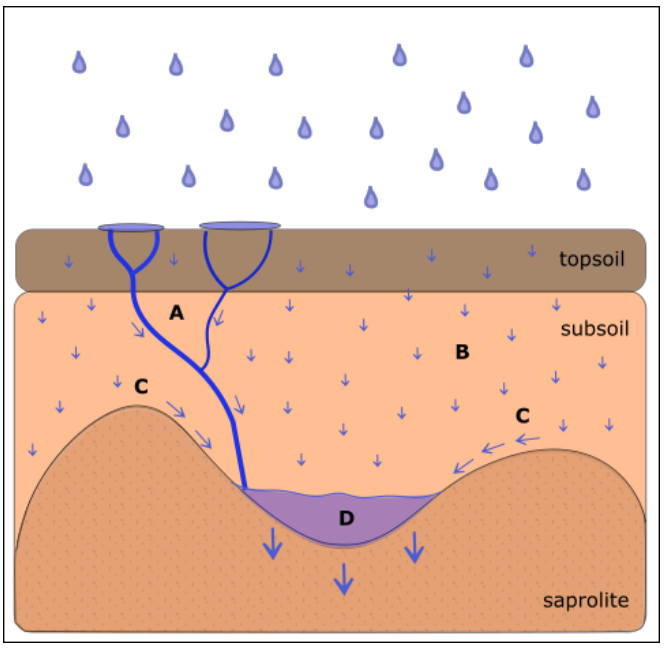

Figure 46 *Schematic representation of the fill-and-drain mechanism at the soil-saprolite interface. Rain water is conducted to the soil-saprolite interface via macropores (A) or via matrix flow (B) in the topsoil and in the subsoil. Due to the undulating sub-surface topography and the higher field-saturated conductivity (K_{fs}) of the saprolite as compared to the soil matrix of the subsoil, infiltrating water is deflected to the depressions in the saprolite topography as a result of capillary diversion (C). When saturated conditions are reached in the depressions, a complete break through occurs and water is transmitted to the saprolite (D).*

The quick response of the interflow to the rainfall event analysed in November 2017 together with the change in NO_3-N concentrations in the interflow suggests that, besides the delayed component, also a quick interflow component and thus preferential flow was present. This is further supported by the high interflow volumes of 907 l/day at P10 and 1180 l/day at P11 in April 2017, which were measured some hours after a rainfall event. In addition, also Burghof (2017) in accordance with Wright (1992) assumes preferential flow to be active in “channels of rapid flow” in the saprolite. Several different mechanisms might have been active in this regard (see chapter 2.2.1). One possibility would be the presence of a network of continuous macropores from the soil surface or at least over longer distances (Beven and Germann, 2013; Jarvis, 2007). At the trench interfaces and at the bottom of the trench interflow entered via visible macropores (of about 0.5 - 2 cm in diameter) in the matrix of the saprolite and in the sandy loam layer (see Figure 47). Throughout the soil body above the saprolite macropores of about 0.3 cm were observed. These macropores favoured the quick delivery of water to the saprolite once being activated by water entry from the saturated matrix or by high hydraulic pressures at the soil surface. Macropores of that size could also be observed in the upper saprolite as such. As higher K_{fs} values could not always be attributed to coarser texture, these macropores were most likely responsible for the higher hydraulic conductivity of this upper part of the saprolite. It is not known though, whether these macropores belong to a continuous pore network, especially as according to Burghof (2017) the lower saprolite is sandier and

contains less quartzites. Nevertheless, she also characterises the texture of the saprolite as very heterogeneous which leads to highly variable hydraulic conductivities within the weathering profile. Thus, even disconnected macropores might temporally get connected via nodes as described in Nieber and Sidle (2010), Noguchi et al. (1999) and Sidle et al. (2001). They state, that under unsaturated conditions water might be trapped behind less permeable structures in the soil leading to local saturation and activation of macropores even in deeper soil layers. In addition, pockets of more permeable material might connect macropores in otherwise less permeable sediments. The before mentioned authors describe this phenomenon to get more important at the end of a rainy season, leading to very extended networks of preferential flow pathways. Unfortunately, there is not sufficient event-based interflow data, to state that there was more preferential flow at the end of the rainy seasons. Yet, the nodes-theory might also help to explain the general increase in interflow during these periods.

Figure 47 *Macropores in the sandy loam layer (a) and in the saprolite (b) at the trench interface. Interflow water was also found to well up in macropores in the upper saprolite at the bottom of the trench (c).*

The weak or lacking correlation of interflow volumes and soil moisture in the soil above the saprolite (rho= 0.3) as well as of interflow volumes and the 7-day precipitation index (rho= 0.2) suggest that the hydrological conditions (i.e., the degree of saturation) in the saprolite built up and persisted over longer periods of time. This is supported by the contorted relation of total rainfall and cumulative interflow volumes during the single rainy seasons. The high interflow volumes in season 2016.2 probably reflect the strong delayed component of the previous rainy season. The sparse rains in season 2016.2, on the other hand, might have caused the slow increase in interflow at the beginning of season 2017.1 as well as partly also the short duration of high flow levels as well as the exsiccation of interflow under crop production in

and after season 2017.2. Nevertheless, these phenomena were further driven by the rainfall distribution and intensity of these seasons. As rainfall intensities were higher in season 2017.1 than during the other seasons, more surface runoff occurred and hence less water was transferred to the saprolite to balance the deficit from season 2016.2. In season 2017.2 on the other hand, most of the rainfall fell during two rainfall events, so again less water could be transferred to the saprolite compared to season 2016.1 which was characterised by equally distributed rainfall events of moderate intensities. Hence, other than in season 2016.1, interflow ceased after the end of the rainy season 2017.2. Nevertheless, it is not known whether higher rainfall intensities during these seasons actually led to an increased quick interflow component, as continuous measurements would be needed to capture this effect. In literature, rainfall intensity was often found to strongly influence the quick component of interflow as it favours surface ponding of rain water and the establishment of (near)-saturated conditions near the surface which can then activate continuous macropores and lead to preferential subsurface flow (Beven and Germann, 1982; Jarvis, 2007; Lin and Zhou, 2008). Analysis of nitrate concentration in the interflow would suggest such processes, as will be discussed in chapter 7.2.

In literature, opinions on the effect of perennial vegetation on lateral flow processes differ. Some authors state that there is more lateral subsurface runoff and especially preferential flow under perennial vegetation (Jarvis, 2007; Yang et al., 2013) or after the re-cultivation with grassy and shrub-like vegetation (Ziegler et al., 2004). Different reasons are reported to be responsible for that matter. Most importantly, infiltration increases due to higher macroporosity caused by root channels and soil faunal activity. This can be enhanced further, when soil fauna leaves hydrophobic coatings at the walls of the macropores. Nevertheless, other authors describe that lateral flow components are less likely to develop under perennial vegetation (Ribolzi et al., 2018). They refer to the fact that deeper roots and a denser root network of grasses, trees and shrubs extract larger volumes of water and that, hence, the evapotranspiration is higher, leading to drier conditions and hence less lateral flow. Others suggest that there is actually less macropore flow from grassland sites due to the extended network of rather small, densely spaced and very tortuous macropores, which rather store water or transfer it back to the soil matrix (Edwards et al., 1992). In this study, K_{fs} and infiltration were found to be higher under semi-natural vegetation for the soil surface and the B horizon. In addition, there was less surface runoff from the plot under semi-natural vegetation. Therefore, more water infiltrated at this plot. Nevertheless, soil moisture was found to be higher than at the other land use types only at 10 cm and 30 cm depth but not at 20 cm and 40 cm depth during the rainy season. The comparably lower values at 40 cm show that higher infiltration rates did not lead to higher degrees of saturation at depth. Hence, despite the increased infiltration of rainwater, probably less or at least not more water was transferred down to the soil saprolite interface and to the deeper saprolite than at the plot under crop production over the rainy period. This fits to the lower interflow values throughout the study period and the faster decrease in interflow at the onset of the dry season and also to the smaller reaction to rainfall events under semi-natural vegetation. The very high flow levels of 1180 l/day under semi-natural vegetation in April 2017 measured some hours after a rainfall event do not match the other data. Here, more event-based measurements would be needed to rule out the existence of a very pronounced fast component of interflow under this land use type. Using ArcSWAT and SWATgrid, Gabiri et al. (2019) modelled the impact

of different land management options on the water balance components in the Nasirye catchment. Their results partly correspond to the observations made here. For the ArcSwat, lateral flow decreased under the slope conservation scenario in which afforestation with tropical highland rainforest of the previously cultivated slopes was simulated. For the SWATgrid on the other hand, lateral flow was found to increase under slope conservation. Either way, processes in a heterogeneous unsaturated soil matrix might not be well represented by models like SWAT, which are based on the Richard's equation (Beven and Germann, 2013).

A third trench was installed beneath the plot under bare fallow. Yet, quantification of interflow at this trench was not possible, as interflow ceased some hours after installing the gutter in the upper saprolite. When digging deeper into the ground to reinstall the gutter, the same happened at every attempt. At the same time, water pooled at the bottom of the trench and there was a constant flow of water in the drainage down to the wetland. One explanation of that behaviour could be that at this position the actual connection of the upper saprolite and the soil body to the interflow from deeper areas of the saprolite occurred further downslope. Thus, the perched water table reached up to the position of P12 but was drained upon digging. The orange stains in the B horizon as well as the yellowish colour of the soil matrix indicate that in contrast to the other two trenches at the slope toe this layer did not constantly experience saturated conditions (see chapter 5.2.1). This supports the before mentioned hypothesis, as the perched water created by the impounding interflow a little further down slope only reached up to the position of the trench during very wet periods.

Several limitations are inherent to the research approach followed by this study, which impede the conclusions on total flow volumes as well as on the interflow related processes. The most important factor was the choice of the measurement interval. As demonstrated above, a quick and a delayed component of interflow were present at the slope under investigation. Yet, due to the measurement interval mostly the delayed component was measured. This implies that the cumulative interflow volumes per season described above were most likely underestimated and the peaks not captured in the description of the interflow dynamics over time. To elaborate on the effect of rainfall and soil moisture characteristics as well as on the influence of the land use type, continuous measurements would be necessary, which capture both, the delayed as well as the quick interflow component. Another source of uncertainty related to interflow quantities and the calculation of the cumulative interflow volumes lies in the setup of the trenches and in the choice of a trench study as such. Blume and Meerveld (2015) point out that trenches must be deep enough to capture all the lateral flow and wide enough to capture spatially varying flow pathways. Due to constructional difficulties and monetary limitations both criteria were probably not fully met in this study. Furthermore, no lateral subsurface boundary, like a plastic sheet, etc. was installed. Therefore, the subsurface catchment for each trench remained unknown, which makes spatial extrapolation of the results as well as area-related statements rather imprecise. Apart from that, maintenance of the trenches is critical as was proven by the very low flow levels captured at P11 in March 2017, when the makeover of the trench led to a rapid increase in the interflow volumes of about 800 %. In addition, continuous soil moisture measurements down to the surface of the saprolite would be needed, to proof the concept of the "fill-and-drain"- mechanism introduced above. Soil moisture measurements of that kind would also help to further elaborate on the different processes under crop

production and semi-natural vegetation regarding water storage, the activation of macropores and drying of the soil. Moreover, the extrapolation of the results to other parts of the catchment as well as general conclusion on the effect of different land use types is restricted by the poor spatial coverage of the experiments, as only one hillslope was considered in this study. Due to the high heterogeneity of the saprolite and the role this plays for the development of perched waters as well as for the activation of preferential flow paths, interflow levels might actually vary strongly between different sites. Even the reduced outflow at P11 might not only be determined by the land use type but also by structural differences of the underlying saprolite. Yet, the trouble of capturing the spatial and temporal variability of preferential lateral flow lies at the heart of hillslope hydrology (Angermann et al., 2017; Beven and Germann, 2013) and gets aggravated by the fact that preferential flow paths are as such dynamic and evolve over time (Nieber and Sidle, 2010).

6.2.2 Contribution of interflow to the wetland

The first part of this section reflects on the hydrogeological connection of the interflow to different ground water bodies in the wetland. In the second part, soil moisture dynamics at the wetland fringe are related to water inputs by the interflow in order to deduct the relevance of water inflow from the slopes on soil moisture conditions at the wetland fringe.

In her study on the hydrogeological characteristics of the Namulonge wetland, Burghof (2017) differentiated three aquifers at the valley bottom (see chapter 3.3). From her geochemical analysis she concluded that the aquifer and the vadose zone in the wetland soils and locally also the aquifer in the valley sediments get recharged by lateral fluxes from the slopes. She as well as Gabiri et al. (2018) found that rainfall dynamics were better reflected in the piezometers at the fringe than at the middle and centre position, which confirms her hypothesis. In this study, we aimed to verify these conclusions regarding slope water input by direct observations and extent them to account for nutrient delivery (see chapter 7.4).

As described above, interflow at the slope toe was found in the first meter of the saprolite as well as in a sandy loam layer above it. Drilling results showed that this sandy loam layer continued laterally into the wetland, where a clayey layer was found beneath it (see chapter 5.2.1). This supports the hypothesis of Burghof (2017) that water from the slopes recharges the shallow aquifer in the wetland soils, which is separated from the aquifer in the valley sediments by the clay layer. In addition, field observations as well as the geo-electrical measurements did not revealed the presence of a paleo-dambo clay, which prevents interflow water from entering the shallow aquifer in the wetland soils, at this position. Therefore, interflow water from the slopes contributed to plant available water for agricultural production in the wetland. At the position investigated in this study, interflow was further found to contribute to the aquifer in the valley sediments. As the clay-muscovite layer in the saprolite was found to meet the valley sediments well below the clay layer which separates the two aquifers in the wetland, the water conducted in the topmost part of the saprolite is expected to enter the aquifer in the valley sediments (see Figure 48). Nevertheless, the situation might be different at other sites within the wetland, if the geological connection is different from the one described above, and the clay-muscovite layer meets the valley sediments above the wetland clay layer. In addition, the water passage from the saprolite into the aquifer

in the valley sediments might be blocked by the presence of a paleo-dambo clay layer, depending on the vertical extend of that layer.

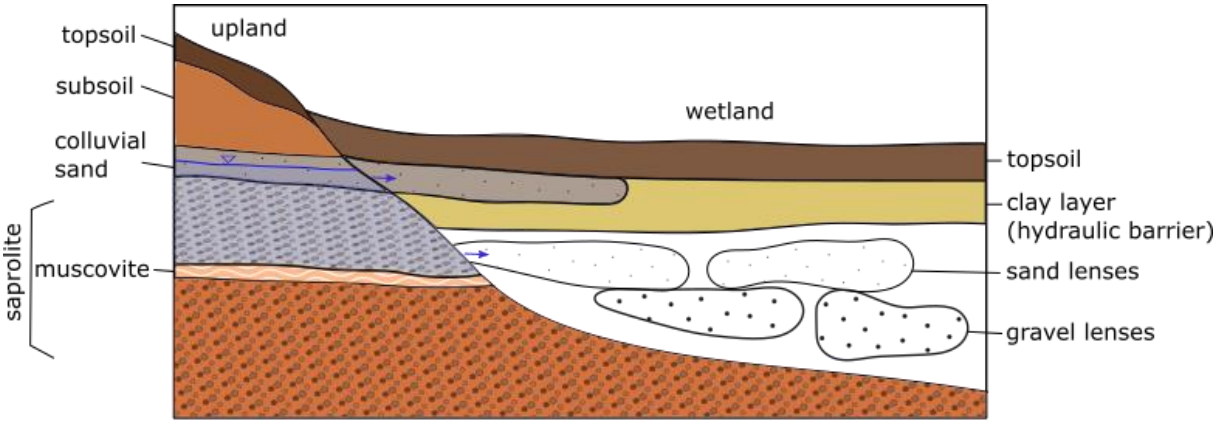

Figure 48 *Schematic representation of the geology at the slope toe and the transition to the wetland (as related to the first and second scenario presented in the text). The blue area indicates the presence of interflow above the muscovite layer in the saprolite and the blue arrows mark its connection and hence water passage to the shallow aquifer in the wetland soils as well as to the aquifer in the valley sediments. Colours were chosen according to field observations where possible. Note that the extend of the different layers is not true to scale.*

Figure 49 shows the dynamics of interflow and soil moisture at the wetland measuring points as well as the mean soil moisture of the upland measuring points on the plot under crop production in relation to the daily rainfall amounts during the study period. For both measuring points in the wetland, soil moisture conditions at 20 - 40 cm depth remained close to saturation throughout the study period. At 0 - 20 cm depth, dynamics were more pronounced. As described in chapter 6.1, soil moisture in the upper 20 cm of the wetland reacted to rainfall inputs in a similar way as soil moisture at the slope. This fits to the observation that the aquifer in the valley sediments was mostly separated from the shallow aquifer in the wetland soils so that soil moisture in the wetland was influenced strongly by rainfall dynamics. Nevertheless, the reduction of soil moisture at the wetland fringe at the beginning of the dry season was delayed compared to the upland positions. In addition, soil moisture in the wetland was still rising further after maximum values at the slope had already been reached at the beginning of the rainy season. As both effects could be caused by water input from the interflow, relations of soil moisture in the wetland and interflow dynamics at the slope toe are discussed in more detail. For point W1 the reduction of soil moisture at the beginning of the first dry season 2017 was delayed compared to soil moisture at the slope but already set in at a time, when interflow levels had not yet reduced. At the beginning of the second dry season 2017, reduction in soil moisture in the first 20 cm at W1 was parallel to the reduction of interflow. The same applies to the rewetting at the beginning of the first and second rainy season in 2017, which mostly followed the dynamics of the interflow. During the drier weeks of the second rainy season 2017 though, soil moisture in the wetland remained rather stable even when soil moisture at the slope as well as interflow levels reduced intensely. At point W0, soil moisture was rather stable at about 90 % saturation even at 0 - 20 cm depth throughout the study period. Interestingly, the slightly drier periods corresponded to times of very little interflow in September and late October 2017. During the exceptionally dry conditions at point W0 in January 2018, interflow had not yet reached its lowest values, as it dried out

completely three weeks later. At this stage, no more soil moisture data were available for the wetland, but the last measurement showed a slight increase in moisture, which does not fit to the interflow dynamics at the plot under crop production. For both measuring points, highest values were reached after the heavy rainfall event in November 2017 and remained very high for some weeks afterwards, when interflow levels had already dropped again. The correlation analysis revealed a strong correlation between soil moisture in the wetland at 0 - 20 cm depths and interflow levels at the slope toe (Spearman's rho= 0.69 for W0 and rho= 0.7 for W1), while no correlation was detected at 20 - 40 cm depth at both points. At this depth soil moisture was close to saturation throughout the measurement period. These findings reveal that water input from the interflow was only one driving force for soil moisture at the wetland fringe, but that the input from other sources should not be neglected. This is not surprising, as interflow does not only contribute to soil water but also to the aquifer in the valley sediments, and the distribution is not known. In addition, the different aquifers in the wetland are locally connected, as described before. Positive hydraulic heads might lead to water input from the aquifer in the valley sediments into the shallow aquifer in the wetland soils. This hydraulic head of the aquifer in the valley sediments was not only driven by water input from the interflow but also by water input from the deep aquifer as well as piston flow from the upper catchment. Another contributor to soil water in the wetland was surface runoff from the slope, which is discussed further in chapter 6.3. The signal of interflow in the soil moisture data can, thus, only be diffuse. Therefore, even if interflow levels could be determined exactly at the slope toe, their contribution to the soil water status of the wetland soils would be difficult to quantify due to the high number of interrelated components contributing to the shallow aquifer in the wetland soils.

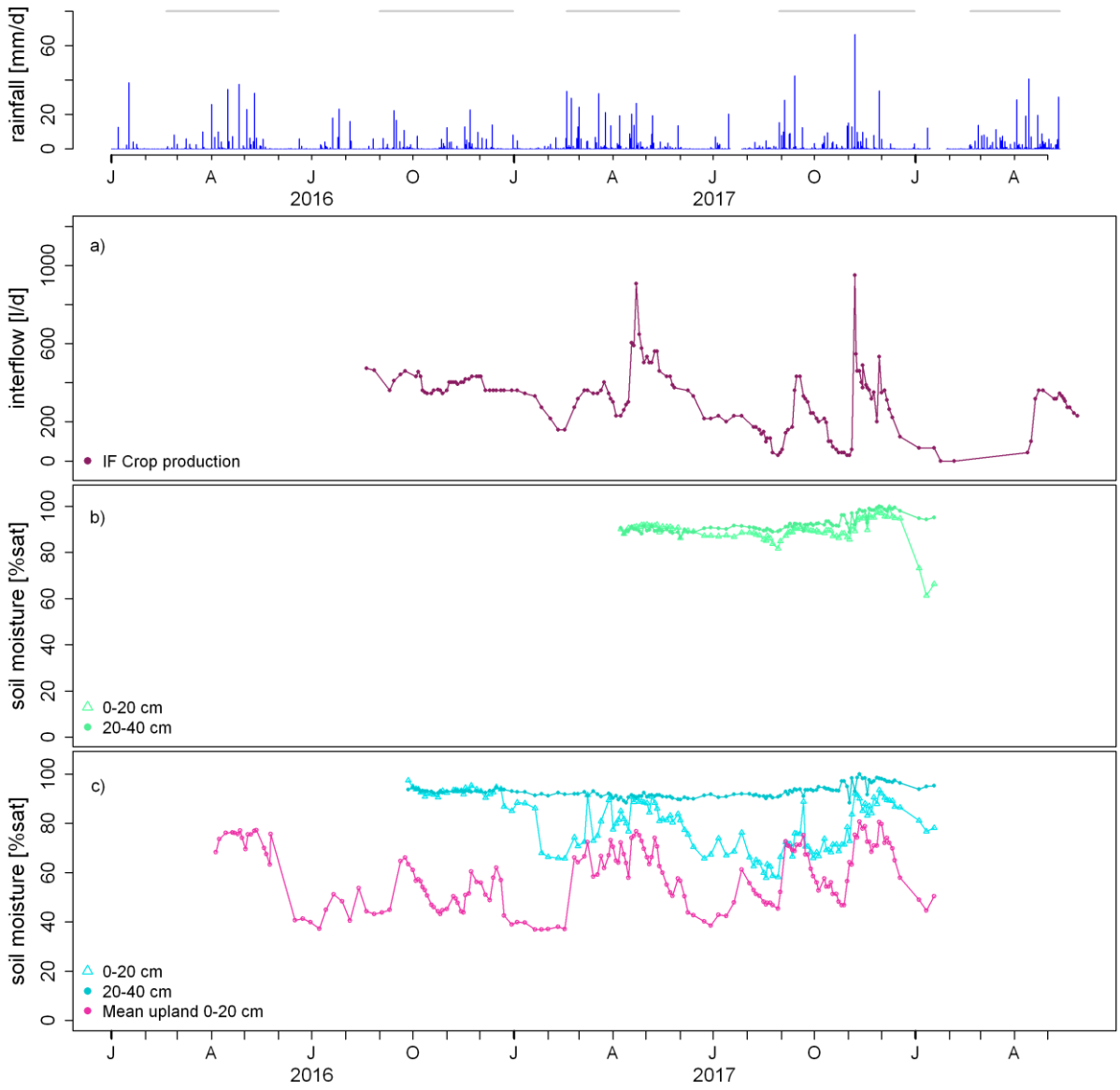

Figure 49 *Interflow [l/d] at the plot under crop production (a) compared to rainfall (top panel) and soil moisture in the wetland at 0 - 20 cm and 20 - 40 cm depths at measuring point W0 (b) and measuring point W1 (c). Panel c) further shows the mean soil moisture of the measuring points in the upland at the plot under crop production (pink line).*

6.3 Surface runoff

Slopes contribute to the water balance of the wetland not only via subsurface interflow but also via surface runoff. Therefore, also the dynamics of water inputs by surface runoff were analysed regarding the impact of the land use type, seasonality and rainfall characteristics as presented in the following chapter. In the second part of this chapter soil moisture at the wetland fringe is related to water inputs from the surface runoff.

As described in chapter 4.4.3, surface runoff was collected on three runoff plots at the lower slope of each land use type. Statistical analysis revealed that the variability of surface runoff volumes between the plots (intra-treatment variability) was not pronounced at the plot under crop production and under bare fallow, as there was no significant difference between the three repetitions. Nevertheless, coefficients of variation ranged from 4 % to 108 % at the plot under crop production and from 6 % to 167 % at the bare fallow plot (excluding days when the collectors overflew). For semi-natural vegetation, surface runoff during the study period at plot P5 was significantly different from the other two repetitions (at p=0.05). For this land use type, coefficients of variations ranged from 10 % to 167 %. Nevertheless, only the mean runoff value for each land use type was used for further analysis. Figure 50 shows the mean runoff from each land use type related to mean soil moisture along the slope at 0 - 40 cm depth, rainfall intensity and rainfall amounts. During some intense rainfall events the volume of the collectors on the plot under crop production and on the plot under bare fallow was not sufficient to capture all the runoff. This is indicated by a black “x” on top of the corresponding runoff bar. To minimize this effect, the collector volume on the bare fallow plot was increased in October 2016 (2 drums which could capture 245 l of water each). Furthermore, the sampling area was reduced from 42 m² to 30 m² on 31st of March 2017. This explains why overflow of the collectors occurred at different runoff quantities (note the unit is l/m²).

The frequently reported effect of land use types on surface runoff generation, including an increase in surface runoff with decreasing soil cover, e.g., Molina et al. (2007), was also found in this study. Surface runoff volumes were different between the three land use types. The Kruskal-Wallis test showed that at p= 0.05 there was significantly less runoff at the plot under semi-natural vegetation than at the bare fallow and the plot under crop production. Further, there was more surface runoff from the bare fallow plot than from the plot under crop production but the difference was not significant according to the Kruskal-Wallis test. Nevertheless, the observed difference between the mean ranks was very close to the critical difference indicating that surface runoff quantities at the bare fallow plot were still considerably higher than at the plot under crop production. At the bare fallow plot, surface runoff could be measured if there was a rainfall event of at least 1.7 mm, while at the plots under crop production and semi-natural vegetation the threshold was 2.8 mm and 3 mm respectively. The thresholds did not noticeably differ between dry and wet conditions. Surface runoff is generated, when water input exceeds the infiltration capacity of the soil or when the soil body is saturated. Both is strongly influenced by the plant cover, as it increases interception and influences infiltration stimulating soil properties, such as macroporosity due to faunal activities, humus content and aggregate stability as well as the overall pore space which dictates the water storage volume of a soil (Weil and Brady, 2017). As agricultural practices included physical soil treatments and periods of no and little plant cover at the beginning of the growing season, differences

between the plots under crop production and bare fallow were not as pronounced compared to the plot under semi-natural vegetation.

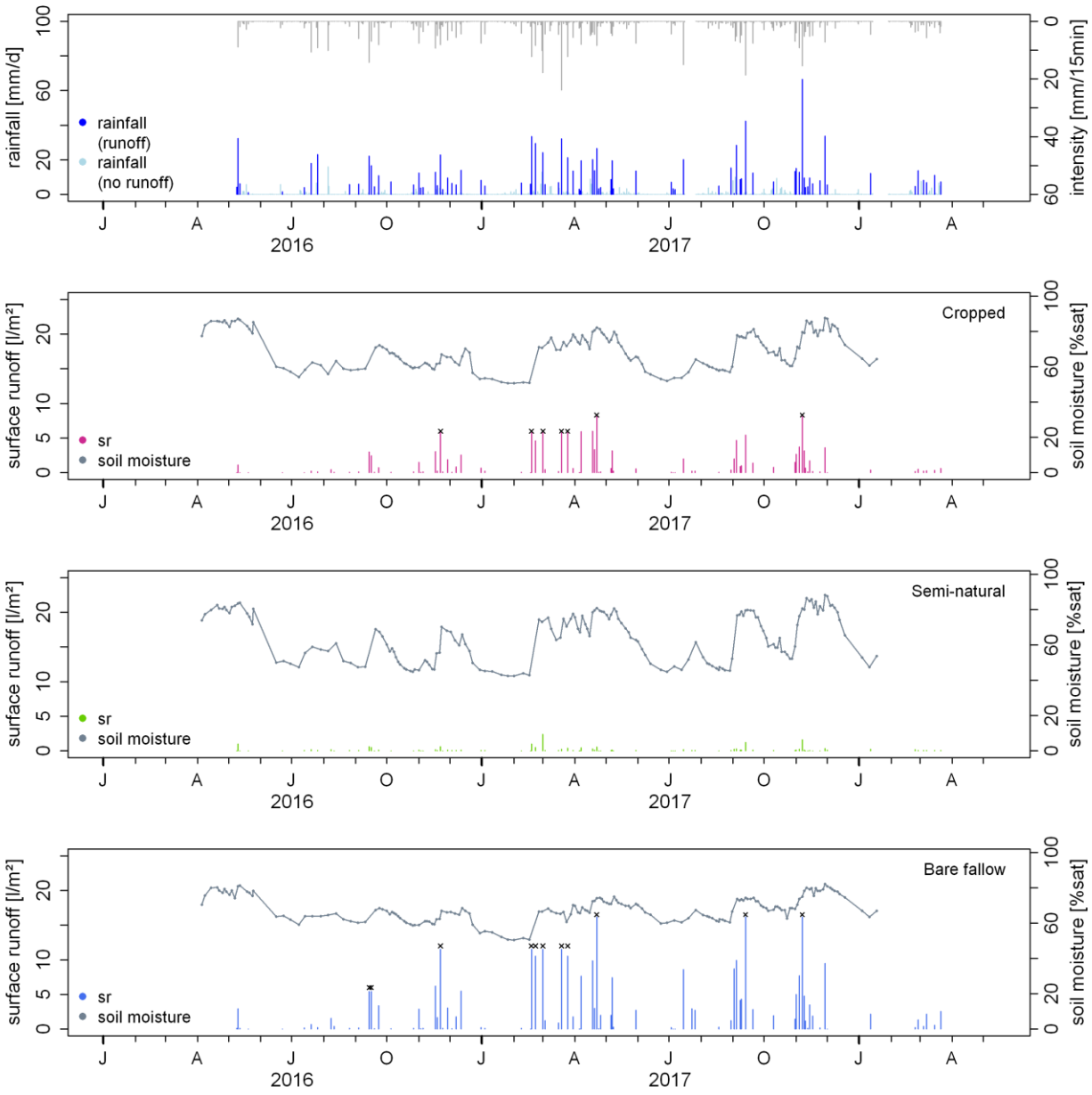

Figure 50 *Mean surface runoff from the plot under crop production, the plot under semi-natural vegetation and the plot under bare fallow (panels 2-4 respectively). The dark lines represent the mean soil moisture at the slope under the respective land use type. The black x on top of a runoff bar indicates that the drums overflowed. The first panel depicts rainfall (light blue and blue bars) and rainfall intensity (grey bars). In this panel, the dark blue bars show rainfall amounts on days when surface runoff was generated, while the light blue bars show rainfall amounts when no surface runoff was generated.*

Table 10 *Correlation coefficients describing the correlation of surface runoff volumes [l/m²], rainfall characteristics, and rainfall characteristics combined with mean soil moisture (0-40 cm).*

Land use type	Rainfall characteristics	r (Pearson)	R^2	n	p	rho (Spearman)	n	p
Crop production	Rainfall event [mm]	0.76	0.57	359	<0.05	0.66	359	0<0.05
	Max 15min intensity [mm]	0.66	0.44	359	<0.05	0.65	359	0<0.05
	Rainfall*intensity	0.68	0.46	359	<0.05	0.66	359	0<0.05
	Rainfall*intens.* moisture	0.81	0.65	133	<0.05	0.74	133	<0.05
Semi-natural vegetation	Rainfall event [mm]	0.68	0.47	359	<0.05	0.64	359	<0.05
	Max 15min intensity [mm]	0.61	0.38	359	<0.05	0.64	359	<0.05
	Rainfall*intensity	0.69	0.48	359	<0.05	0.65	359	<0.05
	Rainfall*intens.* moisture	0.64	0.41	133	<0.05	0.71	133	<0.05
Bare fallow	Rainfall event [mm]	0.77	0.60	359	<0.05	0.65	359	<0.05
	Max 15min intensity [mm]	0.69	0.47	359	<0.05	0.65	359	<0.05
	Rainfall*intensity	0.71	0.50	359	<0.05	0.66	359	<0.05
	Rainfall*intens.* moisture	0.83	0.69	133	<0.05	0.73	133	<0.05

Surface runoff quantities were well related to rainfall amount and rainfall intensity as can be seen in Figure 50. Analysis of correlation supports these findings, as correlation coefficients revealed moderate to strong correlations (see Table 10). There was no clear signal of seasonality. As described in Podwojewski et al. (2008), the first rains after the dry season often cause severe surface runoff in tropical regions. This was only partially reflected in the data collected in the frame of this study. When comparing single rainfall events which occurred during or after dry periods to rainfall events of similar magnitude during moist periods, several times more surface runoff was generated under or following dry conditions, especially at the bare fallow plot. For the bare fallow plot this can be seen in September and November 2016 as well as at the onset of the first and second rainy season 2017 (also after the drier period in October 2017) and

after the intermittent rainfall event in the second dry season 2017. At the plot under crop production, the rainfall events in September 2016 and the intermittent rains of the second dry season 2017 did not cause a strong runoff response. Equally, the differences at the onset of the first and second rainy season in 2017 were less pronounced. It has to be considered, though, that during the first rainy season 2017 the collectors frequently overflowed at both plots so that it was not possible to compare the runoff responses at the beginning of that rainy season with those at a later stage. Nevertheless, under both land use types, there were also various examples of rainfall events of similar magnitudes causing more runoff during the rainy season, when soil moisture of the upper soil was high, e.g., August 2017 and rainfall events during dry periods which produced very little surface runoff, e.g., January 2018. In addition, the strong correlation of surface runoff volumes and rainfall properties was increased again, when antecedent soil moisture was factored in (see Table 10). This indicates that the highest surface runoff volumes occurred as a result of big heavy rainfall events during high soil moisture conditions. Nevertheless, analysis of correlation of soil moisture and surface runoff only has limited explanatory power due to the fact that soil moisture was measured at a constant interval of 2-3 days and, therefore, was oftentimes not measured on the day surface runoff occurred.

Figure 51 has the same setup as Figure 50 but shows the runoff coefficients instead of the runoff volumes. Intra-plot comparison of runoff coefficients did not reveal a significant difference at p= 0.05 for the three repetitions at the plot under crop production. Coefficients of variation ranged from 4 % to 111 %. On the bare fallow plot, runoff coefficients on plot 9 were significantly smaller than on the other two plots and coefficients of variation ranged from 6 % to 111 %. On the plot under semi-natural vegetation runoff coefficients on P5 were significantly smaller than on the other two plots and coefficients of variation ranged from 10 % to 172 %.

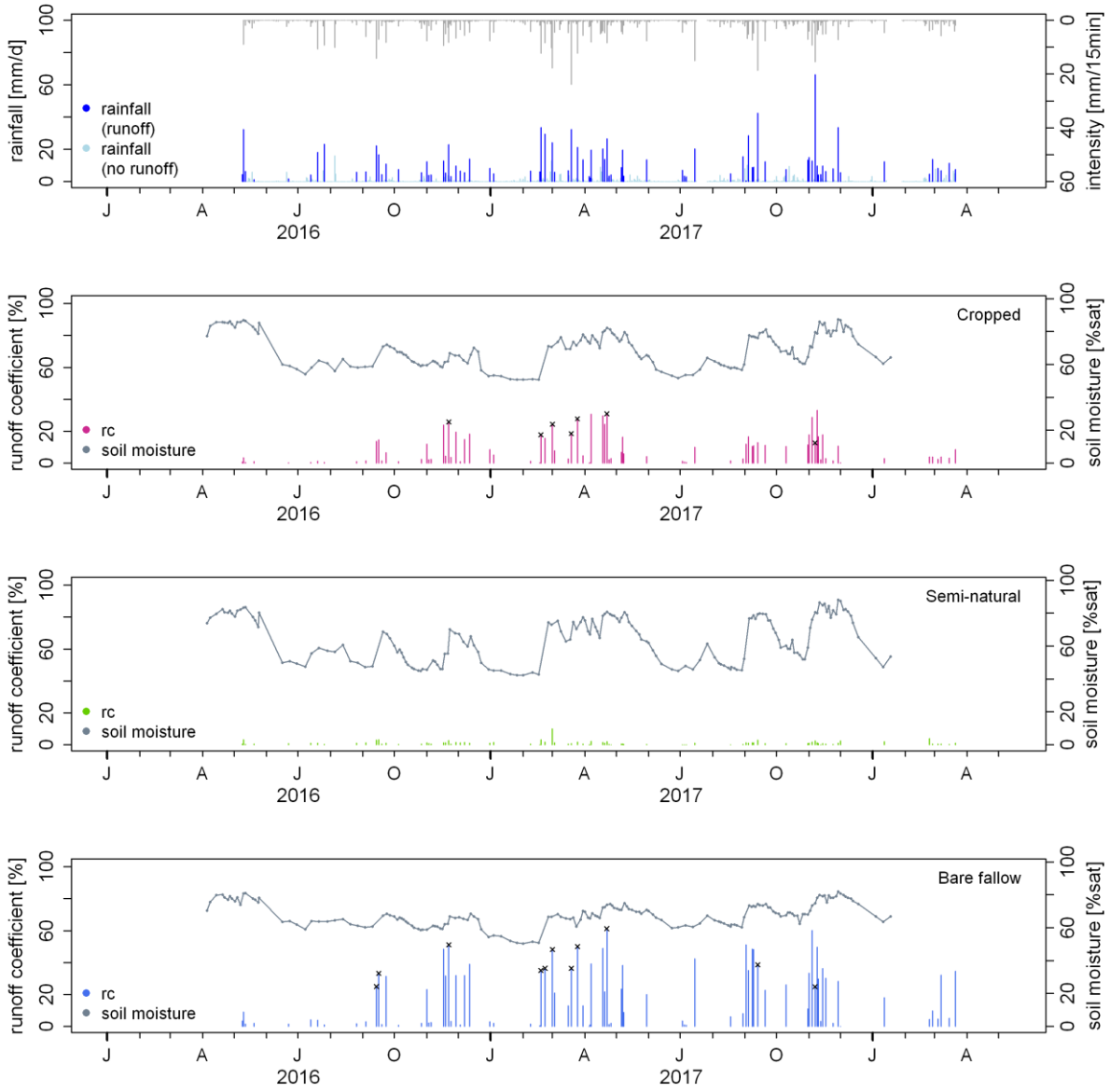

Figure 51 *Mean runoff coefficients on the plot under crop production, the plot under semi-natural vegetation and the plot under bare fallow (panels 2-4 respectively). The dark lines represent the mean soil moisture at the slope under the respective land use type. The black x on top of a runoff bar indicates that the drums overflowed. The first panel depicts precipitation (light blue and blue bars) and rainfall intensity (grey bars). In this panel, the dark blue bars show rainfall amounts on days when surface runoff was generated, while the light blue bars show rainfall amounts when no surface runoff was generated.*

Table 11 *Correlation coefficients describing the correlation of runoff coefficients [%], rainfall characteristics, and rainfall characteristics combined with mean soil moisture (0-40 cm).*

Land use type	Rainfall characteristics	r (Pearson)	R^2	n	p	rho (Spearman)	n	p
Crop production	Rainfall event [mm]	0.60	0.36	359	<0.05	0.65	359	<0.05
	Max 15min intensity [mm]	0.60	0.36	359	<0.05	0.65	359	<0.05
	Rainfall*intensity	0.45	0.21	359	<0.05	0.66	359	<0.05
	Rainfall*intens.* moisture	0.67	0.44	133	<0.05	0.74	133	<0.05
Semi-natural vegetation	Rainfall event [mm]	0.57	0.32	359	<0.05	0.64	359	<0.05
	Max 15min intensity [mm]	0.60	0.36	359	<0.05	0.64	359	<0.05
	Rainfall*intensity	0.51	0.26	359	<0.05	0.65	359	<0.05
	Rainfall*intens.* moisture	0.60	0.36	133	<0.05	0.72	133	<0.05
Bare fallow	Rainfall event [mm]	0.60	0.36	359	<0.05	0.65	359	<0.05
	Max 15min intensity [mm]	0.62	0.39	359	<0.05	0.65	359	<0.05
	Rainfall*intensity	0.46	0.21	359	<0.05	0.66	359	<0.05
	Rainfall*intens.* moisture	0.67	0.45	133	<0.05	0.73	133	<0.05

The data at hand do not allow to further characterize the prevailing runoff processes regarding infiltration or saturation excess runoff. The fact that combining soil moisture with rainfall characteristics gives the strongest correlations might indicate that high runoff volumes in the frame of this study were connected to saturation excess runoff. Nevertheless, the non-significant difference between runoff coefficients in wet and dry periods would not support that. Furthermore, the moisture values collected in this study do not allow to infer on the soil moisture status of the entire soil body, as only the upper 40 cm are considered. Kleinman et al. (2006) described that well-drained mid-slope positions (Conacher and

Dalrymple, 1977) favour the generation of infiltration excess runoff. In addition, Needelman (2002) found that the generation of saturation excess runoff is commonly related to subsurface discontinuities, i.e., an impermeable layer. As discussed in section 6.2.1, complete saturation of the soil profile was unlikely, as in case that saturated condition developed in the lower soil profile above the saprolite, the activation of macropores in the upper saprolite and, thus, the drainage of the soil profile is expected. Therefore, generally, the prevailing geological conditions as well as the slope position would rather suggest that infiltration excess runoff was the prevailing process. Nevertheless, an event based monitoring of the matrix potential in the soil or an analysis of the timely development of rainfall/runoff ratios as in Kleinman et al. (2006) would be necessary to confirm this hypothesis.

Figure 52 shows surface runoff coefficients at the plot under crop production and at the plot under semi-natural vegetation compared to soil moisture at 0 - 20 cm and interflow volumes at the respective plot (panel b and c). Panel a displays daily rainfall amounts. When analysing surface runoff coefficients in relation to the interflow, some general trends emerge. The data generally show rather high runoff coefficients and low interflow levels at the plot under crop production at the beginning of the rainy seasons or when soil moisture was low. That does not apply though at the beginning of the second rainy season 2017, when runoff coefficients were low even if interflow levels had not yet risen again. During the rainy season, when soil moisture levels were high, generally more interflow was generated and runoff coefficients were lower. Nevertheless, big rainfall events during the rainy season produced high levels of interflow and high runoff coefficients alike. At the plot under semi-natural vegetation, this was even the predominant pattern and higher coefficients at low flow levels could only be found at the beginning of the first and, to a smaller extent, of the second rainy season 2017. For both land use types, analysis of correlation (Spearman) presents a weak but positive correlation between surface runoff coefficients and interflow volumes (rho= 0.4). This can be explained by the fact that both, interflow levels and runoff coefficients, were strongly influenced by rainfall amounts. Concerning the interflow, no event-based coefficients could be calculated, as a reference area could not be delineated due to subsurface mixing of infiltrating water, constructional trench layout and temporal resolution of the measurements. Furthermore, the delayed component of interflow could not be attributed to single events, and the direct component was quantified only once. Therefore, coefficients can only be compared to interflow volumes reflecting the rainfall signals over longer time spans, which limits the informative value.

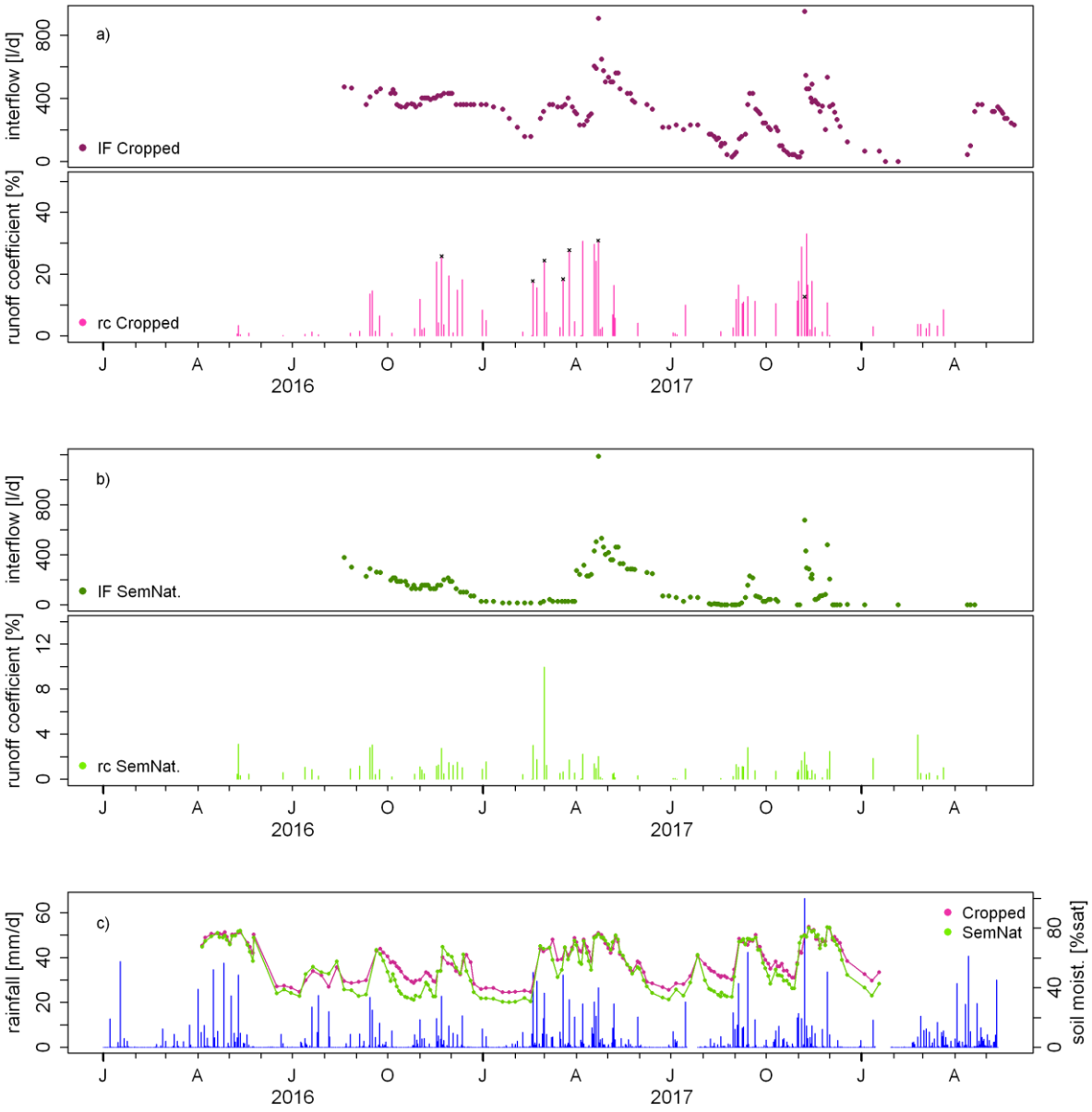

Figure 52 *Dynamics of interflow and runoff coefficients (surface runoff) at the plot under crop production (a) and at the plot under semi-natural vegetation (b) compared to rainfall and mean soil moisture at the slope at 0 - 20 cm under both land use types (c). The black x on some bars in panel a) indicates that surface runoff collectors overflowed on the respective day.*

A pronounced correlation of interflow and surface runoff volumes could also hint to infiltration of surface runoff at the slope toe. Yet, the behaviour described above would not support that. If infiltrating surface runoff made up for an essential part of the interflow at the slope toe, high surface runoff volumes would not subside with low interflow values at the beginning of the rainy season, when the water contribution by the weathering body was still small. In addition, the very pronounced delayed component of the interflow does not allude to an essential contribution of infiltrating surface runoff to interflow. On the other hand, a correlation of rho= 0.5 between nutrient input via the interflow and via surface runoff was found at the plot under crop production (see chapter 7.2). Soil moisture at the slope toe showed a very similar pattern as soil moisture across the slope for each land use type (see Figure 53). Nevertheless,

correlation coefficients with the surface runoff volumes were higher (rho ~0.5) than correlation coefficients of surface runoff and mean soil moisture at the slope. Soil texture at this slope position was sandier compared to the upslope positions. This might favour infiltration of surface runoff and could explain the concurrence of high runoff coefficients and high interflow levels during the rainy season as well as the higher correlation coefficients of soil moisture at the slope toe and surface runoff. Yet, as explained before, the explanatory power of a correlation analysis of volumes and coefficients is limited and continuous interflow measurements are needed to reliably relate surface runoff and interflow. In conclusion, evolution of interflow over time does not suggest that infiltrating surface runoff offers a major contribution to interflow at the slope toe, but it might add to it during moist periods.

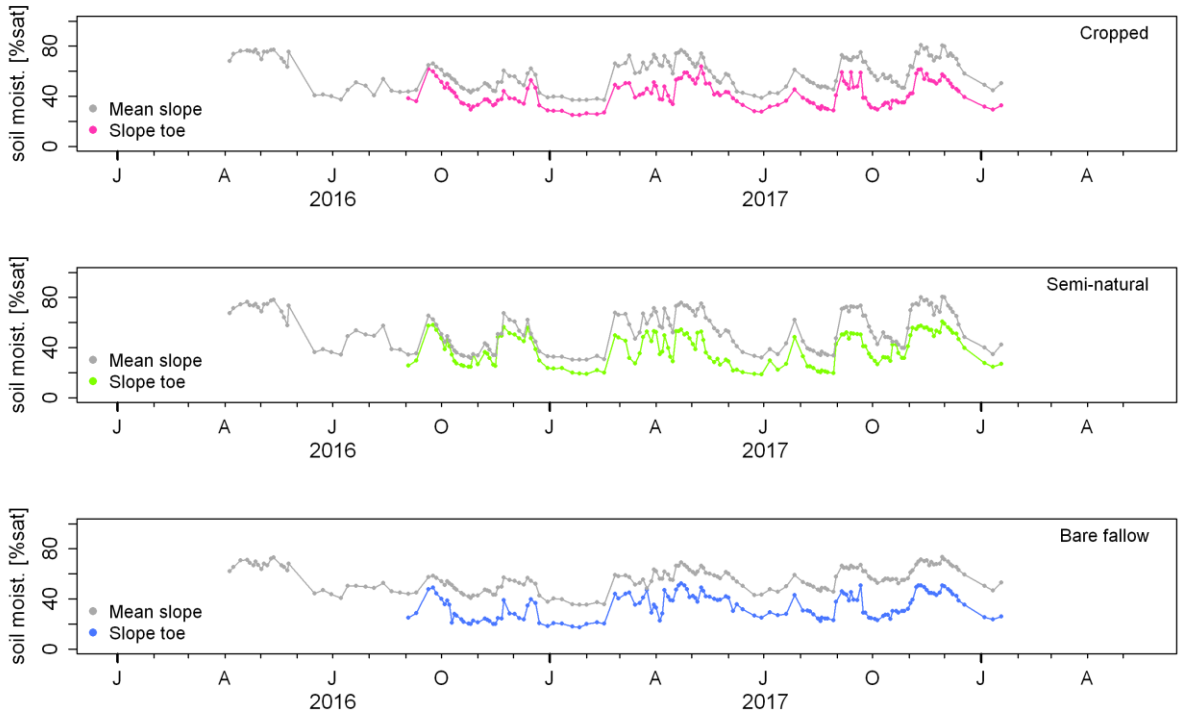

Figure 53 *Mean soil moisture at the slope (upper 20 cm) compared to soil moisture at the slope toe (upper 20 cm) for the three land use types respectively.*

Even if infiltrating surface runoff at the slope toe contributed to the interflow during heavy rainstorms, the biggest share was expected to enter the wetland directly as surface runoff. Here, part of the water infiltrated into the wetland soil while another share continued as surface runoff flowing towards the outlet of the wetland or towards the central stream in the wetland. Analysis of soil moisture at the fringe of the wetland and surface runoff did not reveal a strong connection between the two components. Correlation coefficients between both, surface runoff volumes as well as runoff coefficients and soil moisture at the fringe, were very weak (R^2< 0.1 and rho< 0.2). Comparison of the timelines of surface runoff and soil moisture at the wetland fringe generally supported that (see Figure 54). Most of the time, dynamics of soil moisture did not follow surface runoff dynamics. Except for some few days (e.g., in Nov. 2016 and in April and Sep. 2017), bigger volumes of surface runoff did not cause a strong increase in the soil moisture at the wetland fringe, even at the positions where soil moisture of the topsoil varied considerably over the year (W1 after Nov. 2016 and W2). This hints to the fact that infiltration of surface

runoff at the fringe did not substantially contribute to soil moisture at that position. Nevertheless, it has to be considered that soil moisture was measured at a fixed interval, which often did not match the days, when surface runoff was collected. Therefore, some dynamics in the soil moisture were probably smoothed out. As the slope was very gentle at the fringe, some infiltration of surface runoff is expected to have occurred on days, when the soil at the fringe was not saturated, even if it could not be seen in the moisture data presented in this study. Yet, it can be concluded that infiltrating surface runoff was not a major component of water input at the wetland fringe. Concerning nutrient input though, surface runoff played a more decisive role as discussed in chapter 7.4.

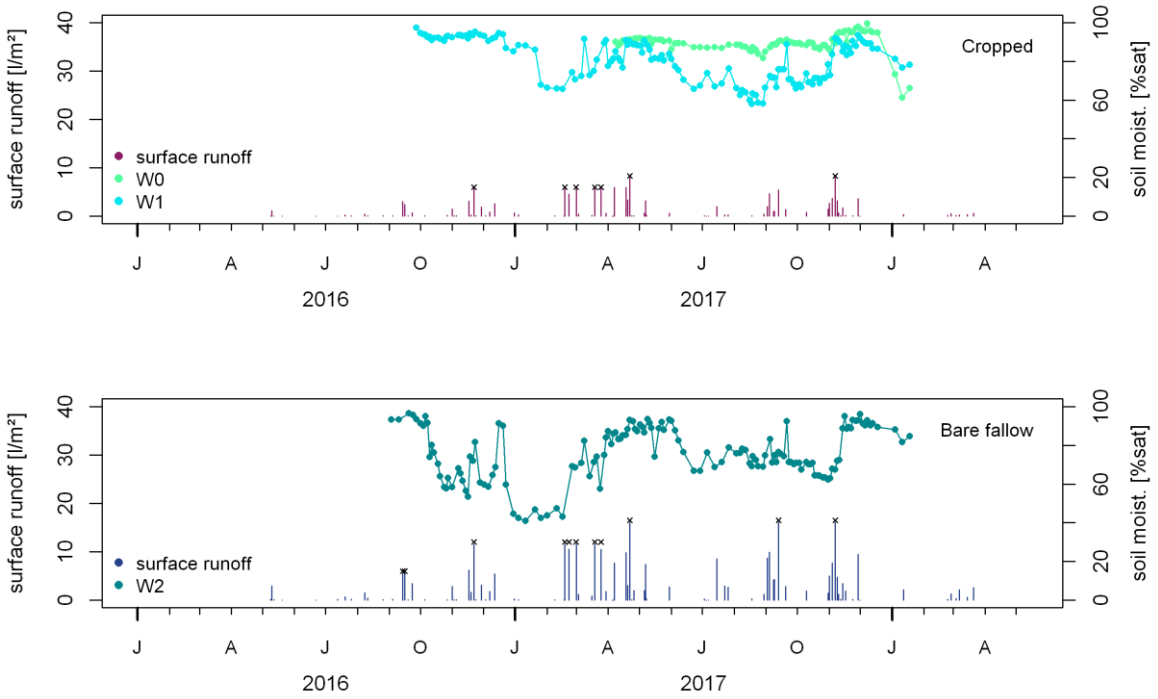

Figure 54 *Dynamics of soil moisture (upper 20 cm) at the wetland fringe compared to surface runoff volumes at the plot under crop production and under bare fallow. The black x on some bars indicate that collectors overflowed on the respective day.*

As described in Hudson (1993), there are many limitations and uncertainties related to field measurements on surface runoff plots. Installation and maintenance of the plots is time consuming and costly and shortcomings may impact the quality of data. Tightening the boundaries of plot is not trivial and water might have escaped from the plot or entered from the outside areas during heavy rain events, even if boundaries were checked regularly. One major issue related to this kind of field installation is that runoff volumes may exceed the collector volume and therefore runoff generated during heavy and intense rainstorms is captured only partially. This also happened in this study. Thus, it was not possible to correlate subsurface flow and surface runoff during heavy rainstorms, so that the contribution of surface runoff data to process understanding under these conditions is limited. Another common problem is the high natural variability of runoff generation rates across the slope, which is related to the spatial heterogeneity of soil properties and thus infiltration rates. In this study, natural variability at the plot

under crop production and under bare fallow was not significant most of the time. Nevertheless, coefficients of variation were sometimes high, mostly on days of smaller event magnitudes. This is a common phenomenon (Pinson et al., 2004). At the plot under semi-natural vegetation, natural variability of surface runoff generation was significant. This might be related to the differential development of grasses and shrubs on the plot, which influenced, e.g., the interception or root network characteristics. Additionally, termites were more common on this plot than at the other land use types and their activities varied considerably at the small scale, leading to differential infiltration. High spatial variability further limits the validity of the findings from surface runoff plots when it comes to extrapolation. Nevertheless, the data collected in the scope of this study provided useful information regarding the connectivity of different runoff components and finally of the slopes and the wetland, and showed trends regarding the impact of different land use types on the generation of surface runoff.

7 Nitrate dynamics and translocation

In this chapter, findings on nitrate dynamics in the soil solution on the slope (7.1) as well as in the interflow (7.2) and the surface runoff along the slope (7.3) are presented. The data are analysed regarding vertical and lateral translocation of nitrate and the conditions and processes involved. In section 7.4, the nitrate dynamics at the fringe of the wetland are discussed pertaining to nitrate inputs from the adjacent slopes.

7.1 Nitrate in the soil solution

Nitrate content in the soil solution was analysed regarding the mineralization of native soil N and the leaching dynamics as influenced by land use type, soil moisture, rainfall characteristics and soil properties. The findings on in-situ dynamics and vertical translocation of nitrate are presented in the first part of this chapter, while the second part focusses on the lateral translocation of nitrate in the soil above the saprolite. To capture the nitrate dynamics, a timely resolution of 2 - 3 days during the rainy seasons was chosen. These data are complemented by information on the cumulative bioavailability of nitrate over the growing period. All measurements were taken at two depths in the topsoil. The data collected at the first measurement depth represents the upper section of the topsoil (0 - 15 cm depth), while the second measurement depths represents the lower topsoil (15 - 30 cm depth). In the following section the two measurement depths are referred to as “upper topsoil” and “lower topsoil”. As this chapter focusses on dissolved nutrients, the water in the soil pores is referred to as “soil solution”.

7.1.1 In-situ dynamics and vertical translocation

Prevenient considerations on nitrate content and nitrate concentration

The amount of nitrate per unit area, i.e., the nitrate content, is a function of the nitrate concentration in the soil solution and the volumetric soil moisture (solution amount per unit area). Figure 55 depicts a near linear relation of the nitrate concentration [mg NO_3-N/l] measured directly in the soil solution and the nitrate content [kg NO_3-N/ha]. Considering the nitrate concentration, no dilution effects were found, as the nitrate concentration generally increased with increasing soil moisture (see Figure 56). Therefore, further analysis of nitrate dynamics in the soil solution is based on the nitrate content only.

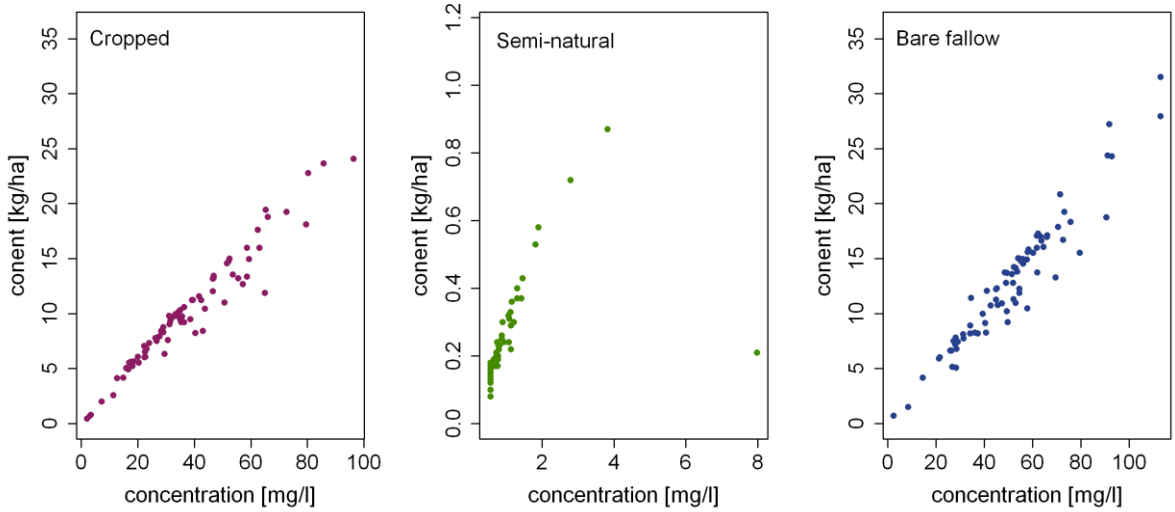

Figure 55 *Relation of nitrate content [kg NO_3-N /ha] and nitrate concentration [mg NO_3-N/l] as a function of land use and vegetation cover, comparing crop production, semi-natural vegetation and bare fallow.*

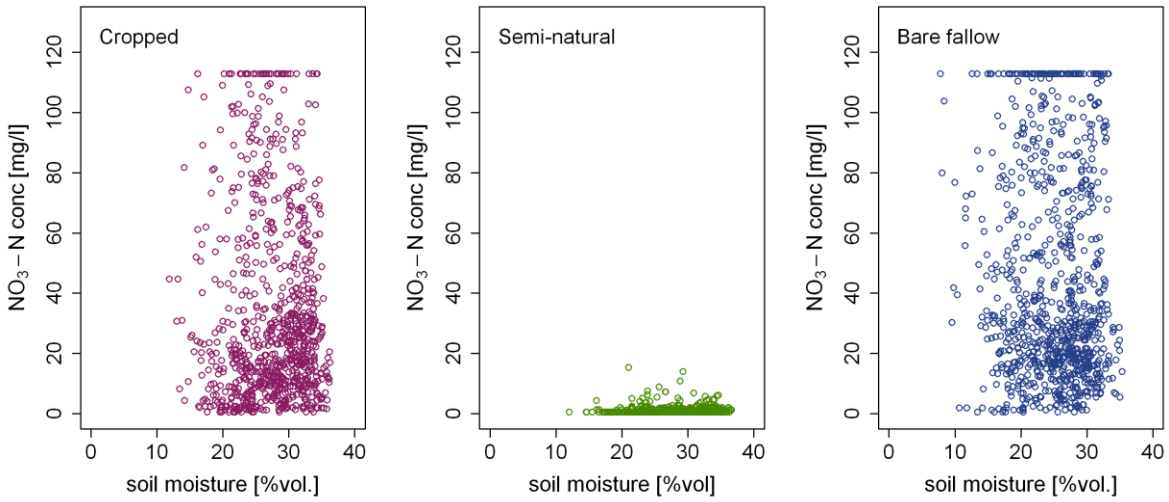

Figure 56 *Relation of volumetric soil moisture content and NO_3-N concentration [mg NO_3-N/l] during four consecutive rainy seasons (2016-2017) as a function of land use and vegetation cover, comparing crop production, semi-natural vegetation and bare fallow. Straight lines at the minimum and maximum concentrations result from censored data caused by the detection limits of the Nitracheck device.*

Intra-seasonal nitrate dynamics

As explained in chapter 2.3, the mineralisation of native soil N to nitrate as well as leaching and denitrification losses are closely related to changes in soil moisture. Hence, in tropical regions, the nitrate content in the soil solution frequently follows a distinct pattern over the course of the rainy season, known as the Birch effect (Birch, 1958) and found in various studies, i.e., in Nepal (Pande and Becker, 2003) or in the Ivory Coast (Bognonkpe and Becker, 2009). This pattern includes a fast increase in mineralization after the onset of the rains with a peak at the beginning of the main rainy season, which is followed by a steep decrease in nitrate due to denitrification and leaching as the rains proceed.

In the present study, this trend could generally be observed as well. In Figure 57, the dynamics of the nitrate content in the soil solution measured at the different measuring points on each plot in the upper topsoil (light colours) and in the lower topsoil (dark colours), as well as the resulting mean nitrate content of the topsoil (large points) are displayed for each land use type. In accordance with the Birch effect theory, the highest nitrate content was generally observed at the beginning of the rainy season, before it declined as the main rains established and soils got increasingly water-saturated. With the ceasing of the rains at the end of the season, the nitrate content increased again as the soil moisture content decreased. This trend was detected under bare fallow and under crop production alike. Nevertheless, the data also reveal a high variation of the nitrate content at the different measuring points on each measurement day, which hints to the high spatial variability of nitrate accumulation in the soil even within the same land use type. It can further be seen that on some days only few measurements were conducted, as the extraction of soil solution was impeded by dry soil conditions, which makes the mean values less representative.

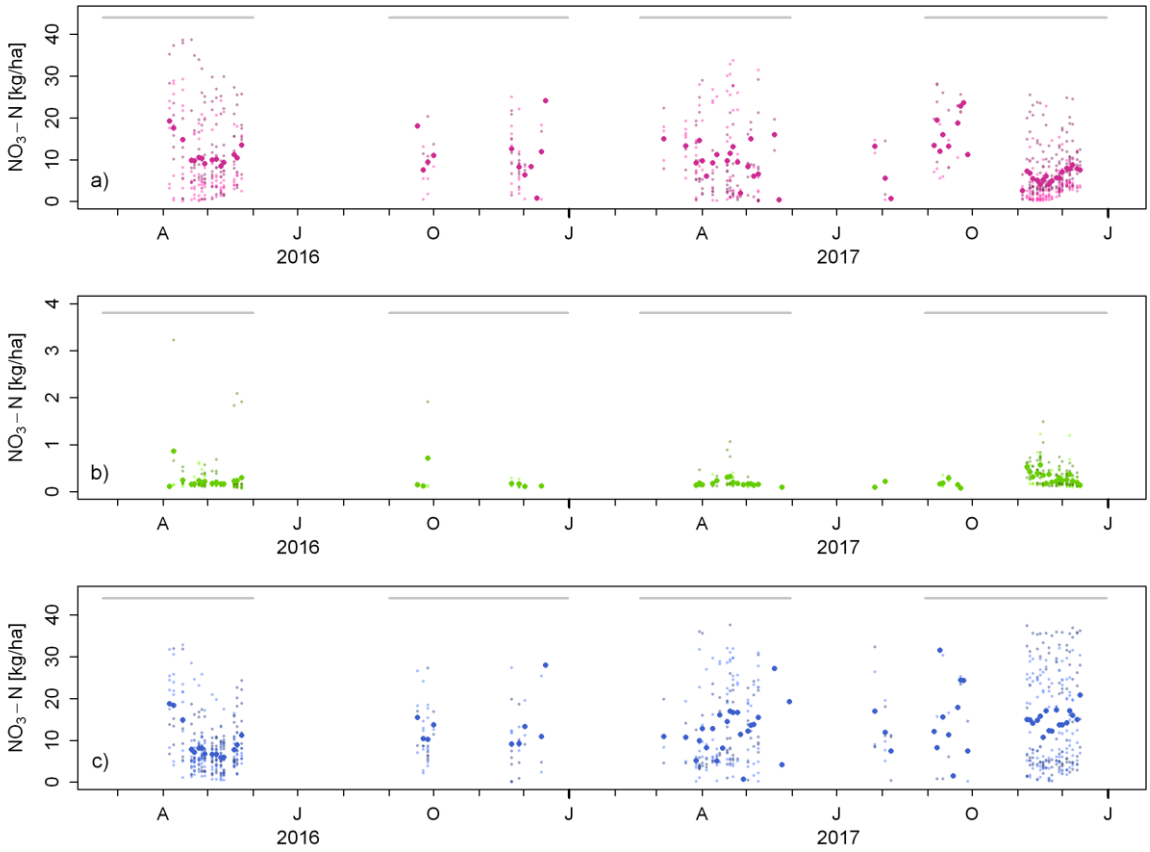

Figure 57 *Nitrate content [kg NO_3-N/ ha] in the upper topsoil (light colours) and in the lower topsoil (deep colours) and the resulting mean nitrate content on each measurement day (big dots) at the plot under crop production, semi-natural vegetation and bare fallow. Grey bars indicate the duration of the rainy seasons.*

Figure 58 depicts the change in soil moisture (positive = increase, negative = decrease) related to the nitrate content in the soil solution. Even if correlation coefficients were very weak (<0.2) for both depths, the data confirm the stimulating effect of an increase in the soil moisture on nitrate mineralization. Especially in the upper topsoil an increase in soil moisture is rather related to higher nitrate contents,

while a decrease in soil moisture coincides with lower nitrate contents. In the lower topsoil this trend is less pronounced, as at this depth also the soil moisture dynamics are extenuated.

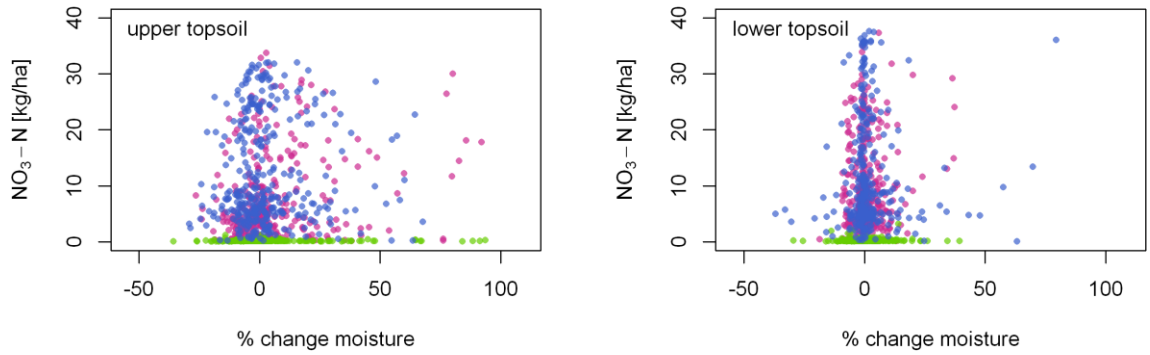

Figure 58 *Relative change in soil moisture from one measurement day to the following measurement day related to the nitrate content in the soil solution [kg NO_3-N/ha]. Colours were chosen according to the land use type (blue: bare fallow, green: semi-natural vegetation, magenta: crop production).*

Even if the intra-seasonal nitrate dynamics generally followed the typical trend described by the Birch effect, a more comprehensive analysis of the effect of variable climatic conditions, soil moisture dynamics and crop development stages is crucial to understand the dynamics of the nitrate content in the soil solution on the slopes.

Nitrate and soil moisture dynamics by season

The following section presents the observed differences of nitrate dynamics between the four observation seasons (2016.1, 2016.2, 2017.1 and 2017.2) as well as under the three land use types (bare fallow, crop production and permanent ground cover by semi-natural vegetation). The seasons were differentiated by the amount of rainfall, as well as by their intensity and (dis)continuity (see Table 12). The implications of such differential patterns for the accumulation and translocation of soil nitrate are presented hereafter. The analysis is based on the data on the cumulative potentially bio-available nitrate per season as shown in Figure 59 and on the dynamics of the mean nitrate content in the soil solution in relation to rainfall dynamics and soil moisture as shown in Figure 60.

Table 12 *Rainfall characteristics and main trends in the soil moisture dynamics during the four rainy seasons 2016 - 2017*

Season	Rainfall total [mm]	Rainfall pattern at the start of the season	Rainfall pattern during the main rainy season	Soil moisture
2016.1	256	Small rainfall events of low intensity	Constant, low to intermediate intensity	Constantly high
2016.2	214	Single rainfall events of intermediate intensity	Sporadic, low intensities	Repeated wetting and drying
2017.1	388	Efficient rainfall events of high intensity	Constant, intermediate intensity	Slow increase at the beginning followed by high values during the main rainy season
2017.2	387	Small rainfall events of low intensity	Bi-modal with single events of high intensity and high rainfall amounts	Bio-modal, very high during the second wet period

First season (2016.1)

The beginning of the first rainy season 2016 was characterized by smaller rainfall events of low intensity and rather equally distributed efficient rainfalls of low to intermediate intensities during the main season. This constant rainwater supply led to soil moisture contents of 60 - 70 % in the upper topsoil and of over 70 % in the lower topsoil with very little intra-seasonal variations. The soil nitrate content was high after the initial flash of soil N mineralization and reached up to 15 - 21 kg NO_3-N /ha in the upper topsoil, depending on the land use type. With the onset of the main rains, it rapidly declined to 6 kg NO_3-N /ha before, at the end of the rainy season and with beginning of soil drying, renewed soil N mineralization resulted again in a slight increase in soil nitrate to 7 kg NO_3-N/ha. The dynamics in the lower topsoil followed a similar pattern, but at a higher level (about 1 kg NO_3-N/ha higher under the bare fallow and about 5 kg NO_3-N/ha higher under crop production). While the dynamics showed similar patterns under bare fallow and under crop production, the nitrate content was constantly up to 10 kg NO_3-N/ha higher under crop production. The nitrate content under semi-natural vegetation remained close to the detection limit (around 0.2 kg NO_3-N/ha) throughout the season. The tendency of nitrate to be leached and to accumulate in the deeper soil layer is further supported by the results of the seasonally aggregated adsorption of nitrate by the ion exchange resin capsules. For the plot under bare fallow and under crop

production, the mean cumulative potentially bio-available nitrate content was smaller in the upper than in the lower topsoil. At the plot under bare fallow, contents reached 32 µmol/cm² in the upper topsoil as compared to 46 µmol/cm² in the lower topsoil, while under crop production, 23 µmol/cm² were detected in the upper topsoil and 35 µmol/cm² in the lower topsoil. Under semi-natural vegetation, cumulative potentially bio-available nitrate was generally very low (1.3 - 1.5 µmol/cm²) and did not differ between soil depths.

Second season (2016.2)

Due to the impact of the La Niña phenomenon, the second rainy season 2016 was very dry and rainfall intensities were low. In the month of October almost no rainfall was recorded and rainfall events remained erratic during most of the season. Therefore, soil moisture in the upper topsoil showed high fluctuations with repeated soil drying and wetting cycles, but generally conditions were too dry for substantial soil N mineralization and the accumulation of nitrate in the soil solution. Consequently, the nitrate content in the soil solution under bare fallow and crop production was lower than in the other seasons. This was also found in the resin data, with mean cumulative potentially bio-available nitrate amounts of 2 - 12 µmol/cm² in the upper and 1 - 4 µmol/cm² in the lower topsoil. In the lower topsoil, soil moisture was less variable, but also lower than during the other seasons and never exceeded 70 % sat.. At this depth, also the nitrate content measured in the soil solution was lower than a in the upper topsoil and only reached 12 kg NO_3-N/ha, as very little nitrate was leached from the upper topsoil. Hence, under the prevailing moisture conditions of season 2016.2, the seasonal pattern of nitrate mineralization and subsequent disappearance of nitrate was also less pronounced than in the other seasons. As before, very little nitrate was detected at the plot under semi-natural vegetation.

Third season (2017.1)

The first rainy season 2017 was characterized by an abrupt beginning with large rainfall events of high intensities relative to the other seasons. Soil moisture in the upper and lower topsoil showed a steady increase towards the end of the season. At the plot under crop production, soil moisture conditions in the upper topsoil were most favourable for nitrate mineralization at the beginning of the season, while under bare fallow, stimulating conditions were only reached later in the season. In the lower topsoil, wet conditions of 70 - 85 % sat. were found under crop production, while under bare fallow, soil moisture conditions in the lower topsoil were still favourable for nitrate mineralization during the beginning of the season. Hence, at the plot under crop production, a high nitrate content of 14 kg NO_3-N/ha was found in the upper topsoil at the beginning of the season, while in the later stages nitrate leaching dominated and the nitrate content dropped to 5 kg NO_3-N/ha in the upper and 2 kg NO_3-N/ha in the lower topsoil. At the plot under bare fallow, the opposite trend was found as the nitrate content in the soil solution increased from 12 kg NO_3-N/ha to 20 kg NO_3-N/ha in the upper topsoil towards the middle of the season before it slightly declined at the end of the season. At the same time, the nitrate content in the lower topsoil increased from 12 kg NO_3-N/ha to 27 kg NO_3-N/ha at the end of the season, indicating the accumulation of leached nitrate. The ion exchange resin data showed that under all land use types less potentially bio-available nitrate was present in the soil solution than during the other two rainy seasons which were also not impacted by drought. In the upper topsoil, the mean cumulative nitrate accumulation reached 18

µmol/cm² under bare fallow and 14 µmol/cm² under crop use. In the lower topsoil, values reached 12 µmol/cm² under bare fallow and 19 µmol/cm² under crop production, indicating a vertical translocation of nitrate under crop production. Similar to previous seasons, little nitrate was detected under cover of the semi-natural vegetation with 0.15 µmol/cm² and 0.3 µmol/cm² in the upper and lower topsoil, respectively.

Fourth season (2017.2)

The second rainy season 2017 was characterized by a bi-modal distribution of rainfall, whereas both wet periods had a gentle start. In both periods, there was an unconventionally efficient rainfall event considering the rainfall recorded in this study, the larger event taking place at the beginning of November with 64 mm of precipitation. The soil moisture also showed a bi-modal behaviour with a rapid increase after the first rain fall events at both measurement depths. Here, values amounted to 60 % in the upper and 70 - 85 % in the lower topsoil during the wet period in September and to 65 - 73 % in the upper and 80 - 90 % in the lower topsoil during the wet period in November, with highest values recorded under crop production and semi-natural vegetation. During the intermittent dry spell, soil moisture decreased rapidly to 50 % in the upper and to 50 - 70 % in the lower topsoil, with lowest values found under semi-natural vegetation. During the wet period in September, the nitrate content in the soil solution under crop production rose from low values at the beginning of the season to 23 kg NO_3-N/ha in the upper topsoil, while values were constantly very high (26 kg NO_3-N/ha) in the lower topsoil, except for the measurement day following the large rainfall event in September. During the following dry spell, values decreased to about 2 kg NO_3-N/ha at both measurement depths. Under bare fallow, the pattern was reversed. In the upper topsoil, very high values of 25 - 31 kg NO_3-N/ha were recorded during the first wet period with a short drop to 2 kg NO_3-N/ha after the large rainfall event in September, while in the lower topsoil, the nitrate content rose from low values at the beginning of the first wet period to about 23 kg NO_3-N/ha. During the wet period in November, the nitrate content in the soil solution under bare fallow amounted to 14 - 16 kg NO_3-N/ha at both measurement depths without much fluctuation. Under crop production, the nitrate content in the soil solution remained very low in the upper topsoil during this second wet period, while it rose to 8 kg NO_3-N/ha in the lower topsoil after the large rainfall event in November and to 11 kg NO_3-N/ha at the end of the season, after a short decrease. During this season, the nitrate content at the plot under semi-natural vegetation increased with increasing soil moisture far beyond the 60 % sat. moisture optimum, and reached values of 0.6 kg NO_3-N/ha at the beginning of November. With 0.5 µmol/cm² in the upper and 1.6 µmol/cm² in the lower topsoil, also the cumulative potentially bio-available nitrate recovered under semi-natural vegetation was higher than during the other seasons under investigation. For the other two land use types, values were comparable to those retrieved in season

2016.1, with 34 µmol/cm² and 48 µmol/cm² under bare fallow and 16 µmol/cm² and 27 µmol/cm² under crop production in the upper and lower topsoil respectively.

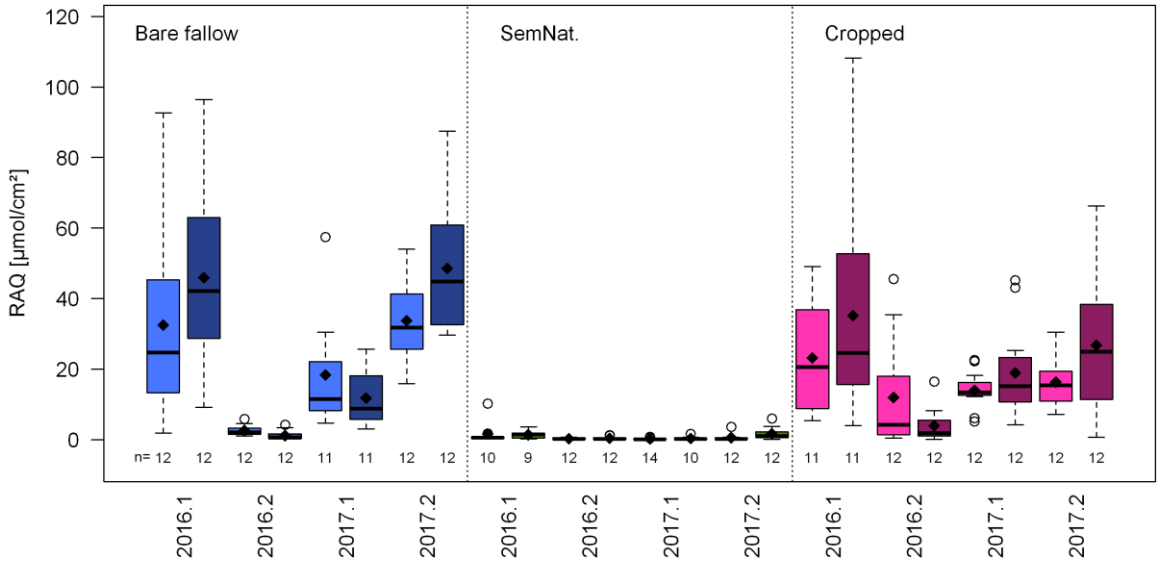

Figure 59 *Seasonal cumulative bio-available nitrate displayed as resin adsorption quantities (RAQ) [µmol/cm²] in the upper (light colours) and in the lower topsoil (dark colours) at each land use type.*

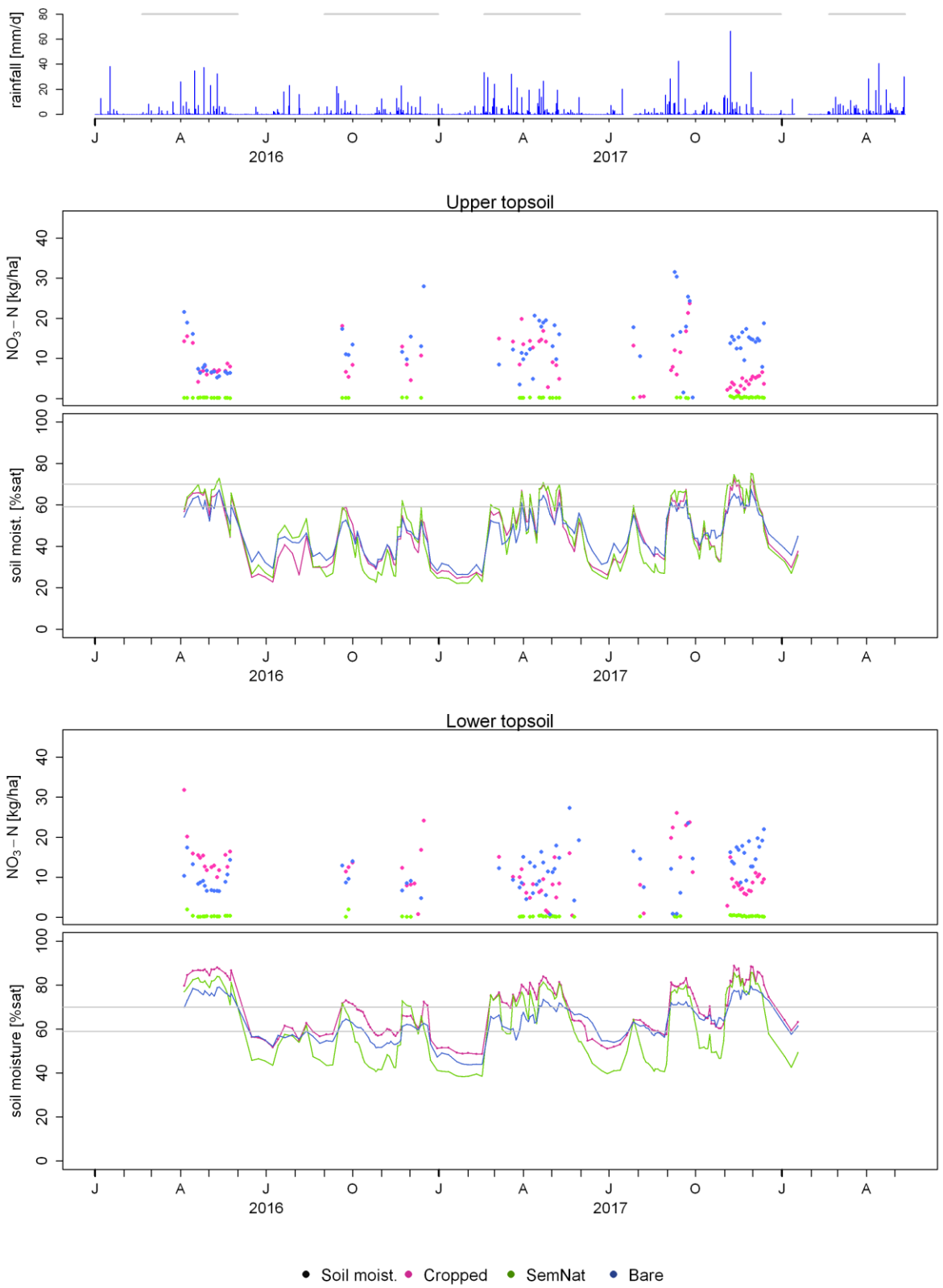

Figure 60 *Rainfall amounts [mm/d] (top panel), nitrate dynamics [kg NO_3-N/ha] and soil moisture dynamics [%sat.] in the upper and lower topsoil. The grey lines mark 59 % and 70 % water saturation of the soil indicating the optimum moisture conditions for mineralization and the denitrification threshold.*

In the following paragraph, the data presented above are further discussed regarding the influence of variable climatic conditions on nitrate mineralization and translocation in the topsoil.

During all rainy seasons, the nitrate content in the soil solution seemed rather high regarding the fact that no fertilizer was applied to the soil. Nevertheless, Krohm (2015, unpublished) found comparable nitrate contents in the soil solution about 100 m further upstream. In addition, the values still fall in the range of values reported in literature. In Kenya, Sheppard et al. (2001) for example, found a nitrate content of 1 - 50 kg NO_3-N/ha in the top 50 cm of fields of smallholder farmers and Russo et al. (2017) reported nitrate concentrations of 0.37 - 130 mg NO_3-N/l (mean 16 mg NO_3-N/l).

The peak nitrate contents during the early rainy season 2016.1 resulted from the high mineralization rates of native soil N following the rewetting of the soil after an extended dry period, as first described by Birch (1960, 1958). The gentle rains at the beginning of the season infiltrated well into the soil, creating favourable moisture conditions for the mineralization of soil organic matter and subsequent nitrification. In the upper topsoil, these conditions remained favourable during the entire season, but the large rainfall events of intermediate intensity caused considerable leaching of the mineralized nitrate, which explains the higher nitrate contents in the lower topsoil. At the same time, nitrate was possibly leached even from deeper layers as shown by the steep decrease in nitrate content in the lower topsoil and concomitant high nitrate levels in the interflow, which will be discussed in chapter 7.2. The high nitrate content under crop production as compared to bare fallow at both soil depths later in the season was surprising, as significant losses were expected due to plant uptake as well as denitrification, as moisture levels under crop production in the lower topsoil always exceeded 80 % sat. Higher potential infiltration rates as determined by infiltration tests (see chapter 4.3.3) under bare fallow (62 mm/hr compared to 47 mm/hr under crop production) might have stimulated nitrate leaching losses. Nevertheless, surface runoff coefficients at the plot under bare fallow were also higher, which would not suggest higher actual infiltration rates. Thus, the only plausible explanation at hand are a higher initial nitrate content at the plot under crop production, which might have resulted from fertilizer application or the cultivation of legumes by the small scale farmers who cultivated this area some years before this study. Unfortunately, there were no data available concerning former land use practices and initial nitrate content in the topsoil. Data on bioavailability gave a different picture, with mean values being higher for the bare fallow than for the plot under crop production. Nevertheless, the variability of the RAQ values was by many times higher than the difference between the two land use types and therefore this shall not be taken into further consideration.

The intermittent peaks in the nitrate content in season 2016.2 again correspond to the effect of rewetting of the soil and the associated rapid release of nitrate (Birch effect). Nevertheless, even if there were more frequent and pronounced wetting and drying cycles in this season, the nitrate content in the soil solution was not higher than in the other seasons. This can be explained by the generally dry soil conditions in 2016.2, which reduced the mineralization of organic matter and the subsequent nitrification of ammonium. This assumption is further confirmed, as reduced nitrate uptake by the poorly developed crops would otherwise be expected to leave a higher nitrate content in the soil solution. The fact that the nitrate content in the soil solution as well as the cumulative potentially bio-available nitrate were higher

in the upper than in the lower topsoil indicates that leaching losses were very small. This is in line with the comparably low nitrate concentration in the interflow during this period. Nevertheless, the nitrate content in the soil solution in the upper topsoil was higher at the plots under bare fallow than under crop production, while in the lower topsoil the nitrate content was higher under crop production. Therefore, some plant uptake and relocation of nitrate is expected to have occurred despite the dry conditions. However, the data retrieved from the resin capsules suggest that over the course of the entire rainy season, more nitrate was present under crop production than under bare fallow, which is probably related to the more favourable moisture conditions under this land use type. The high nitrate content at the end of the season was based on very few data points, as under dry conditions removal of soil solution by the rhizons was often not possible. Therefore, this trend remains speculative.

The nitrate dynamics in season 2017.1 well reflect the effect of rainfall intensities on soil moisture and, consequently, on nitrate mineralization and leaching. During rainstorms of high intensity, the water supply rate exceeds the infiltration capacity of the uppermost soil layers. As a consequence, surface ponding occurs and part of the water runs off superficially as surface runoff or infiltrates into the soil as bypass flow via macropores. Therefore, following the intense rainfall events at the beginning of the season, soil moisture in the topsoil increased very slowly despite the high rainfall amounts, as only a small share of the precipitation infiltrated into the soil matrix. At the plot under crop production, the resulting soil moisture was sufficient to stimulate the mineralization of organic matter but not yet to cause leaching of nitrate from of the soil matrix, as water was transferred directly to the saprolite via preferential flow paths. With increasing soil moisture towards the end of the season, more matrix flow occurred, and hence more nitrate was leached resulting in an increase of the nitrate content in the lower and subsequently a decrease in the upper topsoil. At the plot under bare fallow, soil moisture increased more slowly, as without a protective plant cover, runoff coefficients were higher and hence less water infiltrated into the soil matrix. This explains the delay in nitrate mineralization as well as in the onset of nitrate leaching under this land use type as compared to the plot under crop production. Like in the previous season, the remarkably high and low values at the end of the rainy season at the plot under bare fallow and crop production resulted from very few measuring points and are therefore probably not representative.

In season 2017.2 the close relation of soil moisture and nitrate content in the soil solution as well as the impact of single very large rainfall events on leaching losses became apparent. As in the previous seasons, the stimulating effect of rewetting of the soil after dry periods on nitrate mineralization was shown at the beginning of both wet periods under bare fallow and crop production. Nevertheless, the high infiltration of rainwater under moist conditions resulted in substantial nitrate leaching from the upper topsoil at the plot under crop production already at the beginning of the season. This is shown by the accumulation of nitrate in the lower topsoil and the comparably low nitrate content in the upper topsoil. The large rainfall event in mid-September then also caused leaching from the lower topsoil, which can be deducted from the lower nitrate content after the rainfall event at even this soil depth. In the following two weeks, nitrate was then accumulated at both depths as no further rainfall occurred. During the intermittent dry spell, the crops continued to take up nitrate from the upper soil horizons. This explains the drop in nitrate content at the plot crop production, which cannot be found at the plots under bare fallow. The large rainfall event in the beginning of November again caused major leaching from the plot under crop

production, which is also depicted in the high N content in the interflow during that time (see chapter 7.2). After the rainfall event, high soil moisture contents did not stimulate nitrification, which explains why the nitrate content at the plot under crop production did not significantly increase again until the end of the season. At first, it seems surprising that so much nitrate was leached to the lower topsoil and to the interflow despite the low nitrate content in the soil solution at the last measurement day before the event. Firstly, the nitrate content on the day of the rain fall event was probably higher than depicted here, as there were three days between the last measurements and the event and soil moisture during that time was very favourable for nitrification. Furthermore, the high amount of rainfall led to very high soil moisture values, which means that nitrate could have been washed out of pores which were not drained during previous events. This will be discussed further in chapter 7.2 when looking at nitrate in the interflow in more detail. Different dynamics were found at the plot under bare fallow. Under bare fallow conditions, less water infiltrated into the soil and hence less leaching of nitrate occurred. A vertical translocation of nitrate to the lower topsoil was only found after the very large rainfall events. Otherwise, favourable moisture conditions in the upper topsoil rather stimulated the mineralization of nitrate which led to a high nitrate content throughout the season. The high nitrate content compared to the other seasons at the plot under semi-natural vegetation, which occurred under high soil moisture conditions during the second wet period of the season 2017.2, remain enigmatic. Here as well, the leaching of nitrate from pores which were less frequently saturated or the diffusion of nitrate enclosed in soil aggregates might have played a role. Furthermore, some input of nitrate from areas upslope of the experimental plots could have occurred, which under drier conditions did not reach the plots.

The effect of variable climatic conditions during the rainy season on nitrate mineralization and vertical translocation of nitrate can be summarized as follows: In all four rainy seasons, the soil moisture conditions were the driving factor for the stimulation or inhibition of the mineralization of organic matter and the subsequent nitrification of ammonium. Rainfall events of high intensity at the beginning of the rainy season resulted in higher surface runoff coefficients (and hence less infiltration) and thus delayed the rewetting of the soil and the associated mineralization of nitrate. Intra-season wetting and drying cycles of the soil only stimulated nitrification when favourable moisture conditions were reached over several days. Leaching of nitrate generally occurred under moist soil conditions only. Very large rainfall events led to substantial leaching of nitrate even from the lower topsoil, while the effect was more pronounced when the land use type favoured the infiltration of the rainfall.

Effect of land use types

The land use type had a strong impact on the dynamics and the total amounts of nitrate in the soil solution. The nitrate content under bare fallow and under crop production was significantly higher than under semi-natural vegetation, where only very little nitrate could be detected. Considering the entire investigation period, the mean nitrate content in the soil solution, as well as the mean cumulative potentially bio-available nitrate, were also higher under bare fallow than under crop production (12 kg NO_3-N/ha or 25 µmol/cm² as compared to 9 kg NO_3-N/ha or 18 µmol/cm²). The difference was significant at p= 0.05 for the mean nitrate content as determined by the rhizon measurements. The analysis of the nitrate dynamics during the single seasons (previous section) further revealed that under crop production and bare fallow mineralization as well as leaching and denitrification dominated at different times during each season. Hence, nitrate availability in the soil solution was different between these two land use types in the course of each rainy season, depending on the prevailing rainfall characteristics and the resulting soil moisture conditions. These also affected the total amount of potentially bio-available nitrate at the plot under bare fallow and under crop production in the four rainy seasons, as shown in Figure 59. The effect was statistically significant in season 2017.2 only. It can thus be concluded that the influence of the land use type on nitrate accumulation in the soil solution and nitrate losses from the topsoil on the slopes also depended on the climatic conditions during the rainy seasons, but that the effect of a dense vegetation cover superimposed that of variable climatic conditions.

Overall, the findings presented here agree with literature in many aspects. Several authors reported a very low nitrate content under grasses and shrubs and under early to mid-successional vegetation (Dividson et al., 1990; Robertson and Groffman, 2015; Szott et al., 1999; Warren et al., 1997). They explained these low values by high nutrient demands due to high rates of photosynthesis, rapid increase in leaf area and biomass, a dense and extensive root system of grass vegetation and high turnover rates of nitrates. In contrast, a faster nutrient release and accompanying nitrate losses are caused by an accelerated turnover of the labile SOM pool due to tillage, incorporation of crop residues and the removal of primary vegetation at sites under crop production (Mathers et al., 2007; Zech et al., 1997). Warren et al. (1997) also found the nitrate content under bare fallow and under crop production to be strongly associated with soil moisture and rainfall incidence during their research on the dynamics of soil nitrate under bare fallow, grassland and sorghum crops in semi-arid Kenya. Yet, they constantly detected a higher nitrate content at the plots under bare fallow but could not witness significant leaching processes on neither of the plots.

7.1.2 Lateral translocation of nitrate in the soil

In the following section, the findings on lateral translocation of nitrate in the soil from the upper slope towards the slope toe are introduced. Firstly, a comparison of four different positions along a slope transect regarding the nitrate content in the soil solution as well as the cumulative potentially bio-available nitrate is presented. In the second part, data on nitrate in the soil solution at the positions which were isolated from near-surface slope water by dug-out pits (see chapter 4.1) are related to these retrieved at nearby positions.

Comparing the nitrate content in the soil solution at the different slope positions did not suggest the presence of significant down-slope translocation of nitrate in the soil (see Figure 61). Instead, differences between the slope positions were rather caused by different soil properties than by lateral translocation of nitrate. Considering the two-year period during which the experiment was running, the nitrate content in the soil solution was lower at the mid-slope position than at the lower slope position for all three land use types. The difference was not pronounced though at the plot under semi-natural vegetation, and also at the other two land use types, the difference was not statistically significant (P= 0.05). The nitrate content measured in the soil solution at the slope toe were lower than at both upslope positions, the difference being statistically significant at the plot under bare fallow. This pattern was generally found during all the rainy seasons covered by this study. Divergent results were found at the plot under crop production in season 2016.2, when the nitrate content in the soil solution was highest at the slope toe and slightly higher at the mid-slope than at the lower slope position (see Figure 63), even if there was no change in the crops cultivated at the plot. At the bare fallow plot, the nitrate content in the soil solution at the mid-slope position was higher than at the lower slope position in season 2017.1. The pattern described before- higher values at the lower slope position than at the mid-slope position and lowest values at the slope toe- was generally confirmed by the data on cumulative bio-available nitrate (see Figure 62). Only at the plot under crop production, similar amounts of cumulative potentially bio-available nitrate were found at the slope toe and at the lower slope, with both values being higher than at the mid-slope position. Nevertheless, cumulative bio-available nitrate at the slope toe was measured during two seasons only, as the experimental setup was adjusted after one year. The four data points generated during this time show a high variation and therefore, the data collected from the rhizons repeatedly during each rainy season seem more reliable.

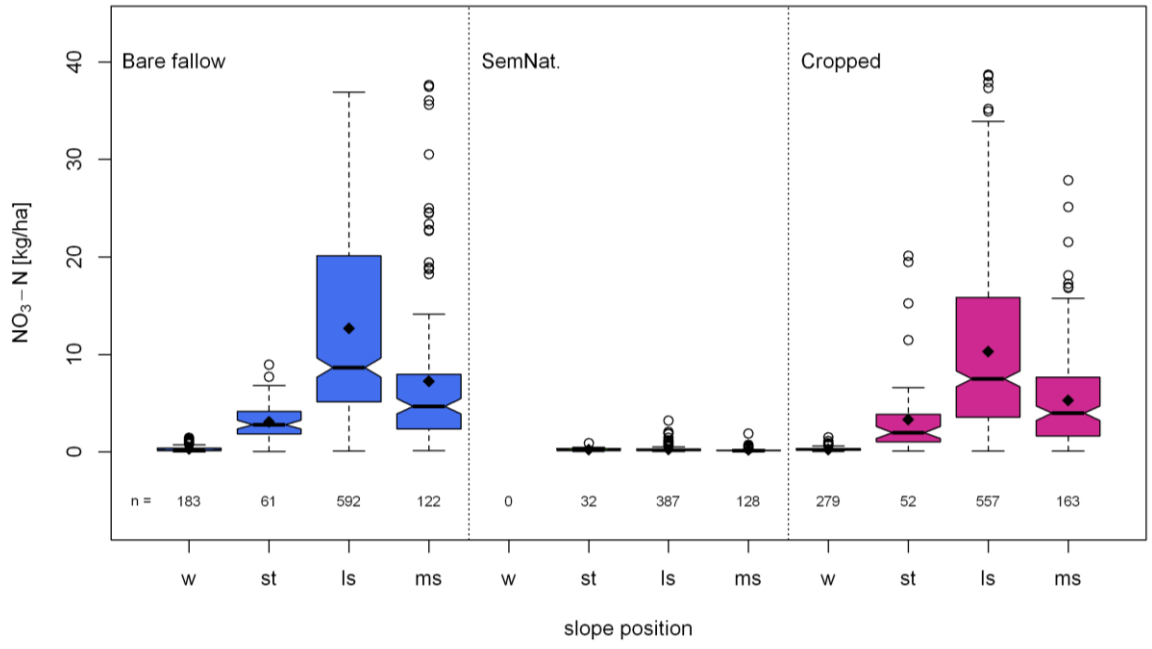

Figure 61 *Nitrate content in the soil solution [kg NO_3-N/ha] at the three different land use types for each slope position (w= wetland, st= slope toe, ls= lower slope, ms= mid-slope) over the two-year measurement period.*

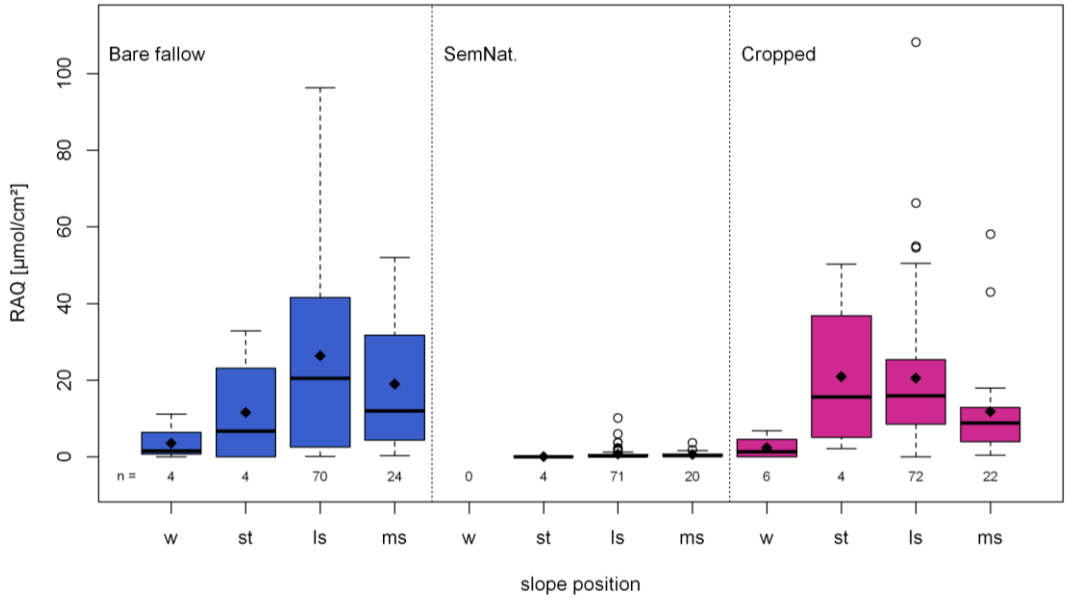

Figure 62 *Cumulative bio-available nitrate [µmol/cm²] at the three different land use types for each slope position (w= wetland, st= slope toe, ls= lower slope, ms= mid-slope) over the two-year measurement period.*

The low nitrate content in the soil solution at the slope toe does not suggest the presence of nitrate fluxes in the soil as otherwise, considering the topography, nitrate would accumulate at this position. At the plots under crop production and semi-natural vegetation, though, this effect could have been biased by higher nitrate uptake by the crops or grasses respectively, but data on nitrate uptake by the plants were not available. Despite the slightly higher share of organic C at this position, the lower nitrate content at the mid-slope position compared to the lower slope position was caused by limited in-situ mineralisation rather than lateral translocation of nitrate in the soil body. The clay content at this slope position was significantly higher than at the lower slope. As a result, soil moisture here was also higher and more frequently reached moisture levels which inhibit mineralization and favour denitrification (see chapter 6.1.2). On the other hand, more nitrate was found in the bulk soil at the mid-slope position (see chapter 5.2.2). Therefore, it might be possible that organic matter was more likely to become part of the stable humus pool than at the lower slope, as the presence of clay minerals favours humus build up (Weil and Brady, 2017). The low value at the slope toe can also be explained by lower nitrification rates and a lower share of organic C in the bulk soil. Here, the soil is significantly sandier than at the lower slope and thus soil moisture is frequently too low to stimulate high mineralisation rates or at least it is less favourable than at the lower slope position. Furthermore, nitrate which had been mineralized can be washed out more easily by infiltrating rainwater when the texture is sandier. The deviant conditions at the plot under crop production in season 2016.2 might be caused by a very limited number of data points during this season. Regarding the nitrate content measured at the bare fallow plot in 2017.1, the prevailing moisture conditions during this season were more favourable for nitrification at the mid-slope position than at the lower slope, whereas in 2016.1 and 2017.2 the mid-slope position was rather too wet compared to the lower slope position.

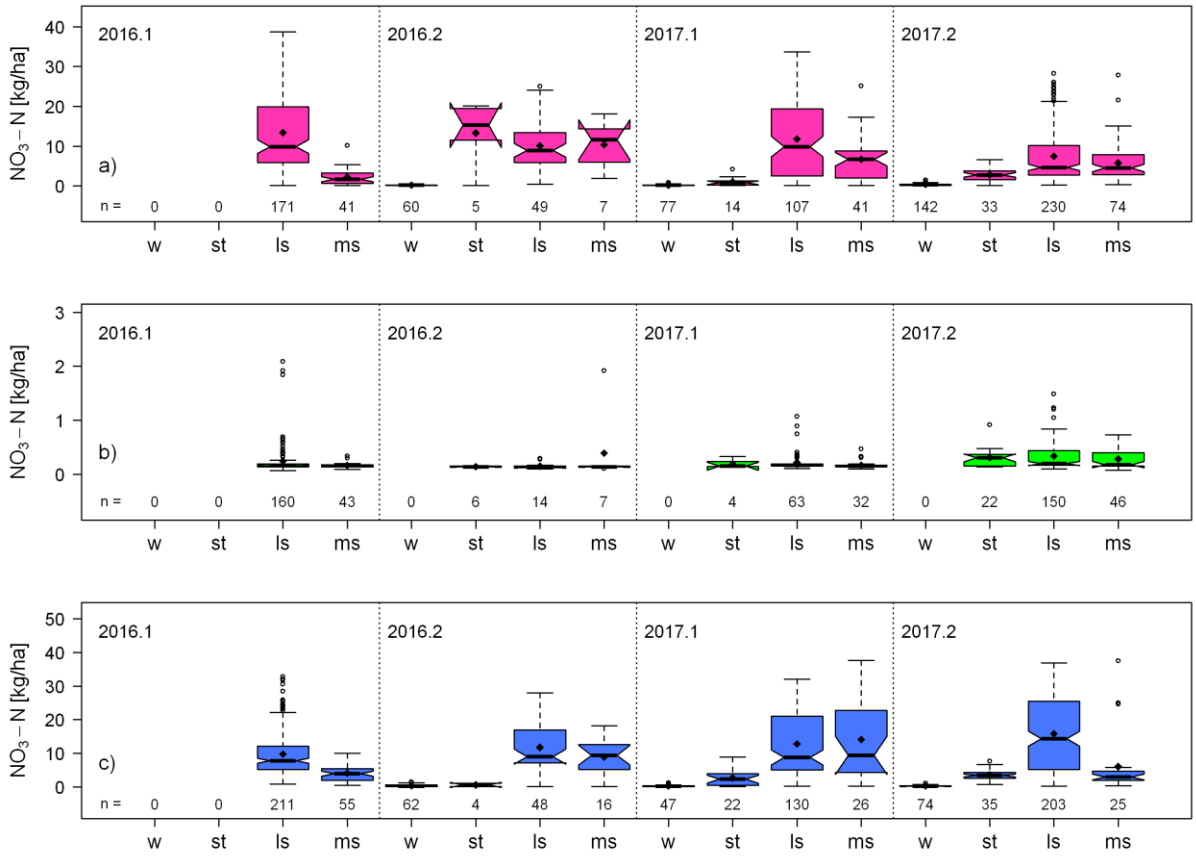

Figure 63 *Nitrate content in the soil solution [kg NO_3-N/ha] per season at the plot under crop production (a), under semi-natural vegetation (b) and under bare fallow (c). Results of the measurements taken in the upper and lower topsoil are summarized in the boxplots.*

The absence of a noteworthy lateral subsurface runoff within the soil body was confirmed by the results from the pit trials. The effect of the pits on the seasonal cumulative bio-available nitrate in the soil solution is shown in Figure 64 and Figure 65, which compare data collected upslope of the pits (=input of shallow subsurface flow) and downslope of the pits (=no input of shallow subsurface flow) and at the reference plots. In case of nitrate transport in the shallow subsurface flow, less nitrate would have been found at the measuring points downslope of the pits than at the measuring points upslope of the pits and on the reference plots, while a higher nitrate content would have been found at the lower positions at the reference plots than downslope of the pits. This effect would be expected to be most pronounced on the plot under bare fallow, as no differential nitrate uptake by plants could cover up the effect there. In Figure 64 the difference between the cumulative bio-available nitrate content measured upslope and downslope of the pits (Px2-Px1) is related to the difference between the measuring points at the same slope positions on the reference plots, i.e., without the effect of the pits (Rx2-Rx1), for each season. In case that the pits prevented the afflux of nitrate via shallow subsurface flow, Rx2-Rx1 would be negative or close to zero, while Px2-Px1 would be positive, i.e., most data points would be positioned in the lower right quarter of the coordinate system. As can be seen, this is not the case as most data points are close to the origin, while the others show a very diverse distribution. Differentiating further between the different land use types and the four measurement positions, Figure 65 reveals that at the plot under crop production, more cumulative bio-available nitrate was found downslope of the pits than at the other positions. Furthermore, values were higher than at the reference plots. The same was true for the plot under semi-natural vegetation. At the plot under bare fallow, though, less cumulative bio-available nitrate was found at the lower positions and the smallest content was detected downslope of the pits.

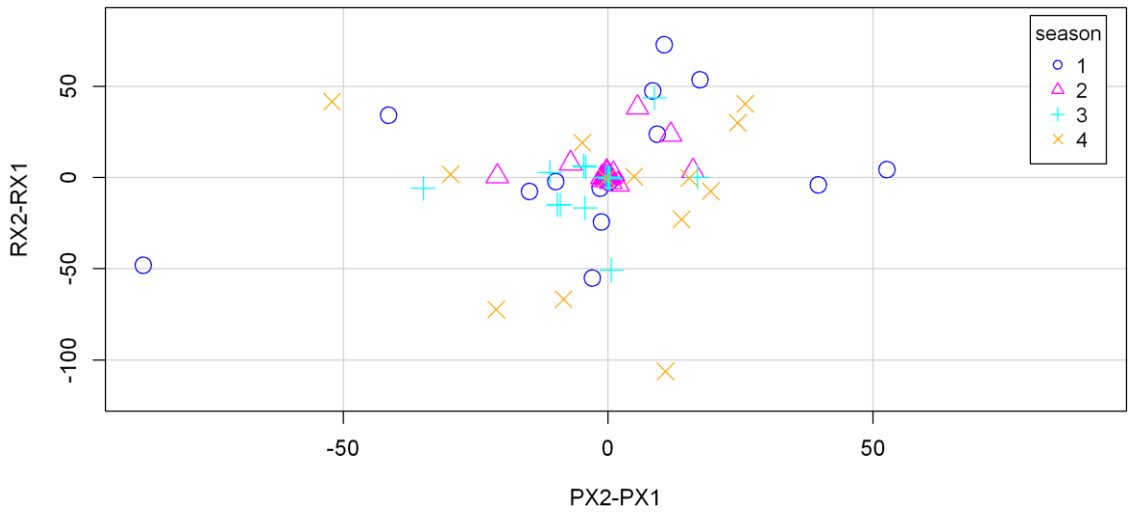

Figure 64 *Effect of the dug-out pits on cumulative bio available nitrate [µmol/cm²] during each season. Displayed is the difference between the upslope and downslope positions separated by the dug-out pits (x-axis) related to the difference between the upslope and downslope position on the reference plots, i.e. without the effect of the dug-out pits (y-axis) for all pits.*

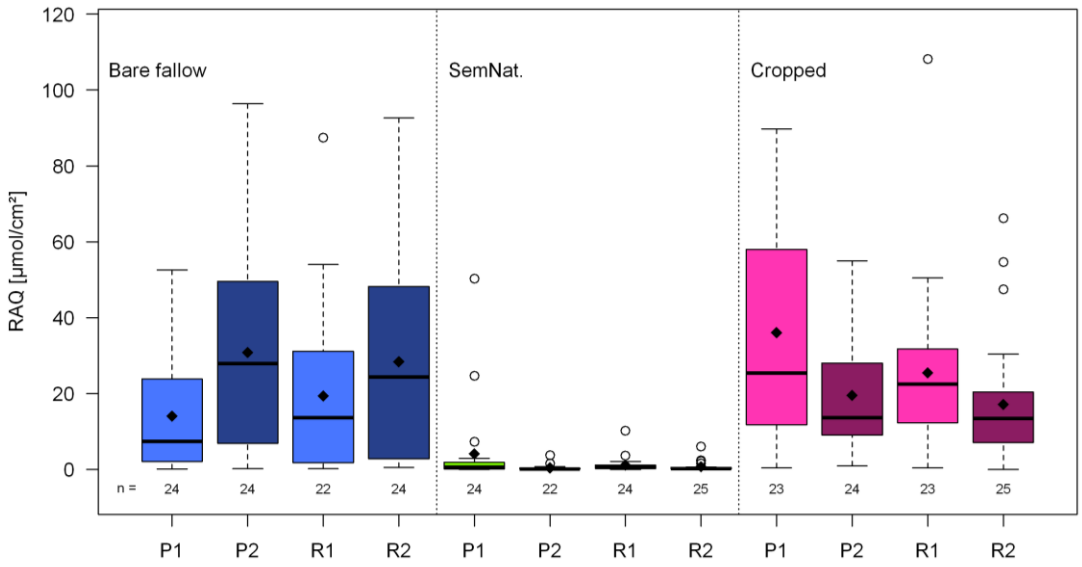

Figure 65 *Effect of the dug-out pits on cumulative bio available nitrate [µmol/cm²] over the two year measurement period at each land use type, P1 being the position downslope of the dug-out pits while P2 is located upslope of the pits. R1 and R2 are the corresponding positions on the reference plots.*

Similar trends were found when analysing the data on the nitrate content in the soil solution collected every two to three days during each rainy season (see Figure 66). Yet, for this data set, the difference between the nitrate collected downslope of the pits at the plot under bare fallow and the corresponding position at the reference plots was not pronounced. None of the differences described in the previous section was statistically significant and differences amongst the measuring points not affected by the pits were bigger than the differences between the positions upslope and downslope of the pits. Furthermore, different trends were observed for the respective seasons and at the two measurement depths and no common trends or overlying factors could be identified. This was further complicated by the fact, that concerning the nitrate content in the soil solution, the amount of data varied strongly from season to season and within each season between the different repetitions at each land use type, due to instrument failures caused by termite activity and dry soil conditions. Therefore, single seasons and single repetitions (and thus very small scale phenomena) carry more weight than others and thus impose a bias on the dataset, which makes it difficult to infer greater contexts. Nevertheless, the data at hand suggest that the nitrate content in the soil solution downslope of the pits was not the result of missing nitrate inputs by shallow subsurface flow but was rather related to soil properties. This was not surprising as no shallow subsurface flow was found in the pits as described in chapter 6.1.2. The lower nitrate content downslope of the pits at the plot under bare fallow, for example, probably resulted from drier soil moisture conditions at these positions as compared to the positions in front of the pits, which did not favour nitrification. The drier conditions were not caused by the missing water contribution from upslope but rather by a sandier soil structure and shallower soils (see chapter 5.2.1). The high mean values downslope of the pits at the plot under crop production on the other hand, were mainly driven by a higher number of data points retrieved in season 2017.2 compared to the other seasons. During this season, the nitrate content in the upper topsoil downslope of the pits was significantly higher than at the reference plots and upslope of the pits, and also significantly higher than during the other seasons. Also the soil moisture content in the

upper and lower topsoil was higher downslope of the pits, and higher than during the other seasons. Nevertheless, the nitrate content in the soil solution in the upper topsoil downslope of the pits was also significantly higher than in the lower topsoil so that it can be assumed that very little leaching of nitrate occurred at this position during that season. This effect could be seen in all three spatial repetitions. So far, no explanation for the high nitrate content downslope of the pits in season 2017.2 was found.

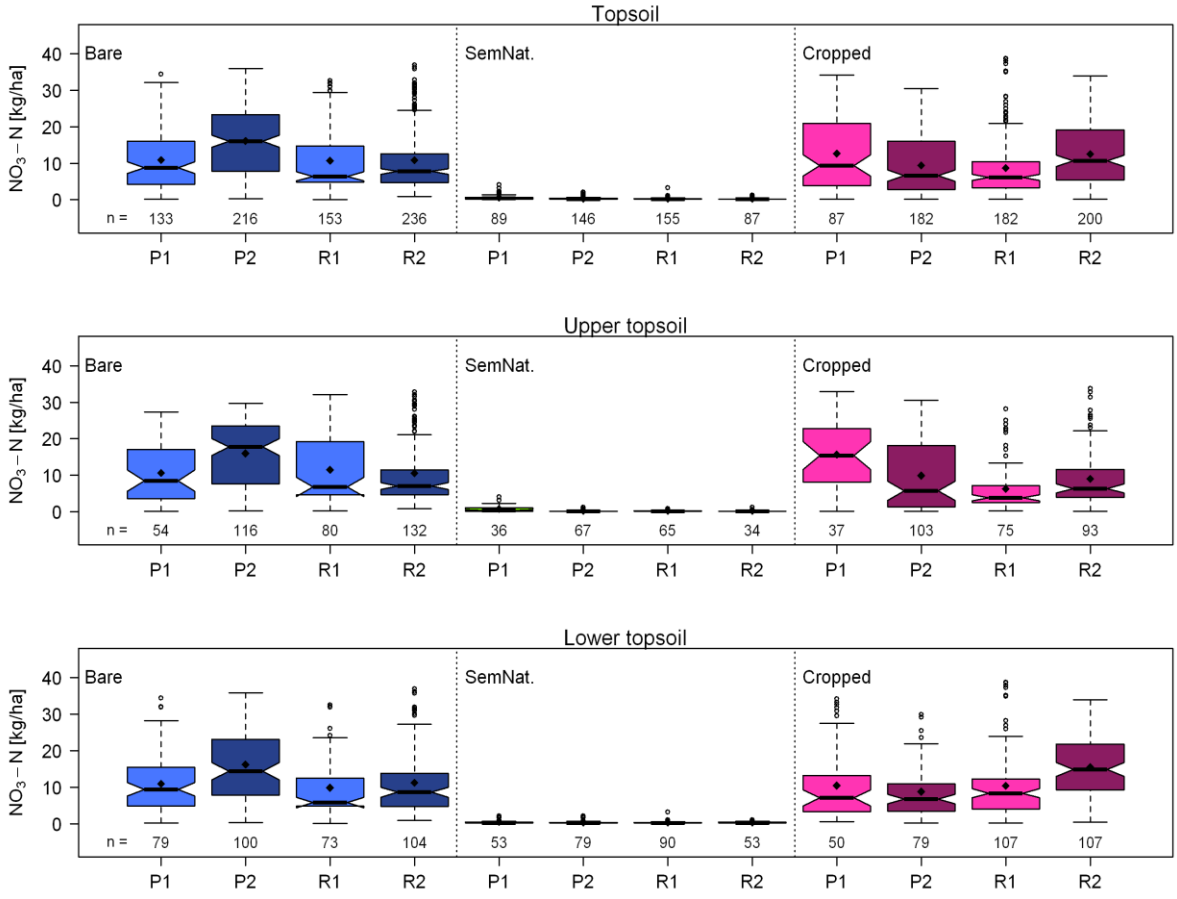

Figure 66 *Effect of dug-out pits on the nitrate content in the soil solution [kg NO_3-N/ha] at each land use type, a) mean over topsoil, b) upper topsoil and c) lower topsoil, P1 being the position downslope of the dug-out pits while P2 is located upslope of the pits. R1 and R2 are the corresponding positions on the reference plots.*

To conclude, the data did not suggest the lateral translocation of nitrate in the soil body, instead variance in the nitrate content at the different slope positions and upslope and downslope of the dug-out pits was related to the soil texture, depth of the soil body and soil moisture conditions.

7.2 Nitrate dynamics in the interflow

This section describes the nitrate dynamics in the interflow in relation to the climatic conditions and nitrate dynamics in the soil solution on the slope and gives a first approximation of nitrate inputs from the slopes to the wetland fringe. Nitrate concentrations in the interflow were measured in dug-out trenches at the slope toe on the same days as soil moisture and the nitrate content in the soil solution along the slope. For the plot under crop production and the plot under semi-natural vegetation, data were retrieved during the entire 2 years the experiment was running. For the bare fallow plot, data are only

available from September 2016 until June 2017 due to the delayed installation of the trench and the desiccation of the trench at the end of June 2017.

Overall, data analysis did not reveal any simple correlations over the entire dataset. Statistical correlations between interflow quantity and nitrate concentration in the interflow were non-existent (R^2= 0.02 and rho= -0.05). Nevertheless, when looking at the time series, one can deduct that high interflow quantities always coincided with high nitrate concentrations. At the same time, there were days when nitrate concentrations were high even if there was only little interflow captured. The correlation between the nitrate content in the soil solution and nitrate concentration in the interflow was also extremely weak (R^2= 0.01 and rho <= 0.2) for all land use types. The same is true for the correlation between nitrate concentration in the soil solution and in the interflow (R^2<= 0.05 and rho= 0.2 at the plot under crop production and semi-natural vegetation and R^2= 0.02 and rho= -0.05 at the bare fallow plot). Thus, a more detailed analysis of the nitrate dynamics in the interflow is needed to understand which factors drive the nitrate input by the interflow to the wetland and to reflect on the underlying processes.

During the two years the experiment was running, nitrate concentrations in the interflow were significantly different between the three land use types at p= 0.05 (see Figure 67). Therefore, it is justified to analyse the data regarding the impact of the different land use types even if the plots did not reach up to the hilltop and the land use types were not established over the total slope area (see chapter 4.1).

Nitrate concentration as well as the nitrate delivery to the wetland were influenced by the variable climatic conditions and the resulting soil water contents of the soil and of the saprolite during the four rainy seasons 2016 - 2017. Therefore, in the following section the nitrate dynamics in the interflow are described and discussed regarding the impact of different climatic conditions on source factors (N-mineralization in the topsoil) and transport factors (interflow pathways in the saprolite) during the different seasons. In the first rainy season 2016, measurements on the plots under crop production and semi-natural vegetation started in mid-April. By then, the nitrate concentration in the interflow at the plot under crop production was very high compared to the values collected during the two years the experiment was running (see Figure 67). The concentration then decreased from 6 to 2 mg NO_3-N/l towards the end of the rainy season and remained at that level throughout the following dry season and also during the second rainy season 2016. The only exception was an increase in the nitrate concentration to values of 5 mg NO_3-N/l before the two small rainfall events at the end of December and beginning of January. This increase persisted for about three weeks (during this time only three measurements were taken). Nitrate concentrations in the interflow at the plot under semi-natural vegetation was about 2 mg NO_3-N /l during the first rainy season 2016 and around 1 mg NO_3-N/l during the following dry season. At the bare fallow plots, measurements started in September 2016. Here, concentrations increased steadily towards the end of the season before they dropped from 4 mg NO_3-N/l to 2 mg NO_3-N/l after the rains had stopped and remained at that level until the beginning of the next rainy season. During the first rainy season 2017, nitrate concentrations in the interflow at the plot under crop production were rather low (2 mg NO_3-N/l) but showed three distinct short peaks of around 4 mg NO_3-N/l on the 1st, 18th and 22nd of April. On the 1st of April, the peak did not appear until two days after the last rainfall event, while on the other two days rain had just stopped some hours before the measurement. On these days, the nitrate

content in the soil solution in the lower topsoil also reached the highest values of that season (see chapter 7.1.1). On the 18th and 22nd of April 2017, high nitrate concentrations coincided with large volumes of interflow. At the plot under semi-natural vegetation, the nitrate concentration also showed a peak on the 18th of April (2.5 mg NO_3-N/l) coinciding with the highest interflow volumes measured during the experiment. Afterwards, concentrations decreased to about 1 mg NO_3-N/l. During the rest of the season and the following dry season, the nitrate concentration was similar to that measured in in season 2016.1. At the plot under bare fallow, nitrate concentrations in the interflow increased to 3.5 mg NO_3-N/l with the onset of the rains at the end of February 2017 and then remained rather stable until the end of the season. After that season, interflow in the trench at the plot under bare fallow dried up, so no more measurements could be conducted. The second dry season 2017 was interrupted by two weeks with several small rainfall events. Even if interflow volumes were not impacted by that, nitrate concentrations in the interflow at the plot under crop production and under semi-natural vegetation increased to 3 mg NO_3-N/l and 2 mg NO_3-N/l respectively and remained at that level until the onset of the second rainy season 2017. In 2017.2, the nitrate concentration in the interflow at the plot under crop production was generally high in relation to the other seasons and there was a pronounced dynamic reflecting the bi-modal distribution of rainfall during this period. The first peak of 5 mg NO_3-N/l was reached after a large rainfall event of 42 mm on the 13th of September, following very high nitrate contents in the soil solution measured during the week before the event. A similar peak was reached after the large rainfall event of 66 mm on the 7th of November and values only decreased again to 2 mg NO_3-N/l at the end of the month. A short increase to 4 mg NO_3-N/l was found on the 4th of December, following a rainfall event of 33 mm on the 29th of November coinciding with an increase in the nitrate content in the lower topsoil on the slope. The interflow then dried up during the following dry season. When it reinitiated after the first week of more efficient rain showers in April 2018, nitrate concentrations quickly increased to 4 mg NO_3-N/l and then sharply decreased to 2.5 mg NO_3-N/l in mid-May. At the plot under semi-natural vegetation, nitrate dynamics in the interflow were also more pronounced in 2017.2 than during the previous seasons, but often showed a different pattern as compared to the dynamics in the interflow at the plot under crop production. Here, concentrations were highest from end August to early September and at the beginning of the second wet interval in early November (around 2 mg NO_3-N/l) and, more importantly, values steeply decreased after the large rainfall events in September and November. In the beginning of January, when interflow volumes were already very small, concentrations suddenly increased to about 2 mg NO_3-N/l. At the beginning of the first rainy season 2018, values were still at a high level (3 mg NO_3-N/l) and then quickly decreased to about 1.5 mg NO_3-N/l during the rest of the rainy season until measurements stopped.

On the 14th of November 2017, interflow and nitrate concentrations in the interflow were measured before and one hour after a rainfall event of 7.2 mm (max. 15 min. intensity of 5.2 mm) to get further insights into the fast component of the interflow (see chapter 6.2.1). At the plot under crop production, the nitrate concentration increased by 54 % from 2.8 mg NO_3-N/l before to 4.3 mg NO_3-N/l one hour after the event. The nitrate concentration at the plot under semi-natural vegetation, on the other hand, decreased by 21 % from 1.4 mg NO_3-N/l to 1.1 mg NO_3-N/l. This proves that water from the upper soil is transported to the slope toe via preferential flow paths in the saprolite. At the plot under crop production,

the increase in the nitrate concentration after the rain event was caused by leaching of nitrate in the soil solution. At the plot under semi-natural vegetation, though, only very little nitrate (0.4 kg NO_3-N/ha) was present in the soil solution of the residual soil so that no or only little nitrate was added to the subsurface flow. The fact that concentrations even decreased hints to a fast transport of infiltrating rainfall before mixing with water in the matrix of the saprolite could occur.

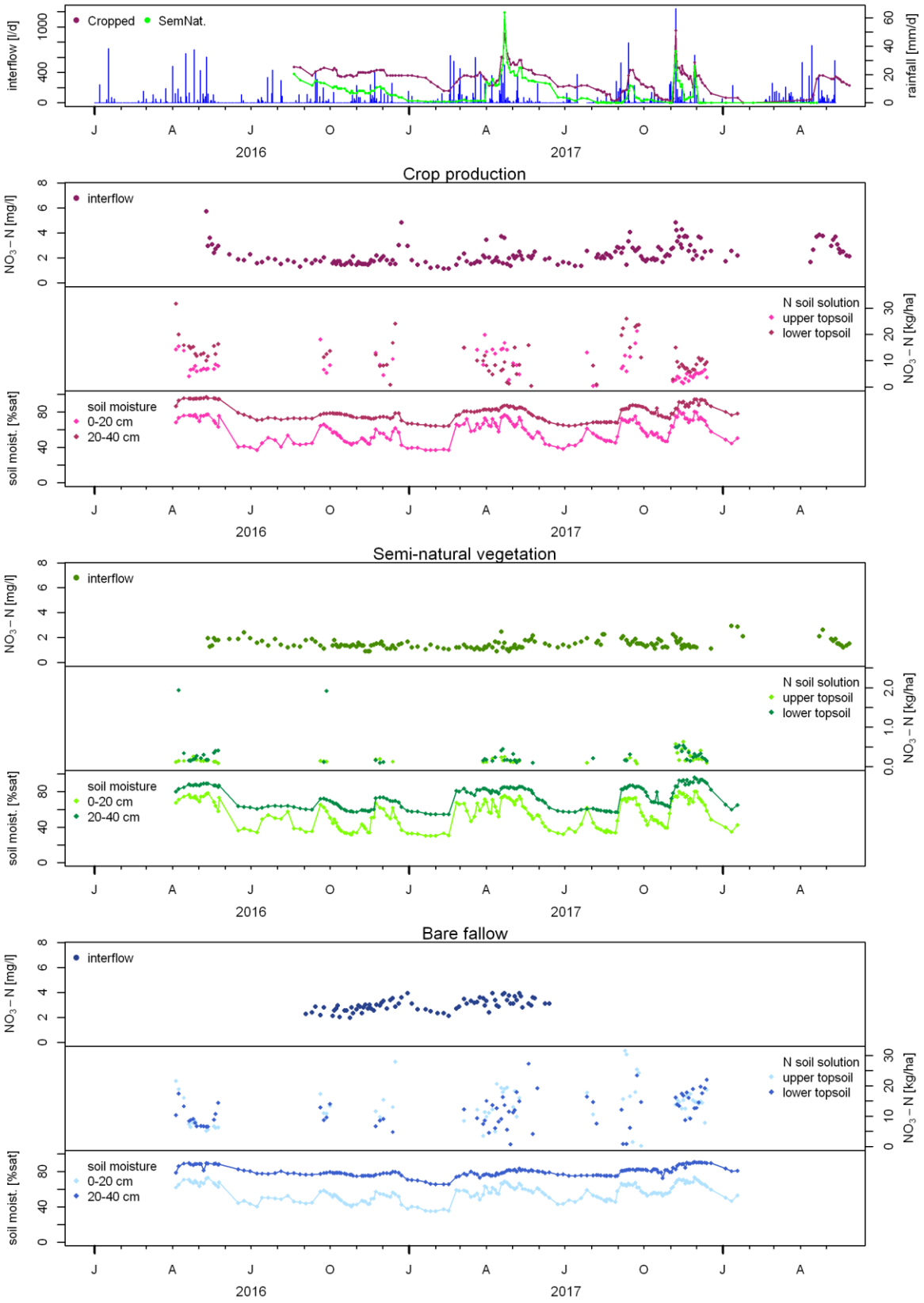

Figure 67 *Nitrate concentration in the interflow [mg NO_3-N/l], mean nitrate content in the soil solution along the slope in the upper and lower topsoil [kg NO_3-N/ha] and mean soil moisture [% sat.] along the slope at 0-20 cm and 20-40 cm depth at a) the plot under crop production, b) the plot under semi-natural vegetation and c) the plot under bare fallow.*

During the first rainy season 2016, high nitrate concentrations measured in the interflow at the plot under crop production, can be explained by the combination of high nitrification in the topsoil on the slope, which was favoured by optimal moisture conditions for nitrifying microorganism during large parts of the season, and by high leaching losses during large rainfall events of moderate intensity during the second half of the rainy season. A higher nitrate content in the lower than in the upper topsoil already suggested intense translocation of nitrate within the soil. The high concentrations during high flow conditions in the interflow show that also significant leaching of nitrate out of the soil profile took place during this period. Nevertheless, it is not known when the leaching began, as the measurements started only a few weeks after the beginning of the first rainy season 2016. Unlike season 2017.2, nitrate concentrations quickly decreased towards the end of the rainy season. Three possible explanations were found for this trend. Firstly, the higher nitrate content in the soil solution in 2016.1 than in 2017.2 could suggest, that the leaching from the topsoil was less efficient in 2016.1 (yet a higher nitrate content could also indicate more nitrate mineralization due to the favourable moisture conditions). Secondly, rainfall patterns in 2016.1 may have led to higher water contents in the deeper soil and the saprolite and thus leached nitrate was diluted on its way down to the slope toe. Thirdly, the reoccurring excessive rainfalls might have quickly conducted nitrate rich water from the topsoil through the saprolite, so that high concentrations pertained for a short time only. In order to prove that hypothesis, it would be necessary to have continuous data which would allow insights in the cumulative nitrate amounts transported by the interflow over the entire season. Following the same line of reasoning, the high nitrate concentrations in the interflow which were observed for several weeks after the large rainfall event in the beginning of November 2017 were caused by high soil moisture in the soil but drier conditions in the saprolite. High amounts of nitrate were washed out from the entire upper soil body due to a very high degree of saturation of the soil following the large rainfall event of November 7. As the deeper saprolite did not contain as much water as in 2016.1, for example, little dilution took place in the saprolite. Finally, sub-surface flow networks did not extend and get connected as effectively in season 2017.2 as during the other seasons due to lower saturation levels in the saprolite. Therefore, the transport of nitrate to the slope toe was delayed and thus high nitrate levels could be detected over a longer time spam. This fits to the calculation of seasonal nitrate input presented below, which was lower in 2017.2 than during the other seasons. Low concentrations during the dry season and the weak second rainy season in 2016 indicate that no significant leaching occurred during this time. Interflow volumes were still moderately high as compared to other dry periods. This supports the assumption of high water contents in the saprolite during and at the end of 2016.1 and, thus, a strong delayed component of the interflow. The short period of high nitrate concentrations in the interflow at the end of the year 2016 follows the increase of the nitrate content in the soil solution in the lower topsoil described in chapter 7.1.1. Interestingly, there was only a small rainfall event of 8.2 mm at that time and soil moisture values were already too low to expect significant nitrate leaching from the soil matrix and infiltration from the soil into the saprolite. The same is true for the increase of nitrate concentrations after the intermittent rains in July 2017. If there was no input from fertilizer or cattle herding from further upslope (and therefore not captured in this experiment), one explanation could be that mineralization of (dissolved) organic compounds also took place in unsaturated parts of the saprolite. More research is needed to follow up on this hypothesis. In 2017.1, nitrate concentrations in the interflow at the plot under crop production were generally lower than in 2016.1 and 2017.2 and only short-time

peaks were detected (see Figure 67). As already suggested by the nitrate content in the soil solution (see chapter 7.1.1), less leaching occurred during this season, as the intense rainfall events at the beginning of the season led to preferential flow in the upper soil and therefore did not leach nitrate from smaller pores. This effect has also been found by several authors before (Creed and Band, 1998; Weiler and McDonnell, 2006; Wild, 1972). Nevertheless, due to the fill-and-drain mechanism described in chapter 6.2.1, water still entered the saprolite causing high interflow volumes, which persisted into the dry season. Therefore, as in season 2016.1, dilution effects within the saprolite might have reduced nitrate concentrations in the interflow. The high concentrations on the 18th and 22nd of April 2017 were measured just some hours after the rainfall event. As they coincide with very high amounts of interflow, they are probably still part of the quick interflow component discussed above and in chapter 6.2.1. As these days were already close to the end of the rainy season, higher saturation levels in the saprolite, which favour the development of a denser network of preferential flow paths and therefore a pronounced quick interflow component, are still expected to persist. On these days, the nitrate content in the soil solution was also very high, which seems surprising. Nevertheless, the nitrate content at the beginning of the rainfall event is not known as there were always 2 - 3 days between the measurements, during which substantial amounts of nitrate can be mineralized (Weil and Brady 2017). So probably nitrate levels before the rain were even higher and the reduction caused by leaching was not captured by the data. As described above, there was less variance of nitrate concentrations in the interflow at the plot under semi-natural vegetation than under crop production. This was caused by the limited availability of leachable nitrate in the soil solution at this land use type, which was also found by other authors before (Dividson et al., 1990; Hill et al., 1999). The excessive rainfall event of the second rainy season 2017 actually led to a decrease in the nitrate concentration, the same effect which was observed when comparing nitrate concentrations in the interflow before and one hour after the rainfall event on the 14th of November. This also supports the assumption of active preferential flow paths in the saprolite. These deliver the fresh rainwater to the slope toe before it can mix with the matrix water, which contains more nitrate due to subsurface mixing of waters stemming from different parts of the slope or due to mineralization of organic compounds within the saprolite. This does not fit, though, to the peak concentration of season 2017.1 measured on the 18th of April some hours after an efficient rainfall event. The subsurface catchment of the trenches at the slope toe is expected to extend beyond the plot boundaries (see below and chapter 6.2.1). Therefore, it might be that nitrate washed out from the plot under crop production or from the plot under bare fallow was mixed up under ground with the water which infiltrated at the plot under semi-natural vegetation before it entered the trench. As explained before, it can be assumed that at this point in time the saprolite already contained a lot of water and, therefore, additional temporary preferential flow paths might have developed. During the entire measurement period, nitrate concentrations in the interflow at the plot under bare fallow were significantly higher than at the other two land use types. Under this land use type, the nitrate which was released by the mineralization of the labile pool of organic matter was not taken up by crops or the semi-natural vegetation and, therefore, more nitrate could be leached to the saprolite and reach the slope toe. Other than at the plot under crop production, the nitrate concentrations in the interflow under bare fallow exhibited very weak reactions to rain fall events. This might hint to the fact that less preferential flow paths in the saprolite were active on that plot, which can be attributed to the heterogeneous properties of the saprolite.

During the dry seasons, a moderate background concentration of nitrate in the interflow was always found at all land use types, with concentrations being lower than during the antecedent rainy season but similar between the different dry seasons (about 1.8 mg NO_3-N/l under crop production, 1.4 mg NO_3-N/l under semi-natural and 2.4 mg NO_3-N/l under bare fallow). Concentrations were still significantly different at p= 0.05 between the different land use types. This supports the assumption of a delayed interflow component as presented in chapter 6.2.1, which is caused by matrix flow or smaller preferential flow paths in the deeper saprolite. Minor fluctuations in the nitrate concentrations during the dry periods and similar concentrations in each dry season at all land use types also hint to the fact, that within the saprolite, water from different rainfall events is mixed up over longer periods of time, as also described in Burghof (2017). Furthermore, bigger similarities in the nitrate concentrations between the different land use types (especially between the plot under semi-natural vegetation and under crop production) were found in the back ground concentrations than during the rainy seasons. This suggests that especially these slowly passing waters mix in the saprolite over larger areas.

Over the entire measurement period, nitrate concentrations and contents in the soil solution at the plot under crop production and under bare fallow were some orders of magnitude higher than nitrate concentrations in the interflow. Several processes might be behind this phenomenon. As described above and in chapter 6.2.1, rainfall partly infiltrated into the soil via macropores (e.g., termite routes) without leaching big quantities of nitrate from the soil matrix. Once this water entered the saprolite, it diluted the nitrate which was leached and transported from the upper soil into the saprolite during previous events. Furthermore, as described above, the subsurface catchment of the pits extended beyond the limits of the plots, on which the different land use types were established. Thus, also nitrate depleted water, which infiltrated from areas further upslope, where elephant grass (*Pennisetum purpureum*) was grown and from the adjacent plot under semi-natural vegetation diluted the interflow further. Due to the long transit times of interflow in the saprolite, some nitrate might also be lost by denitrification. Apart from that, water from the deep aquifer might also contribute to the interflow collected at the trench at the slope toe, as neither the geo-electrical measurements nor the analysis of stable isotopes (see Burghof (2017)) allowed to exclude a connection of the two runoff components at that slope position. The fact, that nitrate concentrations in the interflow at the plot under semi-natural vegetation were higher than in the soil solution at this land use type again supports the hypothesis of a subsurface catchment, which extends beyond the plot limits where water with a higher nitrate concentration was mixed up with the water infiltrated under semi-natural vegetation. In addition, bigger similarities of nitrate concentrations between the two land use types were found in the interflow than in the soil solution, which also supports the latter hypothesis.

There was no correlation between nitrate input to the wetland by the interflow (NO_3-N concentration multiplied by interflow volume per day) and the nitrate content in the soil solution at the slope toe at the plot under crop production and under semi-natural vegetation (R^2 and rho <0.3). This indicates that nitrate leaching at the slope toe did not control the nitrate content in the interflow. Furthermore, there was also no correlation between nitrate input by the interflow and nitrate input via surface runoff at the plot under semi-natural vegetation. At the plot under crop production, though, a moderate correlation of rho = 0.5 was detected. This hints to the fact that infiltrating surface runoff at the slope toe contributes to the

nitrate content in the interflow at the plot under crop production, where nitrate losses by surface runoff were high. This fits to the observation of moderate correlations between surface runoff volumes and interflow volumes presented in chapter 6.3. For the plot under bare fallow, this correlation could not be calculated as interflow volumes could not be measured (see chapter 6.2.1)

Table 13 *Cumulative seasonal nitrate collected over 1 m at the slope toe as well as the deducted seasonal nitrate input from the slope to the wetland and to the wetland fringe. Nitrate inputs to the wetland were calculated based on the assumption that the nitrate is distributed over the entire extend of the wetland in a straight transect below the trench from the slope toe to the stream (180 m²). Nitrate input to the wetland fringe was calculated based on the assumption that nitrate only contributes to the nutrient content of the soil water at the wetland fringe due to the fast uptake of nitrate by the vegetation (according to Gabiri 2018, the fringe extends 60 m from the slope toe into the valley bottom, hence here a transect below the trench of 60m² was considered).*

Season	**Crop production**			**Semi-natural vegetation**		
	Seasonal input collected over 1m at the slope toe [kg NO_3-N]	Seasonal input to the wetland [kg NO_3-N /ha]	Seasonal input to the wetland fringe [kg NO_3-N /ha]	Seasonal input collected over 1m at the slope toe [kg NO_3-N]	Seasonal input to the wetland [kg NO_3-N /ha]	Seasonal input to the wetland fringe [kg NO_3-N /ha]
2016.2	0.11	5.9	17.8	0.03	1.5	4.5
2017.1	0.12	6.5	19.4	0.05	2.6	7.8
2017.2	0.09	4.8	14.3	0.01	0.7	2.0

Table 13 shows the cumulative seasonal nitrate contribution of the slope collected over 1 m at the slope toe below the plot under crop production and under semi-natural vegetation for the three rainy seasons. As the plots were not hydrologically isolated, the values include the input from the areas upslope of the plots. The data show that the input from the plot under crop production was about four times higher than the input from the plot under semi-natural vegetation in season 2016.2 and 2017.1. In season 2017.2, there was less input from both plots but the difference between the two land use types was even higher, as there was seven times as much nitrate input from the plot under crop production. This fits well to the assumption explained above that the saprolite was less saturated during that season due to the distribution and characteristics of rainfall events. As a result, less nitrate-containing water from the saprolite reached the slope toe as the subsurface network of flow paths could not develop well, and, thus, the overall input was less than during the other seasons. This also explains the bigger difference between the plot under crop production and the plot under semi-natural vegetation. Under these conditions, less

subsurface mixing of water in the saprolite took place and therefore the signal of the heavy rainfalls was transmitted more directly, leading to a dilution of nitrate in the interflow under semi-natural vegetation, while causing intense leaching and thus high nitrate concentrations in the subsurface runoff under crop production.

However, the statements concerning nitrate (and water) inputs from the interflow rely on various assumptions, which are known to have some shortcomings. As described before, water in the saprolite mixes over large areas and thus the signal of the land use type established upslope of the individual trenches will always be blurred. This is augmented by the issue, that the plots did not reach up to the hilltop and therefore other land use types and agricultural practices also influenced the interflow water and the corresponding nitrate loads collected at the slope toe. Furthermore, continuous measurements of water and nitrate input from the interflow would be needed to capture nitrate flushing as an immediate reaction to rainfall events, which was shown to be present by the measurements directly before and after a rainfall event. Therefore, most likely the peaks were missed and seasonal water and nitrate inputs to the wetland were underestimated.

7.3 Nitrate loss via surface runoff

This section analyses nitrate transport along the slope via surface runoff regarding the impact of the land use type and climatic conditions as well as the processes involved.

The amount of nitrate transported via surface runoff during each event as well as the cumulative nitrate loss per season were significantly different ($p = 0.05$) between the three land use types. The highest losses were recorded at the plot under bare fallow, followed by the plot under crop production, while only very little nitrate was lost from the plot under semi-natural vegetation. At the plot under crop production, coefficients of variation between the three runoff plots ranged from 3 % to 143 %. At the plot under bare fallow, coefficients ranged from 1 % to 168 %, but overall there was no significant difference between the nitrate losses from the three replicates for these two land use types. At the plot under semi-natural vegetation, coefficients of variation ranged from 14 % to 150 % but one runoff plot (P5) was significantly different from the other two replicates. Nevertheless, for all three land use types further analysis is based on mean values of the three replicates per land use type. Concerning nitrate concentration in the surface runoff, there was a significant difference between the plot under semi-natural vegetation and the plots under crop production and bare fallow ($p = 0.05$), while the difference between the plots under crop production and bare fallow was not significant. Yet, for all three land use types, the differences in the nitrate concentration were not as pronounced as the differences in the nitrate loss. Mean and maximum loss and concentration are shown in Table 14 and cumulative nitrate loss over the study period is presented in Table 15. Nitrate concentrations in the precipitation were not measured during this study. Nevertheless, Burghof (2017) analysed the chemical composition of precipitation in the same study area during the years 2014 - 2016. Her results showed that the nitrate concentration in the rainwater was between <0.1 mg NO_3-N/l and 1 mg NO_3-N/l but could reach up to 2.75 mg NO_3-N/l during single rainfall events.

Table 14 *Mean nitrate loss and mean nitrate concentration in the surface runoff during the measurement period at the three land use types.*

Land use type	Mean nitrate loss [kg NO_3-N/ha]	Max. loss [kg NO_3-N/ha]	Mean nitrate concentration [mg/l]	Max. nitrate concentration [mg/l]
Crop production	0.07	0.4	6	35
Semi-natural vegetation	0.01	0.04	5	39
Bare fallow	0.2	1.1	8	48

Table 15 *Seasonal nitrate loss via surface runoff from the plots under crop production, semi-natural vegetation and bare fallow. Seasons summarize the rainy season and the following dry season so that values can be compared to nitrate loss via the interflow (displayed in the second column of the crop production and semi-natural vegetation section) .*

Season (incl. following off season)	Crop production		Semi-natural vegetation		Bare fallow
	N loss from the slopes via surface runoff [NO_3-N/ha]	N loss from the slopes via interflow [NO_3-N/ha]	N loss from the slopes via surface runoff [NO_3-N/ha]	N loss from the slopes via interflow [NO_3-N/ha]	N loss from the slopes via surface runoff [NO_3-N/ha]
2016.2	0.85	2.67	0.05	0.68	2.06
2017.1	2.31	2.91	0.15	1.16	5.84
2017.2	2.22	2.14	0.23	0.3	5.59

Nitrate loss via surface runoff was strongly positively correlated with runoff volumes (rho= 0.91) and runoff coefficients (rho= 0.9), as shown in Figure 68. The correlations were weaker for the plot under semi-natural vegetation (rho= 0.69 and rho= 0.53 respectively). Looking at the single seasons though, the correlation of surface runoff volume and nitrate loss at the plot under semi-natural vegetation was stronger (rho= 0.8 in 2016.2, rho= 0.93 in 2017.1 and rho= 0.7 in 2017.2). At the plot under bare fallow and under crop production, the correlations were slightly less pronounced in 2017.2 than during the other seasons with rho= 0.74 and rho= 0.83 respectively. A moderate negative correlation between surface runoff volumes and nitrate concentrations in the surface runoff was detected for the plot under bare fallow and under crop production (rho= -0.5), while at the plot under semi-natural vegetation the correlation was weak (rho= -0.3).

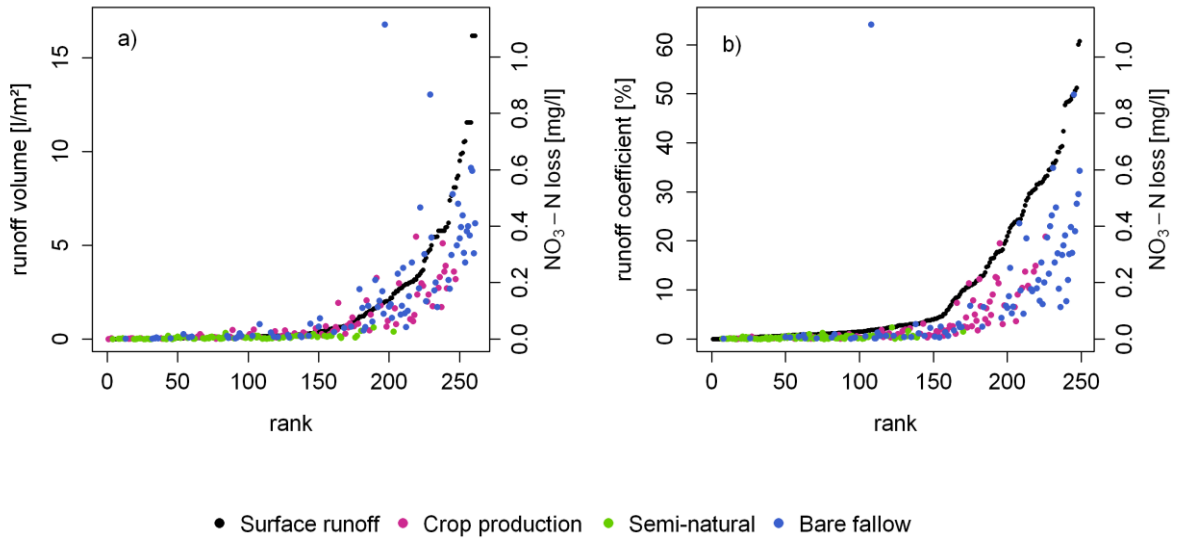

Figure 68 *Nitrate loss via surface runoff [kg NO_3-N/ha] from the plots under crop production, semi-natural vegetation and bare fallow related to a) surface runoff volumes [l/m²] and b) runoff coefficients [%] from April 2016 to December 2017.*

Rainfall amount and max. 15 min. rainfall intensity were well correlated with the nitrate loss via surface runoff at all three land use types (s. Figure 69), with correlations being slightly stronger for the rainfall amount (rho between 0.61 and 0.73 as compared to rainfall intensity for which rho was between 0.51 and 0.64). Regarding the nitrate concentration, a negative correlation to rainfall amount (rho= -0.45 and rho= 0.57) and rainfall intensity (rho= -0.43 and rho= -0.47) was detected at the plots under crop production and bare fallow respectively (see Figure 70). The nitrate concentration in the surface runoff at the plot under semi-natural vegetation was not correlated to rainfall characteristics.

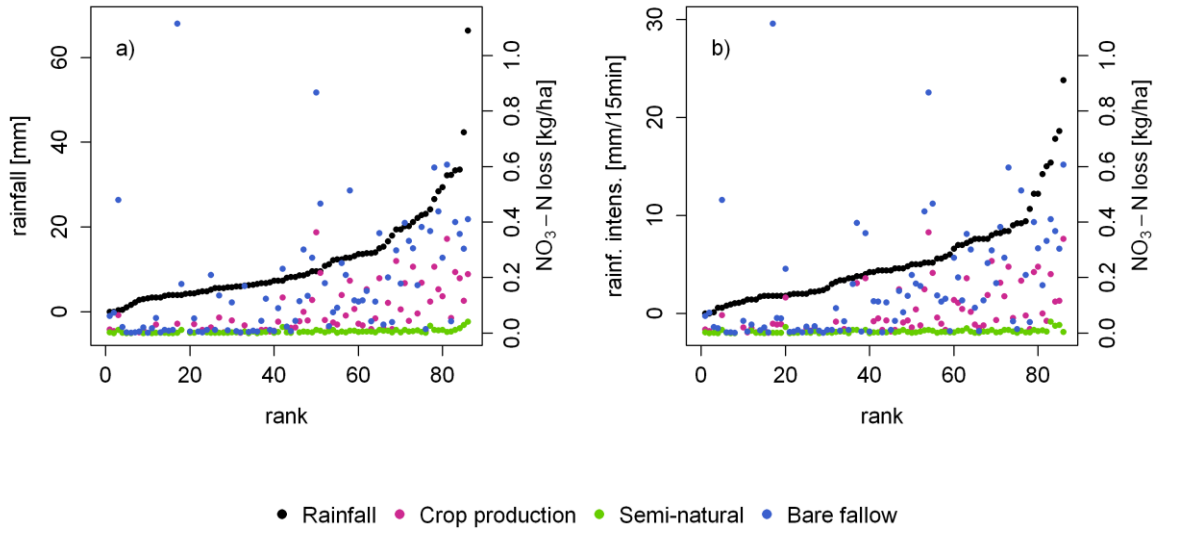

Figure 69 *Nitrate loss via surface runoff [kg NO_3-N/ha] from the plots under crop production, semi-natural vegetation and bare fallow related to a) daily rainfall amounts [mm] and b) max. 15 min. rainfall intensity [mm] from April 2016 to December 2017.*

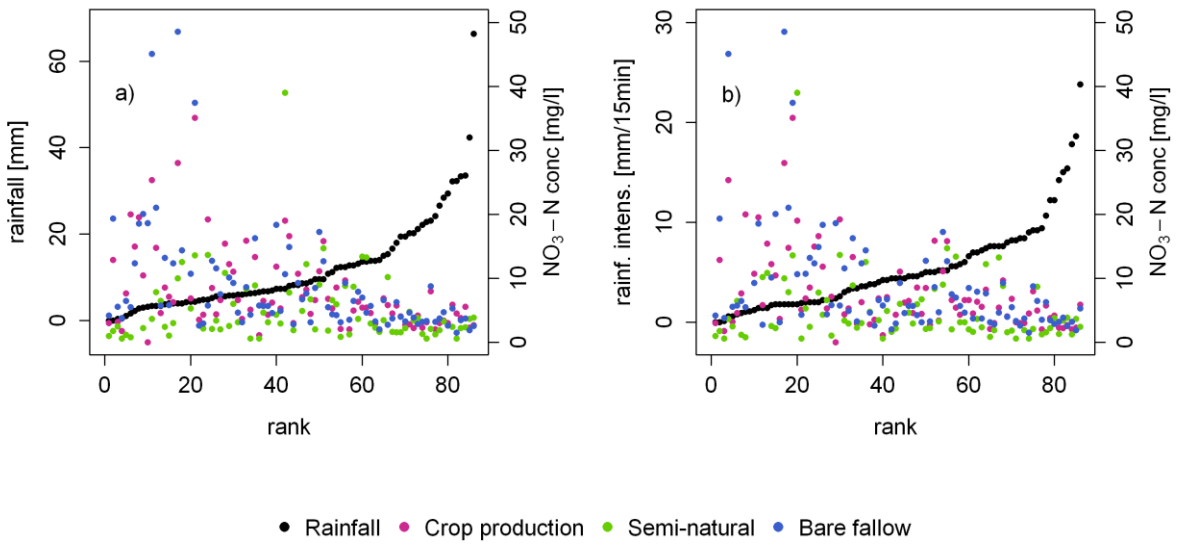

Figure 70 *Nitrate concentrations in the surface runoff [mg NO_3-N/l] from the plots under bare fallow, crop production and under semi-natural vegetation related to a) daily rainfall amounts [mm] and b) max. 15 min. rainfall intensity [mm] from April 2016 to December 2017.*

The correlation of nitrate loss via surface runoff and nitrate content in the soil solution was different between the three land use types. At the plot under crop production, no correlation could be detected (rho= 0.01), while there was a weak correlation at the plot under bare fallow (rho= 0.33) and a moderate correlation at the plot under semi-natural vegetation (rho= 0.62), see Figure 71. Nitrate concentration in the surface runoff was not correlated to the nitrate concentration in the soil solution at the plots under crop production and bare fallow. At the plot under semi-natural vegetation, a weak correlation (rho= 0.32) was found. Surprisingly, at the plot under semi-natural vegetation, the nitrate concentrations measured in the surface runoff were one to two orders of magnitude higher than in the soil solution.

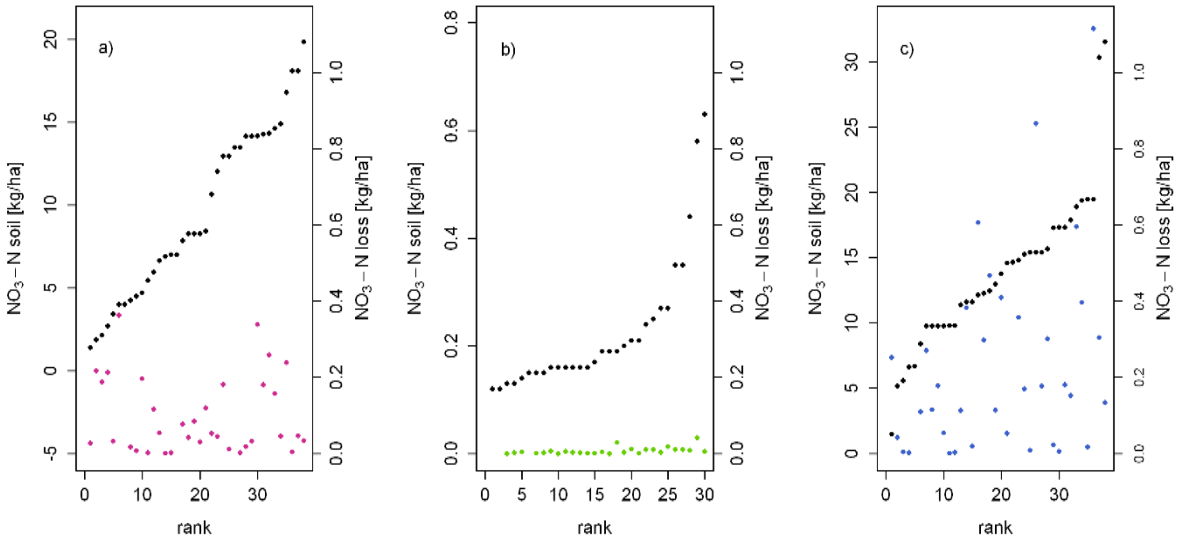

Figure 71 *Nitrate content in the soil solution [kg NO_3-N/ha] (first y-axis) related to nitrate losses via surface runoff [kg NO_3-N/ha] (second y-axis) at the plots under a) crop production, b) semi-natural vegetation and c) bare fallow.*

The common nitrate concentrations in the precipitation reported by Burghof (2017) were significantly lower than the nitrate concentrations measured in the surface runoff in the scope of this study. Therefore, as no fertilizers were applied, nitrate in the surface runoff mainly originated from the upper 6 - 10 cm, i.e., the interaction zone of the topsoil (Elrashidi et al., 2005). Kleinman et al. (2006) described that nitrate loss via surface runoff is determined by source factors (factors controlling nutrient availability in the soil) as well as transport factors (factors controlling runoff generation). The strong correlation of nitrate loss and surface runoff volumes in combination with the weak or missing correlation of nitrate loss and nitrate content in the soil solution at the plots under bare fallow and crop production indicates that, in this study, mainly transport factors controlled the nitrate loss from the slopes. This is further supported by the missing correlation of nitrate concentrations in the surface runoff and in the soil solution at these two plots. In that regard, rainfall characteristics acted as a moderating variable as they controlled surface runoff volumes (see chapter 6.3). The negative correlation of the nitrate concentration and surface runoff volumes shows that dilution effects were prominent at higher runoff volumes. This was also found by Jacobs et al. (2018b) in their study in the Mau Escarpment in Kenya. As described in chapter 6.3, surface runoff is assumed to be mainly generated as infiltration excess runoff. This is supported by the negative correlation of rainfall intensity and nitrate concentration in the surface runoff, as Needelman (2002) found that infiltration excess runoff is dominantly comprised of rainwater. Nevertheless, Kleinman et al. (2006) described that at the beginning of a rainfall event, higher rainfall intensities lead to higher infiltration rates and, thus, cause nitrate leaching to deeper soil layers so that less nitrate is available in the interaction zone. Generally, this process might also have stimulated the negative correlation of rainfall intensity and nitrate concentration in the surface runoff. Nitrate loss, on the other hand, was positively correlated to rainfall intensity, due to higher runoff volumes associated with intense rainstorms. Therefore, nitrate leaching to deeper soil layers during high intensity rainstorms was not the dominant factor here. This proofs that transport factors outweighed the source factors at the plots under bare fallow and crop production. In addition, it can be assumed that the runoff generating processes were very similar at the

two land use types, as there was no significant difference in nitrate concentrations despite the larger runoff volumes and the higher nitrate content in the soil solution at the plot under bare fallow. As described above, compared to the other two land use types, nitrate loss from the plot under semi-natural vegetation was more strongly correlated to the nitrate content in the soil solution. The same applies to the nitrate concentrations in the soil solution and in the surface runoff. One possible explanation could be that due to the high soil moisture contents (see chapter 6.1.1) at this land use type, saturation excess runoff, in which dilution effects are not that prominent, might have developed temporarily. This is supported by the fact that no negative correlation of the nitrate concentration in the surface runoff and the rainfall intensity was found here. Nevertheless, values from the plot under semi-natural vegetation seem dubious, as nitrate concentrations in the surface runoff exceeded these in the soil solution by far. Therefore, external factors must have influenced the results, unless nitrate concentrations in the first centimetres of the soil were significantly higher than at the first measurement depth. One explanation might be that, at this land use type, more nitrate was present at the soil surface due to animal faeces, as animals tended to hide in the high grasses and field rats were living in close proximity to the runoff pits.

In literature, only very few studies reported nitrate losses and nitrate concentration in the surface runoff from plots in tropical regions which were not under the influence of fertilizer application. Lal (1976), for example, found nitrate concentrations of 4 - 6 mg NO_3-N/l and nitrate losses of up to 9 kg NO_3-N/ha from fields under bare fallow in Western Nigeria. Ng Kee Kwong et al. (2002) reported nitrate losses of 0.06 kg NO_3-N/ha and concentrations of 4 mg NO_3-N/l from a sugar cane field in Mauritius. The nitrate concentrations at the plots under crop production and bare fallow measured in this study are comparable to these findings, as is the nitrate loss from the plot under crop production. In their review study, Sharma and Chaubey (2017) found that in all the papers they considered, significantly more nitrate was lost via surface runoff from fields under crop production than from fields under switchgrass (*panicum virgatum*). They reported that on average nitrate loss from corn fields was 2 - 3 times higher than from fields under switchgrass, but single studies within the review revealed that up to 9 times more nitrate was lost from fields under corn production. Nevertheless, in their study all fields were amended with different amounts of mineral nitrogen. In the present study nitrate losses from the plot under crop production were 10 - 17 times higher than losses from the plot under semi-natural vegetation. Nevertheless, it is difficult to compare surface runoff and associated nitrate losses and concentrations between different study sites as many influencing factors such as soil properties, rainfall characteristics, topography and management practices (Nangia et al., 2010) are not identical in the different studies.

At the plot under crop production, similar amounts of nitrate were transported via the interflow and via surface runoff during the wet rainy seasons 2017.1 and 2017.2. This is surprising, as many authors reported nitrate loss via interflow to be significantly higher than nitrate loss via surface runoff (Drury et al., 1993; Lal, 1976; Ng Kee Kwong et al., 2002). Woodley et al. (2018) on the other hand state that portioning of runoff and nitrate loss might end in favour of surface runoff, when the infiltration capacity of the topsoil is severely reduced due to, e.g., intense tillage operations. Yet, the results of the infiltration trials (see chapter 5.2.1) do not suggest that. As discussed above as well as in chapter 6.2.1 and 7.2, there are high uncertainties related to the quantification of interflow and related nitrate losses. Most importantly, peak volumes of interflow and associated nitrate losses could not be captured by the two-

day measurement interval. In addition, transit times of infiltrating water through the saprolite are unknown, and thus denitrification might have taken place. Therefore, nitrate loss via the interflow is very likely to be underestimated in this study, which limits the validity of a comparison of nitrate losses in the different runoff components. Nevertheless, significantly less nitrate was transported down the slope via surface runoff during the La Niña period 2016/2017. This can be related to few and inefficient rainfall events (total rainfall of 214 mm compared to 390 mm in 2017.1) during that season as well as to the strong delayed component of interflow, which still carried the signal of the precedent rainy season. This further indicates that a short-term comparison of the nitrate transported by the two runoff components is difficult and that long-term means need to be considered in order to come up with reliable conclusions. A further difficulty is related to that fact, that some share of the surface runoff most likely infiltrated at the slope toe, as discussed earlier. Therefore, a clear separation of the nitrate transported by the two runoff components is not possible. At the plot under semi-natural vegetation, nitrate loss via interflow was significantly higher than the nitrate transported by the surface runoff except for season 2017.2. This could be explained by the higher infiltration capacity at this land use type. Nevertheless, as explained above, the subsurface catchment of the trenches at the slope toe was larger than the above ground parcels where the different land use types were established. This further complicates the comparison of nitrate contents in the two runoff components.

Some uncertainty also remains regarding the quantification of the nitrate loss via surface runoff. This is mostly related to the well-known problems associated with runoff plots (see chapter 6.3) and thus, imprecise quantification of surface runoff amounts. In addition, nitrate concentrations might have been impacted, as measurements did not always take place immediately after the rainfall events. The same applies to the correlation of nitrate in the surface runoff and in the soil solution, as for some measurements nitrate concentrations in the soil solution were not measured on the same day as the surface runoff event occurred.

In conclusion, nitrate loss via surface runoff is mainly driven by transport factors, i.e., rainfall characteristics and seems to be of similar importance for nutrient delivery to the wetland as the nitrate transport via interflow on slopes under crop production.

7.4 Nitrate dynamics at the wetland fringe

This section presents the findings on nitrate dynamics at the wetland fringe, and relates them to water and nutrient inputs from the slopes via surface runoff and interflow.

Significantly less cumulative bio-available nitrate was recovered by the ion-exchange resins at the wetland fringe downslope of the plots under bare fallow and crop production than at the upland positions. In addition, the nitrate content in the soil solution at the wetland fringe was significantly lower (at $p=0.05$) than at the upslope positions during the entire experiment, and no seasonal dynamics were detected. The mean nitrate content at the measuring point downslope of the plot under bare fallow amounted to 0.31 kg NO_3-N/ha, while a mean nitrate content of 0.34 kg NO_3-N/ha and 0.23 kg NO_3-N/ha was determined at the two measurements points downslope of the plot under crop production. Due to land right issues, no measuring point could be installed downslope of the plot under semi-natural vegetation. The other three measuring points were installed in local farmer's fields and therefore different crops were cultivated at

the different measuring points (see chapter 4.2) so that no bare fallow treatment could be established at the wetland fringe. According to the Kruskal-Wallis test, the nitrate content at the three measuring points at the wetland fringe was significantly different at p= 0.05.

At the measuring points downslope of the plot under crop production (W0 and W1), the nitrate content in the soil solution showed very little fluctuation until season 2017.2, at values of about 0.2 kg NO_3-N/ha. Starting from the second dry season 2017, higher nitrate contents were detected in the upper and lower topsoil alike. At point W0, values reached up to 0.86 kg NO_3-N/ha in the second rainy season 2017, while at point W1 values reached 1.53 kg NO_3-N/ha on November 7th 2017. In general, dynamics in the upper and lower topsoil were very similar at both measuring points but at point W1 the peak nitrate contents were higher in the lower topsoil. The high nitrate contents in season 2017.2 often corresponded with high nitrate input from the interflow. The same was true for an intermediate peak in April 2017, when a nitrate content of 0.73 kg NO_3-N/ha and 0.89 kg NO_3-N/ha was measured in the lower topsoil at point W0 and point W1 respectively. Overall, the correlation of nitrate input per day via interflow and the nitrate content at the wetland fringe was not significant and Pearson's and Spearman's correlation coefficients were below 0.3, except for the lower topsoil of point W1 where a weak correlation of rho= 0.3 could be detected. As described in chapter 6.1.1, soil moisture conditions in the lower topsoil were close to saturation throughout the entire measurement period at both measuring points. At point W0, this applied to the upper topsoil as well, while at the same depth at point W1, intense drying and wetting took place, with moisture values reaching from 40 - 100 %sat.. At point W1, a moderate positive correlation of rho= 0.6 between soil moisture and nitrate content in the soil solution was found for both measurement depths, which goes back to a high soil moisture and simultaneous a high nitrate content in season 2017.2. Analysing the time series, it becomes clear that there neither was an increase in the nitrate content during the dry season nor during the dry-to-wet transition periods, even when soil moisture conditions were favourable for nitrification (see Figure 72). At both measuring points, nitrate input via surface runoff was correlated with the nitrate content in the soil solution (rho= 0.7 at point W0 and rho= 0.35 at point W1), even if the graphical analysis would not suggest such a strong correlation at point W0 (see Figure 73).

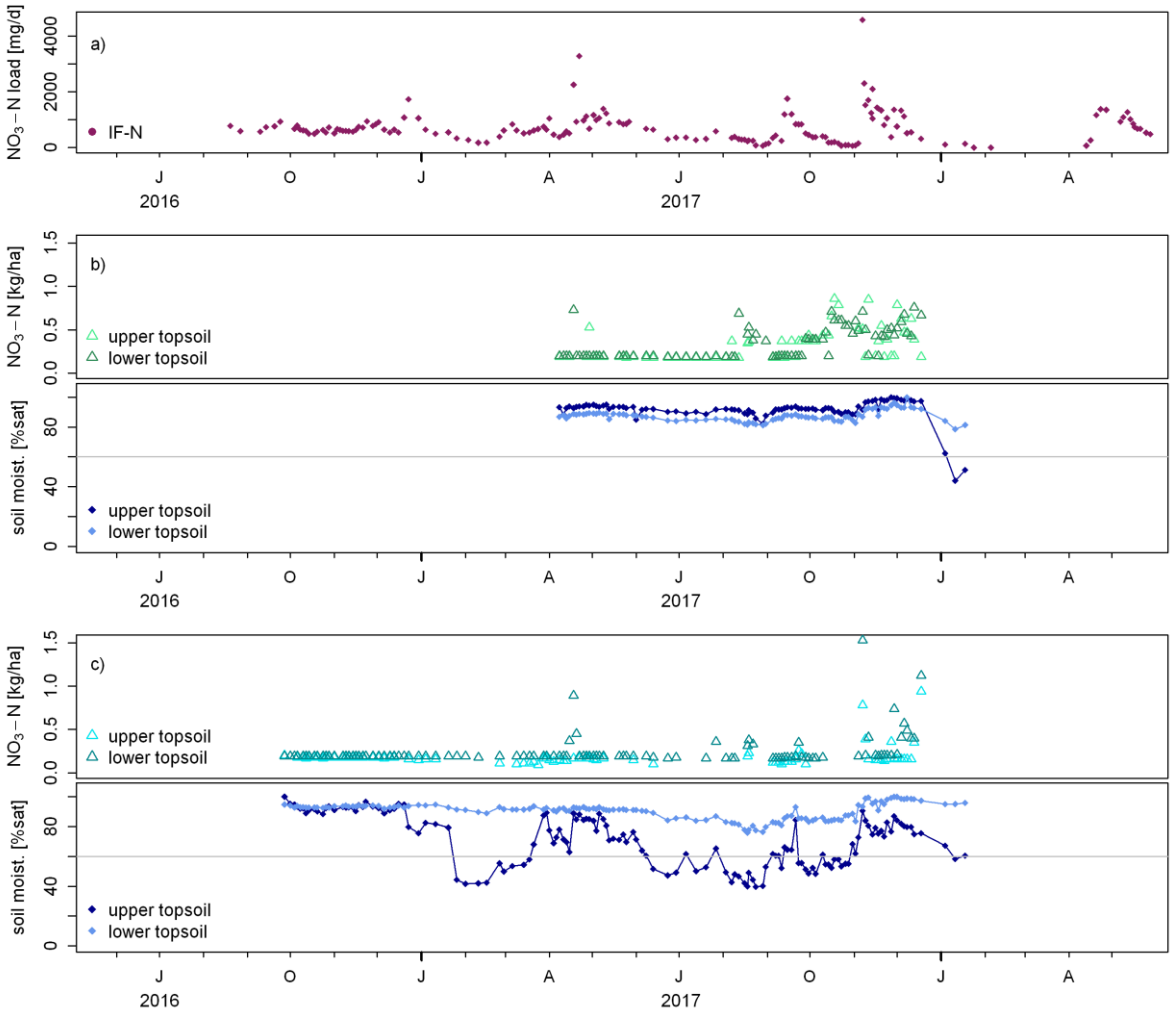

Figure 72 *Nitrate input via interflow [mg NO_3-N/d] (a), nitrate content in the soil solution [kg NO_3-N/ha] and soil moisture at the wetland fringe measured at point W0 (b) and at point W1 (c).*

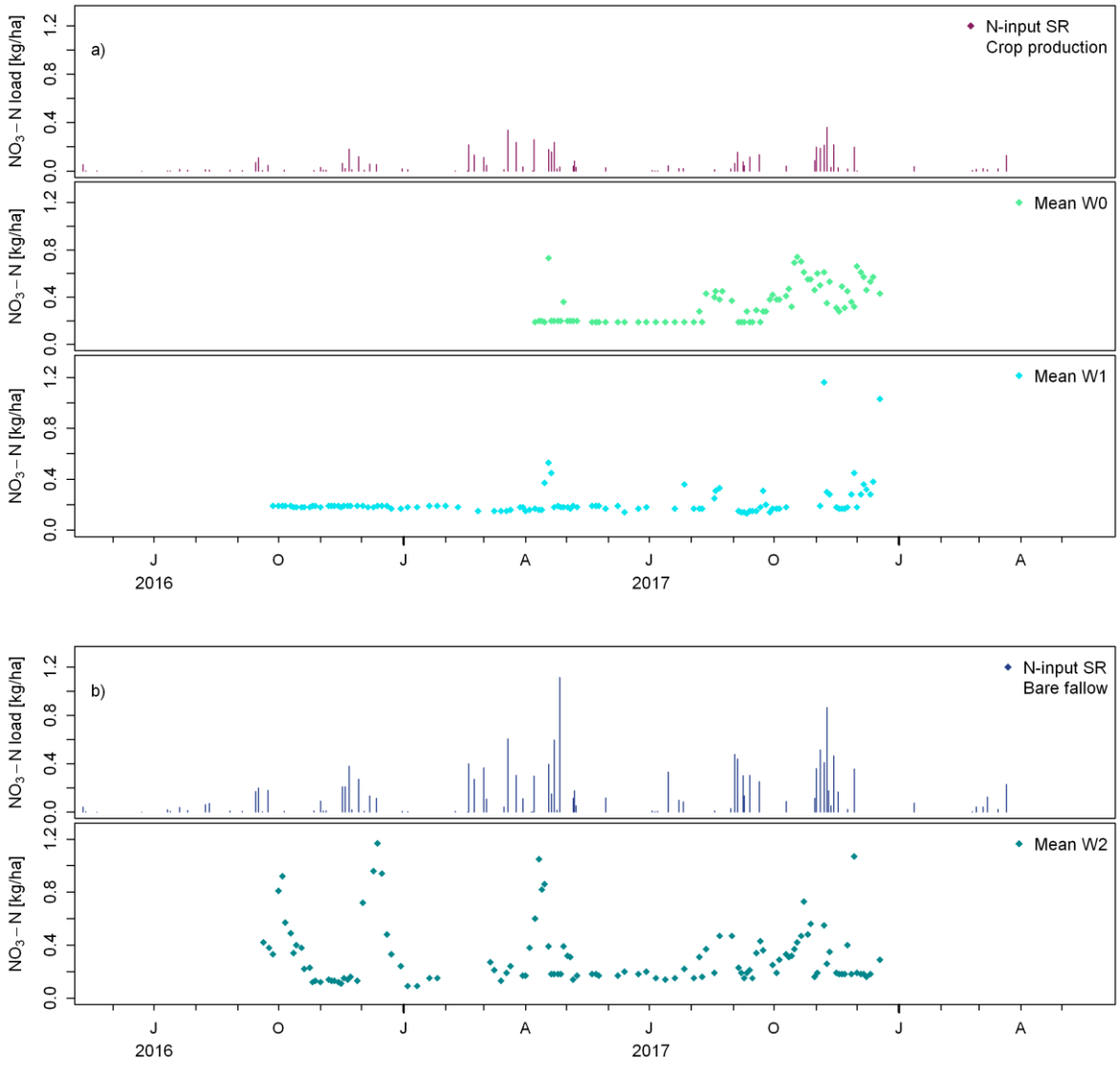

Figure 73 *Nitrate input via surface runoff [kg NO_3-N /ha] related to mean nitrate content in the soil solution [kg NO_3-N/ha] in the topsoil. Panel a) shows the data related to the plot under crop production and the adjacent measuring points at the wetland fringe while panel b) refers to the plot under bare fallow and the adjacent measuring point at the wetland fringe.*

At the measuring point downslope of the plot under bare fallow, the nitrate content was about 0.2 kg NO_3-N/ha most of the time. Like at the other two measuring points, the nitrate content in season 2017.2 was higher than in the other seasons. At the same time, the dynamics over the entire measurement period were more pronounced than at the measuring points adjacent to the plot under crop production. At the beginning and at the end of season 2016.2, the nitrate content increased over several days to 1.31 and 1.46 kg NO_3-N/ha in the upper and lower topsoil respectively before it decreased again over several days to the usual low values. The same pattern can be found in April 2017, when the nitrate content increased to 0.93 kg NO_3-N/ha in the upper and to 1.18 kg NO_3-N/ha in the lower topsoil. Over the entire period, the dynamics were more pronounced in the lower than in the upper topsoil. The second peak in season 2016.2 as well as the peak in April 2017 coincided with high nitrate concentrations in the interflow measured at the plot under bare fallow. For season 2017.2, no interflow data were available. Nevertheless, graphical analysis of the entire time series does not suggest a parallel development of the nitrate concentration in the interflow and the nitrate content in the soil solution at the wetland fringe. Unfortunately, interflow at this trench could not be quantified and therefore, no data regarding nitrate input to the wetland are available. As described in chapter 6.1.1, soil moisture at this measuring point was more variable than at the other two measuring points at the wetland fringe and varied between 25 % and 90 % saturation in the upper topsoil. In the lower topsoil, the fluctuation was less pronounced but still more distinct than at points W0 and W1 and varied between 65 % and 100 % saturation. For both depths, a weak positive correlation of rho= 0.4 was found. Nevertheless, as described for the other two points, the data neither show the effect of mineralization during drier periods nor could any distinct pattern be detected (see Figure 74). A correlation of rho= 0.47 was detected regarding the nitrate content in the soil solution at the wetland fringe and nitrate input via surface runoff from the plot under bare fallow. When comparing the time series, it becomes obvious, though, that the peak nitrate contents do not coincide with the highest nitrate inputs via surface runoff, except for November 29th 2017. High nitrate contents in the soil solution can neither always be found after high inputs via surface runoff nor do they follow any season related logic, so here as well a distinct pattern could not be detected (see Figure 73).

No correlation could be detected between the nitrate content in the soil solution at the wetland fringe and the nitrate content in the soil solution at the corresponding upslope areas. Furthermore, none of the measuring points showed a correlation of the nitrate concentration in the soil solution and rainfall amount or intensity (R^2 and rho <0.3). Hence, dilution effects via direct rainfall inputs seem to be of minor importance. At the same time, no correlation between the nitrate content in the soil solution at the wetland fringe and rainfall amount as well as rainfall intensity could be detected (R^2 and rho < 0.2). This weak correlation suggests that nitrate input via the quick component of interflow is no driving factor of the nitrate content in the soil solution at the wetland fringe, as a pronounced quick interflow component is expected to be related to high rainfall amounts and intensities.

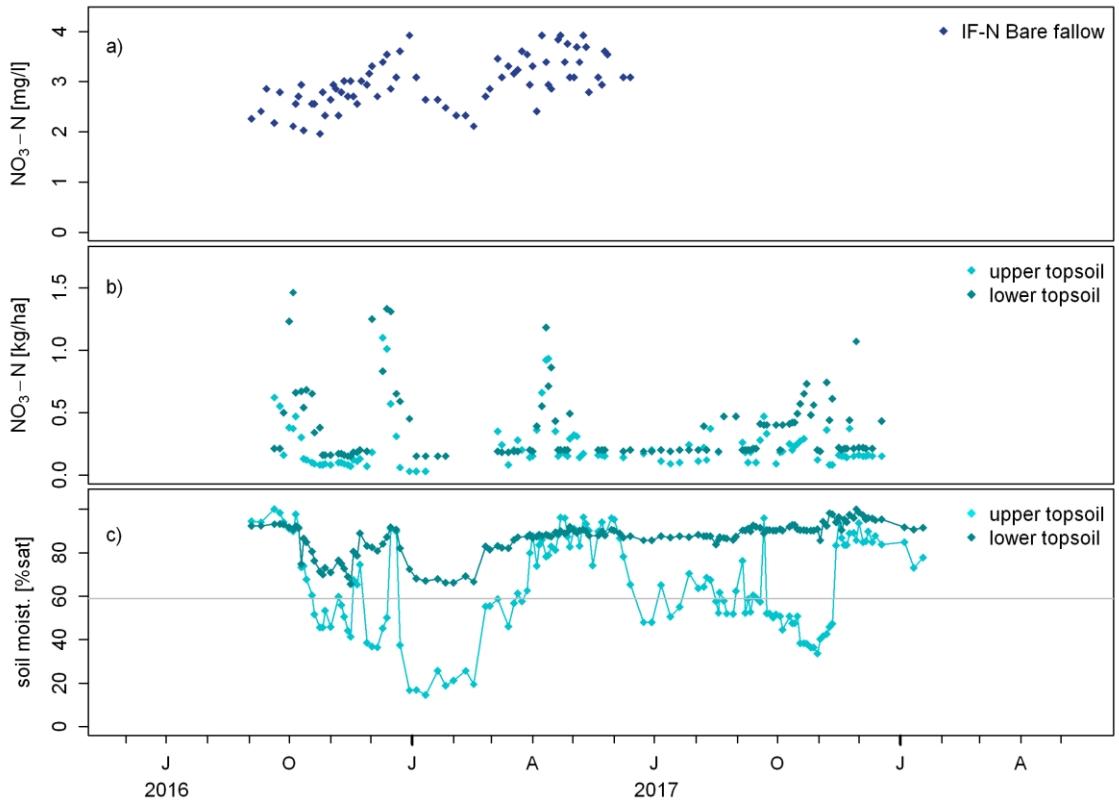

Figure 74 *Nitrate concentration [mg NO_3-N/l] in the interflow below the plot under bare fallow (a), nitrate content [kg NO_3-N/ha] in the soil solution at the wetland fringe in the upper and lower topsoil (b) and soil moisture [%sat] at 10 cm and 20 cm depth (c).*

Generally, the low nitrate content in the soil solution at the wetland fringe as compared to the upslope areas was a result of the hydrological conditions at this toposequence position. Frequent saturation and thus, anaerobic conditions in the soil body, lead to nitrate losses via denitrification and inhibit the mineralization of organic material to NO_3 (Reddy and DeLaune, 2008). The latter would be reflected in higher organic carbon contents in the wetland than in the upland soils. In this study though, higher carbon contents were only present at point W2 (see chapter 5.2.2) indicating that slower decomposition rates were not the main reason behind the low nitrate values in the soil solution at the wetland fringe. In addition to its impact on nitrogen transformation processes, the high water availability at the wetland fringe caused leaching losses to deeper soil layers as well as the translocation of nitrate towards the central stream and towards the outlet of the wetland via surface runoff and subsurface flow. Moreover, free nitrate is quickly taken up by the wetland vegetation and cultivated crops, as nitrate is one of the most limiting factors for plant growth in wetland areas (Mitsch and Gosselink, 2015). All of these processes probably contributed to the low nitrate content in the soil solution at the wetland fringe, despite the nitrate inputs via surface runoff and interflow. Nevertheless, these inputs did influence the dynamics of the nitrate content in the soil solution at the wetland fringe, as was shown by the positive correlation of nitrate in the soil solution and nitrate input to the wetland by the interflow and by surface runoff. Furthermore, a higher nitrate content in the soil solution at the wetland fringe was mostly found in periods of high soil moisture and not during moisture conditions which would favour the in-situ mineralization of

nitrate. This underlines that nitrate inputs from inflowing water and not in-situ mineralization processes dominated the nitrate dynamics at the wetland fringe. Nevertheless, as described above, not all the peaks in the nitrate content in the soil solution could be explained by the present data on nitrate input from the slopes, and high inputs from the slopes did not always cause a positive response in the nitrate content in the soil solution. Therefore, water and nitrate fluxes from the upstream areas of the wetland probably also had a strong impact on the nutrient dynamics at the measuring points at the wetland fringe. As in the study conducted by Wagner (2019) in the same wetland two years earlier, no clear seasonal pattern could be detected. Thus, nitrate input from the upstream wetland areas was most likely impacted by fertilizer application and land management in the upper catchment as well as in the upstream areas of the wetland. Data on fertilizer input from this area would be needed to confirm this hypothesis. In addition, a close monitoring of the redox potential in the soil is needed, to investigate whether higher nitrate inputs during the dry-to-wet transition period were cancelled out by high denitrification rates during these times.

The antecedent analysis stressed that to explain the nitrate dynamics at the wetland fringe, activities in the entire catchment need to be considered and nutrient inputs from the slope need to be captured in a spatially comprehensive study design. Furthermore, nutrient fluxes within the wetland need to be analysed in future studies. Nevertheless, the significant difference between the three measuring points in the wetland, and especially between the two measuring points downslope of the plot under crop production, stresses that at the same time small scale spatial variability was extremely high. Therefore, in-situ processes related to mineralization, macropore structure and other factors impacting flow routing have to be considered as well. Due to the detection limit of the Nitracheck device, dynamics in nitrate concentrations below 5 ppm could not be analysed (see chapter 4.5.1). Using a device which allows to analyse nitrate concentrations below this threshold might give further insights into the nitrate dynamics at the wetland fringe. Additionally, continuous measurements of the nitrate load in the interflow would be needed to capture the quick interflow component and comprehensively quantify the nitrate input by the interflow to the wetland fringe. These measurements would further enable a more detailed correlation analysis of nitrate inputs via interflow and the nitrate dynamics at the wetland fringe.

As rice is the major staple crop cultivated in valley bottom wetlands in East Africa, a comparison of the nitrate input via the interflow and surface runoff from the slopes and the seasonal plant uptake can be used as a reference to assess the significance of nitrate inputs from the slope to the wetland for agricultural production. Mean seasonal total nitrogen uptake of rice plants from indigenous sources was reported to be 54 kg N/ha on 179 plots in South and South-East Asia (Cassman et al., 2002) and between 26 kg N/ha and 62 kg N/ha on 261 study sites in Western Africa (Haefele et al., 2003). In the Namulonge inland valley, Grotelüschen et al. (2021) found the seasonal nitrogen uptake of rice plants on unfertilized plots at the fringe position to be around 70 kg N/ha (as determined from dried and ground dry matter at physiological maturity). It is not known whether the nitrate input from the slopes was transported further into the wetland by lateral flow. Assuming that all nitrate delivered from the slopes is absorbed by the vegetation at the wetland fringe, the mean nitrate input via interflow from the slope was calculated as 17 kg NO_3-N /ha per season (see Table 13), when the slope was under crop production. Mean seasonal nitrate input from the slope under crop production via surface runoff was calculated as 12 kg NO_3-N /ha per season. Hence nutrient inputs to the wetland fringe would be about 30 kg NO_3-N/ha from cultivated slope

areas and would thus contribute almost half of the seasonal nutrient uptake of the rice plants. Even if a direct comparison is difficult due to the different methodological approaches of the studies, these inputs are comparable to those reported from studies in Western Africa. Asante et al. (2017), for example, found seasonal nitrate inputs of 32 kg NO_3-N/ha from slopes under crop production in an inland valley in Ghana, and Bognonkpe and Becker (2000) reported inputs of 47 kg NO_3-N/ha from slopes under bare fallow and of 39 kg NO_3-N/ha from slopes under crop production (*Cajanus cajan*) in an inland valley in Côte d'Ivoire. Nevertheless, there are many uncertainties related to the quantification of the nitrate input to the wetland in the present study, as has been explained in the previous chapters. It should further be considered that the surface runoff partly infiltrates at the slope toe and thus part of its nitrate load is accounted for twice in the previous calculations. Furthermore, part of the interflow is conducted to the aquifer in the valley sediments and thus not available for the plants in the wetland. For both aspects, the respective shares are not known, which limits the informative value of the numbers presented in this paragraph. Regardless of these reflections, the cumulative plant available nitrate as determined by the resin measurements at the wetland fringe, was very low and significantly lower than in the upland. Considering that the ion exchange resins are regarded to be as strong a competitor for nutrients as plant roots are, this hints to the fact that a major part of the nitrate was lost via denitrification even at the edge of the wetland fringe. Therefore, a strong contribution of nitrate inputs from the slopes to the nutrition of plants at the wetland fringe seems unlikely. Nitrate demanding crops cultivated at the slope toe on the other hand, could benefit from the nitrate input via interflow, if their roots grew deep enough to stimulate nutrient fluxes from the interflow in the sandy loam layer towards the plant. Further research is needed to explore the effect of nitrate inputs from the slopes on plant development and plant nutrient uptake at the wetland fringe as well as at the slope toe.

8 Conclusions and outlook

A sound scientific knowledge of the hydrological linkages between the upland and the wetland system enables informed land management decisions that aim to combine environmental protection and sustainable agricultural production in the region. The study at hand successfully contributes to achieving this aim by characterising water and nitrate fluxes that connect the valley slopes to the valley bottom wetland in a catchment in Central Uganda. In the course of the study, interflow processes and the transition from upland to wetland geology were analysed using a combination of geo-electrical sounding, runoff trenches and soil moisture monitoring, while surface runoff was studied on runoff plots (chapters 5 and 6). In addition, nitrate dynamics in the soil solution on the slope and at the wetland fringe were monitored under three different land use types, and nitrate fluxes from the slopes to the wetland were measured in different runoff components (chapter 7). Chapter 8.1 presents conclusions regarding interflow pathways along the slope, while chapter 8.2 summarizes the impacts of different land use types and rainfall characteristics on the slope hydrology. Chapter 8.3 presents the conclusions regarding nitrate dynamics and transport along the slope in relation to environmental conditions and land use type. The relevance of water and nitrate inputs from the slope for water and nitrate dynamics at the wetland fringe, as well as the implications for agricultural production at this toposequence position, are summarized in chapter 8.4.

The present study provides valuable insights into interflow and surface runoff processes and associated nutrient transport to the wetland fringe along a slope which is characterised by a saprolitic geology and a low-input farming system. Nevertheless, the methodological approach entails some limitations which were discussed at the end of each subchapter in the thesis. Chapter 8.5 finally summarizes the contribution of this study to the field of hillslope hydrology, discusses possibilities for spatial extrapolation and defines future research needs as well as recommendations for agricultural production in valley bottom wetlands.

8.1 Interflow processes along the slope and connectivity to the wetland aquifers (Research question 1, objectives i and ii)

The geo-electrical measurements showed that the saprolite at the slopes in the study region is over 30 m thick. The division of the saprolite into an upper and a lower part as shown at the point scale by Burghof (2017) persists up to the hilltop. The upper saprolite increases in thickness towards the hilltop and shows higher electrical resistivities than the lower saprolite which hints to a high skeletal fraction (including rocks with a diameter of up to 1 - 2 m found during field work) and high shares of oxidized metallic minerals. The electrical resistivity of the lower saprolite is too high to indicate saturated conditions, suggesting that no groundwater body is situated in this stratigraphy. Due to the phenomenon of suppression, the presence and course of smaller perched aquifers could not be explored by resistivity sounding, but deep drilling logs proved their existence. The geo-electrical measurements also revealed a small-scale heterogeneity of resistivities in the saprolite suggesting the presence of highly weathered regions favouring the infiltration of rainwater into the saprolite. The upper saprolite is further characterised by an undulating surface structure both parallel and perpendicular to the slope, which was confirmed by shallow drilling logs. In combination with a higher field-saturated conductivity of the upper saprolite as

compared to the overlying B horizon, the prevailing subsurface topography leads to the so-called “fill-and-drain” mechanism. Infiltrating rain water which drains to the soil-saprolite interface via macropores and via matrix flow, is conducted to the depressions in the upper saprolite due to capillary diversion (Heilig et al., 2003). There it is collected until saturated conditions are reached, a complete breakthrough (Walter et al., 2000) occurs and water enters the upper saprolite. As the soil texture of the upper saprolite still has a clay content of about 20 %, higher infiltration rates are most likely the result of macropores. Because of this fill-and-drain mechanism no interflow was observed to occur at the soil-saprolite interface along the slope. Within the saprolite, both, a delayed and a fast interflow component develop. The delayed component is probably caused by matrix flow in the aforementioned smaller perched aquifers which get connected over the span of the rainy season. The fast component on the other hand might go back to a network of macropores or to preferential flow paths which get connected via nodes (Nieber and Sidle, 2010; Noguchi et al., 1999) under wet conditions and are the result of the high heterogeneity in the degree of weathering of the saprolitic material. The electrical resistivities measured at the slope toe do not suggest a connection of the deep ground water and the interflow. This is further supported by shallow drilling logs showing interflow water to impound on a horizontally layered muscovite so that it is found in the uppermost saprolite and a sandy loam layer in the overlying soil body at the slope toe. Infiltrating surface runoff on the other hand, is found to partially contribute to the interflow at the slope toe.

The geo-electrical measurements confirmed the hypothesis of Burghof (2017) that the aquifer in the valley sediments is separated from the shallow aquifer in the wetland soils. In addition, the electrical resistivities measured at the slope toe did not suggest the presence of a pronounced paleo-dambo as described in McFarlane (1992), which suggests a contribution of interflow from the slopes to the wetland hydrology. This contribution was confirmed by the stratigraphy observed in the shallow drilling logs. These revealed that the water bearing sandy loam layer encountered at the slope toe is most likely of colluvial origin and continues into the wetland on top of the clay layer separating the aquifer in the valley sediments from the shallow aquifer in the wetland soils. Interflow water from the slopes is hence partially conducted to the shallow aquifer in the wetland soils via the sandy loam layer as well as to the aquifer in the valley sediments via the upper saprolite.

In a nutshell: The study revealed that the presence of interflow at the soil-saprolite interface depends on the physical properties of the uppermost saprolite and its subsurface topography. In deeply weathered saprolite over crystalline rocks, interflow processes can occur even within the saprolite and comprise a quick as well as a delayed component. In case of long transit times within the saprolite, the delayed component of interflow can continue to deliver water to the wetland even during dry spells. A thorough investigation of the geology at the transition from upland to wetland geology is essential in order to detect whether and to what extent interflow from the slopes recharges the aquifer(s) in the wetland.

8.2 Impact of land use type and rainfall characteristics on the slope hydrology (Research question 2, objective iii)

Land use type and rainfall characteristics strongly influence soil moisture, surface runoff and interflow volumes on the slope. The dense plant cover at the plot under semi-natural vegetation prevents siltation of the soil surface and the generation of surface runoff and hence increases the infiltration of water,

leading to higher soil moisture contents during the rainy season compared to the plots under crop production and bare fallow. On the other hand, high plant transpiration most likely outweighs the increased water supply from infiltration as smaller interflow volumes were measured at the slope toe at the plot under semi-natural vegetation than at the plot under crop production. This is further reflected in the fast and intense decrease in soil moisture and interflow volumes at the beginning of the dry season. In the absence of a vegetation cover on the other hand, heavy siltation and missing interception of rain water cause higher runoff coefficients and surface runoff volumes.

Surface runoff volumes as well as runoff coefficients at the plot under bare fallow and crop production are directly driven by rainfall amount and intensity. Rainfall distribution over the rainy season and hence soil moisture, on the other hand, do not significantly influence surface runoff volumes and runoff coefficients. Continuous soil moisture measurements would be needed to determine the prevailing runoff type, but slope position and the lack of an impeding layer close to the soil surface would suggest that infiltration excess runoff is the dominant runoff process.

Volumes of the delayed interflow component as well as the persistence of interflow in the dry season strongly depend on the amount of water conducted to the saprolite during a rainfall event and over the entire season. Hence, the total rainfall amount during the rainy season as well as the distribution of rainfall over the season have the strongest impact on interflow generation. Persistent high volumes of interflow are related to longer periods, i.e., several weeks, of reoccurring rainfall events, and generally interflow volumes increase towards the end of the rainy season. However, little rainfall, as well as an uneven distribution of rainfall over the rainy season, result in less interflow and shorter persistence of flow in the dry season. In addition, interflow volumes increase more slowly at the beginning of the rainy season when the rainfall intensity of the first rainfall events is high and causes a pronounced surface runoff component. Nevertheless, interflow volumes also reflect the signal of the rainfall properties encountered during the previous rainy season due to the long transit times of water in the saprolite. Due to the lack of continuous or event based measurements, the impact of rainfall characteristics on the quick interflow component could not be determined.

In a nutshell: The study revealed that the land use type along the slopes adjacent to the wetland impacts water delivery to the wetland, as the high water demand of native vegetation can reduce the amount of interflow and surface runoff. Extended durations of wet periods and the repeated occurrence of moderately-intense rainfall events increase flow volumes of the delayed interflow component in a deep saprolite.

8.3 Nitrate dynamics and translocation along the slope as influenced by land use type and rainfall characteristics (Research question 2, objectives iv and v)

Both, land use type and rainfall characteristics strongly impact the nitrate translocation along the slope, as they are the driving factors of the soil moisture conditions and the activation of vertical and lateral flow paths. The land use type further determines the nutrient uptake from the soil solution and hence the amount of nitrate in the soil solution susceptible for leaching. Generally, intra-seasonal dynamics of the nitrate content in the soil solution at the study site follow the typical pattern of the Birch effect. Hence,

the rewetting of the soil at the beginning of the rainy season results in high mineralization rates before nitrate is lost via leaching and denitrification. Nevertheless, rainfall distribution and intensity at the beginning of and during the rainy season cause a distinctive pattern during each rainy season. Rainfall events of high intensities result in more surface runoff and less infiltration of water into the soil matrix. At the beginning of the rainy season, this causes a delayed increase in soil moisture and hence in the mineralization of nitrate, while during the rainy season, higher levels of surface runoff and macropore flow reduce leaching losses from the soil matrix. Drying and rewetting of the soil during the rainy season, only increase the nitrate content in the soil solution, if favourable moisture conditions prevail over several days.

It was shown that nitrate is translocated vertically from the upper to the lower top soil and even to water pathways in the saprolite. Leaching intensity is driven by the prevailing soil moisture conditions as well as the rainfall amount and intensity. The water content of the saprolite, on the other hand, determines how fast the nitrate is translocated to the slope toe via interflow processes. Under wet conditions, more preferential flow paths in the saprolite are activated and hence more nitrate is transferred to the wetland via the quick component of interflow. At the same time, higher water contents in the saprolite enhance the mixing of subsurface waters and hence the dilution and subsurface distribution of the nitrate recently leached from the soil body.

A primary and secondary influence of the land use type on the amount of nitrate which is translocated to the slope toe was demonstrated. As a primary effect, a dense and permanent vegetation cover significantly reduces the nitrate content in the soil solution by uptake and immobilization in the biomass, thus restricting nitrate losses by leaching. The secondary effect is related to the influence of the land use type on soil moisture as well as surface runoff and interflow generation. Optimum conditions for the mineralization as well as the denitrification of nitrate are reached at different points in time and over different time periods under the three different land use types. The same applies to the water availability for leaching processes. Therefore, the temporal dynamics as well as the intensity of nitrate mineralization and loss also vary between the different land use types during each season.

Nitrate is further translocated along the slope by surface runoff. Thereby, nitrate losses are mainly driven by transport factors, i.e., rainfall amount and intensity. Surprisingly the data revealed, that the amount of nitrate which is translocated by the surface runoff at the plot under crop production is similar to the amount delivered to the slope toe by the delayed interflow component.

In a nutshell: The study highlighted that source and transport factors determine the nitrate translocation along the slopes. Both factors are strongly influenced by rainfall characteristics. For one, rainfall characteristics drive the nitrate formation and its accumulation in the soil solution and govern nitrate leaching from the soil. At the same time, rainfall characteristics determine the nitrate supply to the wetland fringe as they control the activation of flow paths within the saprolite.

8.4 Relevance of water and nitrate inputs from the slope for agricultural production at the wetland fringe (Research question 3, objective vi)

Electrical resistivity sounding, soil sampling and field observations showed that interflow and surface runoff contribute to the water availability at the wetland fringe. Analysis of water inputs from the slope and the soil moisture dynamics at the wetland fringe revealed a positive correlation regarding water inputs via the interflow, while water inputs via the surface runoff do not have a significant impact. Nevertheless, water fluxes from the upper catchment and from the deeper aquifers also contribute to the soil moisture content at the wetland fringe, so that even during periods of negligible water inputs by interflow and surface runoff, soil moisture conditions at the wetland fringe are still favourable for agricultural production. Thus, crop production at the wetland fringe in the lower catchment does not mainly depend on water inputs from the slopes. Instead, they are but one driver of the favourable moisture conditions during dry periods but also of the poor soil aeriation and anaerobic conditions during the rainy season.

The nitrate content in the soil solution at the wetland fringe is constantly very low showing no distinct seasonal dynamics. Hence, a nitrate flush from the slopes during the dry-to-wet transitions period, as suggested by the appearance of the Birch effect in the upland, was not detected and nitrate seems to be lost quickly via denitrification after entering the wetland. While a positive correlation between nitrate inputs via the surface runoff and the dynamics of the nitrate content in the soil solution at the wetland fringe was found, the correlation to nitrate inputs via the interflow was very weak throughout the experiment. As nitrate dynamics are not dominated by in-situ mineralisation, additional nitrate fluxes from the upstream areas of the wetland are expected to contribute to the nutrient availability at the wetland fringe in the lower catchment.

Despite the diverging hillslope hydrology, nutrient transport to the slope toe was comparable to that reported for similar wetlands in Western Africa. Nevertheless, some unknowns are related to the calculation of the nitrate input to the wetland in the present study and further research is necessary to quantify the nitrate input from the slopes precisely.

In a nutshell: The study proved that also in a deep weathering profile, nitrate is transported to the slope toe via interflow. It was further shown, that activities in the upper catchment might impact agricultural production in the lower catchment as inflowing water from upstream areas is one driver of water and nutrient availability at this position.

8.5 Relevance of the study and future research needs

Contribution to hillslope hydrology

This study extended the existing knowledge on the hillslope hydrology of valley bottom wetlands by focussing on a hillslope which is characterized by interflow processes within a deep saprolite. It showed that depending on the local geology at the transition from the upland to the valley sediments, interflow in the deeper saprolite can contribute to the shallow aquifer in the wetland soils as well as in the valley sediments. The case study of the Namulonge wetland revealed that interflow processes in the saprolite and their contribution to aquifers in the valley bottom wetland are the result of a rather complex

combination of the subsurface topography, heterogeneous weathering of crystalline rocks and a certain stratigraphy along the slope and at the slope toe. This stresses the importance of a sound geological exploration of the slopes adjacent to valley bottom wetlands when investigating wetland-catchment interactions and when transferring the results to different sites. To this end, the methodology applied in this study, including geo-electrical sounding, shallow drilling logs and single-ring infiltrometer measurements was found to be a cost-effective and quick option to capture important attributes of the local geology and extend the findings of Burghof (2017) on regional and local aquifers in the study area. As most parts of the land surface in East Africa are covered by a thick saprolite (Chilton and Foster, 1995b), the Namulonge wetland can be considered a representative site for valley bottom wetlands in an undulating topography. Hence, processes related to hillslope hydrology and water recharge of the wetland aquifers are generally indicative for other wetlands in the region as well. Nevertheless, as discussed before, hydrogeological properties of the saprolite are finally responsible for interflow processes and the associated translocation of nutrients along the slopes. Therefore, characteristic processes as well as water quantities might vary strongly between different sites and cannot be assumed without previous geological exploration of the site in question.

The methodological approach followed in this study allowed to establish well-founded hypotheses on interflow processes within the saprolite. Nevertheless, further research would be needed to confirm these hypotheses and describe the interflow processes in more detail. Firstly, continuous measurements of the interflow and associated nitrate concentrations are needed to capture the quick component of interflow and hence comprehensively quantify water and nutrient inputs to the wetland. Such a setup would further allow to analyse the influence of rainfall characteristics and moisture conditions on the processes related to the quick interflow component. The same applies to the soil moisture measurements along the slope. In order to prove the fill-and-drain mechanism, continuous measurements of the matrix potential down to the depth of the saprolite would be needed to show the formation of a saturated layer and the consequent break-through and drainage of water to the saprolite during a rainstorm. Secondly, some uncertainties are related to the water pathways within the saprolite. Firstly, the perched aquifers in the saprolite could not be identified by the geo-electrical measurements. A possible approach could be to combine these measurements with GPR (ground penetrating radar) or EM (electromagnetic geophysics) measurements this can be an option to overcome suppression problems during groundwater exploration in highly weathered material (Blume and Meerveld, 2015; Muiuane, 1999). Regarding an enhanced understanding of flow paths and water movement within the saprolite, imaging of water and solute fluxes based on time-lapse measurements could also be an interesting approach. In addition, Guo et al. (2014) developed a method to implement GPR time-lapse measurements for the visualization of preferential flow patterns at a centimetre scale along a hill slope in Pennsylvania, USA. This could be an interesting approach to follow in order to characterise preferential flow pathways within the saprolite and the connection to the sandy loam layer at the slope toe. Nevertheless, the depth of the weathering body as well as the texture of the upper saprolite would be an obstacle to overcome. Besides an extended approach to the geophysical measurements, (multi-)tracer and irrigation trials could give further insights into the complexity of interflow processes and shed light on the magnitude of internal storages, flow generation thresholds and large-scale hydraulic characteristics (Jackson et al. 2016).

Recommendations for agricultural production

Focussing on the Namulonge wetland as a case study, it was shown that in a catchment where low-input farming prevails and which is characterised by interflow processes within the saprolite, nutrients are translocated to the slope toe but do most likely not contribute significantly to agricultural production at the wetland fringe due to quick losses under anaerobic conditions. Therefore, on the one hand, agricultural interventions should focus on the toposequence position of the slope toe, where the cultivation of nitrate demanding crops could prevent the loss of nitrogen from the soil-plant system. Nevertheless, the selection of crops should consider a sufficient rooting depth for plants to be able to absorb the nutrients in the interflow from the subsoil (i.e., the sandy loam layer where the interflow is found), as there is no accumulation of nitrate in the topsoil. On the other hand, agricultural management practices should aim at minimizing nitrate losses via leaching from the fields in the upland. This could include the cultivation of perennial crops like cassava (*Manihot esculenta*) as the timing of high nitrate demands of seasonal crops might not match with the highest nitrate availability after the onset of the rains. In addition, a shift to agroforestry should be considered as an alternative land management strategy along the slopes. For one, the cultivation of deep rooting plants which are able to recover the nitrate which was leached from the soil and consequently collected in the surface depressions of the upper saprolite would help to keep the nitrate in the soil-plant system. At the same time, the continuous ground cover and the interruption of surface runoff paths by tree stems would increase the infiltration of rainwater, reduce water and nitrate losses via surface runoff and hence increase the water use efficiency on the slopes. This is supported by the findings of this study related to the effect of semi-natural vegetation on water and nutrient fluxes along the slope. Here it was shown, that a dense vegetation cover increases the soil moisture during the rainy season but reduces water and nutrient losses from the slope via the interflow and surface runoff as well as the presence of free nitrate in the soil solution. Nevertheless, the implementation of agro-forestry systems could be hindered by the current situation of land tenure, as most of the small-scale farmers in the catchment do not own the land they cultivate and might therefore not be able or motivated to engage in long-term land management practices (van Soest, 2018).

Future research should include the impact of fertilizer application on nitrate fluxes from the slopes to the wetland as superficial fertilizer application might increase nitrate losses via surface runoff, while the incorporation of nitrate into the soil could increase the translocation of nitrate via the interflow.

Final remarks

This study stressed the importance of a thorough understanding of the local hillslope hydrology to include catchment-wetland interactions in wise land management and agricultural decision making, which is at the base of enhancing food security in the region. Nevertheless, the study also revealed the complexity of subsurface runoff processes in saprolitic environments. Therefore, further research on interflow processes is needed at the slope scale, to fully understand water pathways within the saprolite. Such knowledge could help to improve existing models of the catchment hydrology in valley bottom wetlands and thus yield the basis for scenario analysis regarding climate change and land use change impacts on water and nutrient translocation from the slopes to the wetland. Nevertheless, the experiments should further be repeated in other valley bottom wetlands in the region which are characterized by a similar

geology. Such an extension would show whether the results are transferable to valley bottom wetlands in East Africa in general and would allow to explore common attributes which are indicative of the prevailing interflow processes.

9 References

Acres, B.D., Rains, A.B., King, A.B., Lawton, R.M., Mitchell, A.J.B., Rackman, L.J., 1985. African dambos: their distribution, characteristics and use. Zeitschrift für Geomorphologie Supplementband 52, 63–86.

Ali, G.A., Roy, A.G., Turmel, M.-C., Courchesne, F., 2010. Source-to-stream connectivity assessment through end-member mixing analysis. Journal of Hydrology 392, 119-135. doi:10.1016/j.jhydrol.2010.07.049

Aitkenhead, J.A., McDowell, W.H., 2000. Soil C:N ratio as a predictor of annual riverine DOC flux at local and global scales. Global Biogeochemical Cycles 14, 127–138. https://doi.org/10.1029/1999GB900083

Amler, E., Schmidt, M., Menz, G., 2015. Definitions and Mapping of East African Wetlands: A Review. Remote Sensing 7, 5256–5282. https://doi.org/10.3390/rs70505256

Angermann, L., Jackisch, C., Allroggen, N., Sprenger, M., Zehe, E., Tronicke, J., Weiler, M., Blume, T., 2017. Form and function in hillslope hydrology: characterization of subsurface flow based on response observations. Hydrology and Earth System Sciences 21, 3727–3748. https://doi.org/10.5194/hess-21-3727-2017

Anudu, G.K., Essien, B.I., Obrike, S.E., 2014. Hydrogeophysical investigation and estimation of groundwater potentials of the Lower Palaeozoic to Precambrian crystalline basement rocks in Keffi area, north-central Nigeria, using resistivity methods. Arab J Geosci 7, 311–322. https://doi.org/10.1007/s12517-012-0789-x

Appelo, C.A.J., Postma, D., 2005. Geochemistry, groundwater and pollution, 2nd ed. CRC Press, Boca Raton, Florida.

Archie, G.E., 1942. The electrical resistivity log as an aid in determining some reservoir characteristics. Transactions of the AIME 146, 54–62. https://doi.org/10.2118/942054-G

Asante, M., Becker, M., Angulo, C., Fosu, M., Dogbe, W., 2017. Seasonal nitrogen dynamics in lowland rice cropping systems in inland valleys of northern Ghana. Journal of Plant Nutrition and Soil Science 180, 87–95. https://doi.org/10.1002/jpln.201600209

Aulenbach, B.T., Hooper, R.P., Meerveld, H.J. (Ilja) van, Burns, D.A., Freer, J.E., Shanley, J.B., Huntington, T.G., McDonnell, J.J., Peters, N.E., 2021. The evolving perceptual model of streamflow generation at the Panola Mountain Research Watershed. Hydrological Processes 35, e14127. https://doi.org/10.1002/hyp.14127

Bagarello, V., Iovina, M., Reynolds, W.D., 1999. Measuring hydraulic conductivity in a cracking clay soil using the guelph permeameter. Transactions of the ASAE 4, 957–964.

Bamutaze, Y., Tenywa, M.M., Majaliwa, M.J.G., Vanacker, V., Bagoora, F., Magunda, M., Obando, J., Wasige, J.E., 2010. Infiltration characteristics of volcanic sloping soils on Mt. Elgon, Eastern Uganda. Catena 80, 122–130. https://doi.org/10.1016/j.catena.2009.09.006

Barongo, J.O., Palacky, G.J., 1991. Investigations of electrical properties of weathered layers in the Yala area, western Kenya, using resistivity soundings. Geophysics 56, 133–138. https://doi.org/10.1190/1.1442949

Beauvais, A., Ritz, M., Parisot, J.-C., Dukhan, M., Bantsimba, C., 1999. Analysis of poorly stratified lateritic terrains overlying a granitic bedrock in West Africa, using 2-D electrical resistivity tomography. Earth and Planetary Science Letters 173, 413–424. https://doi.org/10.1016/S0012-821X(99)00245-9

Becker, M., Asch, F., Maskey, S.L., Pande, K.R., Shah, S.C., Shrestha, S., 2007. Effects of transition season management on soil N dynamics and system N balances in rice–wheat rotations of Nepal. Field Crops Research 103, 98–108. https://doi.org/10.1016/j.fcr.2007.05.002

Berktold, A., 2005. Geoelektrik, in: Knödel, K., Krummel, H., Lange, G. (Eds.), Handbuch zur Erkundung des Untergrundes von Deponien und Altlasten. Band 3: Geophysik. Springer, Berlin, Heidelberg, pp. 71–387.

Bertrand, I., Delfosse, O., Mary, B., 2007. Carbon and nitrogen mineralization in acidic, limed and calcareous agricultural soils: Apparent and actual effects. Soil Biology and Biochemistry 39, 276–288. https://doi.org/10.1016/j.soilbio.2006.07.016

Beuel, S., Alvarez, M., Amler, E., Behn, K., Kotze, D., Kreye, C., Leemhuis, C., Wagner, K., Willy, D.K., Ziegler, S., Becker, M., 2016. A rapid assessment of anthropogenic disturbances in East African wetlands. Ecological Indicators 67, 684–692. https://doi.org/10.1016/j.ecolind.2016.03.034

Beven, K., Germann, P., 2013. Macropores and water flow in soils revisited. Water Resources Research 49, 3071–3092. https://doi.org/10.1002/wrcr.20156

Beven, K., Germann, P., 1982. Macropores and water flow in soils. Water Resources Research 18, 1311–1325. https://doi.org/10.1029/WR018i005p01311

Binley, A., Kemna, A., 2005. DC resistivity and induced polarization methods, in: Rubin, Y., Hubbard, S.S. (Eds.), Hydrogeophysics, Water Science and Technology Library. Springer Netherlands, Dordrecht, pp. 129–156. https://doi.org/10.1007/1-4020-3102-5_5

Birch, H.F., 1960. Nitrification in soils after different periods of dryness. Plant and Soil 12, 16. https://doi.org/10.1007/BF01377763

Birch, H.F., 1958. The effect of soil drying on humus decomposition and nitrogen availability. Plant and soil 10, 9–31. https://doi.org/10.1007/BF01343734

Bishop, K.H., 1991. Episodic increases in stream acidity, catchment flow pathways and hydrograph separation. University of Cambridge, Cambridge, United Kingdom.

Black, A., Waring, S., 1979. Adsorption of nitrate, chloride and sulphate by some highly weathered soils from South-East Queensland. Soil Res. 17, 271–282. https://doi.org/10.1071/SR9790271

Blume, T., Meerveld, H.J. (Ilja) van, 2015. From hillslope to stream: methods to investigate subsurface connectivity. WIREs Water 2, 177–198. https://doi.org/10.1002/wat2.1071

Boast, R., 1990. Dambos: a review. Progress in Physical Geography 14, 153–177. https://doi.org/10.1177/030913339001400201

Bognonkpe, J.P., Becker, M., 2009. Land use and dynamics of water and native soil N in inland valleys of Côte d'Ivoire. European Journal of Scientific Research 36, 342–356.

Bognonkpe, J.P.I., Becker, M., 2000. Native soil N dynamics and use efficiency by lowland rice as a function of slope management, in: International Agricultural Research: A Contribution to Crisis Prevention. Proceedings of the Deutscher Tropentag 2000. Müllerbader Press, Hohenheim, pp. 197–199.

Böhme, B., Becker, M., Diekkrüger, B., 2013. Calibrating a FDR sensor for soil moisture monitoring in a wetland in Central Kenya. Physics and Chemistry of the Earth 66, 101–111. https://doi.org/10.1016/j.pce.2013.09.004

Bonell, M., 2005. Runoff generation in tropical forests, in: Bonell, M., Bruijnzeel, L.A. (Eds.), Forests, Water and People in the Humid Tropics: Past, Present and Future Hydrological Research for Integrated Land and Water Management, International Hydrology Series. Cambridge University Press, Cambridge.

Borken, W., Matzner, E., 2009. Reappraisal of drying and wetting effects on C and N mineralization and fluxes in soils. Global Change Biology 15, 808–824. https://doi.org/10.1111/j.1365-2486.2008.01681.x

Braun, J.-J., Dupré, B., Viers, J., Ngoupayou, J.R.N., Bedimo, J.-P.B., Sigha-Nkamdjou, L., Freydier, R., Robain, H., Nyeck, B., Bodin, J., Oliva, P., Boeglin, J.-L., Stemmler, S., Berthelin, J., 2002. Biogeohydrodynamics in the forested humid tropical environment: the case study of the Nsimi small experimental watershed (south Cameroon). Bulletin de la Société Géologique de France 173, 347–357. https://doi.org/10.2113/173.4.347

Bullock, A., 1992. Dambo hydrology in southern Africa - review and reassessment. Journal of Hydrology 134, 373–396. https://doi.org/10.1016/0022-1694(92)90043-U

Burghof, S., 2017. Hydrogeology and water quality of wetlands in East Africa - case studies of a floodplain and a valley bottom wetland. Rheinische Friedrich Wilhelms Universität Bonn, Steinmann Institut für Geologie, Mineralogie und Paläontologie, Bonn, Germany.

Burns, D., 2005. What do hydrologists mean when they use the term flushing? Hydrological Processes 19, 1325–1327. https://doi.org/10.1002/hyp.5860

Burns, D.A., Hooper, R.P., McDonnell, J.J., Freer, J.E., Kendall, C., Beven, K., 1998. Base cation concentrations in subsurface flow from a forested hillslope: The role of flushing frequency. Water Resour. Res. 34, 3535–3544. https://doi.org/10.1029/98WR02450

Cassman, K.G., Dobermann, A.R., Walters, D.T., 2002. Agroecosystems, nitrogen-use efficiency, and nitrogen management. Ambio 31, 132–140. https://doi.org/10.1579/0044-7447-31.2.132

Chandran, P., Ray, S., Bhattacharyya, T., Dubey, P.N., Pal, D., Krishnan, P., 2004. Chemical and mineralogical characteristics of ferruginous soils of Goa. Clay Res. 23, 51–64.

Chilton, P.J., Foster, S.S.D., 1995a. Hydrogeological characterisation and water-supply potential of basement aquifers in tropical Africa. HYJO 3, 36–49. https://doi.org/10.1007/s100400050061

Cirmo, C.P., McDonnell, J.J., 1997. Linking the hydrologic and biogeochemical controls of nitrogen transport in near-stream zones of temperate-forested catchments: a review. Journal of Hydrology 199, 88–120. https://doi.org/10.1016/S0022-1694(96)03286-6

Conacher, A., Dalrymple, J.B., 1977. The nine unit landsurface model: an approach to pedogeomorphic research. Geoderma 18, 1–154.

Creed, I.F., Band, L.E., 1998. Export of nitrogen from catchments within a temperate forest: Evidence for a unifying mechanism regulated by variable source area dynamics. Water Resources Research 34, 3105–3120. https://doi.org/10.1029/98WR01924

Delta-T Devices Ltd, 2017. User manual for the moisture meter type HH2. URL: https://www.delta-t.co.uk/wp-content/uploads/2016/10/HH2-UM-4.2.pdf (last accessed 2021/11/01).

Delta-T Devices Ltd, 2016. PR2_user_manual_version_5.0. URL: https://www.delta-t.co.uk/wp-content/uploads/2017/02/PR2_user_manual_version_5.0.pdf (last accessed 2021/11/1).

Delta-T Devices Ltd, 2005. Profile probe augering manual for PR2 and PR1. URL: https://delta-t.co.uk/wp-content/uploads/2016/09/AUG-Augering-User-Manual-v2.0.pdf (last accessed 2021/11/01)

Denef, K., Six, J., Bossuyt, H., Frey, S.D., Elliott, E.T., Merckx, R., Paustian, K., 2001. Influence of dry–wet cycles on the interrelationship between aggregate, particulate organic matter, and microbial community dynamics. Soil Biology and Biochemistry 33, 1599–1611. https://doi.org/10.1016/S0038-0717(01)00076-1

Denny, P. (1993): Eastern Africa. In: Whigham, D.F., Dykyjová, D. & Hejný, S. (eds) (1993): Wetlands of the world, Volume 1: Inventory, Ecology and Management. Kluwer Academic Publishers, Dordrecht, 32-46.

Dewandel, B., Lachassagne, P., Wyns, R., Maréchal, J.C., Krishnamurthy, N.S., 2006. A generalized 3-D geological and hydrogeological conceptual model of granite aquifers controlled by single or multiphase weathering. Journal of Hydrology, Hydro-ecological functioning of the Pang and Lambourn catchments, UK 330, 260–284. https://doi.org/10.1016/j.jhydrol.2006.03.026

Di, H.J., Cameron, K.C., 2002. Nitrate leaching in temperate agroecosystems: sources, factors and mitigating strategies. Nutrient Cycling in Agroecosystems 46, 237–256. https://doi.org/10.1023/A:1021471531188

Di Prima, S., Castellini, M., Abou Najm, M.R., Stewart, R.D., Angulo-Jaramillo, R., Winiarski, T., Lassabatere, L., 2019. Experimental assessment of a new comprehensive model for single ring infiltration data. Journal of Hydrology 573, 937–951. https://doi.org/10.1016/j.jhydrol.2019.03.077

Dick, J., Skiba, U., Wilson, J., 2001. The effect of rainfall on NO and N_2O emissions from Ugandan agroforest soils. Phyton (Austria) 41 Special Issue, 73–80.

Diekkrüger, B., Menz, G. (†), Reichert, B., 2018. Veröffentlichung der Ergebnisse von Forschungsvorhaben im BMBF-Programm GlobE: Wetlands - Feuchtgebiete in Ostafrika: Vereinbarkeit von Naturschutz und künftiger Nahrungsmittelproduktion, Partner C. Förderkennzeichen: 031A250C. Fachgruppe Erdwissenschaften der Rheinischen Friedrich-Wilhelms-Universität Bonn, Bonn, Germany.

Dividson, E.A., Stark, J.M., Firestone, M.K., 1990. Microbial production and consumption of nitrate in an annual grassland. Ecology 71, 1968–1975. https://doi.org/10.2307/1937605

Dobermann, A., Pampolino, M.F., Adviento, M.A., 1997. Resin capsules for onsite assessment of soil nutrient supply in lowland rice fields. Soil Sciences Society of America Journal 61, 1202–1213. https://doi.org/10.2136/sssaj1997.03615995006100040028x

Drury, C.F., McKenney, D.J., Findlay, W.I., Gaynor, J.D., 1993. Influence of tillage on nitrate loss in surface runoff and tile drainage. Soil Science Society of America Journal 57, 797–802.

https://doi.org/10.2136/sssaj1993.03615995005700030028x

Dunne, T., Black, R.D., 1970a. An experimental investigation of runoff production in permeable soils. Water Resour. Res. 6, 478–490. https://doi.org/10.1029/WR006i002p00478

Dunne, T., Black, R.D., 1970b. Partial area contributions to storm runoff in a small New England watershed. Water Resources Research 6, 1296–1311. https://doi.org/10.1029/WR006i005p01296

Edwards, W.M., Shipitalo, M.J., Traina, S.J., Edwards, C.A., Owens, L.B., 1992. Role of lumbricus terrestris (L.) burrows on quality of infiltrating water. Soil Biol. Biochem. 24, 1555–1561. https://doi.org/10.1016/0038-0717(92)90150-V

Eijkelkamp, 2019. Rhizon soil moisture samplers manual. URL: https://de.eijkelkamp.com/produkte/grund-wasser-probennehmer/rhizon-bodenfeuchteprobennehmer.html (last accessed 2021/11/01)

Eijkelkamp, 2004. Nitracheck reflectometer manual. URL: https://en.eijkelkamp.com/products/field-measurement-equipment/nitrachek-reflectometer.html (last accessed 2021/11/01)

Elrashidi, M.A., Mays, M.D., Fares, A., Seybold, C.A., Harder, J.L., Peaslee, S.D., VanNeste, P., 2005. Loss of nitrate-nitrogen by runoff and leaching for agricultural watersheds. Soil Science 170, 969–984. https://doi.org/10.1097/01.ss.0000187353.24364.a8

Erwin, K.L., 2009. Wetlands and global climate change: the role of wetland restoration in a changing world. Wetlands Ecol Manage 17, 71–84. https://doi.org/10.1007/s11273-008-9119-1

Everett, M.E., 2013. Near-surface applied geophysics. Cambridge University Press, Cambridge.

Fan, Y., Clark, M., Lawrence, D.M., Swenson, S., Band, L.E., Brantley, S.L., Brooks, P.D., Dietrich, W.E., Flores, A., Grant, G., Kirchner, J.W., Mackay, D.S., McDonnell, J.J., Milly, P.C.D., Sullivan, P.L., Tague, C., Ajami, H., Chaney, N., Hartmann, A., Hazenberg, P., McNamara, J., Pelletier, J., Perket, J., Rouholahnejad-Freund, E., Wagener, T., Zeng, X., Beighley, E., Buzan, J., Huang, M., Livneh, B., Mohanty, B.P., Nijssen, B., Safeeq, M., Shen, C., Verseveld, W., Volk, J., Yamazaki, D., 2019. Hillslope hydrology in global change research and earth system modelling. Water Resour. Res. 55, 1737–1772. https://doi.org/10.1029/2018WR023903

FAO, 2017. The future of food and agriculture: trends and challenges. Food and Agriculture Organization of the United Nations, Rome.

FAO, IFAD, UNICEF, WFP, WHO, 2021. The state of food security and nutrition in the world 2021. Transforming food systems for food security, improved nutrition and affordable healthy diets for all. FAO, Rome. https://doi.org/10.4060/cb4474en

Fatumah, N., Munishi, L.K., Ndakidemi, P.A., 2021. The effect of land-use systems on greenhouse gas production and crop yields in Wakiso District, Uganda. Environmental Development 37, Article 100607. https://doi.org/10.1016/j.envdev.2020.100607

Field, A., Miles, J., Field, Z., 2012. Discovering statistics using R. Sage Publications Ltd, London.

Fierer, N., Schimel, J.P., Holden, P.A., 2003. Influence of drying-rewetting frequency on soil bacterial community structure. Microbial Ecology 45, 63–71. https://doi.org/10.1007/s00248-002-1007-2

Finlayson, C.M., van der Falk, A.G., 1995. Wetland classification and inventory: a summary. Vegetatio 118, 185–192. https://doi.org/10.1007/BF00045199

Flint, A.L., Childs, S., 1984. Physical properties of rock fragments and their effect on available water in skeletal soils, in: Erosion and Productivity of Soils Containing Rock Fragments. John Wiley & Sons, Ltd, pp. 91–103. https://doi.org/10.2136/sssaspecpub13.c10

Flügel, W.A., 1993. Hierarchically structured hydrological process studies to regionalize interflow in a loess covered catchment near Heidelberg, Germany. IAHS Publication 212, pp. 215–223.

Gabiri, G., 2018. Multi-scale modelling of water resources in a tropical inland valley and a tropical floodplain catchment in East Africa. Rheinische Friedrich Wilhelms Universität Bonn, Geographisches Institut, Bonn, Germany.

Gabiri, G., Diekkrüger, B., Leemhuis, C., Burghof, S., Näschen, K., Asiimwe, I., Bamutaze, Y., 2018. Determining hydrological regimes in an agriculturally used tropical inland valley wetland in Central Uganda using soil moisture, groundwater, and digital elevation data. Hydrological Processes 32, 349–362. https://doi.org/10.1002/hyp.11417

Gabiri, G., Leemhuis, C., Diekkrüger, B., Näschen, K., Steinbach, S., Thonfeld, F., 2019. Modelling the impact of land use management on water resources in a tropical inland valley catchment of central Uganda, East Africa. Science of The Total Environment 653, 1052–1066. https://doi.org/10.1016/j.scitotenv.2018.10.430

Gaskin, J.W., Dowd, J.F., Nutter, W.L., Swank, W.T., 1989. Vertical and lateral components of soil nutrient flux in a hillslope. J. environ. qual. 18, 403–410. https://doi.org/10.2134/jeq1989.00472425001800040002x

George, T., Ladha, J.K., Buresh, R.J., Garrity, D.P., 1993. Nitrate dynamics during the aerobic soil phase in low-land rice based cropping systems. Soil Sciences Society of America Journal 1526–1532. https://doi.org/10.2136/sssaj1993.03615995005700060022x

George, T., Ladha, J.K., Garrity, D.P., Buresh, R.J., 1994. Legumes as nitrate catch crops during the dry-to-wet transition in lowland rice cropping systems. Agron.j. 86, 267–273. https://doi.org/10.2134/agronj1994.00021962008600020011x

Giertz, S., Diekkrüger, B., Steup, G., 2006. Physically-based modelling of hydrological processes in a tropical headwater catchment (West Africa) - process representation and multi-criteria validation. Hydrology and Earth System Sciences Discussions 10, 829–847. https://doi.org/10.5194/hess-10-829-2006, 2006.

Gilkes, R.J., Scholz, G., Dimmock, G.M., 1973. Lateritic deep weathering of granite. Journal of Soil Science 24, 523–536. https://doi.org/10.1111/j.1365-2389.1973.tb02319.x

Government of Uganda, 2016. Uganda wetlands atlas vol. 2, popular version. URL: https://www.mwe.go.ug/sites/default/files/library/Uganda%20Wetlands%20Atlas%20Volume%20II_Popular%20Version.pdf (last accessed 2021/12/12)

Grenfell, S., Grenfell, M., Ellery, W., Job, N., Walters, D., 2019. A genetic geomorphic classification system for Southern African palustrine wetlands: Global implications for the management of wetlands in drylands. Front. Environ. Sci. 7. https://doi.org/10.3389/fenvs.2019.00174

Grotelüschen, K., Gaydon, D.S., Langensiepen, M., Ziegler, S., Kwesiga, J., Senthilkumar, K., Whitbread, A.M., Becker, M., 2021. Assessing the effects of management and hydro-edaphic conditions on rice in contrasting East African wetlands using experimental and modelling approaches. Agricultural Water Management 258, 1–14.

https://doi.org/10.1016/j.agwat.2021.107146

GTK consortium, 2012. Geological map of Uganda 1:100,000. Sheet 61, Bombo.

Guo, L., Chen, J., Lin, H., 2014. Subsurface lateral preferential flow network revealed by time-lapse ground-penetrating radar in a hillslope. Water Resour. Res. 50, 9127–9147. https://doi.org/10.1002/2013WR014603

Haefele, S.M., Wopereis, M.C.S., Ndiaye, M.K., Barro, S.E., Isselmou, M.O., 2003. Internal nutrient efficiencies, fertilizer recovery rates and indigenous nutrient supply of irrigated lowland rice in Sahelian West Africa. Field Crops Research 80, 19–32. https://doi.org/10.1016/S0378-4290(02)00152-1

Halverson, L.J., Jones, T.M., Firestone, M.K., 2000. Release of intracellular solutes by four soil bacteria exposed to dilution stress. Soil Sci. Soc. Am. J. 64, 1630–1637. https://doi.org/10.2136/sssaj2000.6451630x

Heilig, A., Steenhuis, T.S., Walter, M.T., Herbert, S.J., 2003. Funnelled flow mechanisms in layered soil: field investigations. Journal of Hydrology 279, 210–223. https://doi.org/10.1016/S0022-1694(03)00179-3

Heiß, L., 2016 (unpublished). The alluvium of the Namulonge wetland (Uganda), its contribution to subsurface water dynamics and composition (Master thesis). Rheinische Friedrich Wilhelms Universität Bonn, Steinmann Institut für Geologie, Mineralogie und Paläontologie, Bonn, Germany.

Helsel, D.R., Hirsch, R.M., 2002. Statistical methods in water resources. Techniques of water resources investigations. Book 4, chapter A3.

Hentschel, K., Borken, W., Matzner, E., 2007. Leaching losses of inorganic N and DOC following repeated drying and wetting of a spruce forest soil. Plant and Soil 300, 21–34. https://doi.org/10.1007/s11104-007-9385-3

Hewlett, J.D., Hibbert, A.R., 1967. Factors affecting the response of small watersheds to precipitation in humid areas, in: Sopper, W.E., Lull, H.W. (Eds.), Proc Int Symp on Forest Hydrology. Pergamon Press, Oxford, pp. 275–290.

Hill, A.R., Kemp, W.A., Buttle, J.M., Goodyear, D., 1999. Nitrogen chemistry of subsurface storm runoff on forested Canadian Shield hillslopes. Water Resources Research 35, 811–821. https://doi.org/10.1029/1998WR900083

Horton, R.E., 1933. The role of infiltration in the hydrologic cycle. Transactions, American Geophysical Union 14, 446–460. https://doi.org/10.1029/TR014i001p00446

Hudson, N.W., 1993. Field measurement of soil erosion and runoff. Food & Agriculture Organisation of the United Nations, Rome.

Idrissou, M., 2020. Modelling water availability for smallholder farming in inland valleys under climate and land use / land cover change in Dano, Burkina Faso. Rheinische Friedrich Wilhelms Universität Bonn, Geographisches Institut, Bonn, Germany.

Jackisch, C., Angermann, L., Allroggen, N., Sprenger, M., Blume, T., Tronicke, J., Zehe, E., 2017. Form and function in hillslope hydrology: in situ imaging and characterization of flow-relevant structures. Hydrol. Earth Syst. Sci. 21, 3749–3775. https://doi.org/10.5194/hess-21-3749-2017

Jacobs, S.R., Timbe, E., Weeser, B., Rufino, M.C., Butterbach-Bahl, K., Breuer, L., 2018a. Assessment of hydrological pathways in East African montane catchments under different land use. Hydrology and Earth System Sciences 22, 4981–5000. https://doi.org/10.5194/hess-22-4981-2018

Jacobs, S.R., Weeser, B., Guzha, A.C., Rufino, M.C., Butterbach-Bahl, K., Windhorst, D., Breuer, L., 2018b. Using high-resolution data to assess land use impact on nitrate dynamics in East African tropical montane catchments. Water Resources Research 54, 1812–1830. https://doi.org/10.1002/2017WR021592

Jackson, C.R., Du, E., Klaus, J., Griffiths, N.A., Menberu, B. McDonnell, J.J., 2016. Interactions among hydraulic conductivity distributions, subsurface topography, and transport thresholds revealed by a multi-tracer hillslope irrigation experiment. Water Resources Research 52, 6186-6206. doi:10.1002/2015WR018364.

Jarvis, A., Reuter, H.I., Nelson, A., Guevara, E., 2008. Hole-filled SRTM for the globe Version 4. CGIAR-CSI SRTM 90m Database.

Jarvis, N., Koestel, J., Larsbo, M., 2016. Understanding preferential flow in the vadose zone: Recent advances and future prospects. Vadose Zone Journal 15, 1-11. https://doi.org/10.2136/vzj2016.09.0075

Jarvis, N.J., 2007. A review of non-equilibrium water flow and solute transport in soil macropores: principles, controlling factors and consequences for water quality. Eur J Soil Science 58, 523–546. https://doi.org/10.1111/j.1365-2389.2007.00915.x

Jiang, R., Woli, K.P., Kuramochi, K., Hayakawa, A., Shimizu, M., Hatano, R., 2012. Coupled control of land use and topography on nitrate-nitrogen dynamics in three adjacent watersheds. Catena 97, 1–11. https://doi.org/10.1016/j.catena.2012.04.015

Jiang, R., Woli, K.P., Kuramochi, K., Hayakawa, A., Shimizu, M., Hatano, R., 2010. Hydrological process controls on nitrogen export during storm events in an agricultural watershed. Soil Science and Plant Nutrition 56, 72–85. https://doi.org/10.1111/j.1747-0765.2010.00456.x

Jones, A., Breuning-Madsen, H., Brossard, M., Dampha, A., Deckers, J., Dewitte, O., Gallali, T., Hallet, S., Jones, R., Kilasara, M., Le Roux, P., Micheli, E., Montanarealla, L., Spargaaren, O., Thiombiano, L., Van Ranst, E., Yemefack, M., Zougmore, R., 2013. Soil atlas of Africa. Publication Office of the European Union, Luxembourg.

Jury, W.A., Flühler, H.F., 1992. Transport of chemicals through soils. Mechanisms, models and field applications. Advances in Agronomy 47, 141–165. https://doi.org/10.1016/S0065-2113(08)60490-3

Kahl, G., Ingwersen, J., Nutniyom, P., Totrakool, S., Pansombat, K., Thavornyutikarn, P., Streck, T., 2007. Micro-trench experiments on interflow and lateral pesticide transport in a sloped soil in Northern Thailand. Journal of Environmental Quality 36, 1205–1216. https://doi.org/10.2134/jeq2006.0241

Kienzler, P.M., Naef, F., 2008. Subsurface storm flow formation at different hillslopes and implications for the 'old water paradox.' Hydrological Processes 22, 104–116. https://doi.org/10.1002/hyp.6687

Kirchner, J.W., 2003. A double paradox in catchment hydrology and geochemistry. Hydrological Processes 17, 871–874. https://doi.org/10.1002/hyp.5108

Kirkby, M., 1988. Slope runoff processes and models. Journal of Hydrology 1–3, 315–339. https://doi.org/10.1016/0022-1694(88)90190-4

Kižlo, M., Kanbergs, A., 2009. The causes of the parameters changes of soil resistivity. Scientific Journal of Riga Technical University. Power and Electrical Engineering 25, 43–46. https://doi.org/10.2478/v10144-009-0009-z

Klaus, J., Jackson, C.R., 2018. Interflow is not binary: A continuous shallow perched layer does not imply continuous connectivity. Water Resour. Res. 54, 5921–5932. https://doi.org/10.1029/2018WR022920

Klaus, J., McDonnell, J.J., 2013. Hydrograph separation using stable isotopes: Review and evaluation. Journal of Hydrology 505, 47-64. http://dx.doi.org/10.1016/j.jhydrol.2013.09.006

Klaus, J., Zehe, E., Elsner, M., Külls, C. and McDonnell, J.J., 2013. Macropore flow of old water revisited: experimental insights from a tile-drained hillslope. Hydrology and Earth System Sciences 17, 103-118. doi:10.5194/hess-17-103-2013

Kleinman, P.J.A., Srinivasan, M.S., Dell, C.J., Schmidt, J.P., Sharpley, A.N., Bryant, R.B., 2006. Role of rainfall intensity and hydrology in nutrient transport via surface runoff. Journal of Environmental Quality 35, 1248–1259. https://doi.org/10.2134/jeq2006.0015

Koch, K., Wenninger, J., Uhlenbrook, S., Bonell, M., 2009. Joint interpretation of hydrological and geophysical data: electrical resistivity tomography results from a process hydrological research site in the Black Forest Mountains, Germany. Hydrological Processes 23, 1501–1513. https://doi.org/10.1002/hyp.7275

Koita, M., Jourde, H., Koffi, K.J.P., Da Silveira, K.S., Biaou, A., 2013. Characterization of weathering profile in granites and volcano-sedimentary rocks in West Africa under humid tropical climate conditions. Case of the Dimbokro Catchment (Ivory Coast). J Earth Syst Sci 122, 841–854. https://doi.org/10.1007/s12040-013-0290-2

Kotze, D.C., Breen, C.M., Klug, J.R., 1994. WETLAND-USE: a decision support system for managing wetlands. WRC Report No. 501/2/94. Water Research Commission, Pretoria.

Kotze, D.C., Ellery, W.N., Macfarlane, D.M., Jewitt, G.P.W., 2012. A rapid assessment method for coupling anthropogenic stressors and wetland ecological condition. Ecological Indicators 13, 284–293. https://doi.org/10.1016/j.ecolind.2011.06.023

Krohm, Y., 2015. Seasonal Soil N Dynamics and Contribution of valley slopes to Matter Fluxes in Wetlands of Uganda. (Master thesis). Rheinische Friedrich Wilhelms Universität Bonn, Steinmann Institut für Geologie, Mineralogie und Paläontologie, Bonn, Germany.

Kung, K.-J.S., 1990. Preferential flow in a sandy vadose zone: 2. Mechanism and implications. Geoderma 46, 59–71. https://doi.org/10.1016/0016-7061(90)90007-V

Lal, R., 1976. Soil erosion on Alfisols in Western Nigeria: IV. Nutrient element losses in runoff and eroded sediments. Geoderma 16, 403–417. https://doi.org/10.1016/0016-7061(76)90004-5

Lassabatère, L., Angulo-Jaramillo, R., Soria Ugalde, J.M., Cuenca, R., Braud, I., Haverkamp, R., 2006. Beerkan estimation of soil transfer parameters through infiltration experiments-BEST. Soil Sci. Soc. Am. J. 70, 521–532. https://doi.org/10.2136/sssaj2005.0026

Li, Z.M., Skogley, E.O., Ferguson, A.H., 1993. Resin adsorption for describing bromide transport in soil under continuous or intermittent unsaturated water flow. Journal of Environmental Quality 22, 715–722. https://doi.org/10.2134/jeq1993.00472425002200040012x

Lin, H., Zhou, X., 2008. Evidence of subsurface preferential flow using soil hydrologic monitoring in the Shale Hills catchment. European Journal of Soil Science 59, 34–49. https://doi.org/10.1111/j.1365-2389.2007.00988.x

Locke, M.H., 2018. Rapid 2-D Resistivity & IP inversion using the least-squares method. Geotomo software sdn bhd. URL: http://www.geotomosoft.com/downloads.php (last accessed 2021/11/01)

Lu, P., Woo, K., Liu, Z., 2002. Estimation of whole-plant transpiration of bananas using sap flow measurements. Journal of Experimental Botany 53, 1771–1779. https://doi.org/10.1093/jxb/erf019

Luo, L., Lin, H., Li, S., 2010. Quantification of 3-D soil macropore networks in different soil types and land uses using computed tomography. Journal of Hydrology, Soil Architecture and Preferential Flow across Scales 393, 53–64. https://doi.org/10.1016/j.jhydrol.2010.03.031

Mahan, S.A., Brown, D.J., 2007. An optical age chronology of late Quaternary extreme fluvial events recorded in Ugandan dambo soils. Quaternary Geochronology, LED 2005 2, 174–180. https://doi.org/10.1016/j.quageo.2006.04.015

Mathers, N.J., Nash, D.M., Gangaiya, P., 2007. Nitrogen and phosphorus exports from high rainfall zone cropping in Australia: Issues and opportunities for research. Journal of Environmental Quality 36, 1551–1562. https://doi.org/10.2134/jeq2006.0464

McCartney, M.P., 2000. The water budget of a headwater catchment containing a dambo. Physics and Chemistry of the Earth, Part B: Hydrology, Oceans and Atmosphere 25, 611–616. https://doi.org/10.1016/S1464-1909(00)00073-3

McCartney, M.P., Neal, C., 1999. Water flow pathways and the water balance within a head-water catchment containing a dambo: inferences drawn from hydrochemical investigations. Hydrology and Earth System Sciences 3, 581–591. https://doi.org/10.5194/hess-3-581-1999

McDonnell, J.J., 1990. A rationale for old water discharge through macropores in a steep, humid catchment. Water Resour. Res. 26, 2821–2832. https://doi.org/10.1029/WR026i011p02821

McDonnell, J.J., Owens, I.F., Stewart, M.K., 1991. A case study of shallow flow paths in a steep zero-order basin. JAWRA Journal of the American Water Resources Association 27, 679–685. https://doi.org/10.1111/j.1752-1688.1991.tb01469.x

McFarlane, M.J., 1992. Groundwater movement and water chemistry associated with weathering profiles of the African surface in parts of Malawi, in: Wright, E.P., Burgess, W.G. (Eds.), Hydrogeology of Crystalline Basement Aquifers in Africa. pp. 101–129.

McFarlane, M.J., 1989. Dambos - their characteristics and geomorphological evolution in parts of Malawi and Zimbabwe with particular reference to their role in the hydrogeological regime of surviving areas of African Surface, in: Groundwater Exploration and Development in Crystalline Basement Aquifers. Common wealth sciences publication, pp. 254–310.

McGlynn, B.L., McDonnell, J.J., 2003. Role of discrete landscape units in controlling catchment dissolved organic carbon dynamics. Water Resources Research 39.

https://doi.org/10.1029/2002WR001525

McHale, M.R., McDonnell, J.J., Mitchell, M.J., Cirmo, C.P., 2002. A field-based study of soil water and groundwater nitrate release in an Adirondack forested watershed. Water Resour. Res. 38, 2.1-2.16. https://doi.org/10.1029/2000WR000102

McNeill, J.D., 1980. Electrical conductivity of soils and rocks. Technical Note T-5. Geonics Ltd., Ontario.

Meerveld, H.J.T., McDonnell, J.J., 2006a. Threshold relations in subsurface stormflow: 1. A 147-storm analysis of the Panola hillslope. Water Resources Research 42. https://doi.org/10.1029/2004WR003778

Meerveld, H.J.T., McDonnell, J.J., 2006b. Threshold relations in subsurface stormflow: 2. The fill and spill hypothesis. Water Resources Research 42. https://doi.org/10.1029/2004WR003800

Millennium Ecosystem Assessment (Ed.), 2005. Ecosystems and human well-being: wetlands and water, Synthesis. World Resources Institute, Washington, DC.

Mindrila, D., Balentyne, P., 2016. Scatterplots and correlation. https://www.westga.edu/academics/research/vrc/assets/docs/scatterplots_and_correlation_notes.pdf (last accessed 2021/12/22)

Mitsch, William J., Gosselink, J.G., 2015. Wetlands, Fifth edition. ed. John Wiley and Sons, Inc, Hoboken.

Miyamoto, K., Maruyama, A., Haneishi, Y., Matsumoto, S., Asea, G., Okello, S., Takagaki, M., Kikuchi, M., 2012. NERICA cultivation and its yield determinants: The case of upland rice farmers in Namulonge, Central Uganda. Journal of Agricultural Science 4, 16.

Molina, A., Govers, G., Vanacker, V., Poesen, J., Zeelmaekers, E., Cisneros, F., 2007. Runoff generation in a degraded Andean ecosystem: Interaction of vegetation cover and land use. Catena 71, 357–370. https://doi.org/10.1016/j.catena.2007.04.002

Mugisa, I.O., Fungo, B., Adur, S.O., Ssemalulu, O., Molly, A., Atim, J., Nakyagaba, W., Kizza, T., Kabanyoro, R., Sseruwu, G., Akello, B.O., 2017. Urban and peri-urban crop farming in Central Uganda: Characteristics, constraints and opportunities for household food security and income. Afr. J. Plant Sci. 11, 264–275. https://doi.org/10.5897/AJPS2016.1477

Muiuane, E., 1999. Hydrogeophysics of tropical Africa. Recent advances and perspectives. Upsala University, Factulty of Science and Technology, Upsala, Sweden.

Mulumba, L.N., 2004. Land use effects on soil quality and productivity in the Lake Victoria Basin of Uganda. The Ohio State University.

Nangia, V., Mulla, D.J., Gowda, P.H., 2010. Precipitation changes impact stream discharge, nitrate–nitrogen load more than agricultural management changes. Journal of Environmental Quality 39, 2063–2071. https://doi.org/10.2134/jeq2010.0105

Nash, D., Halliwell, D., Cox, J., 2002. Hydrological mobilization of pollutants at the field/slope scale, in: Haygarth, P.M., Jarvis, S.C. (Eds.), Agriculture, Hydrology and Water Quality. CABI, Wallingford, pp. 243–264. https://doi.org/10.1079/9780851995458.0243

Nicholson, S.E., 2017. Climate and climatic variability of rainfall over eastern Africa. Rev. Geophys. 55, 590–635. doi:10.1002/2016rg000544

Needelman, B.A., 2002. Surface runoff hydrology and phosphorus transport along two agricultural hillslopes with contrasting soils. The Pennsylvania State University, USA.

NEMA, 2019. State of environment report for Uganda 2018/2019. National Environmental Management Authority, Kampala, Uganda.

Ng Kee Kwong, K.F., Bholah, A., Volcy, L., Pynee, K., 2002. Nitrogen and phosphorus transport by surface runoff from a silty clay loam soil under sugarcane in the humid tropical environment of Mauritius. Agriculture, Ecosystems & Environment 91, 147–157. https://doi.org/10.1016/S0167-8809(01)00237-7

Nichols, G., 2009. Sedimentology and Stratigraphy, 2nd ed. Wiley-Blackwell, Oxford.

Nieber, J.L., Sidle, R.C., 2010. How do disconnected macropores in sloping soils facilitate preferential flow? Hydrological Processes 24, 1582–1594. https://doi.org/10.1002/hyp.7633

Noguchi, S., Tsuboyama, Y., Sidle, R.C., Hosoda, I., 1999. Morphological characteristics of macropores and the distribution of preferential flow pathways in a forested slope segment. Soil Science Society of America Journal 63, 1413–1423. https://doi.org/10.2136/sssaj1999.6351413x

Nsubuga, F.N.W., Namutebi, E.N., Nsubuga-Ssenfuma, M., 2014. Water resources of Uganda: An assessment and review. Journal of Water Resource Protection 6, 1297–1315.

Nsubuga, F.W., Olwoch, J.M., Rautenbach, C.J. de W., 2011. Climatic trends at Namulonge in Uganda: 1947-2009. Journal of Geography and Geology 3. https://doi.org/10.5539/jgg.v3n1p119

Ogallo, L.A., 1993. Dynamics of the East African climate. Proceedings of the Indian Academy of Sciences (Earth Planet Sciences) 102, 203–217.

Oguntunde, P.G., 2005. Whole-plant water use and canopy conductance of Cassava under Iimited available soil water and varying evaporative demand. Plant Soil 278, 371–383. https://doi.org/10.1007/s11104-005-0375-z

Ollis, D., Ewart-Smith, J., Day, J., Job, N., Macfarlane, D., Snaddon, C., Sieben, E., Dini, J., Mbona, N., 2015. The development of a classification system for inland aquatic ecosystems in South Africa. WSA 41, 727. https://doi.org/10.4314/wsa.v41i5.16

Ollis, D., Snaddon, K., Job, N., Mbona, N., 2013. Classification system for wetlands and other aquatic ecosystems in South Africa. User manual: inland systems, SANBI Biodiversity Series. South African National Biodiversity Institute, Pretoria.

Op de Hipt, F., 2017. Modelling climate and land use change impacts on water resources and soil erosion in the Dano catchment (Burkina Faso, West Africa). Rheinische Friedrich Wilhelms Universität Bonn, Geographisches Institut, Bonn, Germany.

Palacky, G.J., 1987. Resistivity characteristics of geological targets, in: Nabighian, M.N. (Ed.), Electromagnetic Methods in Applied Geophysics. Society of exploration geophysics, Tulsa, pp. 131–311.

Pampolino, M.F., Urushiyama, T., Hatano, R., 2000. Detection of nitrate leaching through bypass flow using pan lysimeter, suction cup, and resin capsule. Soil Science and Plant Nutrition 46, 703–711. https://doi.org/10.1080/00380768.2000.10409135

Pande, K.R., Becker, M., 2003. Seasonal soil nitrogen dynamics in rice-wheat cropping systems of Nepal. Journal of Plant Nutrition and Soil Science 166, 499–506.

https://doi.org/10.1002/jpln.200320315

Peel, M.C., Finlayson, B.L. and McMahon, T.A., 2007. World map of the Köppen-Geiger climate classification updated. *Hydrol. Earth Syst. Sci.* 11, 1633–1644. doi:10.1127/0941-2948/2006/0130.

Peric, M., 1981. Exploration of Burundi nickeliferous laterites by electrical methods. Geophysical Prospecting 29, 274–287. https://doi.org/10.1111/j.1365-2478.1981.tb00405.x

Phillips, J., McIntyre, B., 2000. ENSO and interannual rainfall variability in Uganda: implications for agricultural management. Int. J. Climatol. 20, 171–182. https://doi.org/10.1002/(SICI)1097-0088(200002)20:2<171::AID-JOC471>3.0.CO;2-O

Pierret, A., Capowiez, Y., Belzunces, L., Moran, C.J., 2002. 3D reconstruction and quantification of macropores using X-ray computed tomography and image analysis. Geoderma 106, 247–271. https://doi.org/10.1016/S0016-7061(01)00127-6

Pincus, L., Margenot, A., Six, J., Scow, K., 2016. On-farm trial assessing combined organic and mineral fertilizer amendments on vegetable yields in central Uganda. Agriculture, Ecosystems & Environment 225, 62–71. https://doi.org/10.1016/j.agee.2016.03.033

Pinson, W.T., Yoder, D.C., Buchanan, J.R., Wright, W.C., Wilkerson, J.B., 2004. Design and evaluation of an improved flow divider for sampling runoff plots. Applied engineering in agriculture 20, 433–437.

Podwojewski, P., Orange, D., Jouquet, P., Valentin, C., Nguyen, V.T., Janeau, J.L., Tran, D.T., 2008. Land-use impacts on surface runoff and soil detachment within agricultural sloping lands in Northern Vietnam. CATENA 74, 109–118. https://doi.org/10.1016/j.catena.2008.03.013

Prosser, J.I., 2011. Soil Nitrifiers and Nitrification, in: Ward, B.B., Arp, D.J., Klotz, M.G. (Eds.), Nitrification. John Wiley & Sons, Ltd, pp. 347–383. https://doi.org/10.1128/9781555817145.ch14

Ramsar Convention Secretariat, 2016. An introduction to the Ramsar Convention on wetlands, 7th ed. Gland.

Rawls, W.J., Brakensiek, D.L., 1985. Prediction of soil water properties for hydrologic modelling, in: Proceedings of the American Society of Civil Engineers Watershed Management in the Eighties Symposium. ASCE, New York, pp. 293–299.

Rebelo, L.-M., McCartney, M.P., Finlayson, C.M., 2010. Wetlands of Sub-Saharan Africa: distribution and contribution of agriculture to livelihoods. Wetlands Ecol Manage 18, 557–572. https://doi.org/10.1007/s11273-009-9142-x

Reddy, K.R., DeLaune, R.D., 2008. Biogeochemistry of wetlands: Science and applications, 1st ed. CRC Press, Boca Raton. https://doi.org/10.1201/9780203491454

Reynolds, W.D., 2008. Chapter 77: Saturated hydraulic properties: Ring infiltrometer, in: Carter, M.R., Gregorich, E.G. (Eds.), Soil Sampling and Methods of Analysis. Canadian Society of Soil Science, CRC Press, Boca Raton.

Reynolds, W.D., Elrick, D.E., 1990. Ponded infiltration from a single ring: I. Analysis of steady flow. Soil Science Society of America Journal 54, 1233. https://doi.org/10.2136/sssaj1990.03615995005400050006x

Ribolzi, O., Lacombe, G., Pierret, A., Robain, H., Sounyafong, P., de Rouw, A., Soulileuth, B., Mouche, E., Huon, S., Silvera, N., Latxachak, K.O., Sengtaheuanghoung, O., Valentin, C., 2018. Interacting land

use and soil surface dynamics control groundwater outflow in a montane catchment of the lower Mekong basin. Agriculture, Ecosystems & Environment 268, 90–102. https://doi.org/10.1016/j.agee.2018.09.005

Riddell, E., Lorentz, S., Kotze, D., 2012. The hydrodynamic response of a semi-arid headwater wetland to technical rehabilitation interventions. Water SA 38. https://doi.org/10.4314/wsa.v38i1.8

Riddell, E.S., Lorentz, S.A., Kotze, D.C., 2010. A geophysical analysis of hydro-geomorphic controls within a headwater wetland in a granitic landscape, through ERI and IP. Hydrology and Earth System Sciences 14, 1697–1713. https://doi.org/10.5194/hess-14-1697-2010

Ritsema, C.J., Dekker, L.W., 1995. Distribution flow: A general process in the top layer of water repellent soils. Water Resources Research 31, 1187–1200. https://doi.org/10.1029/94WR02979

Robertson, G.P., 1989. Nitrification and denitrification in humid tropical ecosystems: potential controls on nitrogen retention. Mineral nutrients in tropical forest and savannah ecosystems, Special publication series of the British Ecological Society 9, 55–69.

Robertson, G.P., Groffman, P.M., 2015. Nitrogen transformations, in: Soil Microbiology, Ecology and Biochemistry. Elsevier, pp. 421–446. https://doi.org/10.1016/B978-0-12-415955-6.00014-1

Rodenburg, J., 2013. Inland valleys: Africa's future food baskets., in: Wopereis, M.C.S., Johnson, D.E., Ahmadi, N., Tollens, E., Jalloh, A. (Eds.), Realizing Africa's Rice Promise. CABI, Wallingford, pp. 276–293. https://doi.org/10.1079/9781845938123.0276

Rusjan, S., Brilly, M., Mikoš, M., 2008. Flushing of nitrate from a forested watershed: An insight into hydrological nitrate mobilization mechanisms through seasonal high-frequency stream nitrate dynamics. Journal of Hydrology 354, 187–202. https://doi.org/10.1016/j.jhydrol.2008.03.009

Russo, T.A., Tully, K., Palm, C., Neill, C., 2017. Leaching losses from Kenyan maize cropland receiving different rates of nitrogen fertilizer. Nutr Cycl Agroecosyst 108, 195–209. https://doi.org/10.1007/s10705-017-9852-z

Sabiiti, E.N., Katongole, B., 2016. Chpt. 23: Role of Peri-Urban Areas in the Food System of Kampala, Uganda, in: Balanced Urban Development: Options and Strategies for Liveable Cities. Springer International Publishing, Cham, pp. 387–392.

Sahrawat, K.L., 2008. Factors Affecting Nitrification in Soils. Communications in Soil Science and Plant Analysis 39, 1436–1446. https://doi.org/10.1080/00103620802004235

Sakané, N., Alvarez, M., Becker, M., Böhme, B., Handa, C., Kamiri, H.W., Langensiepen, M., Menz, G., Misana, S., Mogha, N.G., Möseler, B.M., Mwita, E.J., Oyieke, H.A., van Wijk, M.T., 2011. Classification, characterisation, and use of small wetlands in East Africa. Wetlands 31, 1103–1116. https://doi.org/10.1007/s13157-011-0221-4

Sanuade, O.A., Amosun, J.O., Olaojo, A.A., Fagbemigun, T.S., Faloyo, J.I., 2019. Analysis of principles of equivalence and suppression in resistivity sounding technique. Journal of Physics Conference Series 1299 (12065). https://doi.org/10.1088/1742- 6596/1299/1/012065

Scheffer, F., Schachtschabel, P., Blume, H.-P., Thiele, S., 2010. Lehrbuch der Bodenkunde, 16. Auflage. ed. Spektrum, Akademischer Verlag, Heidelberg.

Scheu, S., Parkinson, D., 1994. Changes in bacterial and fungal biomass C, bacterial and fungal biovolume and ergosterol content after drying, remoistening and incubation of different layers of cool temperate forest soils. Soil Biology and Biochemistry 26, 1515–1525. https://doi.org/10.1016/0038-0717(94)90093-0

Schimel, J., Balser, T.C., Wallenstein, M., 2007. Microbial stress-response physiology and its implications for ecosystem function. Ecology 88, 1386–1394. https://doi.org/10.1890/06-0219

Schimel, J.P., Gulledge, J.M., Clein-Curley, J.S., Lindstrom, J.E., Braddock, J.F., 1999. Moisture effects on microbial activity and community structure in decomposing birch litter in the Alaskan taiga. Soil Biology and Biochemistry 31, 831–838. https://doi.org/10.1016/S0038-0717(98)00182-5

Schlüter, T., 1997. Geology of East Africa, Beiträge zur regionalen Geologie der Erde. Gebrüder Borntraeger, Berlin, Stuttgart.

Sharma, S., Chaubey, I., 2017. Surface and subsurface transport of nitrate loss from the selected bioenergy crop fields: Systematic review, analysis and future directions. Agriculture 7, 27. https://doi.org/10.3390/agriculture7030027

Sheppard, G., Buresh, R.J., Gregory, P.J., 2001. Inorganic soil nitrogen distribution in relation to soil properties in smallholder maize fields in the Kenya highlands. Geoderma 87–103.

Shuaib, L., Nyakaana, J.B., Sengendo, H., 2005. Assessment of environmental impacts of land use land cover change: A challenge for urban planning in metropolitan Kampala. Proceedings of Informatics for Environmental Protection - Networking Environmental Information, Masaryk University Brno, pp. 252–257.

Sidle, R.C., Noguchi, S., Tsuboyama, Y., Laursen, K., 2001. A conceptual model of preferential flow systems in forested hillslopes: evidence of self-organization. Hydrological Processes 15, 1675–1692. https://doi.org/10.1002/hyp.233

Sidle, R.C., Tsuboyama, Y., Noguchi, S., Hosoda, I., Fujieda, M., Shimizu, T., 2000. Stormflow generation in steep forested headwaters: a linked hydrogeomorphic paradigm. Hydrological Processes 14, 369–385. https://doi.org/10.1002/(SICI)1099-1085(20000228)14:3<369::AID-HYP943>3.0.CO;2-P

Sieben, E.J.J., Khubeka, S.P., Sithole, S., Job, N.M., Kotze, D.C., 2018. The classification of wetlands: integration of top-down and bottom-up approaches and their significance for ecosystem service determination. Wetlands Ecol Manage 26, 441–458. https://doi.org/10.1007/s11273-017-9585-4

Sierra, J., 2002. Nitrogen mineralization and nitrification in a tropical soil: effects of fluctuating temperature conditions. Soil Biology and Biochemistry 34, 1219–1226. https://doi.org/10.1016/S0038-0717(02)00058-5

Sililo, O.T.N., Tellam, J.H., 2000. Fingering in unsaturated zone flow: A qualitative review with laboratory Experiments on heterogeneous systems. Groundwater 38, 864–871. https://doi.org/10.1111/j.1745-6584.2000.tb00685.x

Skogley, E.O., 1992. The universal bioavailability environment/soil test unibest. Communications in Soil Science and Plant Analysis 23, 2225–2246. https://doi.org/10.1080/00103629209368736

Skogley, E.O., Dobermann, A., 1996. Synthetic ion-exchange resins: Soil and environmental studies. Journal of Environmental Quality 25, 13–24.

https://doi.org/10.2134/jeq1996.00472425002500010004x

Smaling, E.M.A., Bouma, J., 1992. Bypass flow and leaching of nitrogen in a Kenyan Vertisol at the onset of the growing season. Soil Use and Management 8, 44–47. https://doi.org/10.1111/j.1475-2743.1992.tb00892.x

Smith, R.C., Sjogren, D.B., 2006. An evaluation of electrical resistivity imaging (ERI) in Quaternary sediments, southern Alberta, Canada. Geosphere 2, 287–298. https://doi.org/10.1130/GES00048.1

Stange, F., Diekkrüger, B., Nordmeyer, H., 1998. Measurement and simulation of herbicide transport in macroporous soils. Pesticide Sciences 52, 241–250. https://doi.org/10.1002/(SICI)1096-9063(199803)52:3<241::AID-PS721>3.0.CO;2-1

Stark, J.M., Firestone, M.K., 1995. Mechanisms for soil moisture effects on activity of nitrifying bacteria. Appl Environ Microbiol 61, 218–221. https://doi.org/10.1128/aem.61.1.218-221.1995

Sugita, F., Nakane, K., 2007. Combined effects of rainfall patterns and porous media properties on nitrate leaching. Vadose Zone Journal 6, 548–553. https://doi.org/10.2136/vzj2006.0095

Szott, L.T., Palm, C.A., Buresh, R.J., 1999. Ecosystem fertility and fallow function in the humid and subhumid tropics. Agroforestry Systems 47, 163–196. https://doi.org/10.1023/A:1006215430432

Taylor, R., Howard, K., 2000. A tectono-geomorphic model of the hydrogeology of deeply weathered crystalline rock: Evidence from Uganda. Hydrogeology Journal 8, 279–294. https://doi.org/10.1007/s100400000069

Taylor, R.G., Howard, K.W.F., 1998. Post-Palaeozoic evolution of weathered land surfaces in Uganda by tectonically controlled deep weathering and stripping. Geomorphology 25, 173–192. https://doi.org/10.1016/S0169-555X(98)00040-3

Taylor, R.G., Howard, K.W.F., 1996. Groundwater recharge in the Victoria Nile basin of East Africa: support for the soil moisture balance approach using stable isotope tracers and flow modelling. Journal of Hydrology 180, 31–53. https://doi.org/10.1016/0022-1694(95)02899-4

Touré, A., Becker, M., Johnson, D.E., Koné, B., Kossou, D.K., Kiepe, P., 2009. Response of lowland rice to agronomic management under different hydrological regimes in an inland valley of Ivory Coast. Field Crops Research 114, 304–310. https://doi.org/10.1016/j.fcr.2009.08.015

Tully, K., Sullivan, C., Weil, R., Sanchez, P., 2015. The state of soil degradation in Sub-Saharan Africa: Baselines, trajectories, and solutions. Sustainability 7, 6523–6552. https://doi.org/10.3390/su7066523

Turrion, M.B., Gallardo, J.F., Gonzalez, M.I., 1997. Nutrient availability in forest soils as measured with anion-exchange membranes. Geomicrobiology Journal 14, 51–64. https://doi.org/10.1080/01490459709378033

UBOS (Uganda Bureau of Statistics), 2018. Annual agricultural survey (AAS). URL: https://uganda.opendataforafrica.org/yyyatvd/agricultural-household-characteristics-in-uganda-at-zardi-level-aas-2018 (last accessed 2022/02/19)

UBOS (Uganda Bureau of Statistics), 2021. Annual agricultural survey (AAS). URL: https://www.ubos.org/africa-statistics-week-launch-of-annual-agricultural-survey-2019-15th-november-2021/ (last accessed 2021/12/12)

Uhlenbrook, S., Wenninger, J., Lorentz, S., 2005. What happens after the catchment caught the storm? Hydrological processes at the small, semi-arid Weatherley catchment, South-Africa. Advances in Geosciences 2, 237–241. https://doi.org/10.5194/adgeo-2-237-2005

United States Department of Agriculture, n.d. Soil Survey Technical Note 8 (NRCS Soils). URL: https://www.nrcs.usda.gov/wps/portal/nrcs/detail/soils/ref/?cid=nrcs142p2_053575 (last accessed 2021/11/01).

van Breugel, P., Kindt, R., Lillesø, J.P.G., Bingham, M., Demissew, S., Dudley, C., Friis, I., Gachathi, F., Kalema, J., Mbago, F., Moshi, H.N., Mulumba, J., Ndangalasi, H.J., Ruffo, C.K., Védaste, M., Jamnadass, R., Graudal, L., 2015. Potential natural vegetation map of East Africa (Burundi, Ethiopia, Kenya, Malawi, Rwanda, Tanzania, Uganda and Zambia). URL: //vegetationmap4africa.org (last accessed 2021/11/01)

Van Soest, M., 2018. The political ecology of malaria - emerging dynamics of wetland agriculture at the urban fringe in central Uganda. Universtiät zu Köln, Cologne, Germany.

van Stempfoort, D.R., MacKay, D.R., Koehler, G., Collins, P., Brown, S.J. (2021): Subsurface hydrology of tile drained headwater catchments: compatibility of concepts and hydrochemistry. Hydrological processes 35, e14342. DOI: 10.1002/hyp.14342

van Verseveld, W.J., McDonnell, J.J., Lajtha, K., 2009. The role of hillslope hydrology in controlling nutrient loss. Journal of Hydrology 367, 177–187. https://doi.org/10.1016/j.jhydrol.2008.11.002

Vizy, E.K., Cook, K.H., 2020. Interannual variability of East African rainfall: role of seasonal transitions of the low-level cross-equatorial flow. Clim Dyn 54, 4563–4587. https://doi.org/10.1007/s00382-020-05244-z

von der Heyden, C.J., 2004. The hydrology and hydrogeology of dambos: a review. Progress in Physical Geography: Earth and Environment 28, 544–564. https://doi.org/10.1191/0309133304pp424oa

von der Heyden, C.J., New, M.G., 2003. The role of a dambo in the hydrology of a catchment and the river network downstream. Hydrol. Earth Syst. Sci. 7, 339–357. https://doi.org/10.5194/hess-7-339-2003

Voroney, R.P., 2007. The soil habitat, in: Paul, E.A. (Ed.), Soil Microbiology, Ecology and Biochemistry. Academic Press, San Diego, pp. 25–49. https://doi.org/10.1016/B978-0-08-047514-1.50006-8

Wagner, K.X.X., 2019. Impact assessment of land-use change and agricultural treatments on greenhouse gas emissions from wetlands of Uganda and Tanzania. Rheinische Friedrich Wilhelms Universität Bonn, Geographisches Institut, Bonn, Germany.

Walter, M.T., Kim, J.-S., Steenhuis, T.S., Parlange, J.-Y., Heilig, A., Braddock, R.D., Selker, J.S., Boll, J., 2000. Funnelled flow mechanisms in a sloping layered soil: Laboratory investigation. Water Resources Research 36, 841–849. https://doi.org/10.1029/1999WR900328

Warren, G.P., Atwal, S.S., Irungu, J.W., 1997. Soil nitrate variations under grass, sorghum and bare fallow in semi-arid Kenya. Ex. Agric. 33, 321–333. https://doi.org/10.1017/S0014479797003025

Weil, R.R., Brady, N.C., 2017. The nature and properties of soils, 15th ed. Pearson Education, Essex.

Weiler, M., McDonnell, J.J., 2006. Testing nutrient flushing hypotheses at the hillslope scale: A virtual experiment approach. Journal of Hydrology 319, 339–356. https://doi.org/10.1016/j.jhydrol.2005.06.040

Weiss Peter T., Gulliver John S., 2015. Effective saturated hydraulic conductivity of an infiltration-based stormwater control measure. Journal of Sustainable Water in the Built Environment 1, 04015005. https://doi.org/10.1061/JSWBAY.0000801

Wenninger, J., Uhlenbrook, S., Lorentz, S., Leibundgut, C., 2008. Identification of runoff generation processes using combined hydrometric, tracer and geophysical methods in a headwater catchment in South Africa / Identification des processus de formation du débit en combinat la méthodes hydrométrique, traceur et géophysiques dans un bassin versant sud-africain. Hydrological Sciences Journal 53, 65–80. https://doi.org/10.1623/hysj.53.1.65

Westerhof, A.B., Härmä, P., Isabirye, E., Katto, E., Koistinen, T., Kuosmanen, E., Lehto, T., Lehtonen, M.I., Mäkitie, H., Manninen, T., Mänttäri, I., Pekkala, Y., Pokki, J., Saalmann, K., Virransalo, P., 2014. Geology and geodynamic development of Uganda with explanation of the 1:1,000,000-scale geological map, Special paper. Geological Survey of Finland, Espoo.

Wild, A., 1972. Nitrate leaching under bare fallow at a site in Northern Nigeria. Journal of Soil Science 23, 315–324. https://doi.org/10.1111/j.1365-2389.1972.tb01663.x

Williams, A.G., Dowd, J.F., Meyles, E.W., 2002. A new interpretation of kinematic stormflow generation. Hydrological Processes 16, 2791–2803. https://doi.org/10.1002/hyp.1071

Windmeijer, P.N., Andriesse, W. (Eds.), 1993. Inland valleys in West Africa: an agro-ecological characterization of rice-growing environments, ILRI publications. Wageningen.

Wong, M.T.F., Hughes, R., Rowell, D.L., 1990. The retention of nitrate in acid soils from the tropics. Soil Use and Management 6, 72–74. https://doi.org/10.1111/j.1475-2743.1990.tb00805.x

Woodley, A.L., Drury, C.F., Reynolds, W.D., Tan, C.S., Yang, X.M., Oloya, T.O., 2018. Long-term Cropping effects on partitioning of water flow and nitrate loss between surface runoff and tile drainage. Journal of Environmental Quality 47, 820–829. https://doi.org/10.2134/jeq2017.07.0292

Wright, E.P., 1992. The hydrogeology of crystalline basement aquifers in Africa. Geological Society, London, Special Publications 66, 1–27. https://doi.org/10.1144/GSL.SP.1992.066.01.01

Wyns, R., Baltassat, J.-M., Lachassagne, P., Legchenko, A., Vairon, J., Mathieu, F., 2004. Application of proton magnetic resonance soundings to groundwater reserve mapping in weathered basement rocks (Brittany, France). Bulletin de la Société Géologique de France 175, 21–34. https://doi.org/10.2113/175.1.21

Wyns, R., Gourry, J.C., Baltassat, J.M., Lebert, F., 1999. Caracterisation multiparametres des horizons de subsurface 0-100m en contexte de socle altere, in: Geofcan : Actes Du 2ème Colloque de Géophysique Des Sols et Des Formations Superficielles : Résumés Étendus. BRGM, Orléans, pp. 105–110.

Yameogo, P.L., Becker, M., Segda, Z., 2021. Seasonal soil nitrogen dynamics affect yields of lowland rice in the savannah zone of West Africa. Journal of Plant Nutrition and Soil Science 184, 98–111. https://doi.org/10.1002/jpln.202000275

Yang, Y., Wendroth, O., Walton, R.J., 2013. Field-scale bromide leaching as affected by land use and rain characteristics. Soil Science Society of America Journal 77, 1157–1167. https://doi.org/10.2136/sssaj2013.01.0018

Yost, D., Eswaran, H., 1990. Major land resources Uganda, World Soil Resources. Soil Conservation Service, USDA, Washington DC.

Zech, W., Senesi, N., Guggenberger, G., Kaiser, K., Lehmann, J., Miano, T.N., Miltner, A., Schroth, G., 1997. Factors controlling humification and mineralization of soil organic matter in the tropics. Geoderma 79, 117–161. https://doi.org/10.1016/S0016-7061(97)00040-2

Zehe, E., Flühler, H., 2001. Slope scale variation of flow patterns in soil profiles. Journal of Hydrology 247, 116–132. https://doi.org/10.1016/S0022-1694(01)00371-7

Zheng, F.-L., Huang, C.-H., Norton, L.D., 2004. Effects of near-surface hydraulic gradients on nitrate and phosphorus losses in surface runoff. Journal of Environmental Quality 33, 2174–2182. https://doi.org/10.2134/jeq2004.2174

Ziegler, A.D., Giambelluca, T.W., Tran, L.T., Vana, T.T., Nullet, M.A., Fox, J., Vien, T.D., Pinthong, J., Maxwell, J.F., Evett, S., 2004. Hydrological consequences of landscape fragmentation in mountainous northern Vietnam: evidence of accelerated overland flow generation. Journal of Hydrology 287, 124–146. https://doi.org/10.1016/j.jhydrol.2003.09.02

Appendix

Appendix 1 *Overview of the experimental site showing each measuring point and the corresponding label.*

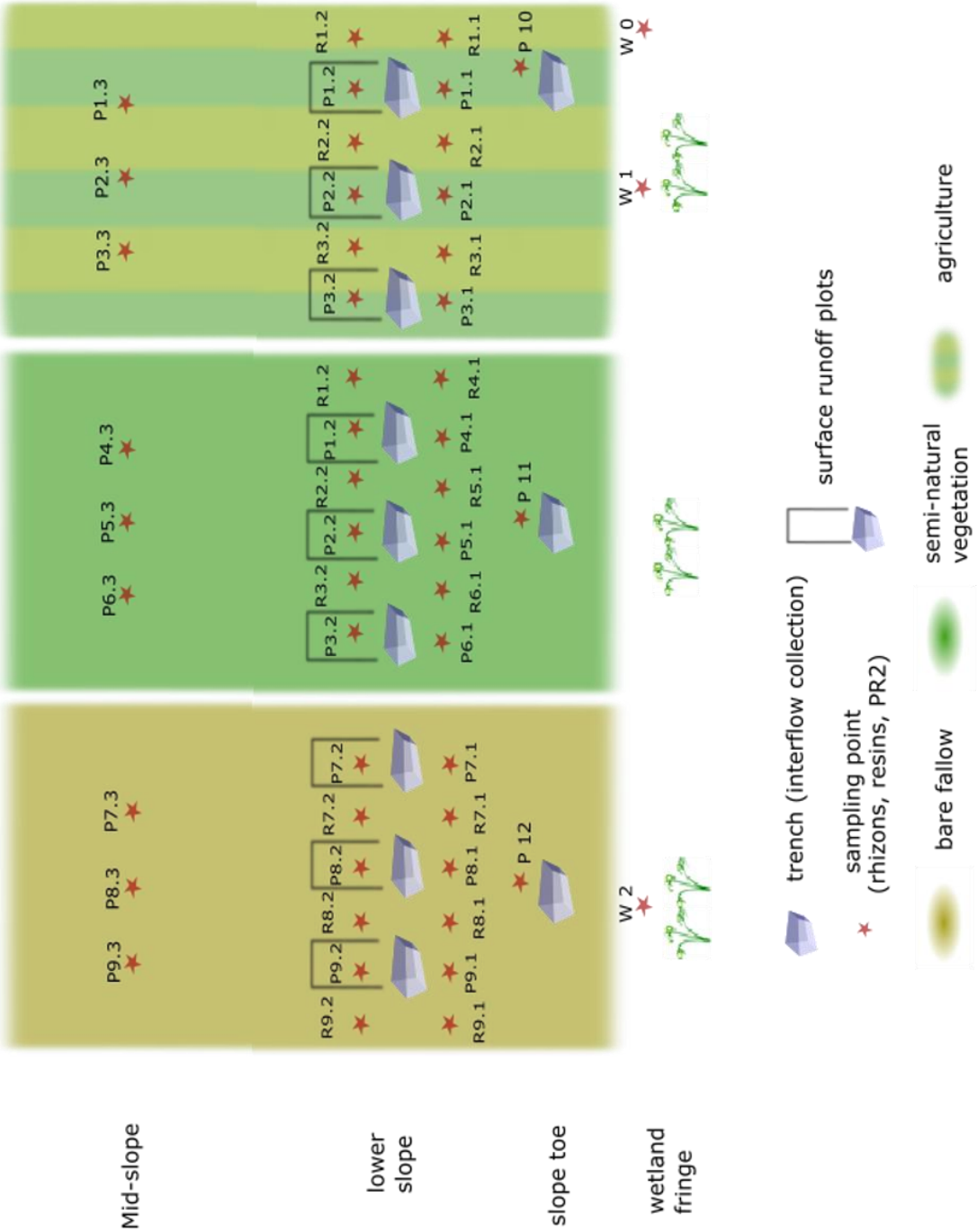

Appendix 2 *Model resistivity with topography of the geo-electrical measurements at transect 1 (profile 1, electrode spacing of 5 m) as modelled by the inversion software "Bert" (http://resistivity.net/bert/).*

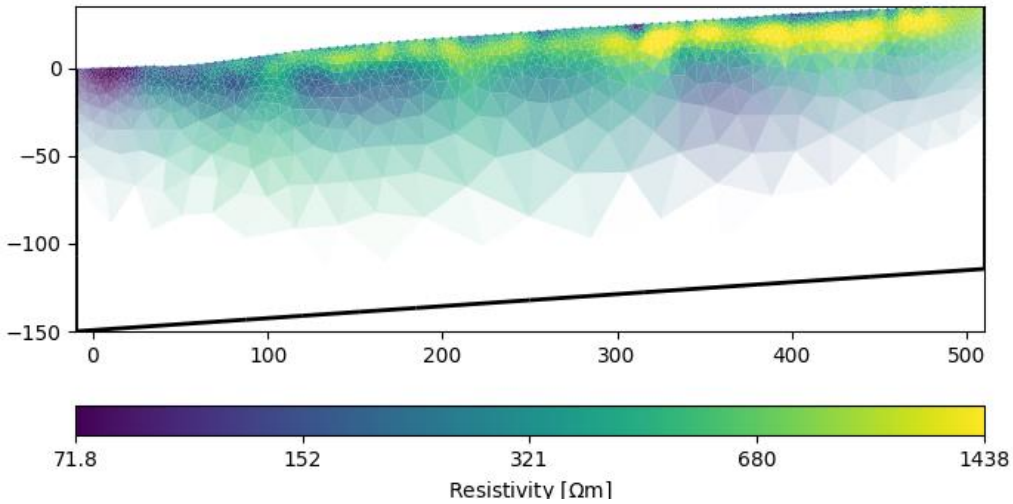

Appendix 3 *Model resistivity and depth of investigation index (DOI) of Transect 1, profile N° 1. The DOI is a measure of how strongly the resistivity value of each model cell is influenced by the measured data, with values close to zero indicating a strong signal of the measured data.*

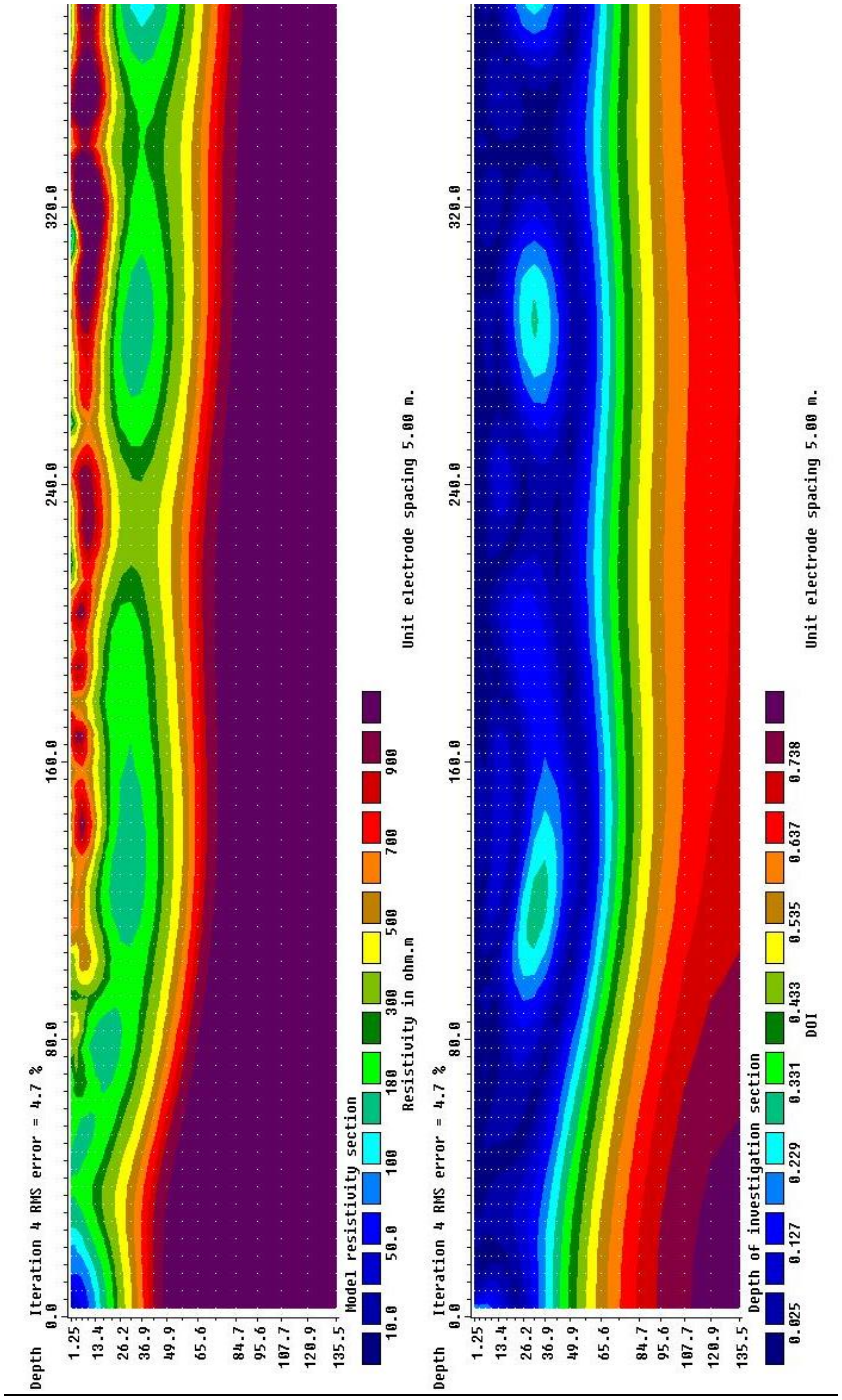

Appendix 4 *Model resistivity and the model resolution per unit area index of transect 1, profile N° 1. Lower values indicate a weaker resolution. To evaluate whether the resolution of a model cell is acceptable Loke (2018) proposes a cutoff value of 5 -10 to be a reasonable threshold.*

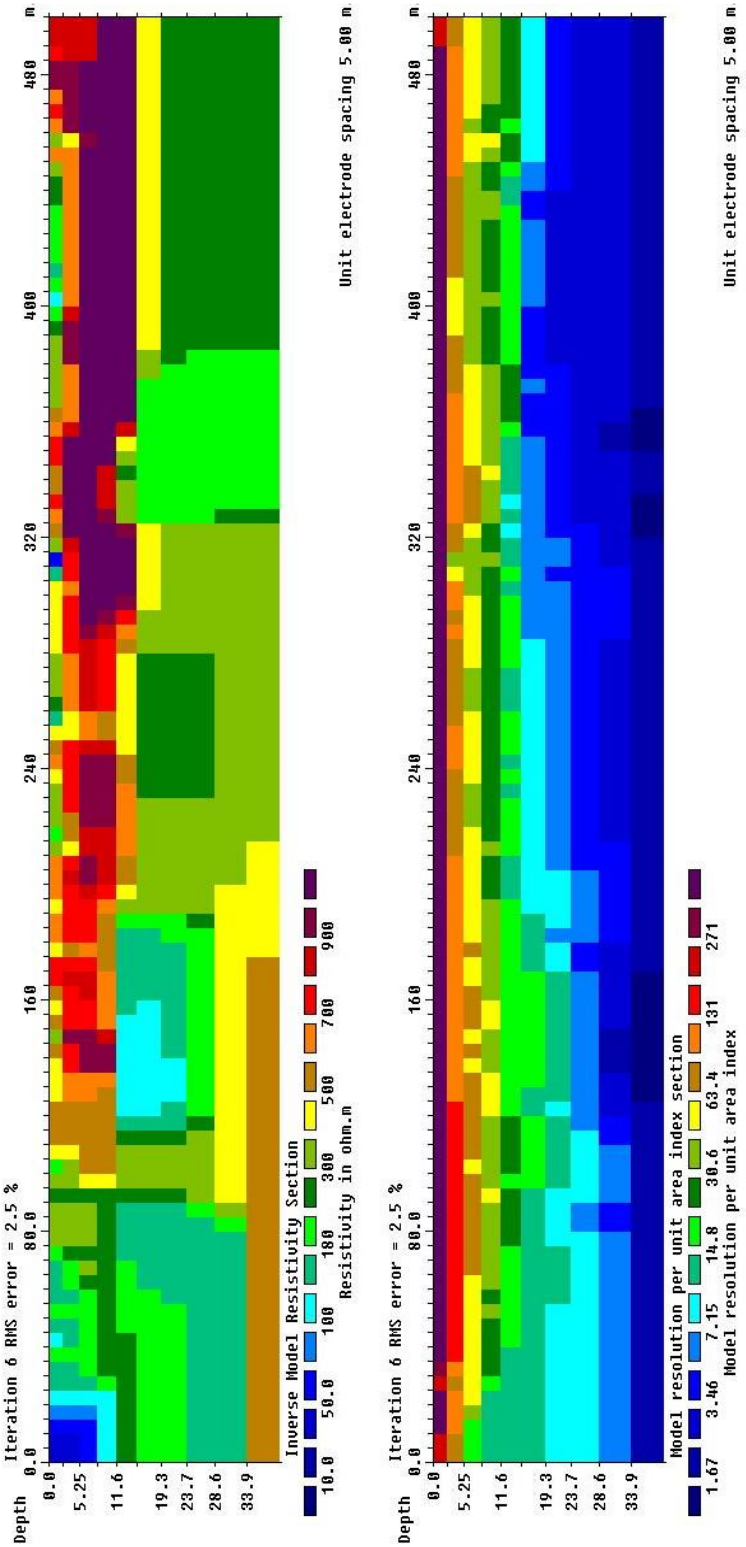

Appendix 5 *Description of two deep drilling logs which were sunk close to the experimental site (data provided by the Ugandan Ministry for Water and Environment)*

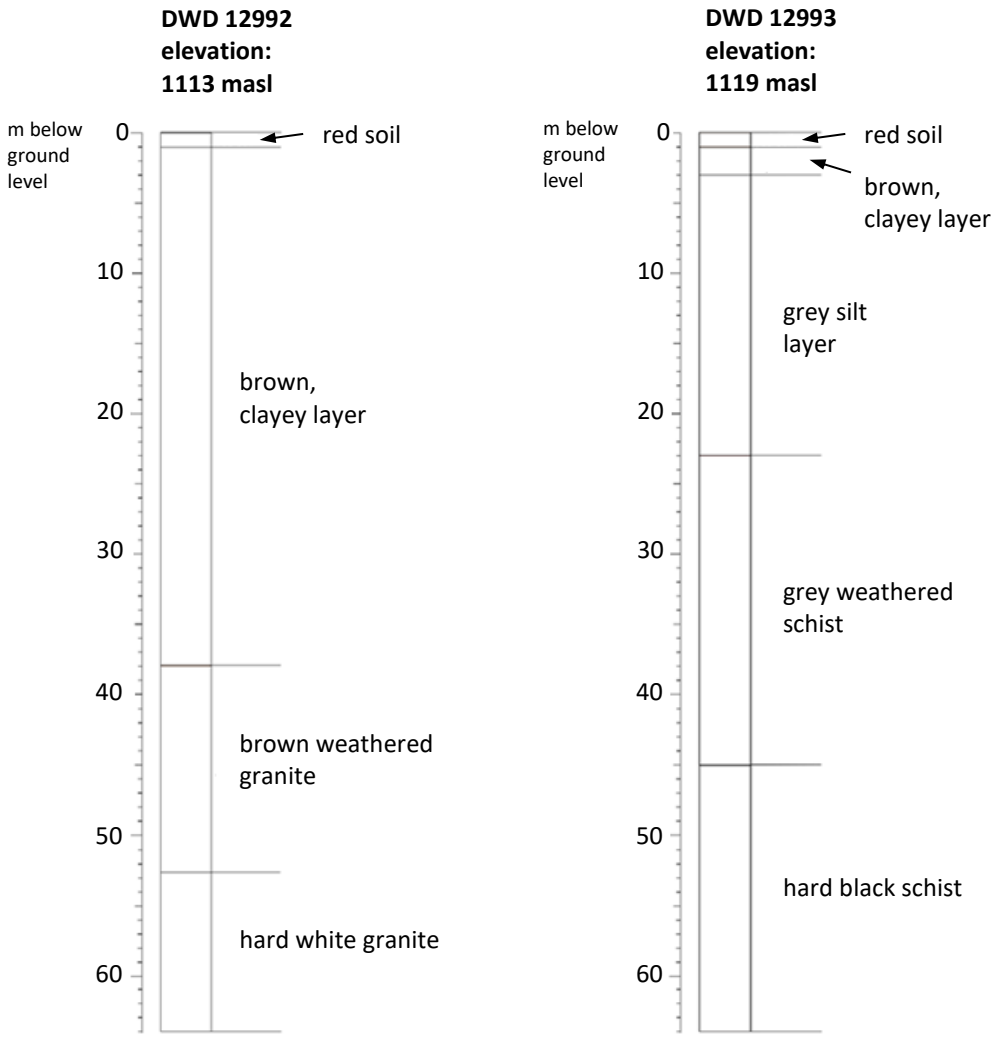

Appendix 6 *Soil profiles of the shallow drilling logs at each measuring point. Displayed are soil texture classes and the skeletal fraction (volume percentage represented by the area share of the box filled with dots). Colours were chosen following the soil colour observed in the field. Depth is shown as depth below ground level.*

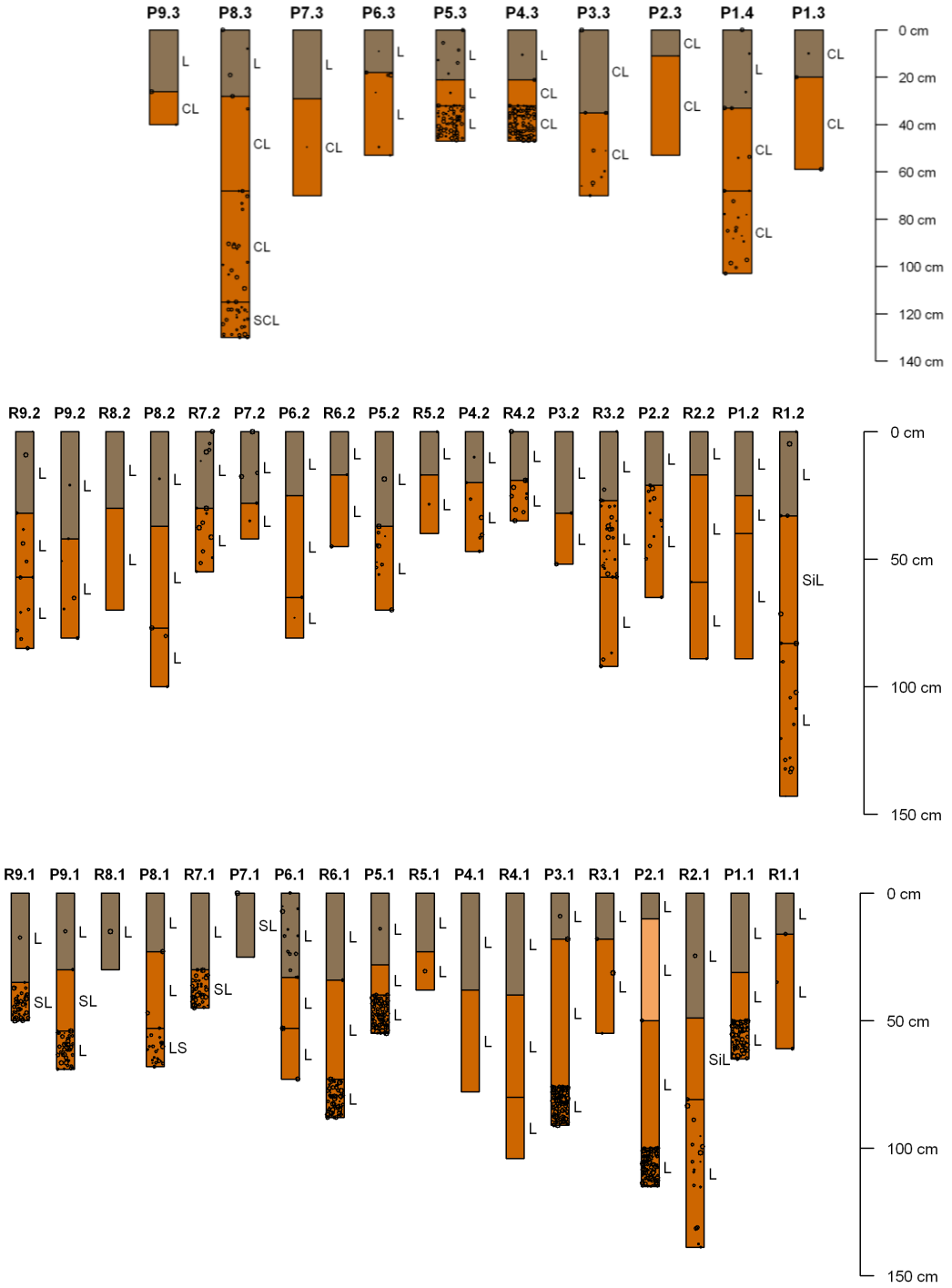

***Appendix 7** Soil properties at the single measuring points.*

	Top [cm]	Bottom [cm]	grain size distribution [%] sand	silt	clay	texture	skeletal fraction [%]	silt/clay ratio	colour (field obs.)	Density [g/cm³]	pH (H2O)	pH (KCl)	Δ pH	C [%]	C/N
W 0	0	25	57.1	32.1	10.9	SL	0.0	2.9	dark brown black	1.34	6	5.1	-0.9	1.86	16
W 0	25	30	64.6	27.1	8.3	SL	0.4	3.3	beige, grey brown		5.8	4.4	-1.4	0.62	22
W 0	30	60	69.7	22.7	7.6	SL	0.1	3.0	grey	1.60	6	4.1	-1.9	0.13	18
W 0	60	100	67.5	21.9	10.6	SL	0.2	2.1	grey		5.2	4	-1.2	0.13	21
W 0	100	160	55.1	26.4	18.5	SL	0.7	1.4	grey		5.4	3.9	-1.5	0.12	20
W 0	160	180	43.7	30.9	25.5	L	26.7	1.2	grey		5.3	3.9	-1.4	0.12	27
W 0	180	202	36.4	35.6	28.0	CL	4.4	1.3	beige		5.3	3.8	-1.5	0.17	28
W 0	202	217	46.3	34.6	19.1	L	29.6	1.8	grey		4.8	3.7	-1.1	0.15	20
P 1.1	0	31	35.6	44.4	20.0	L	0.0	2.2	dark brown	1.40	5.2	4.7	-0.5	1.67	13
P 1.1	31	50	37.8	43.8	18.5	L	0.1	2.4	reddish brown	1.55	4.6	4	-0.6	0.69	13
P 1.1	50	65	43.9	41.9	14.1	L	42.4	3.0	reddish brown		4.7	4.3	-0.4	0.28	11
P 1.2	0	25	39.0	41.7	19.3	L	0.0	2.2	dark brown	1.19	5.2	4.6	-0.6	1.96	14
P 1.2	25	40	27.8	47.4	24.8	L	0.0	1.9	reddish brown	1.49	5.1	4.4	-0.7	0.78	12
P 1.2	40	89	27.3	46.9	25.8	L	0.0	1.8	reddish brown		5.3	4.6	-0.7	0.76	11
P 1.3	0	20	32.5	38.9	28.6	CL	0.3	1.4	dark brown	1.25	5.4	4.6	-0.8	1.99	13
P 1.3	20	59	30.4	36.9	32.8	CL	0.5	1.1	reddish brown	1.56	4.7	4.2	-0.5	0.89	14
P 1.4	0	33	38.5	38.3	23.2	L	1.1	1.7	dark brown	1.51	5.5	4.5	-1	2.0	15
P 1.4	33	68	35.5	37.3	27.2	CL	1.1	1.4	reddish brown	1.55	5.2	4.2	-1	0.8	9
P 1.4	68	103	27.9	38.6	33.5	CL	4.4	1.2	reddish brown		5.3	4.1	-1.2	0.5	8
R 1.1	0	16	32.1	46.4	21.5	L	0.2	2.2	dark brown	1.26	5.3	4.8	-0.5	1.88	15
R 1.1	16	61	33.7	45.0	21.3	L	0.6	2.1	reddish brown	1.51	4.6	4	-0.6	0.66	13
R 1.2	0	33	33.7	46.1	20.2	L	0.8	2.3	dark brown	1.26	5.9	5.1	-0.8	2.2	15
R 1.2	33	83	27.6	50.0	22.4	SiL	0.7	2.2	reddish brown	1.52	5.1	4	-1.1	0.8	20
R 1.2	83	143	32.9	45.0	22.1	L	2.3	2.0	reddish brown		5.2	4.1	-1.1	0.5	15
W 1	0	17	50.9	36.8	12.3	L	0.3	3.0	dark brown black	1.36	5.6	4.6	-1	1.72	14
W 1	17	28	54.9	31.9	13.2	SL	0.1	2.4	beige, grey brown		5.2	4.1	-1.1	0.51	22
W 1	28	55	67.9	24.4	7.8	SL	0.4	3.1	grey	1.91	5.7	4	-1.7	0.13	23
W 1	55	90	60.7	23.3	16.0	SL	0.4	1.5	grey		5.4	3.8	-1.6	0.12	12
W 1	90	100	58.4	25.2	16.4	SL	0.9	1.5	grey		5.7	3.9	-1.8	0.12	14

	Top	Bottom	grain size distribution [%]				skeletal	silt/clay	colour	Bulk					
	[cm]	[cm]	sand	silt	clay	texture	fraction [%]	ratio	(field obs.)	Density	pH (H2O)	pH (KCl)	Δ pH	C [%]	C/N
W 1	100	115	50.0	29.6	20.3	L	22.1	1.5	grey		5.4	3.9	-1.5	0.11	15
P 2.1	0	10	36.3	45.3	18.5	L	0.0	2.4	dark brown	1.25	5.5	4.5	-1	2.12	14
P 2.1	10	50	32.3	47.2	20.5	L	0.0	2.3		1.56	5.2	4	-1.2	1.56	20
P 2.1	50	100	32.6	46.8	20.5	L	0.4	2.3	reddish brown	1.62	5.3	4.2	-1.1	0.61	14
P 2.1	100	115	37.5	42.2	20.3	L	61.8	2.1	reddish brown		5	4.2	-0.8	0.60	12
P 2.2	0	21	37.6	43.6	18.8	L	0.2	2.3	dark brown	1.27	5.6	4.9	-0.7	2.28	14
P 2.2	21	65	35.8	42.2	22.0	L	2.8	1.9	reddish brown	1.69	5	4.4	-0.6	0.69	14
P 2.3	0	11	29.6	42.1	28.3	CL	0.3	1.5	dark brown	1.20	5.9	5	-0.9	2.48	13
P 2.3	11	53	30.5	39.6	29.9	CL	0.4	1.3	reddish brown	1.64	5.1	4.2	-0.9	0.88	14
R 2.1	0	49	33.8	46.4	19.7	L	0.2	2.4	dark brown	1.47	5.9	5	-0.9	1.77	15
R 2.1	49	81	27.4	50.7	21.9	SiL	0.1	2.3	reddish brown	1.58	5	4.2	-0.8	0.65	14
R 2.1	81	139	29.8	49.3	20.9	L	2.9	2.4	reddish brown		5.5	4.1	-1.4	0.51	12
R 2.2	0	31	35.1	45.4	19.5	L	0.6	2.3	dark brown	1.51	5.4	4.8	-0.6	2.0	15
R 2.2	0	17	36.1	44.0	19.9	L	0.1	2.2	dark brown	1.54	5	4.4	-0.6	1.50	14
R 2.2	17	59	32.3	44.3	23.4	L	0.1	1.9	reddish brown	1.64	4.7	4.1	-0.6	0.58	14
R 2.2	59	89	28.6	49.5	21.9	L	0.7	2.3	reddish brown		5.1	4.2	-0.9	0.60	12
W 2	0	30	55.2	34.2	10.7	SL	0.0	3.2	dark brown black	1.35	5.7	4.7	-1	1.91	14
W 2	30	50	69.4	24.7	5.9	SL	0.0	4.2	beige, grey brown		5.3	4.2	-1.1	0.54	21
W 2	50	85	70.3	24.9	4.8	SL	0.2	5.2	grey		5.8	4.4	-1.4	0.07	72
W 2	85	115	58.8	23.4	17.8	SL	0.2	1.3	grey		5.2	3.8	-1.4	0.12	15
W 2	115	160	39.1	33.6	27.3	CL	0.7	1.2	beige		5.5	3.8	-1.7	0.14	18
W 2	160	175	35.5	32.7	31.8	CL	31.7	1.0	grey		4.9	3.7	-1.2	0.17	14
P 3.1	0	18	34.7	44.1	21.2	L	0.3	2.1	dark brown	1.33	5.8	5	-0.8	2.51	14
P 3.1	18	76	31.1	47.9	20.9	L	0.4	2.3	reddish brown	1.63	4.9	4.2	-0.7	0.55	12
P 3.1	76	91	37.8	42.5	19.7	L	63.3	2.2	reddish brown		4.6	4.2	-0.4	0.56	11
P 3.2	0	32	36.3	44.3	19.4	L	0.1	2.3	dark brown	1.25	5.6	5.1	-0.5	2.18	15
P 3.2	32	52	30.6	45.9	23.4	L	0.9	2.0	reddish brown	1.56	4.9	4.3	-0.6	0.69	13
P 3.3	0	35	34.1	33.4	32.4	CL	0.5	1.0	dark brown	1.38	5.8	5	-0.8	2.4	8
P 3.3	35	70	30.4	36.1	33.5	CL	2.7	1.1	reddish brown	1.58	5.8	4.8	-1	0.9	14
R 3.1	0	18	33.8	46.0	20.2	L	0.2	2.3	dark brown	1.43	5.6	5.1	-0.5	2.02	14
R 3.1	18	55	36.8	41.5	21.8	L	0.8	1.9	reddish brown	1.57	4.9	4.3	-0.6	0.66	13

	Top	Bottom	grain size distribution [%]				skeletal	silt/clay	colour	Bulk					
	[cm]	[cm]	sand	silt	clay	texture	fraction [%]	ratio	(field obs.)	Density	pH (H2O)	pH (KCl)	Δ pH	C [%]	C/N
R 3.2	0	27	35.3	45.0	19.7	L	1.0	2.3	dark brown	1.39	5.7	5	-0.7	2.5	9
R 3.2	27	57	36.8	40.6	22.6	L	7.7	1.8	reddish brown	1.59	5.5	4.3	-1.2	0.6	16
R 3.2	57	92	30.6	46.0	23.4	L	1.0	2.0	reddish brown		5.5	4.2	-1.3	0.5	13
P 4.1	0	38	32.2	46.9	21.0	L	0.1	2.2	dark brown	1.31	5.6	4.7	-0.9	2.21	14
P 4.1	38	78	32.9	45.7	21.4	L	0.1	2.1	reddish brown	1.54	5.6	4.6	-1	0.85	14
P 4.2	0	20	44.6	36.4	19.1	L	0.5	1.9	dark brown	1.42	5.7	4.7	-1	2.05	14
P 4.2	20	47	36.9	39.9	23.2	L	2.4	1.7	reddish brown	1.66	5.5	4.2	-1.3	0.81	16
P 4.3	0	21	33.8	39.9	26.3	L	0.3	1.5	dark brown	1.35	5.4	4.4	-1	2.19	13
P 4.3	21	32	37.8	34.4	27.8	CL	1.6	1.2	reddish brown	1.65	5.2	4.1	-1.1	0.94	15
P 4.3	32	47	44.6	26.9	28.5	CL	59.8	0.9	reddish brown		5.2	4.1	-1.1	0.96	13
R 4.1	0	40	38.4	44.7	16.8	L	0.0	2.7	dark brown	1.32	5.7	4.7	-1	2.15	17
R 4.1	40	80	33.9	45.0	21.1	L	0.0	2.1	reddish brown	1.69	5.5	4.2	-1.3	0.62	14
R 4.1	80	104	35.3	43.0	21.7	L	0.2	2.0	reddish brown		5.3	4.2	-1.1	0.48	13
R 4.2	0	19	44.1	36.7	19.2	L	0.9	1.9	dark brown	1.30	5.6	4.7	-0.9	2.17	14
R 4.2	19	35	37.0	39.2	23.8	L	4.7	1.6	reddish brown	1.66	5.7	4.6	-1.1	1.03	15
P 5.1	0	28	40.7	42.8	16.5	L	0.4	2.6	dark brown	1.30	5.5	4.5	-1	2.08	15
P 5.1	28	40	40.1	46.4	13.5	L	0.0	3.4	reddish brown	1.55	5.3	4.3	-1	1.25	16
P 5.1	40	55	36.4	45.3	18.2	L	54.0	2.5	reddish brown		4.8	4.1	-0.7	0.71	14
P 5.2	0	37	38.5	41.5	20.0	L	0.2	2.1	dark brown	1.26	5.3	4.3	-1	1.79	15
P 5.2	37	70	35.2	43.4	21.5	L	2.9	2.0	reddish brown	1.66	5.2	4.1	-1.1	0.55	16
P 5.3	0	21	38.0	39.4	22.7	L	3.3	1.7	dark brown	1.30	5.6	4.6	-1	2.26	13
P 5.3	21	32	36.3	38.1	25.6	L	0.9	1.5	reddish brown	1.61	5.4	4.2	-1.2	0.99	15
P 5.3	32	47	35.4	39.0	25.6	L	42.2	1.5	reddish brown		5.5	4.2	-1.3	0.87	15
R 5.1	0	23	37.6	45.6	16.8	L	0.2	2.7	dark brown	1.25	5.7	4.7	-1	2.12	14
R 5.1	23	38	35.3	48.0	16.7	L	0.5	2.9	reddish brown	1.63	5.4	4.2	-1.2	0.79	15
R 5.2	0	17	36.5	45.2	18.4	L	1.0	2.5	dark brown	1.28	5.6	4.8	-0.8	2.0	15
R 5.2	17	40	35.8	45.6	18.6	L	0.4	2.5	reddish brown	1.52	5.8	4.2	-1.6	0.9	10
P 6.1	0	33	46.4	36.4	17.3	L	3.6	2.1	dark brown	1.31	5.8	4.9	-0.9	1.8	15
P 6.1	33	53	38.3	41.5	20.2	L	0.9	2.1	reddish brown	1.61	5.9	5	-0.9	0.8	15
P 6.1	53	73	40.5	39.6	19.8	L	0.9	2.0	reddish brown		5.9	5.1	-0.8	0.7	16
P 6.2	0	25	45.5	36.5	18.0	L	0.0	2.0	dark brown	1.52	5.8	4.8	-1	1.68	15

	Top	Bottom	grain size distribution [%]				skeletal	silt/clay	colour	Bulk					
	[cm]	[cm]	sand	silt	clay	texture	fraction [%]	ratio	(field obs.)	Density	pH (H2O)	pH (KCl)	Δ pH	C [%]	C/N
P 6.2	25	65	41.7	36.4	21.9	L	0.5	1.7	reddish brown	0.68	5.4	4.3	-1.1	0.69	15
P 6.2	65	81	39.5	38.4	22.0	L	0.6	1.7	reddish brown		5.5	4.5	-1	0.63	13
P 6.3	0	18	38.4	42.1	19.6	L	0.5	2.1	dark brown	1.30	5.5	4.5	-1	2.1	15
P 6.3	18	53	36.1	44.2	19.7	L	1.6	2.2	reddish brown	1.59	5.4	4	-1.4	1.1	21
R 6.1	0	34	45.1	36.0	18.9	L	0.0	1.9	dark brown	1.52	5.6	4.5	-1.1	1.71	18
R 6.1	34	73	39.8	37.4	22.8	L	0.6	1.6	reddish brown	1.70	5.4	4.3	-1.1	0.44	13
R 6.1	73	88	47.2	32.0	20.8	L	38.6	1.5	reddish brown		4.8	4.3	-0.5	0.35	13
R 6.2	0	17	39.5	44.5	16.0	L	0.2	2.8	dark brown	1.53	5.5	4.9	-0.6	1.93	14
R 6.2	17	45	38.9	41.2	19.9	L	0.8	2.1	reddish brown	1.64	5.1	4.1	-1	0.73	16
P 7.1	0	25	59.6	28.7	11.7	SL	0.8	2.5	dark brown	1.27	5.2	4.4	-0.8	1.61	14
P 7.2	0	28	41.2	37.2	21.6	L	1.4	1.7	dark brown	1.24	4.8	4.4	-0.4	1.67	13
P 7.2	28	42	50.6	31.9	17.6	L	0.7	1.8	reddish brown	1.66	4.9	4.2	-0.7	0.74	16
P 7.3	0	29	38.2	38.1	23.8	L	0.0	1.6	dark brown	1.37	5.1	4.8	-0.3	2.50	14
P 7.3	29	70	38.1	33.4	28.5	CL	0.2	1.2	reddish brown	1.48	5.1	4.5	-0.6	0.96	14
R 7.1	0	30	50.0	34.2	15.8	L	0.0	2.2	dark brown	1.27	4.9	4.4	-0.5	1.56	13
R 7.1	30	45	60.3	27.4	12.3	SL	26.9	2.2	reddish brown		5.1	4.5	-0.6	0.37	18
R 7.2	0	30	47.6	33.1	19.3	L	1.9	1.7	dark brown	1.50	5.2	4.5	-0.7	0.1	9
R 7.2	30	55	44.0	33.9	22.1	L	3.6	1.5	reddish brown	1.65	5.3	4.3	-1	0.5	10
P 8.1	0	23	44.0	36.8	19.2	L	0.1	1.9	dark brown	1.28	4.8	4.3	-0.5	1.65	14
P 8.1	23	53	50.8	34.2	15.1	L	0.9	2.3	reddish brown	1.57	4.7	4.4	-0.3	0.54	13
P 8.1	53	68	80.3	14.1	4.2	LS	14.3	3.4	reddish brown		4.4	4.2	-0.2	0.28	10
P 8.2	0	37	47.3	33.9	18.8	L	0.2	1.8	dark brown	1.37	5.1	4.5	-0.6	1.52	15
P 8.2	37	77	40.3	35.7	24.0	L		1.5	reddish brown	1.69	5.2	4.3	-0.9	0.40	13
P 8.2	77	100	43.7	32.8	23.5	L	1.2	1.4	reddish brown		4.9	4.3	-0.6	0.35	12
P 8.3	0	28	43.6	33.1	23.2	L	1.3	1.4	dark brown	1.44	5.7	4.5	-1.2	2.2	10
P 8.3	28	62	44.1	27.6	28.2	CL	0.7	1.0	reddish brown	1.59	5.4	4.4	-1	0.7	8
P 8.3	68	115	35.5	31.4	33.0	CL	3.3	1.0	reddish brown		5.1	4.2	-0.9	0.4	7
P 8.3	115	130	49.4	23.6	26.1	SCL	17.3	0.9	reddish brown		5.7	4.4	-1.3	0.4	14
R 8.1	0	30	45.6	36.7	17.7	L	0.2	2.1	dark brown	1.29	5	4.3	-0.7	1.65	14
R 8.2	0	30	45.0	36.2	18.8	L	0.0	1.9	dark brown	1.36	5	4.6	-0.4	1.62	13
R 8.2	30	70	47.9	30.9	21.2	L	0.1	1.5	reddish brown	1.67	4.8	4.3	-0.5	0.50	14

	Top	Bottom	grain size distribution [%]				skeletal	silt/clay	colour	Bulk					
	[cm]	[cm]	sand	silt	clay	texture	fraction [%]	ratio	(field obs.)	Density	pH (H2O)	pH (KCl)	Δ pH	C [%]	C/N
P 9.1	54	69	43.6	33.5	22.9	L	26.3	1.5	reddish brown		6	4.6	-1.4	0.2	9
P 9.2	0	42	41.4	36.8	21.7	L	0.3	1.7	dark brown	1.46	5.4	4.6	-0.8	1.68	15
P 9.2	42	81	38.5	36.1	25.5	L	1.4	1.4	reddish brown	1.72	4.9	4.3	-0.6	0.65	17
P 9.3	0	26	41.5	37.1	21.5	L	0.0	1.7	dark brown	1.37	4.9	4.4	-0.5	1.98	15
P 9.3	26	40	34.8	31.9	33.3	CL	1.2	1.0	reddish brown	1.54	5	4.4	-0.6	0.92	13
R 9.1	0	35	51.0	33.4	15.6	L	0.2	2.1	dark brown	1.25	5.4	4.5	-0.9	1.76	15
R 9.1	35	50	58.8	31.1	10.2	SL	28.2	3.1	reddish brown		4.9	4.3	-0.6	0.55	18
R 9.2	0	32	49.3	32.9	17.8	L	0.8	1.9	dark brown	1.50	5.6	4.7	-0.9	2.0	15
R 9.2	32	57	38.4	34.6	26.9	L	2.1	1.3	reddish brown	1.62	5.4	4.3	-1.1	0.6	13
R 9.2	57	85	37.3	36.4	26.3	L	2.4	1.4	reddish brown		5.1	4.2	-0.9	0.4	14
P 10	0	17	37.1	42.7	20.2	L	1.5	2.1	dark brown	1.29	6	5.3	-0.7	2.4	14
P 10	17	47	37.2	49.0	13.8	L	0.8	3.5	dark grey	1.47	6	4.8	-1.2	1.8	19
P 10	47	75	54.7	38.4	6.9	SL	6.3	5.6	grey	1.81	5.9	4.1	-1.8	0.2	13
P 10	75	90	51.7	41.1	7.2	L	52.4	5.7	grey		6.1	4.7	-1.4	0.2	27
P 11	0	18	51.8	36.2	12.1	L	0.7	3.0	dark brown	1.20	5.4	4.4	-1	1.5	10
P 11	18	40	50.2	37.2	12.6	L	3.9	3.0	dark brown reddish	1.52	6.1	4.1	-2	0.8	27
P 11	40	68	58.7	33.8	7.5	SL	6.4	4.5	grey	1.93	5.9	4.3	-1.6	0.1	26
P 11	68	83	52.4	34.3	13.3	SL	51.2	2.6	grey	1.65	5.4	4.1	-1.3	0.1	24
P 12	0	25	58.4	31.2	10.4	SL	0.6	3.0	dark brown	1.21	5.5	4.4	-1.1	1.4	17
P 12	25	54	54.3	32.5	13.2	SL	0.5	2.5	beige, grey brown	1.50	5.6	4.1	-1.5	0.9	14
P 12	54	88	59.7	28.9	11.4	SL	0.8	2.5	beige	1.69	5.5	4.1	-1.4	0.3	24
P 12	88	114	46.8	34.3	18.9	L	1.4	1.8	grey	1.78	5.8	4	-1.8	0.2	16
P 12	114	140	42.3	36.2	21.5	L	8.5	1.7	grey	1.76	5.8	4	-1.8	0.2	14
P 12	140	155	43.9	35.1	21.0	L	12.4	1.7	grey		5.6	4	-1.6	1.4	9